Augmentation of Rotator Cuff Tendon-Bone Healing using Demineralised Bone Matrix and Mesenchymal Stem Cells

Tanujan Thangarajah

Submitted for the degree of Doctor of Philosophy

University College London

November 2016

John Scales Centre for Biomedical Engineering

Institute of Orthopaedics and Musculoskeletal Science

University College London

Royal National Orthopaedic Hospital

Stanmore

HA7 4LP

United Kingdom

Declaration

I, Tanujan Thangarajah, confirm that the work presented in this thesis is my own. Where information has been derived from other sources, I confirm that this has been indicated in the thesis.

Abstract

Background:

The results of surgery for tears of the rotator cuff are variable, with failure occurring in up to 94% of cases. Demineralised bone matrix (DBM) consists of a collagen scaffold containing multiple growth factors and has been used successfully to improve tendon-bone healing. By combining DBM with stem cells its effects may be enhanced given that many of the growth factors it contains are able to direct stem cell differentiation down tenogenic, chondrogenic, and osteogenic lineages. These cell lines produce elements essential to the formation of a naturally graded enthesis.

Aim:

To investigate the effect of DBM on regeneration of the tendon-bone interface, and whether its function can be enhanced by mesenchymal stem cells (MSCs).

Hypothesis:

DBM will improve tendon-bone healing in an enthesis defect model, and its effect may be further enhanced by the incorporation of MSCs.

Methods:

The following experiments were undertaken in order to investigate the hypothesis:

1. Tensile testing of allogenic and xenogenic cortical/cancellous DBM.
2. Evaluating the effect of allogenic and xenogenic DBM, incorporated with MSCs, on regeneration of the enthesis in a large animal model of severe tendon retraction.
3. Development of a chronic rotator cuff tear model.
4. Investigation of tendon-bone healing using DBM in a chronic rotator cuff tear model.
5. Investigation of tendon-bone healing using DBM and MSCs in a chronic rotator cuff tear model.

Results:

Allogenic cortical DBM possessed the greatest tensile strength and was used *in vivo* to examine tendon-bone healing complicated by retraction. In this, DBM regenerated a direct enthesis characterised by fibrocartilage. A similar effect was noted in a chronic rotator cuff tear model with no additional effect conferred by the stem cells.

Conclusion:

This thesis has shown that DBM can regenerate a fibrocartilaginous enthesis in models of tendon retraction and chronic rotator cuff degeneration.

Acknowledgements

I wish to express my sincere gratitude to Professor Gordon Blunn for giving me the opportunity to undertake this PhD. His guidance, mentorship, and support have been invaluable throughout this process and I am truly honored to have worked under his tutelage. A debt of gratitude is also owed to Dr Catherine Pendegrass and Ms Susan Alexander without whom this project would not have been possible.

To all those at the John Scales Centre for Biomedical Engineering/Institute of Orthopaedics and Musculoskeletal Science who have helped me throughout this journey, I cannot thank you enough. A special thanks goes to Mark Harrison, Frederick Henshaw, Hyat Khan, Simon Lambert, Josie Marshall, Aadil Mumith, Charlotte Page, Rebecca Porter, Anita Sanghani-Kerai, and Shirin Shahbazi.

Finally, I would like to thank my wife Arani for her unwavering support and dedication. She has been instrumental during my research tenure and has worked tirelessly in the background to ensure that I can achieve success in my professional career. For this, I am eternally grateful.

I dedicate this thesis to my parents.

Table of contents

List of Figures

List of Tables

Abbreviations

α-Gal: Galactose-alpha-1, 3-galactose

ACL: Anterior cruciate ligament

Ad-MT1-MMP: Adenoviral membrane type 1 matrix metalloproteinase

ASES: American Shoulder and Elbow Surgeons

β: Beta

B: Bone

bFGF: Basic fibroblast growth factor

BMPs: Bone morphogenic proteins

cc: Cubic centimeter

CD: Cluster of differentiation

CI: Confidence interval

cm: Centimeters

CXCR: Chemokine ligand 12- chemokine receptor

DBM: Demineralised bone matrix

DMEM: Dulbecco's Modified Eagle Medium

° C: Degrees centigrade

DNA: Deoxyribonucleic acid

ECM: Extracellular matrix

EDTA: Ethylenediaminetetraacetic acid

FC: Fibrocartilage

FCS: Fetal calf serum

FGF: Fibroblast growth factor

FITC: Fluorescein isothiocyanate

FWB: Functional weight bearing

GP: General practitioner

GPa: Gigapascals

g: Grams

GRFz: Ground reaction force

H&E: Hematoxylin and eosin

HLA DR: Human Leukocyte Antigen – antigen D Related

HCL: Hydrochloric acid

IGF: Insulin like growth factor

IU: International units

kg: Kilogram

kV: Kilovolts

µl: Microlitre

µm: Micrometers

M: Molar

MFC: Mineralised fibrocartilage

mg: milligrams

ml: Milliliter

mm: Millimeters

mmMSCs: Minimally manipulated Mesenchymal stem cells

MMP: Matrix metalloproteinases

MPa: Megapascal

MRI: Magnetic resonance imaging

MSC: Mesenchymal stem cell

MT1-MMP: Membrane type 1 matrix metalloproteinase

N: Newtons

N: Normal

NaCl: Sodium chloride

NB: Normal bone

NHS: National Health Service

pQCT: Peripheral quantitative computer tomography

PBS: Phosphate-buffered saline

PDGF: Platelet-derived growth factor

PDO: Polydioxanone

PGA: Polyglycolyic acid

PGS: Polyglycolyic acid

PLGA: Poly (lactic-co-glycolic) acid

PLLA: Poly-L-lactic acid

PRF-M: Platelet-rich fibrin matrix

PRP: Platelet rich plasma

QDs: Quantum dot nanoparticles

rpm: Revolutions per minute

SH2: Src Homology 2

Stro-1: Stromal cell surface marker-1

T: Tendon

TN: Tennessee

TGF-β: Transforming growth factor beta

3D: Three-dimensional

UK: United Kingdom

USA: United States of America

UTS: Ultimate tensile strength

VEGF: Vascular endothelial growth factor

Chapter One: Introduction

1.1 Aims and Hypotheses

This thesis aims to investigate the effect of demineralised bone matrix (DBM) on regeneration of the tendon-bone interface, and whether its function can be augmented by mesenchymal stem cells (MSCs). To achieve this, the following overarching hypothesis will be tested:

DBM will improve tendon-bone healing in an enthesis defect model, and its effect may be further enhanced by the incorporation of MSCs.

The introductory chapter provides an overview of tendon biology and rotator cuff tears. Specific attention is given to tissue engineering strategies that are currently employed to enhance tendon-bone healing and the rationale for using DBM in this setting.

Chapter Two examines the mechanical properties of ovine and porcine demineralised cortical and cancellous bone matrix. Given the low costs associated with xenogenic scaffolds its use in tendon-bone healing would be advantageous, but it is essential to first establish whether it possesses the appropriate mechanical properties. The second part of this chapter aims to determine whether there is a difference in tensile strength between cortical and cancellous DBM, since the latter may be a superior carrier of MSCs due to its porosity. Thus, it was hypothesised that the tensile strength of cancellous DBM would be significantly lower than that of cortical DBM, and that there would be no difference between ovine and porcine scaffolds.

Chapter Three applies the information gained about DBM in Chapter Two to investigate its effect on tendon-bone healing in a non-degenerative ovine model of tendon retraction, to simulate an irreparable rotator cuff tear. This involved creating a 1 centimeter (cm) ovine patellar tendon defect and then repairing it with either xenogenic cortical DBM (porcine) + minimally manipulated MSCs (mmMSCs) or allogenic cortical DBM (ovine) + mmMSCs. Autogenic MSCs were derived from the buffy layer obtained from bone marrow aspirates, which were harvested from the iliac crest of each animal at the time of surgery. Functional outcome was measured using force plate analysis at six, nine, and 12 weeks post-operatively. Histology was used to assess morphological recovery of the enthesis at 12 weeks. The hypothesis tested was that tendon-bone healing augmented with autologous mmMSC-enhanced xenogenic and allogenic DBM, would result in restored function and morphology of the enthesis by 12 weeks.

Chapter Four outlines the development of a clinically relevant chronic rotator cuff tear model in order to evaluate the presence of osteopenia at the enthesis and the time taken for degenerative changes to become apparent. The latter was examined by determining the extent of muscle atrophy, changes in muscle architecture, and fatty infiltration of the musculotendinous unit. It was hypothesised that detachment of supraspinatus from the humerus would result in osteopenia and tendon degeneration akin to what is seen in clinical practice.

Chapter Five utilises the animal model established in Chapter Four to examine rotator cuff tendon-bone healing. The supraspinatus tendon was first detached and then reattached to its bony insertion at the time point identified in Chapter Four. Healing

was augmented with either cortical DBM or GraftJacket [Wright Medical Technology, Inc., Arlington, TN (Tennessee)]. It was hypothesised that compared to a commercially available scaffold (GraftJacket), DBM would regenerate a functionally and morphologically superior enthesis in a rat model of chronic rotator cuff degeneration.

Chapter Six investigates whether the effect of DBM can be enhanced by the incorporation of culture-expanded MSCs at the repair site of a chronic rotator cuff tear. Using a similar operative protocol to Chapter Five, the supraspinatus tendon was detached and then later reattached to the humerus using either DBM + MSCs, GraftJacket + MSCs, or MSCs alone. The hypothesis was that compared to GraftJacket + MSCs and MSCs alone, the addition of cortical DBM + MSCs to the healing enthesis would regenerate a functionally and morphologically superior enthesis in a rat model of chronic rotator cuff degeneration.

1.2 The Clinical Problem

Shoulder pain is a significant socioeconomic burden and accounts for 2.4% of all General Practitioner (GP) consultations in the United Kingdom (UK) and 4.5 million visits to physicians annually in the United States (Carr et al., 2015a). This equates to 500,000 adults in England and Wales and costs the National Health Service (NHS) £310 million per year (Littlewood et al., 2012).

Rotator cuff disease encompasses a wide spectrum of pathological conditions including tendinitis, partial/full-thickness tears, and calcific tendinitis. The natural history and progression of rotator cuff tendinitis to a subsequent tear remains poorly understood (Iannotti, 1994). Rotator cuff tears affect 30-50% of patients over the age of 50 years and are a common cause of function-limiting pain and weakness of the shoulder (Zhao et al., 2014, Isaac et al., 2012). Approximately 75% of all rotator cuff tears only involve supraspinatus (Dunn et al., 2014). Many patients choose to have surgery due to disabling or progressive symptoms and this has been reflected in a 500% increase in the rate of repair since 2001, in the UK (Hakimi et al., 2013). In the United States an estimated 75,000 rotator cuff surgeries are performed annually and this number is likely to rise given an ageing population with greater functional demands (Vitale et al., 2007). By effectively augmenting healing of the rotator cuff the number of retears and tendons that failure to heal should decline, and in turn fewer revision surgeries would be required. Reducing the time taken for the rotator cuff to heal and increasing the strength of the initial repair will allow patients to rehabilitate more effectively and result in the restoration of normal tendon strength and function

at an earlier stage. Patients will consequently be able to return to work sooner and thereby minimise the amount of money lost by their employers through sick days.

Understanding the patho-anatomy of rotator cuff tears has improved over the last decade and treatment strategies have evolved considerably. Poor biological healing is still problematic with failure of tendon-bone fixation occurring in up to 26% of small to medium tears and up to 94% in large and massive tears (Galatz et al., 2004, Bishop et al., 2006, Iannotti et al., 2006, Klepps et al., 2004, Sclamberg et al., 2004). The cause of the high retear rate is multifactorial and may be attributed to the older age of the patient, quality of the tissue, chronicity and size of the tear, muscle atrophy, fatty infiltration, bone mineral density, and repair technique (single vs double row repair) (Deniz et al., 2014, Chung et al., 2013, Chung et al., 2011, Tashjian et al., 2010). In selected patients, mechanical and biological enhancement of the tendon-bone interface may be integral to a successful outcome following surgery (Aurora et al., 2012).

1.3 Tendon

Microstructure

Tendons connect muscle to bone and allow the transmission of forces generated by muscular contraction in order to produce movement at a joint. Healthy tendons are white in appearance and have a fibro-elastic texture. Their form is varied and can adopt the shape of either rounded cords, strap-like bands, or flattened ribbons. Water accounts for 70% of total tendon mass. The remaining 30% is dry mass and is primarily made up of collagen type I (65-80%) (Sharma and Maffulli, 2005). Between the densely pack collagen fibers are rod- or spindle-shaped fibroblast-like cells (tenoblasts and tenocytes) aligned parallel to the longitudinal axis of tensile load. These are embedded within a well-organised extracellular matrix (ECM) that contains glycoproteins and proteoglycans such as decorin and aggrecan (James et al., 2008).

Tenoblasts are spindle-shaped immature tendon cells that contain numerous cytoplasmic organelles to maintain their high metabolic activity. As they mature and transform into tenocytes their shape becomes elongated. Tenocytes synthesise collagen and all components of the ECM. Collagen constitutes the basic functional unit of a tendon. It is organised in hierarchical levels of increasing complexity commencing with a triple helix polypeptide chain that unites into fibrils with cross-links between adjacent helices. At the myotendinous interface these fibrils are inserted into deep recesses formed by myocytes and absorb the tension created from muscular contraction thereby limiting the stresses exerted on the tendon (Kvist et al., 1991, Michna, 1983, Trotter and Baca, 1987, Tidball and Daniel, 1986). In the

remaining tendon, collagen fibrils are bundled together to form large fibers that are visible under light microscopy as a crimped pattern. This characteristic facilitates elongation of the tendon and prevents damage from sudden mechanical loading. Fibers are subsequently arranged into bundles (fascicles) by the endotenon, which in turn are held together by an epitenon to form the tendon (Amiel et al., 1984, Dykyj and Jules, 1991, Kastelic et al., 1978) (Figure 1.1). Surrounding the epitenon is a loose connective tissue layer (paratenon) consisting of type I and type III collagen fibrils, elastic fibrils, and synovial cells (Kvist et al., 1985).

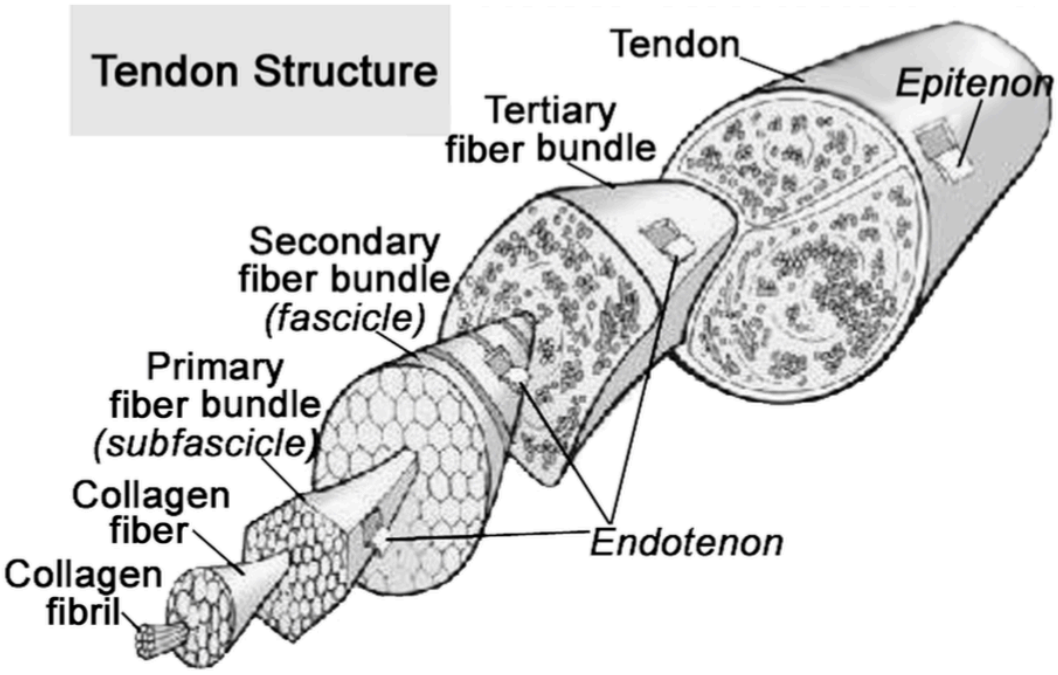

Figure 1.1: Hierarchical structure of tendon. Reproduced with permission from Sharma and Maffulli, 2005.

Biomechanics

Tendons possess a number of unique properties in order to carry out their normal function of load transfer: high mechanical strength, flexibility, and elasticity (Kirkendall and Garrett, 1997, O'Brien, 1992, Oxlund, 1986). The mechanical behaviour of collagen determines the physical properties of tendon and can be demonstrated using a stress-strain curve (Figure 1.2).

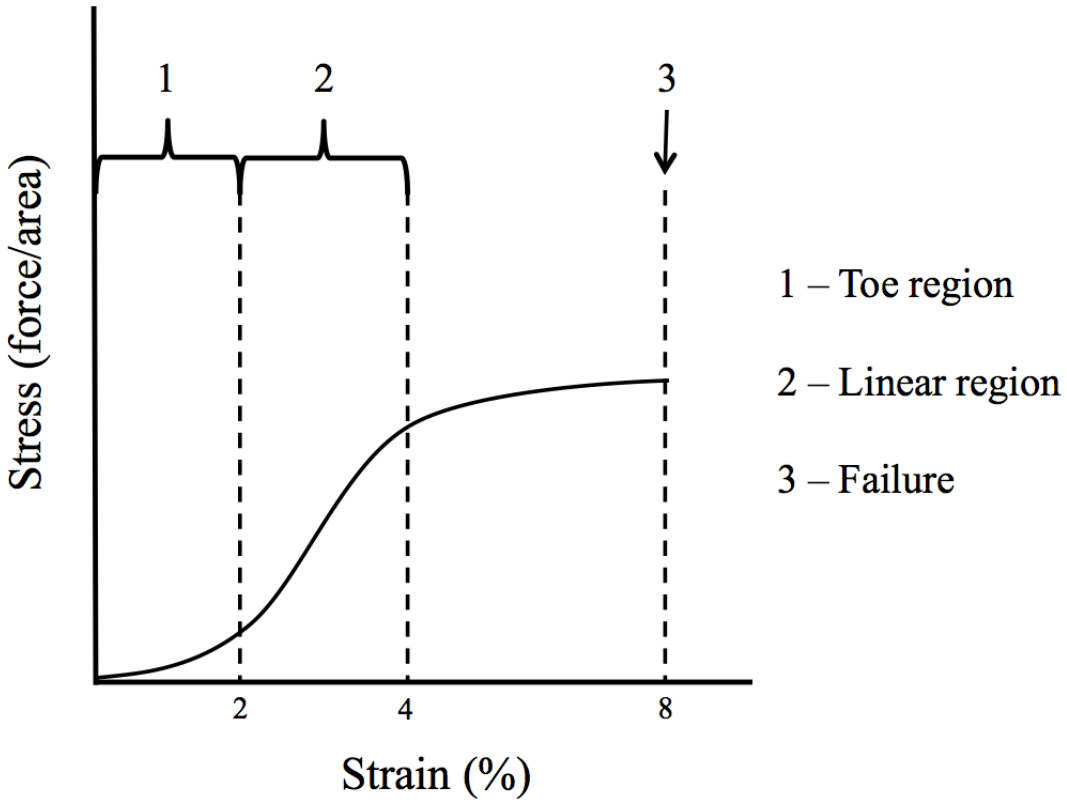

Figure 1.2: Stress-strain curve demonstrating the basic physical properties of tendon.

The initial part of the curve (toe region) represents flattening of the crimped pattern that characterises collagen fibrils at rest. This occurs when the tendon is strained up to 2% (Hess et al., 1989, Butler et al., 1978, Viidik, 1973). Beyond this, the tendon deforms in a linear fashion as the collagen triple helices slide and the fibers become more parallel (Young's modulus/stiffness) (Mosler et al., 1985). Below 4% strain the tendon retains its elastic properties and returns to its original length when unloaded (Sharma and Maffulli, 2005). Beyond 8-10% strain macroscopic failure occurs (O'Brien, 1992, Butler et al., 1978, Kastelic and Baer, 1980).

The Enthesis

Tendon and bone demonstrate different mechanical properties. Tendon has a tensile modulus of approximately 200 Megapascals (MPa) in the direction of muscular contraction but fails under compression (Thomopoulos et al., 2010). In contrast, cortical bone has a modulus of 20 Gigapascals (GPa) in both tension and compression making it relatively brittle and rigid compared to tendon (Thomopoulos et al., 2010). The attachment of a flexible material such as tendon to a stiff material such as bone is challenging. This has been overcome by the native enthesis, which is the anatomical region located between these two distinct structures.

The enthesis has two forms: direct and indirect (Woo and Buckwalter, 1988). Indirect entheses attach to the metaphysis and diaphysis of bone by merging with periosteum via the superficial layers of tendon, supported by deeper penetrating Sharpey's fibers anchoring it to the underlying bone. In contrast, a direct enthesis such as the rotator cuff inserts onto bone by a naturally graded fibrocartilaginous structure comprising

mineralised and demineralised tissue-types (Figure 1.3). The demineralised component resists compression within the distal tendon, and the mineralised component resists shearing across the bone surface (Benjamin et al., 1986).

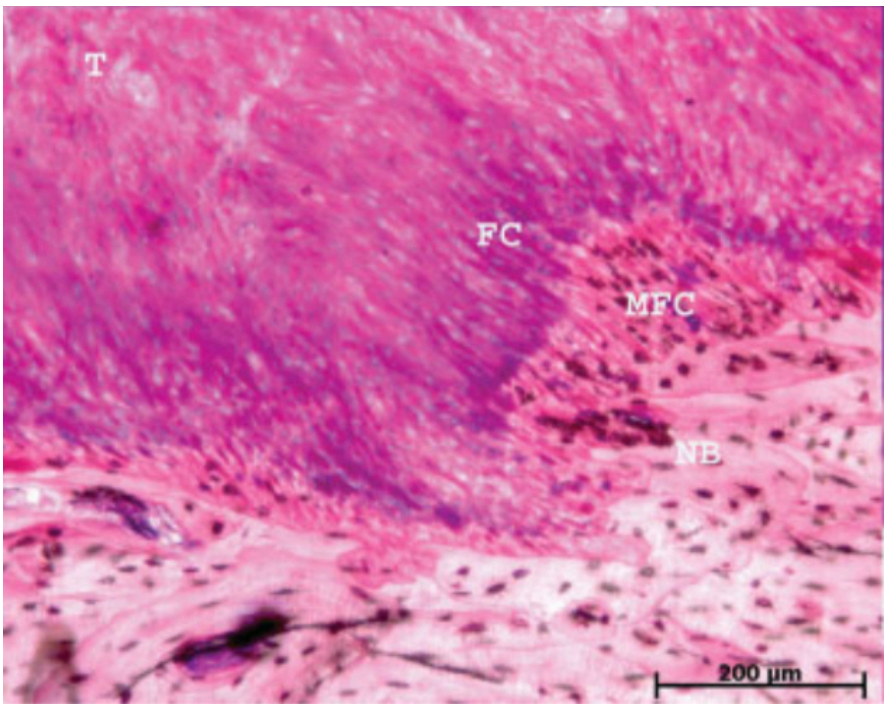

Figure 1.3: Morphology of the supraspinatus tendon-bone insertion site illustrating tendon (T), fibrocartilage (FC), mineralised fibrocartilage (MFC), and normal bone (NB).

The first zone is tendon proper, and consists of well-aligned type I collagen fibers and small quantities of decorin (Waggett et al., 1998, Woo SL, 2000). Zone two is the transitional region between tendon and bone. This is primarily composed of fibrocartilage, which is characterised by types II and III collagen, and small amounts of the proteoglycans aggrecan and decorin (Waggett et al., 1998, Thomopoulos et al., 2003, Kumagai et al., 1994, Fukuta et al., 1998, Sagarriga Visconti et al., 1996). The

third zone is mineralised fibrocartilage and corresponds to the gradual change to bony tissue. In this area, types II and X collagen predominate (Ralphs et al., 1998, Thomopoulos et al., 2003, Kumagai et al., 1994, Fukuta et al., 1998, Sagarriga Visconti et al., 1996). Bone is the final part of the enthesis and is made of type I collagen with a high mineral content.

Although the enthesis has been recognised to consist of several distinct tissue-types, there is evidence to suggest that there is a natural gradation along its length that is responsible for the effective distribution of forces. This encompasses a variation in collagen structure, ECM composition, mineral content, and viscoelastic properties (Thomopoulos et al., 2010).

1.4 The Rotator Cuff

Structure and Function

The muscles of the rotator cuff (subscapularis, supraspinatus, infraspinatus, and teres minor) play an important role in glenohumeral motion and stability (Escamilla et al., 2009). All four tendons fuse around the tuberosities of the humerus to form an insertion site that is made up of 'footprints,' corresponding to each muscle (Figure 4) (Curtis et al., 2006). Subscapularis is the largest musculotendinous unit of the rotator cuff and inserts onto the lesser tuberosity. It predominantly functions to internally rotate the shoulder and produces a maximum force of 1725 Newtons (N) at 90 ° of abduction (Escamilla et al., 2009, Hughes and An, 1996). Infraspinatus and teres minor constitute the posterior cuff (by way of their insertion on the greater tuberosity) and mediate external rotation, whilst exerting a postero-inferior force on the humeral head to resist antero-superior translation (Escamilla et al., 2009, Sharkey and Marder, 1995). Both muscles are strongest in 0 ° of abduction, with teres minor generating 159 N and infraspinatus generating 909 N (Hughes and An, 1996).

Supraspinatus inserts onto the greater tuberosity above infraspinatus, which occupies a larger cross-sectional area (Curtis et al., 2006). In a study examining the tendon of supraspinatus, the anterior portion resembled a tendinous band whereas the posterior portion was thin and membranous. These anatomical variations contribute to the greater strength associated with the anterior part (Itoi et al., 1995). Supraspinatus is often regarded as an initiator of shoulder abduction, but it also provides weak

rotational movements. At 90 ° of abduction in the scapular plane it generates a peak force of 117 N (Figure 1.4) (Curtis et al., 2006, Hughes and An, 1996).

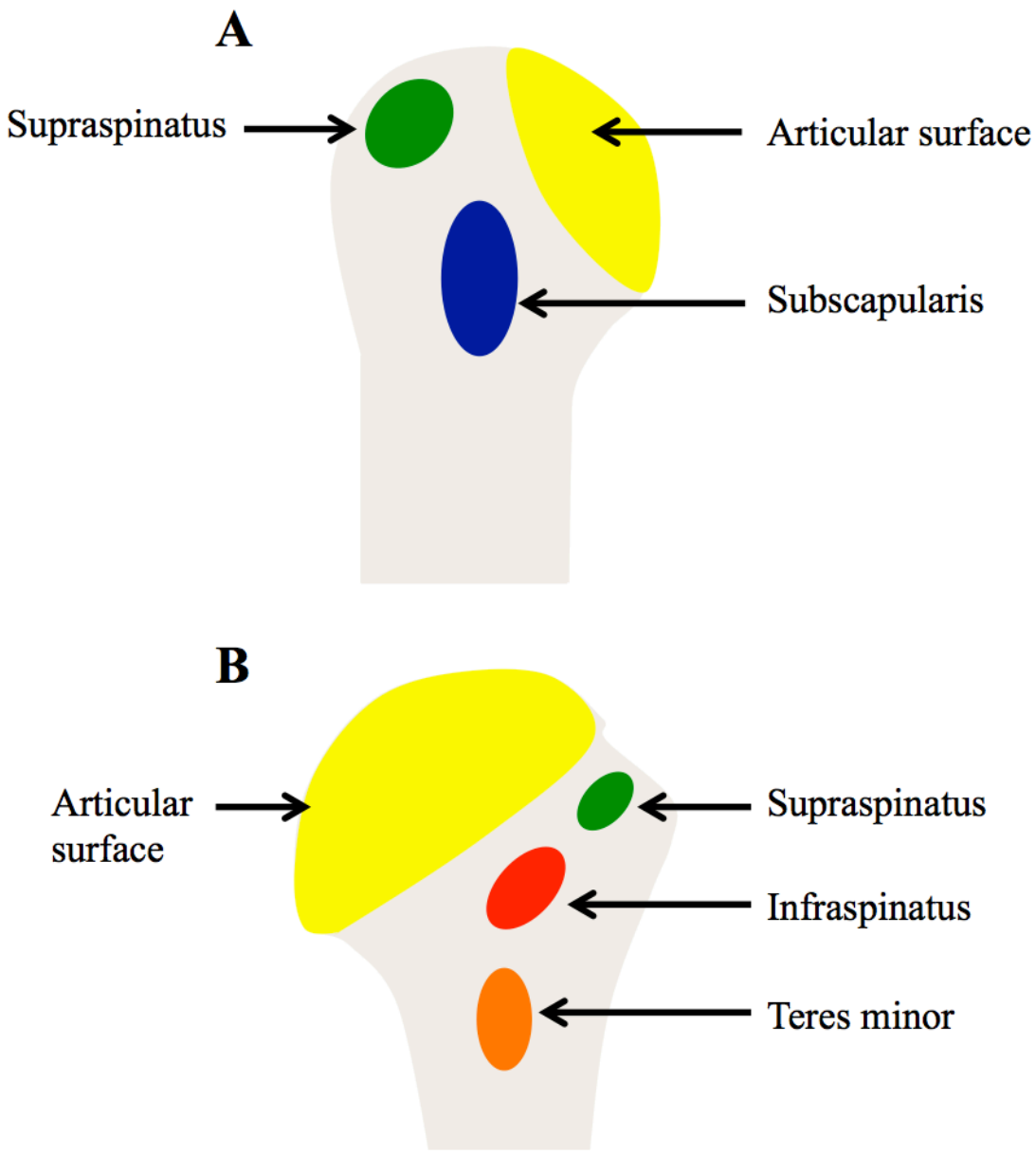

Figure 1.4: Anterior (A) and posterior (B) views of the right humeral head showing attachments of subscapularis (blue), supraspinatus (green), infraspinatus (red), and teres minor (orange). The yellow area denotes the articular surface.

Considerable inter-digitation exists between tendon fibers making it difficult to identify specific insertion points (Curtis et al., 2006). This tendinous portion is confluent with the capsule of the shoulder joint, the coracohumeral ligament, and the glenohumeral ligaments. The rotator cuff is therefore divided into five histological layers with the orientation of the tendon fascicles varying according to depth. This allows it to resist tensile forces throughout all planes of glenohumeral motion (Figure 1.5) (Clark and Harryman, 1992).

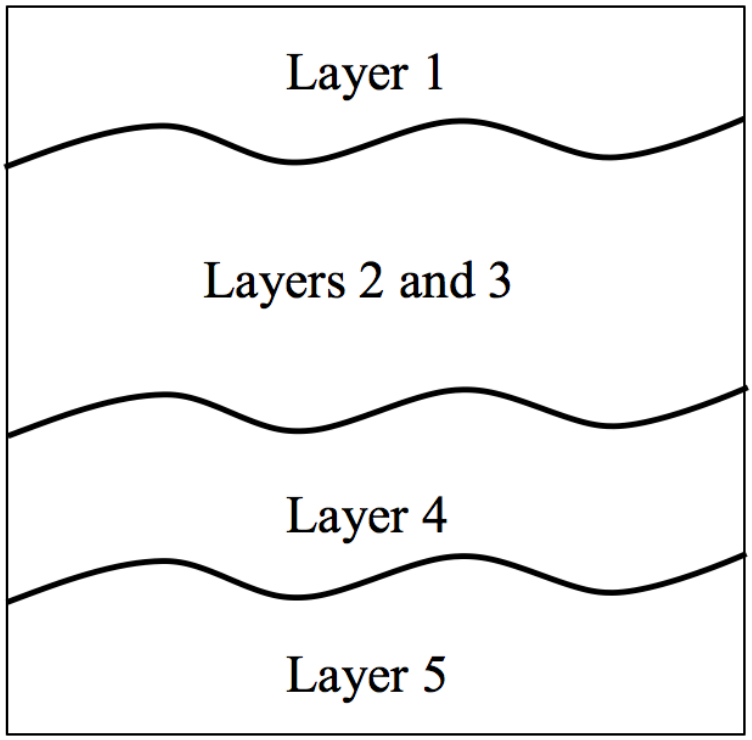

Figure 1.5: The five layers of the rotator cuff. Layers 1 and 4 contain fibers from the coraco-humeral ligament. Layers 2 and 3 demonstrate a predominance of fibers that course medial to lateral. Layer 5 is the glenohumeral joint capsule.

From the glenohumeral joint the superior aspect of the rotator cuff resembles a capsular thickening (rotator cable) surrounding, and protecting, a thinner portion of tissue (the crescent region) inserting onto the greater tuberosity (Burkhart et al., 1993) (Figure 1.6). The rotator crescent comprises the distal portions of the supraspinatus and infraspinatus tendon insertions, located within the 'critical (watershed) zone' of avascularity. This makes it vulnerable to tendinopathy and eventual tearing (Karthikeyan et al., 2015, Burkhart et al., 1993).

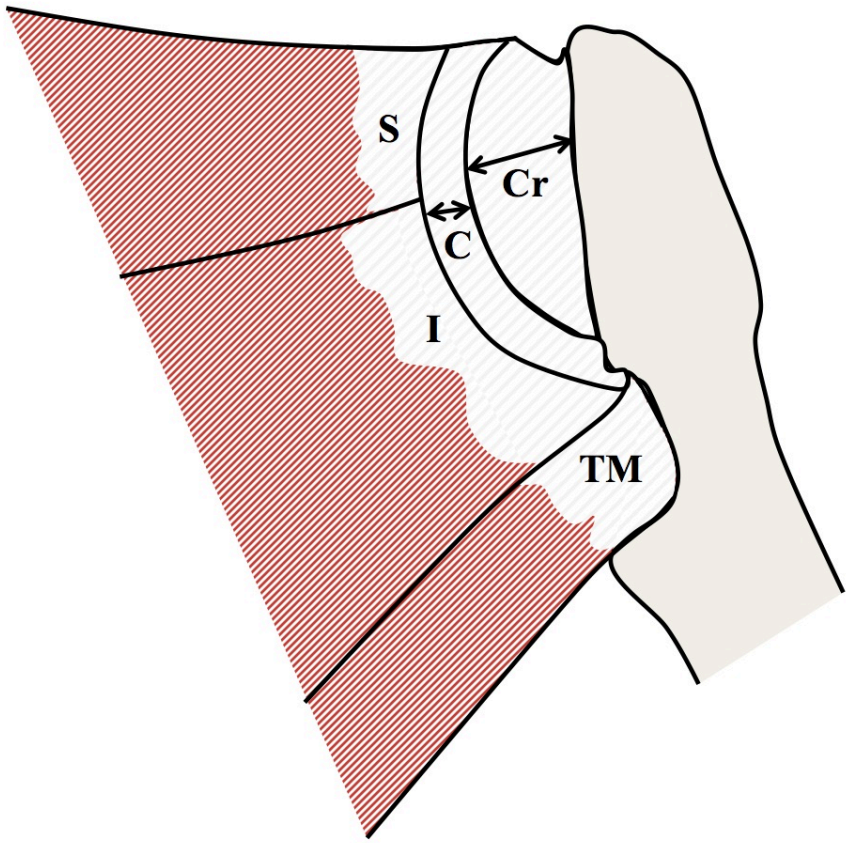

Figure 1.6: Posterior aspect of the rotator cable and crescent in a right shoulder. Rotator cable (C), mediolateral diameter of rotator crescent (Cr), supraspinatus (S), infraspinatus (I), and teres minor (TM).

Types of Rotator Cuff Tear

1.1.1.1. Acute vs Chronic Tears

Less than 10% of rotator cuff tears occur as a result of acute trauma. The majority are degenerative in nature (Loew et al., 2015, Bassett and Cofield, 1983). In patients less than 40 years only a forceful injury, such as a shoulder dislocation, is capable of tearing the rotator cuff tendon (Loew et al., 2015). Alternatively, in the elderly population minor traumatic events may exacerbate long-standing degenerative changes to result in a tear (acute-on-chronic tear) (Loew et al., 2015). Distinguishing between these two entities is crucial since the results of surgery are superior in traumatic tears (Braune et al., 2003). Indicators of acute tears include muscle oedema and 'kinking' of the proximal tendon, in contrast to chronic injuries that are characterised by advanced atrophy, loss of cellularity, loss of vascularity, loss of fibrocartilage at the enthesis, fatty infiltration, calcification, and degeneration of the muscle (Loew et al., 2015, Nho et al., 2008). Fatty infiltration can be graded on magnetic resonance imaging (MRI) according to the classification proposed by Goutallier et al (1994): Grade 0 – normal muscle, Grade 1 – some fatty streaks, Grade 2 – more muscle than fat, Grade 3 – equal amounts of fat and muscle, and Grade 4 – more fat than muscle.

1.1.1.2. Full Thickness vs Partial Thickness Tears

Several rotator cuff tear classification systems have been proposed in the literature (Patte, 1990, DeOrio and Cofield, 1984, Harryman et al., 1991, Wolfgang, 1974). Many of these were derived from the simple concept that tears maybe either partial or full-thickness. Partial thickness tears typically begin approximately 13 to 15 millimeters (mm) posterior to the biceps tendon, near the junction of the supraspinatus and infraspinatus tendons, and exhibit a low rate of progression (Maman et al., 2009, Kim et al., 2010). Full-thickness tears allow communication between the glenohumeral joint and subacromial-subdeltoid bursa and are considered 'massive' when they are greater than 5 cm in the largest diameter and involve at least two tendons (Chang and Chung, 2014, Pill et al., 2012).

The difficulty with having so many categories of tear is that agreement between clinicians may vary thus defeating the main objective of any classification system, which is to guide treatment. Kuhn et al (Kuhn et al., 2007) examined several classifications systems for partial and full-thickness rotator cuff tears to assess inter-observer variation and inter-observer agreement. With the exception of distinguishing partial-thickness from full-thickness tears and identifying the side (articular vs bursal vs intratendinous) of involvement with partial-thickness tears, other methods of categorising tears had little inter-observer agreement. For full-thickness tears, the degree of retraction in the frontal plane was found to be the most reliable: Stage 1: close to the bony insertion, stage II: at the level of the humeral head, or stage III: at the level of the glenoid (Figure 1.7) (Patte, 1990).

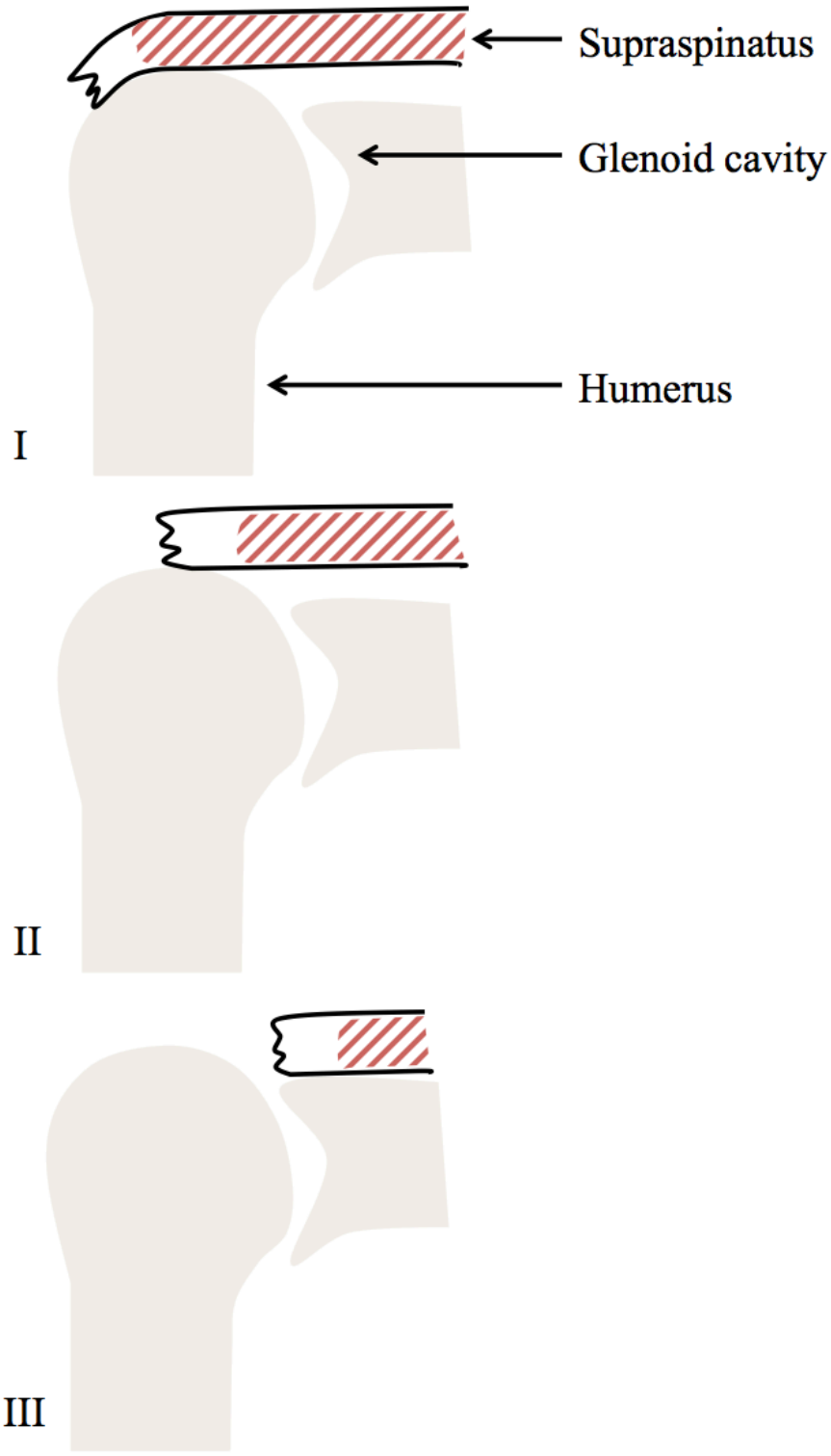

Figure 1.7: Grading rotator cuff tears according to the level of retraction in the frontal plane. Stage 1: close to the bony insertion, stage II: at the level of the humeral head, or stage III: at the level of the glenoid.

Rotator Cuff Healing

Healing of the rotator cuff takes place in three stages (inflammation, proliferation, and remodeling):

1. Inflammation

Immediately following injury, bleeding within the tendon produces a haematoma. This activates several chemotactic factors that recruit inflammatory cells from surrounding tissue to remove tissue debris by phagocytosis. Fibroblasts enter the area and synthesise various components of the ECM, and angiogenic proteins promote the formation of a vascular network (Lindsay and Birch, 1964).

2. Proliferation

Recruitment of fibroblasts continues and their rapid proliferation is responsible for the deposition of type III collagen to form callus. Once this collagen-rich ECM has been laid down it is remodeled, causing scar contraction. The resultant tissue has a higher ratio of type III collagen to type I collagen, a property that renders it weaker and more prone to re-rupture (Galatz et al., 2007, Gao et al., 1996, Bedi et al., 2012, Isaac et al., 2012, Rodeo et al., 1993). One factor that may contribute to the formation of this scar tissue is the mechanical strain during the initial phases of healing. At birth, the rotator cuff tendon is attached to the perichondrium of the cartilaginous humeral head by an attachment that bears no histological resemblance to the adult insertion site. This changes first at seven days post-natally where a fibrocartilaginous bridge is seen and

then at 56 days postnatal where the typical four zones of the enthesis are visible. Since the mechanical environment changes substantially following birth, it is plausible that this loading of the cuff is the primary agonist for change (Galatz et al., 2007). Furthermore, studies have indicated that compressive forces lead to the production of proteins associated with fibrocartilage (e.g. aggrecan) and tensile forces lead to the production of proteins associated with tendon (e.g. type I collagen) (Evanko and Vogel, 1990, Vogel et al., 1994). Other factors contributing to a poor healing response include an inadequate population of undifferentiated stem cells at the healing tendon-bone interface, the presence of macrophages at the site of tissue injury, and insufficient bony ingrowth into the tendon (Bedi et al., 2012, Kovacevic and Rodeo, 2008).

3. Remodeling

Remodeling begins six to eight weeks after injury and is characterised by a decrease in cellularity, reduction in matrix synthesis, decrease in type III collagen, and an increase in type I collagen. Type I collagen fibers align parallel to the mechanical axis of the tendon and interact with one another to result in an improvement in tensile strength, albeit less than the native uninjured tendon (James et al., 2008).

Factors Affecting Rotator Cuff Healing

Healing of the rotator cuff is associated with an improvement in function (Carr et al., 2015a, Mihata et al., 2011). It is affected by both patient and surgical factors, which if optimised, may result in better outcomes (Mall et al., 2014).

1.1.1.3. Surgical Factors

Rotator cuff repairs can be undertaken using either arthroscopic or open surgery. For many years there has been conflicting evidence as to which is the most effective method. Arthroscopic surgery causes less damage to surrounding soft tissues such as the deltoid, and has the theoretical advantage of causing less postoperative pain while permitting earlier mobilisation. This comes at the expense of longer surgical time and the use of expensive equipment. A recent randomised controlled trial evaluated the effectiveness of these two techniques and determined that in patients over the age of 50 years with a degenerative tear, there was no difference in functional outcome or cost. Healed repairs gave the best outcome followed by a repair that subsequently re-tore (Carr et al., 2015a).

Tendon-bone fixation is often achieved using suture anchors (Figure 1.8). Failure of this mechanism has been noted to occur at the suture-tendon interface, suture anchor-bone interface, or within the suture material itself (Kim et al., 2006). During rotator cuff repair, suture anchors can be place in either a single or double-row. Double-row repairs have the perceived advantage of increasing compression of the tendon against its bony footprint, but are associated with increased costs and surgical time. Mimata et

al (Mimata et al., 2015) reviewed 206 shoulders in 201 patients with full-thickness rotator cuff tears that underwent arthroscopic rotator cuff repair. Retear rates were 10.8%, 26.1%, and 4.7% for single-row, double-row, and compression double-row techniques respectively. In a randomised controlled trial Franceschi et al (Franceschi et al., 2016) demonstrated a significantly lower full-thickness retear rate for patients who underwent a double-row repair compared to those that had a single-row repair (8% vs 24% respectively). Other surgical factors that affect healing of the rotator cuff include location of the knot used to repair the tendon, the use of knotless repairs, the material of suture anchor, and postoperative rehabilitation (early vs delayed motion) (Mall et al., 2014).

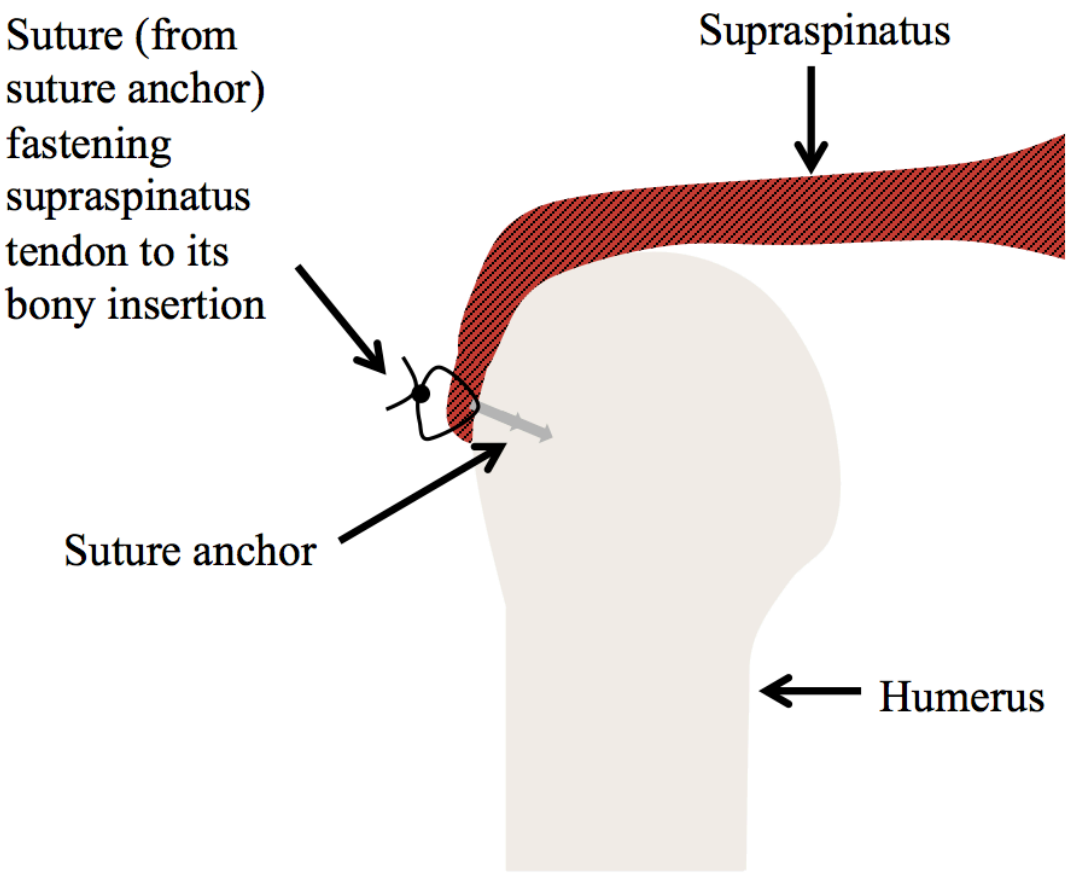

Figure 1.8: Supraspinatus tendon-bone fixation using a suture anchor.

1.1.1.4. Patient Factors

Despite optimising surgical techniques some rotator cuff repairs still fail to heal (Mall et al., 2014). Several studies have demonstrated an age difference in healing rates after surgery (Boileau et al., 2005, Charousset et al., 2010, Cho and Rhee, 2009). Yamaguchi et al (Yamaguchi et al., 2006) undertook an observational study of 588 consecutive patients with shoulder pain and found that the average age was 49 years for patients with no rotator cuff tear, 59 years for those with a unilateral tear, and 68 years for those with a bilateral tear. In a large cohort study of 272 patients who

underwent arthroscopic rotator cuff repair the failure rate was significantly higher in older patients although this was not a consistent finding on multivariate analysis, which identified bone mineral density, fatty infiltration of the infraspinatus, and the amount of tear retraction at the time of surgery as the only independent predictors of healing (Chung et al., 2011).

Tear characteristics influence rotator cuff healing with larger tears and those involving multiple tendons exhibiting the highest failure rates (Mihata et al., 2011, Charousset et al., 2010, Nho et al., 2009, Tashjian et al., 2010). Tissue quality also plays an important role with fatty infiltration and degenerative changes contributing the most to poor healing (Nho et al., 2009, Pedowitz et al., 2012, Chung et al., 2011).

Osteopenia in the greater tuberosity is a common finding in patients with rotator cuff tears due to the loss of physical stimuli at the enthesis (Cadet et al., 2008, Postl et al., 2013, Waldorff et al., 2011). This reduces the pull-out strength of suture anchors and therefore the quality of tendon fixation (Braunstein et al., 2015). Accordingly, bone mineral density has been identified as an independent risk factor for rotator cuff healing (Chung et al., 2011).

1.5 Diagnosing Rotator Cuff Tears

1.5.1 Clinical Presentation

Rotator cuff tears present in three clinical settings: acute traumatic, acute-on-chronic, and chronic atraumatic (Green, 2003). Pain radiating down the arm (due to involvement of the subdeltoid and subacromial bursae), stiffness, and weakness of the arm are the most commonly reported symptoms and suggest tendon degeneration when present before an injury (Wolff et al., 2006, Iannotti, 1994). Pain typically occurs during overhead activities (in a 'painful arc' of movement) or at night, and is more severe in partial-thickness tears (Fukuda, 2000). Chronic tears present with insidious symptoms and are often associated with preserved range of motion due to compensatory deltoid muscle strength (Green, 2003).

Some rotator cuff tears may be asymptomatic but approximately 50% of these become painful within three years (Yamaguchi et al., 2001). While this may indicate tear extension in some cases, in others, pain can develop without tear extension and tear extension can develop without pain (Yamaguchi et al., 2001, Dunn et al., 2014). The importance of pain in decision-making has yet to be determined, particularly since psychosocial factors have been demonstrated to play a more important role in patient-reported pain and function than tear severity (Wylie et al., 2016).

A detailed physical examination is crucial to accurately evaluate the rotator cuff. Both shoulders and scapulae must be exposed. Swelling and bruising may be present in acute tears, whereas muscle atrophy is a more common feature of chronic injuries.

Active and passive range of movement should be examined. A ‘painful arc’ of movement indicating impingement may be present during passive motion, and should be further evaluated with provocative maneuvers such as the Hawkins-Kennedy test. In this, a positive impingement sign is denoted by pain in the subacromial space when the arm is passively internally rotated in 90° of forward elevation and 90° of elbow flexion (Hawkins and Kennedy, 1980). Strength is often preserved with small tears but weakness is often present with larger tears. Approximately 95% of rotator cuff tears involve supraspinatus and consequently lead to weakness in abduction and elevation of the arm (Dunn et al., 2014). This can be assessed using the ‘empty can test’ (Jobe test) where shoulder abduction is resisted in internal rotation (Hughes et al., 2008).

Findings consistent with a chronic massive rotator cuff tear include antero-superior subluxation of the humeral head, infraspinatus muscle atrophy, external rotation weakness (due to infraspinatus involvement), and rupture of the proximal part of the tendon of the long head of biceps (Green, 2003). Specific attention should be given to tears of the subscapularis, as these may be under-diagnosed. Subscapularis involvement occurs in less than 10% of cases and can be associated with weakness of internal rotation and excessive passive external rotation (Gerber and Krushell, 1991, Dunn et al., 2014).

1.5.2 Radiographic Evaluation

1.5.2.1 Plain Radiographs

Several imaging modalities can be used to assist in the diagnosis of rotator cuff tears. Plain radiographs are often taken when a patient presents to a health-care provider (General Practitioner, surgeon, or other health professional) with shoulder pain and should involve two views: antero-posterior and axillary. Bony anatomy can be evaluated for arthritis (rotator cuff arthropathy) and acromiohumeral distance. The latter is defined as the distance between the acromion and the humeral head and is consistent with chronic rotator cuff pathology when less than 7 mm (Green, 2003). Specialised projections, such as when the X-Ray beam is directed 10° caudally, can examine acromial morphology (flat, curved, or hooked) and identify acromial spurs (Iannotti, 1994).

1.5.2.2 Ultrasonography

Ultrasonography is a noninvasive, cost-effective tool that can be utilised as an initial screening study to determine the size and level of retraction of a tear (Crass et al., 1984, Mack et al., 1988). Sensitivity and specificity of ultrasound has been reported to be as high as 94% and 93% respectively but its accuracy is highly dependent upon the operator and can be enhanced by obtaining dynamic images through the range of shoulder motion (Green, 2003, Brenneke and Morgan, 1992, Wiener and Seitz, 1993).

1.5.2.3 Magnetic Resonance Imaging

MRI provides a comprehensive assessment of the rotator cuff and has the advantage of being able to measure the size of a tear, the magnitude of tendon retraction, the extent of fatty infiltration, and the degree of muscle atrophy (Iannotti, 1994, Green, 2003, Iannotti et al., 1991). MRI is similar to ultrasonography in its ability to estimate the size of a rotator cuff tear but it is a more useful preoperative investigation because it can define other associated pathology such as arthritis and rupture of the long head of the biceps tendon (Bryant et al., 2002, Iannotti et al., 2005, Teefey et al., 2004).

1.5.2.4 Arthrography

Arthrography is an imaging technique in which a radio-opaque contrast in injected into the shoulder joint. It has been reported to have an accuracy of greater than 95% in the diagnosis of full-thickness rotator cuff tears but it is limited in its ability to estimate the size of a tear and to identify a partial-thickness tear (Mink et al., 1985).

1.6 Treatment of Rotator Cuff Tears

In the United States more than 300,000 rotator cuff repairs are performed annually (Colvin et al., 2012). Quantifying the risk and rate of tear progression is fundamental to formulating appropriate indications for surgery. In a long-term prospective study of 224 patients with an asymptomatic rotator cuff tear (118 initial full-thickness tears, 56 initial partial-thickness tears, and 50 controls) in one shoulder and pain due to rotator cuff disease in the contralateral shoulder, tear enlargement was observed in 49% of cases within 2.8 years. This was related to the magnitude of the initial tear, with a greater proportion of full-thickness tears increasing in size when compared to partial-thickness tears (61% vs 41%). Tear enlargement was significantly associated with ongoing degeneration and the onset of new pain (Keener et al., 2015).

Without repair, the rotator cuff has limited capacity to heal; yet conservative treatment often yields a satisfactory outcome (Kukkonen et al., 2015, Lambers Heerspink et al., 2015, Yamaguchi et al., 2001). The main drawbacks of a non-operative approach are tear progression, ongoing pain, and deterioration in function over time. These problems are still a concern following surgery, particularly retears. These most frequently occur between six and 26 weeks postoperatively and have been noted to occur in up to 94% of cases (Galatz et al., 2004, Iannotti et al., 2013).

Optimal treatment of symptomatic, non-traumatic (degenerative) rotator cuff tears is unknown. In a randomised controlled-trial of 160 patients over the age of 55 years with symptomatic, non-traumatic rotator cuff tears there were no significant differences in function between surgery and conservative treatment at two years

follow-up. Surgery was associated with a significantly smaller tear size and increased costs. Long-term monitoring of tear progression and its effect on function was not undertaken (Kukkonen et al., 2015). In a similar trial comparing the results of surgery and non-operative treatment for degenerative rotator cuff tears in patients over 60 years, no significant difference was observed in functional outcome at short-term follow-up (12 months). Surgery did yield a significant improvement in pain, but retears were still reported in 73% of cases (Lambers Heerspink et al., 2015). In order to determine whether this difference in conservative and surgical treatment was maintained in the medium-term, Moosmayer et al (Moosmayer et al., 2014) compared the outcome of patients with small and medium-sized tears treated with either primary tendon repair or, physiotherapy and optional secondary repair. Degenerative and acute cases were included for study and participants were followed-up for five years. Twelve patients (24%) initially randomised to have physiotherapy underwent surgery. At five years, 14 tears (38%) treated with physiotherapy alone increased in size, and this was associated with an inferior outcome. The retear rate in the surgical cohort was 25%. Overall, a better outcome was associated with repaired tears.

Treatment of massive rotator cuff tears poses a considerable challenge to current management strategies. The prevalence of massive tears has been reported to be as high as 40% of all tears and the rate of retears following surgery is recognised to be higher than for smaller tears (Bedi et al., 2010, Galatz et al., 2004). Shoulders with massive tears involving the postero-superior cuff demonstrate weakness in active external rotation and increase in passive internal rotation, whereas tears involving the antero-superior cuff lead to weakness in active internal rotation and increased passive external rotation (Giphart et al., 2013). Large retracted tears have been shown to

cause traction on the suprascapular nerve thereby propagating atrophy and fatty infiltration of the supraspinatus and infraspinatus through disuse (Costouros et al., 2007, Mallon et al., 2006, Shi et al., 2014).

To restore normal glenohumeral kinematics several surgical strategies have been introduced: debridement with biceps tenotomy (detachment of the tendon)/tenodesis (detachment of the tendon and subsequent re-fixation to surrounding bone/soft tissue), complete repair, partial repair, biological augmentations using scaffolds, superior capsular reconstruction, muscle-tendon transfer, and reverse anatomy total shoulder arthroplasty (Greenspoon et al., 2015). Failure to heal and retears are still common and therefore further work is required to develop new strategies and to improve existing ones (Chung et al., 2013, Zumstein et al., 2008).

1.7 Tissue Engineering Strategies for Rotator Cuff Tears

Scaffolds

Scaffolds have emerged as a potential solution to the problems (high retear rate and failure to heal) associated with surgical repair of the rotator cuff. They currently exist in three main forms: Xenografts (tissue taken from a donor of one species and transplanted into a recipient belonging to another species), allografts, and synthetic matrices.

1.1.1.5. Xenografts

Adverse immune reactions are the main concern with using xenografts in the clinical setting. In order to avoid these, decellularisation is carried out using gamma irradiation or physical, chemical, or enzymatic techniques. Physical methods entail freezing or mechanical agitation to lyse native cells whereas chemical-based strategies use hypotonic solutions or detergents to lyse the cells in the harvested tissue, which is then washed to remove them. Trypsin, an enzyme that hydrolyses proteins, is found in the digestive system of vertebrates. When used as a single agent it is capable of degrading cellular material within a matrix, but its effect can been enhanced when used in combination with gamma irradiation (Cheung et al., 2010, Fini et al., 2012).

Porcine small intestinal submucosa contains type I collagen and growth factors such as fibroblast growth factor (FGF)-2, transforming growth factor (TGF)-β and vascular

endothelial growth factor (VEGF) (Badylak et al., 1998, McPherson et al., 2000). Clinical studies evaluating the efficacy of porcine xenografts to augment rotator cuff repairs have shown variable results. In one of the few randomised controlled trials investigating rotator cuff healing with a xenograft, Iannotti et al (Iannotti et al., 2006) treated 15 shoulders with porcine small intestinal mucosa (Restore Orthobiologic Implant; DePuy, Warsaw, Indiana) and compared them to 15 non-augmented open repairs. No significant improvement in healing or functional outcome was found.

Phipatanakul and Petersen (Phipatanakul and Petersen, 2009) used porcine small intestinal mucosa to augment the repair of massive rotator cuff tears. Despite an improvement in functional outcome scores only 44% of repairs were partially or completely intact postoperatively. Furthermore, three complications occurred including one infection and two skin reactions. Poor results were additionally reported by Walton et al (Walton et al., 2007) who found that patients whose rotator cuffs were repaired using the Restore Orthobiologic Implant (DePuy, Warsaw, Indiana), a collagen-based material derived from the small intestinal mucosa of pigs, had decreased muscle strength, greater impingement in external rotation, slower rate of pain resolution, and reduced participation in sport. Two years postoperatively MRI demonstrated comparable retear rates between the study group and non-augmented controls. Due to the high number of severe inflammatory reactions that required further surgery, use of this material was discouraged.

The current body of evidence suggests that xenografts do not appear to enhance rotator cuff repair in humans, with retear rates similar to non-augmented controls (Iannotti et al., 2006, Walton et al., 2007). Major concerns have been raised over their

immunogenic potential and severe inflammatory reactions (Malcarney et al., 2005, Zheng et al., 2005). This could be due to traces of deoxyribonucleic acid (DNA) and TGF-β remaining in the graft material despite thorough decellularisation. Another less commonly found cell-associated marker responsible for hyper-acute rejection of porcine xenografts is Galactose-alpha-1,3-galactose (α -Gal). The α-Gal epitope is synthesised on glycolipids and glycoproteins present in non-primate mammals by the glycosylation enzyme alpha 1,3-galactosyltransferase. This epitope is not present in humans, who instead have the anti-Gal antibody, which constitutes approximately 1% of circulating immunoglobulins and specifically targets α -Gal (Zheng et al., 2005, McDevitt et al., 2003, Mathapati et al., 2011).

1.1.1.6. Allografts

Allogenic matrices are produced by the decellularisation of cadaveric material from humans and are capable of bridging soft tissue defects whilst reducing the risk of graft rejection. Bond et al (Bond et al., 2008) reviewed the outcome of 16 patients with massive, contracted, immobile rotator cuff tears that were treated with arthroscopic placement of a GraftJacket allograft (acellular human dermal matrix) (Wright Medical Technology, Arlington, TN). This yielded a failure rate of 19%, which is considerably lower than the 30-94% quoted in the literature (Isaac et al., 2012). No complications were noted and follow-up analysis of the graft at 12 months illustrated its viability. Furthermore, in one of the patients who had a documented failure, a biopsy revealed partial neo-tendon formation at the site of graft insertion. Histological analysis of the remaining specimens was not undertaken and therefore the extent of any tendon remodeling remains unknown. Barber et al (Barber et al., 2012) further assessed the

effectiveness of the GraftJacket in a randomised, prospective, multicenter clinical study of 42 patients undergoing arthroscopic repair of large (> 3cm) rotator cuff tears. At 24 months follow-up, using the American Shoulder and Elbow Surgeons (ASES) and Constant scores, superior functional outcomes were noted in the augmented group compared to non-augmented controls. Significantly more intact repairs were also found in the GraftJacket group using enhanced MRI and no adverse reactions related to the graft were observed.

Although the results of acellular dermal matrices are promising there have been no large human studies conducted evaluating their effectiveness. Bony ingrowth into a healing tendon is essential for regeneration of a functional enthesis, but little sign of bone integration is seen with current allografts (Bedi et al., 2012). Despite no serious complications being reported there have been concerns over the presence of residual DNA that may cause an inflammatory response and increase tendon degeneration (Gilbert et al., 2009, Zheng et al., 2005).

1.1.1.7. Synthetic Grafts

Degradable polyesters such as poly (lactic-co-glycolic) acid (PLGA), poly-L-lactic acid (PLLA) and polydioxanone (PDO) have emerged as potential biomaterials (Hakimi et al., 2013). Upon their initial conception rapidly absorbable sheets of polyglycolyic acid (PGA) were used to regenerate the enthesis however they displayed poor mechanical properties and created a tendon insertion comprised primarily of type III collagen (Yokoya et al., 2008).

Few human studies examining the effect of synthetic scaffolds on regeneration of the enthesis have been conducted. In a non-randomised retrospective three-year follow-up study, Ciampi et al (Ciampi et al., 2014) compared the results of mini-open repair of postero-superior massive rotator cuff tears between non-augmented controls, augmentation with an absorbable collagen patch, and augmentation with a synthetic non-absorbable polypropylene patch. The polypropylene patch performed the best, exhibiting a significantly lower 12-month retear rate and superior functional outcome (using the University of California, Los Angeles shoulder rating scale), abduction and elevation at 36-months. No adverse reactions were related to patch application. Proctor (Proctor, 2014) evaluated the functional results of 18 consecutive patients with large to massive rotator cuff tears treated with a woven mesh of absorbable PLLA (X-Repair; Synthasome Inc., San Diego, CA, USA). A combination of ultrasound and MRI showed that 83% of patients had intact repairs 12 months following surgery. At 42 months one additional failure occurred, which reduced long-term survival to 78%. There was a progressive improvement in functional outcome in the cuff repair-'survivor' group, assessed by the ASES scoring system, at all time points.

Although many studies investigating synthetic scaffolds have yielded encouraging results there are several concerns over the degradation products of the polymers used to produce them. High levels of lactic and glycolic acid have been shown to impair osteoblast proliferation and inhibit matrix mineralisation whereas in non-toxic concentrations they were found to decrease cellular proliferation and increase differentiation of osteoblasts (Meyer et al., 2012b). These toxic effects have been shown to vary between polymers and thus further research is required to ensure that

the liberation of these degradation-products remains within safe levels for the duration that the implant is in situ (Taylor et al., 1994).

Mesenchymal Stem Cells

MSCs are multipotent stromal cells derived from mesenchymal tissue that have the capacity to self-renew and differentiate into cells capable of producing bone, fat, muscle, and tendon (Castro-Malaspina et al., 1980). Stem cells can be sourced from bone marrow, adipose tissue, muscle, synovia, periosteum, tendon, dermis, and umbilical cord but their numbers decline with age (Nixon et al., 2012). Techniques to optimise the proportion of stem cells isolated from bone marrow include using a Ficoll-induced density gradient and flow cytometry (Kastrinaki et al., 2008).

1.1.9.1 Mesenchymal Stem Cell Characterisation

MSCs are frequently isolated from the mononuclear layer of bone marrow and can be expanded *in vitro* following separation by a density gradient (Hernigou et al., 2005). Cells produced in this manner are spindle-shaped and adhere to plastic flasks (features commonly observed in MSCs) but further characterisation is often necessary because of the lack of a single cell surface marker present ubiquitously on MSCs (Chamberlain et al., 2007). The Mesenchymal and Tissue Stem Cell Committee within the International Society for Cellular Therapy proposed criteria to define MSCs within a cell population: (1) plastic adherence *in vitro*; (2) positive expression of CD105, CD90, and CD73 in greater than 95% of cells in the culture and negative expression of CD34, CD45, CD14 or CD11b, CD79a or CD19, and HLA-DR; (3) the

capacity to tri-differentiate into chondrocytes, adipocytes, and osteoblasts (Dominici et al., 2006).

Human MSCs express on their surface CD105 (SH2), CD73 (SH3/4), CD44, CD90 (Thy-1), CD71, and Stro-1, while lacking the expression of CD45, CD34, CD14, or CD11 hematopoietic markers (Haynesworth et al., 1992, Galmiche et al., 1993, Pittenger et al., 1999, Conget and Minguell, 1999, Sordi et al., 2005, Le Blanc et al., 2003a). By negatively and positively selecting these markers antibodies can identify MSCs within a mixed cell population (Baddoo et al., 2003, Jones et al., 2002, Gindraux et al., 2007). Another method that can be used is to evaluate the capacity of cells to tri-differentiate into bone, fat, and cartilage (Chamberlain et al., 2007).

Osteoblastic differentiation is accomplished by incubating a confluent layer of MSCs with ascorbic acid, β-glycerophosphate, and dexamethasone for two-to-three weeks. MSCs express alkaline phosphatase and produce calcium deposits that can be stained with Alizarin Red (Pittenger et al., 1999). Culturing MSCs with dexamethasone, insulin, isobutyl methyl xanthine, and indomethacin can induce adipogenic differentiation by causing the accumulation of lipid-rich vacuoles within cells. These can be positively stained by Oil Red O (Pittenger et al., 1999). To induce chondrogenic differentiation, MSCs are centrifuged in order to form a cell pellet. Culturing this with TGF-β will cause the production of type II collagen (a typical marker of articular cartilage) that can be positively stained with toluidine blue (Pittenger et al., 1999, Kopen et al., 1999).

1.1.9.2 Therapeutic Mechanisms of Mesenchymal Stem Cells

Several functions of MSCs highlight their ability to enhance tendon-bone healing: migration to sites of tissue damage, differentiation potential, growth factor production, and immunosuppression (Wei et al., 2013). Together, these limit degeneration and ongoing degradation associated with tendon fiber rupture (Caplan, 2007, Caplan and Dennis, 2006, Wagner et al., 2009).

1. Migration to sites of tissue damage

MSCs migrate to damaged/inflamed tissue from the circulation by adhering to and rolling on endothelial cells using adhesion molecules such as integrins and selectins (Chamberlain et al., 2007). This process is similar to leukocyte recruitment and is mediated by chemokines, adhesion molecules, and matrix metalloproteinases (MMPs) (Wynn et al., 2004, Belema-Bedada et al., 2008). Specifically, the chemokine (C-X-C motif) ligand 12- chemokine (C-X-C motif) receptors 4, 5, and 10 (CXCR4, CXCR5, and CXCR 10 respectively) have been demonstrated to enhance the engraftment and effect of MSCs (Von Luttichau et al., 2005, Cheng et al., 2008). However, these receptors are expressed to varying degrees on MSCs thus highlighting their heterogeneity (Chamberlain et al., 2007).

2. Production of growth factors

After MSCs enter damaged tissue they interact with local cytokines and produce growth factors critical to tissue regeneration (Crisostomo et al., 2008, Caplan and Dennis, 2006, Jing et al., 2011). These include VEGF, insulin-like growth factor 1 (IGF-1), and basic fibroblast growth factors (bFGFs) (Caplan and Dennis, 2006, Xu et al., 2007, Liu et al., 2011).

3. Immunosuppression

MSCs suppress the activity of B cells, T cells, macrophages, and natural killer cells (Uccelli et al., 2008, Han et al., 2012). By modulating the function of these inflammatory cells, MSCs are able to exert an immunosuppressive effect (Bartholomew et al., 2002). Reports suggest that this is achieved through direct cell-cell contact and/or the presence of chemokines (Di Nicola et al., 2002, Krampera et al., 2003, Le Blanc et al., 2003b). In tendon healing, the anti-inflammatory effect of MSCs has been shown to reduce tendon fiber degeneration (Nixon et al., 2008, Schnabel et al., 2009).

1.1.9.3 Mesenchymal Stem Cell use in Rotator Cuff Healing

MSCs are an appealing tissue-engineering strategy because they can differentiate into several cell types and possess a non-immunogenic phenotype making them suitable for allogenic transplantation without immunosuppression (Javazon et al., 2004). In rotator cuff tears the levels of MSCs at the enthesis decrease as a function of a

number of clinical factors such as tear size, time between the onset of a tear and treatment, and stage of fatty infiltration (Hernigou et al., 2015). The effects of MSCs on tendon-bone healing have been investigated in a number of animal studies with varying outcomes, ranging from an improvement in fibrocartilage and reduction in fatty infiltration, to no change in histology or mechanical properties of the resultant tissue (Gulotta et al., 2009, Gulotta et al., 2010, Gulotta et al., 2011a, Oh et al., 2014a).

Few human studies have investigated the role of MSCs in rotator cuff healing and there are currently no evidence-based guidelines outlining when they should be used (Hernigou et al., 2014, Ellera Gomes et al., 2012). Ellera Gomes et al (Ellera Gomes et al., 2012) reported the results of 14 patients who underwent mini-open repair of a rotator cuff tear using autologous bone marrow mononuclear cells. Tear characteristics included injury to three tendons with fatty infiltration grade II (Goutallier classification) or higher (five patients), injury to two tendons with fatty infiltration grade II or higher (eight patients), and injury to one tendon (one patient). The stem cell population was derived from bone marrow aspirates concentrated using a Ficoll density gradient. Subsequent flow cytometry analysis of this suspension revealed that it contained 3.81×10^8 mononuclear cells. After 12 months follow-up all tendons were intact and there was an improvement in functional outcome. Evidence from this series is limited due to the lack of a control group and the small heterogeneous sample.

In a case-controlled study, Hernigou et al (Hernigou et al., 2014) reviewed 45 patients that received concentrated bone marrow-derived MSCs as an adjunct to single-row

rotator cuff repair and compared them to a matched control group who did not receive MSCs. The concentration of MSCs (the number of connective-tissue progenitor cells per 1.0 cc of aspirate) and the prevalence of MSCs (the number of MSCs per million nucleated cells) were estimated by counting the number of colony forming unit fibroblasts. The average number of MSCs per milliliter (ml) of concentrated cells returned to the 45 patients was 4,300 + 1,00 per mL of bone marrow concentrate. The average total number of MSCs returned to the patient was 51,000 ± 25,000 cells in 12 mL of injected bone marrow concentrate. Only tears less than 3 cm were included for study. At six months, all repairs with MSCs had healed, in comparison to 30/45 repairs (67%) without MSCs. At 10 years, intact repairs were noted in 39/45 (87%) patients in the MSC group in contrast to 20/45 (44%) of the controls.

1.1.9.4 Mesenchymal Stem Cell Delivery into Tissues

When MSCs are applied to the enthesis it is imperative that they are localised and maintained in that area. Two strategies that have received considerable attention in the literature are the use of fibrin glue and scaffolds (Beitzel et al., 2014, Kalia et al., 2006, Lee et al., 2005). Fibrin glue, a combination of fibrinogen and thrombin, is a matrix whose principal component fibrin, has an integral role in blood clotting and wound healing (Kalia et al., 2006). It is potentially a suitable carrying media for cellular implantation as it has proven biocompatibility, biodegradability, and binding capacity to cells (Lee et al., 2005). A further advantage of fibrin glue is that it can be injected into a deep layer of tissue and remains confined to that area due to its high viscosity. To examine the use of MSCs in fibrin glue, Lee et al (Lee et al., 2005) used it to treat 1.5 mm rat femoral defects to determine whether it could induce new bone

formation in chemotherapy-treated rats. One hundred thousand cells were suspended in 1.0 mL of the thrombin component of the fibrin glue (Tisseel; Baxter BioScience, Newbury, UK) before mixing the thrombin and fibrin components. After the glue had set, culture medium was added and the cells were cultured. An alamarBlue (Biosource International/Invitrogen, Camarillo, CA) assay was performed to evaluate cell viability and cell proliferation was measured by [^{3}H]thymidine uptake. A cell proliferation assay was performed on cells after 24, 48, 72, and 96 hours in culture. The results of this indicated that cells remained viable up to 96 hours and there was no difference in the rate of proliferation at any time point, thus demonstrating the efficacy of fibrin glue as a potential carrier of MSCs.

As described above, scaffolds exist in different forms and maybe used as a mechanical graft to improve load distribution across the enthesis or as a biological strategy to enhance tissue regeneration. To successfully integrate into the scaffold cells must attach to the surface, proliferate, produce a matrix, and migrate into the deep structure (Beitzel et al., 2014). Beitzel et al (Beitzel et al., 2014) compared the response of human MSCs to several commercially available scaffolds and a control (rotator cuff tendon allograft). Scaffolds used in the study included human highly cross-linked collagen membrane (Arthroflex; LifeNet Health, Virginia Beach, VA), porcine non cross-linked collagen membrane (Mucograft; Geistlich Pharma, Lucerne, Switzerland), a human platelet-rich fibrin matrix (PRF-M), and a fibrin matrix based on platelet-rich plasma (ViscoGel; Arthrex, Naples, FL). Each material was seeded with MSCs and examined for cellular adhesion (24 hours), proliferation (thymidine assay at 96 hours), and viability (live/dead stain at 168 hours). Cellular adhesion and proliferation varied between the different materials with the non cross-linked porcine

collagen scaffold (Mucograft) demonstrating superior results, due to its highly porous structure permitting greater initial cell loading during seeding.

1.1.9.5 Enhancing Stem Cell Therapy

In vivo studies examining the effect of MSCs on enthesis regeneration have reported the absence of a fibrocartilaginous interface, citing the potential lack of signaling as a reason for the transplanted cells not differentiating and creating a naturally graded structure (Gulotta et al., 2009). Methods used to enhance stem cell activity include supplementary growth factors, mechanical stimulation, and scaffolds. Scaffolds are commonly used to carry stem cells (Rutledge et al., 2014, Shen et al., 2015). Their composition has been suggested to affect cell seeding and migration (Beitzel et al., 2014) but may also direct differentiation (Shen et al., 2015, Rutledge et al., 2014). These properties can be enhanced by mechanical stimulation but further studies are required to determine whether this strategy is effective for all materials (Juncosa-Melvin et al., 2007, Butler et al., 2008).

Membrane type 1 matrix metalloproteinase (MT1-MMP) is thought to regulate the formation of mineralised cartilage and thus bony ingrowth into the enthesis. Using an adenovirus to upregulate MSCs with its expression, Gulotta et al (Gulotta et al., 2010) repaired the supraspinatus tendon in rats using either MSCs in a fibrin glue carrier or the adenoviral membrane MT1-MMP (Ad-MT1-MMP)–transduced MSCs. At four weeks, the Ad-MT1-MMP group exhibited more fibrocartilage and superior biomechanical results than the MSC group. Using the same rat model of an acute supraspinatus tear, Gulotta et al (Gulotta et al., 2011a) repaired the tendon using

either MSCs in fibrin glue or adenoviral-mediated scleraxis-transduced MSCs. At four weeks, the adenoviral-mediated scleraxis-transduced MSCs produced more fibrocartilage and had better biomechanical results.

Other Non Cell-Based Strategies

During the initial phases of rotator cuff healing the activation of fibroblasts results in the expression of several growth factors including bone morphogenetic proteins (BMPs), bFGF, platelet-derived growth factor (PDGF), and TGF-β (Bedi et al., 2012). Wurgler-Hauri et al (Wurgler-Hauri et al., 2007) demonstrated that over an eight-week period the concentrations of these growth factors fluctuate before returning to normal, suggesting that administration of a single growth factor is unlikely to promote the formation of a normal enthesis. This has not been addressed by current augmentation strategies and may be partly responsible for their failure.

1.1.1.8. Bone Morphogenic Proteins

BMPs are part of the TGF-β superfamily and are recognised to stimulate bone formation (Isaac et al., 2012). This is an important stage in the formation of a naturally graded enthesis and has eluded many of the augmentation strategies used to date. BMP-12 and BMP-13 regulate fibrocartilage and neotendon formation whilst BMP-13 and BMP-14 increase the tensile strength of a regenerated tendon (Longo et al., 2011, Aspenberg and Forslund, 1999). In an ovine model of rotator cuff repair, BMP-12 resulted in superior biomechanical properties and greater collagen continuity at the healing interface (Seeherman et al., 2008). In contrast, a rat study of rotator cuff

repair did not find a difference in new cartilage formation or collagen fiber organisation between groups treated with BMP-13 and non-augmented controls. There were also no differences in the biomechanical properties of the repairs between groups (Gulotta et al., 2011b). More recently, BMP-2 and BMP-7 have been demonstrated to induce collagen production when added to tenocyte-like cells (Pauly et al., 2012).

1.1.1.9. Basic Fibroblast Growth Factor

Concentrations of bFGF peak between five and nine days after tendon rupture (Wurgler-Hauri et al., 2007, Kobayashi et al., 2006, Takahashi et al., 2002). By improving collagen proliferation and secretion, bFGF has been shown to stimulate tendon-bone healing *in vivo* but further studies are required to evaluate its effect on rotator cuff healing (Ide et al., 2009a, Ide et al., 2009b, Ju et al., 2008).

1.1.1.10. Platelet-Derived Growth Factor

PDGF is expressed in the acute phase of rotator healing and reaches its highest levels between seven and 14 days after injury (Gulotta et al., 2009, Kobayashi et al., 2006, Wurgler-Hauri et al., 2007, Gulotta and Rodeo, 2009). It has been demonstrated to be an essential cytokine responsible for tendon healing because of its ability to promote chemotaxis, cell proliferation, ECM production, and angiogenesis (Hoppe et al., 2013, Kovacevic et al., 2015). In a rat model of an acute supraspinatus tear, administration of PDGF enhanced cellular proliferation and angiogenesis during the early phase of healing, but this did not result in either a more structurally organised or stronger

attachment site at the latter stages of healing (Kovacevic et al., 2015). In a further study examining PDGF in a rat model of an acute supraspinatus tear, greater collagen fiber orientation and superior biomechanical properties were noted in the experimental group when compared to controls (Tokunaga et al., 2015).

1.1.1.11. Transforming Growth Factor-β

TGF-β is present during rotator cuff healing in three isoforms: TGF-β1, TGF-β2, and TGF-β3 (Kobayashi et al., 2006, Wurgler-Hauri et al., 2007). Variable expression of these different proteins has been postulated to be responsible for wound healing similar to what occurs during fetal development (increased TGF-β3), as opposed to adult wounds that are characterised by scar tissue (increased TGF-β1) (Campbell et al., 2004, Klein et al., 2002). In a rat model of rotator cuff repair, application of an osteoconductive calcium-phosphate matrix was associated with new bone formation, increased fibrocartilage, and improved collagen organisation at the healing tendon-bone interface. The addition of TGF-β3 significantly improved strength of the repair at four weeks postoperatively and resulted in a more favorable collagen I/III ratio (Kovacevic et al., 2011). Using a similar model, Manning et al (Manning et al., 2011) administered exogenous TGF-β3 to the healing enthesis and demonstrated that it was associated with increased vascularity and cell proliferation at 56 days compared to controls.

1.1.1.12. Platelet Rich Plasma

Platelet-rich plasma (PRP) is manufactured by centrifuging blood plasma to produce a dense matrix of platelets containing multiple growth factors (TGF-b, bFGF, PDGF, VEGF, connective tissue growth factor, and epidermal growth factor) (Randelli et al., 2008, Everts et al., 2006). For this reason it has received considerable attention in orthopaedics for treating a range of musculoskeletal problems (Dallari et al., 2016, Kilincoglu et al., 2015). However, recent evidence from randomised controlled trials and systematic reviews suggest that PRP does not reduce the retear rate or improve functional outcome following rotator cuff repair (Saltzman et al., 2015, Barber, 2016, Carr et al., 2015b, Wang et al., 2015).

1.8 Demineralised Bone Matrix

DBM first emerged as a biomaterial following pioneering work by Urist who highlighted its potential to be osteoinductive through endochondral ossification (Urist, 1965). It has subsequently been incorporated into an allograft that has been used as a successful surgical adjunct in non-union surgery, spinal fusion, and the filling of bone defects (Chakkalakal et al., 1999, Block and Russell, 1998, Killian et al., 1998). Commercial production of DBM has been achieved by demineralising bone with 0.6 Normal (*N*) hydrochloric acid (HCL) and then washing it in 0.15 molar (M) sodium chloride (NaCl). Prior to implantation it is often sterilised by gamma irradiation. Manufacturing in this manner exposes a type I collagen matrix, which is rich in growth factors such as BMPs (BMP-2, BMP-4, and BMP-7), TGF-β1, TGF-β2, and TGF-β3 (Sawkins et al., 2013, Veillette and McKee, 2007, Urist, 1965, Urist et al., 1983, Reddi, 1998). Evidence suggests that BMP-2 and TGF-β may act on bone marrow-derived stem cells and form new bone in the developing enthesis. This new bony ingrowth may then develop into fibrocartilage and mineralised fibrocartilage as the interface matures creating a structure that resembles the uninjured enthesis (Sundar et al., 2009b).

Rotator cuff healing involves a complex interplay of biological and mechanical factors. Whilst an optimal biological milieu is required to produce a naturally graded enthesis, it is the mechanical environment that stimulates this to happen. Several stratified constructs incorporating different cell groups are available but tend to be unstable and prone to detrimental stress concentrations (Spalazzi et al., 2008, Spalazzi et al., 2006, Dormer et al., 2010). By producing bone through a fibrocartilage

intermediate, DBM may be the ideal scaffold as both of these tissues are seen at the native enthesis. Very few studies though have examined its effect on the tendon-bone interface (Sundar et al., 2009b, Kilicoglu et al., 2012, Sundar et al., 2009a, Hsu and Wang, 2014).

In an ovine model of the extensor mechanism at the knee, Sundar et al (Sundar et al., 2009b) used DBM to augment patellar tendon re-attachment to a metal implant positioned on the tibial tuberosity. This model was used to investigate the attachment of a tendon to a metallic segmental prosthesis typically used to treat bone tumours of the proximal tibia. At six weeks the DBM group exhibited an increase in functional weight bearing (% full weight-bearing) compared to controls and by 12 weeks, there was regeneration of a more direct-type of enthesis made up of regions of fibrocartilage and mineralised fibrocartilage. New bone formation also accompanied these soft tissue changes. A slow release of growth factors by DBM was thought to stimulate the formation of this naturally graded structure. Sundar et al (Sundar et al., 2009a) additionally examined functional recovery of the ovine patella tendon-bone interface following tendon reattachment with DBM. Repair failure was noted in 33% of non-augmented controls. In contrast, none of the repairs failed in the DBM group and the resultant enthesis comprised new bone and fibrocartilage (demineralised and mineralised). Earlier mobilisation and superior function was also noted at all time points. Unlike other animal models of tendon regeneration around the shoulder, the ovine knee is entirely dependent upon an intact extensor mechanism.

Kilicoglu et al (Kilicoglu et al., 2012) assessed the effect of DBM on fixation of the extensor digitorum longus tendon within a proximal tibial bone tunnel in a rabbit

model. At three weeks a greater proportion of Sharpey's fibers, fibrocartilage, and new bone was found in the DBM group when compared to non-augmented controls. This was not maintained throughout the study period and at six weeks there was no significant difference. To further evaluate the influence of DBM on tendon-bone healing within a bony tunnel, Hsu and Wang (Hsu and Wang, 2014) used a rabbit model of anterior cruciate ligament (ACL) reconstruction. Similar to previous reports, DBM was associated with new bone formation, greater mineralised fibrocartilage, and less fibrous tissue.

Demineralised bone has been used successfully to augment tendon-bone healing (Sundar et al., 2009a, Kilicoglu et al., 2012). One of its properties is to induce new bone formation. In doing so, it may improve the strength of the enthesis and reverse osteopenia at the bony insertion as this has been demonstrated to occur following a rotator cuff tear (Meyer et al., 2004a). By combining DBM with stem cells its effects may be enhanced given that many of the growth factors it contains are able to direct MSC differentiation down tenogenic, chondrogenic, and osteogenic lineages (Dorman et al., 2012, Na et al., 2007, Gomiero et al., 2016). These cell lines produce elements essential to the formation of a naturally graded enthesis.

1.9 Chapter Overview

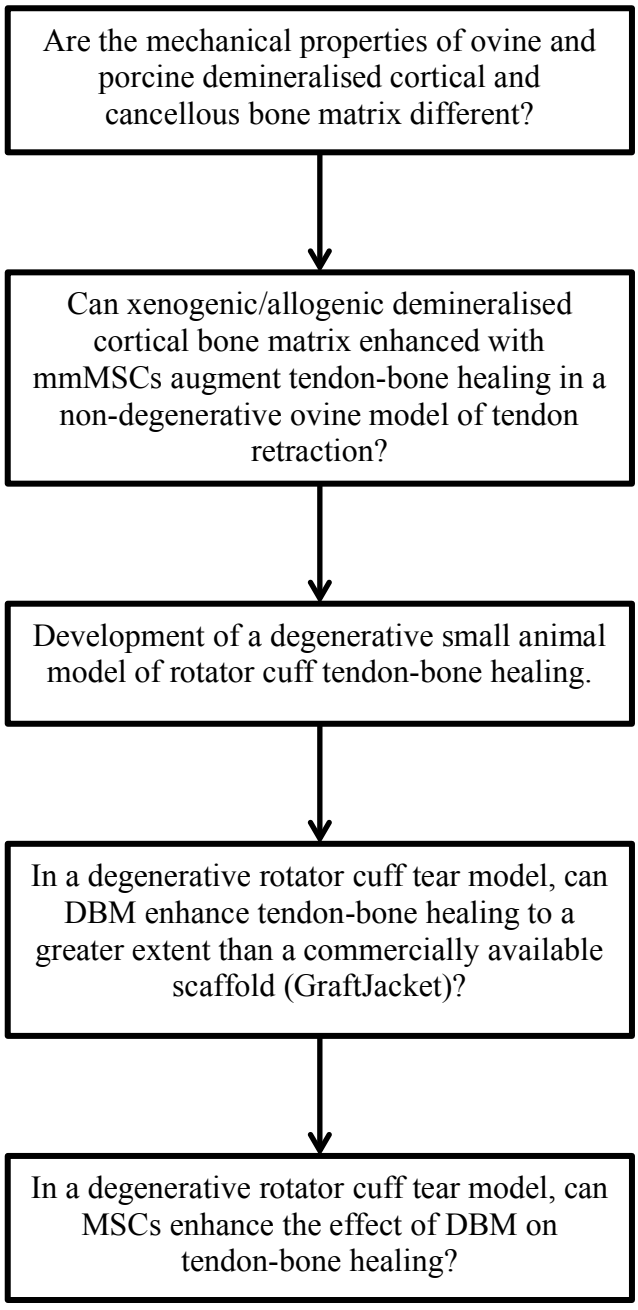

Chapter Two: Allogenic and Xenogenic Demineralised Bone Matrix as a Scaffold for Tendon-Bone Healing

2.1 Introduction

When used to treat rotator cuff tears, scaffolds reinforce the strength of the repair and improve biological healing (Beitzel et al., 2014). Tissue regeneration can be further enhanced by seeding cells into a biomaterial, but for this to happen there needs to be an interaction between the microstructure of the graft and the different types of cell surface receptors (Ide et al., 2009b, Tokunaga et al., 2015, Hidalgo-Bastida and Cartmell, 2010). Integrins in particular play an important role, as they are essential for MSC survival, proliferation, and differentiation (Derwin et al., 2010, Schwartz and DeSimone, 2008). Porous biomaterials facilitate this process as they optimise initial cell loading, and allow neovascularization and haematoma ingrowth, with its endogenous progenitor cells and growth factors (Whang et al., 1999). However, porosity may compromise the biomechanical properties of the repair construct leading to failure if it cannot resist the forces transmitted through the supraspinatus tendon during maximum contraction (196N) (Itoi et al., 1995).

Cancellous bone is a cellular material comprising struts and plates that form a trabecular, porous structure (Gibson, 1985). A network of struts produces open cells whilst one of plates produces closed cells. The stress-strain curve of cancellous bone responds to compressive load in three ways: (1) As it bends or undergoes axial compression, behaviour is initially linear elastic; (2) At high enough loads the cell walls collapse at a constant rate until they meet and touch, creating a plateau phase characterised by a greater resistance to load due to crushing of the cancellous structure; (3) After this, the resistance to load rises and results in an increasingly steep portion to the curve (Figure 2.1).

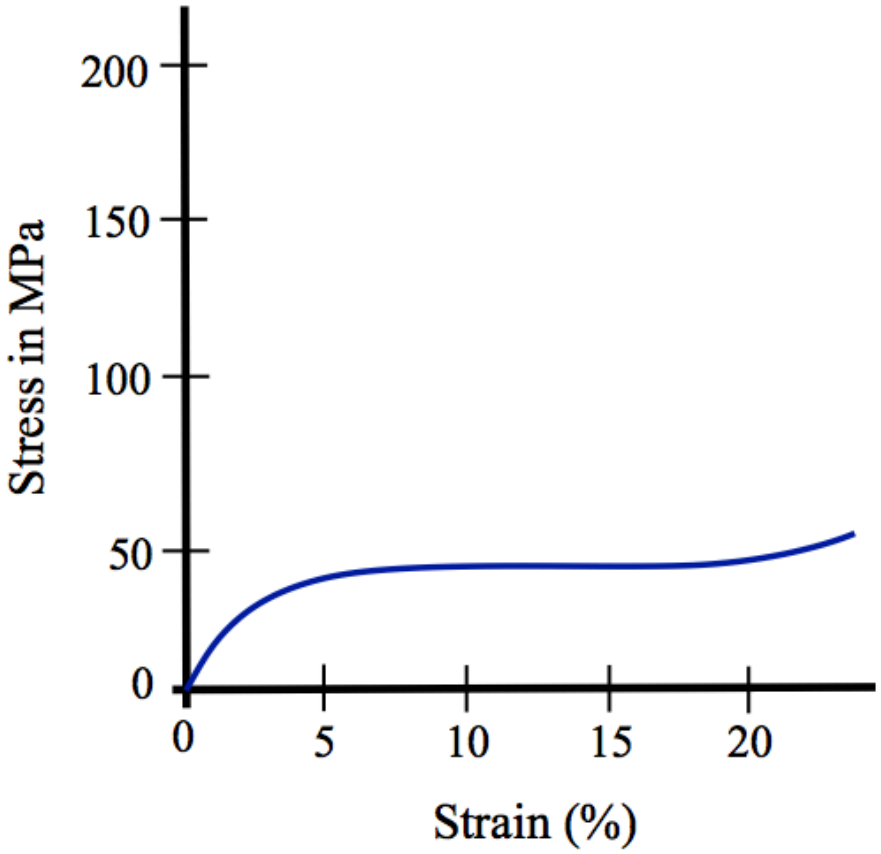

Figure 2.1: Stress-strain curve for cancellous bone under compressive load.

The structural arrangement of cancellous bone depends upon the direction of the load applied to it. When this is uniaxial, such as in vertebrae, the trabeculae develop a columnar structure with cylindrical symmetry. These columns are orientated vertically, giving a relatively high stiffness and strength in the direction of load (Gibson, 1985). This is reflected in cancellous bone exhibiting a significantly higher strength, ultimate strain, and work to failure when it is loaded in tension as opposed to compression (Rohl et al., 1991). This is an important consideration for tendon-bone healing where tensile loads are predominantly encountered.

Compared to their allogenic derivatives, xenografts are cost-effective and have almost unlimited availability (Sachs, 1994). For the purposes of xenotransplantation the most suitable donor is a non-human primate such as the chimpanzee, but the rarity of this species prevents them from being considered (Sachs, 1994). Accordingly, porcine materials have received considerable attention in the literature but due to high failure rates and adverse tissue reactions in clinical studies evaluating their use in tendon-bone healing, they are not widely used (Walton et al., 2007, Phipatanakul and Petersen, 2009). Refining the ways in which xenografts are produced could reduce the costs associated with expensive scaffolds and increase their uptake by healthcare providers.

This study aims to determine whether there is a difference in mechanical properties between porcine and ovine cortical and cancellous DBM in order to establish the scaffold to be used in Chapter Three (*in vivo* study examining tendon-bone healing in a large animal model of tendon retraction). Lumbar vertebrae were used as its cancellous nature gives rise to a porous structure resulting in longitudinal stiffness and strength, thereby making it a suitable graft material to improve tendon-bone healing (Smit et al., 1997, Gibson, 1985). The porous nature would also allow stem cells to penetrate the inner structure of the graft and improve graft remodeling at the healing enthesis. It was hypothesised that the tensile strength of cancellous DBM would be significantly lower than that of cortical DBM, and that there would be no difference between ovine and porcine scaffolds.

2.2 Materials and Methods

2.2.1 Study Overview

The tensile strength of porcine and ovine cancellous/cortical DBM (n = 3) was examined to determine which scaffold possessed appropriate mechanical properties to be used in a large animal model of tendon retraction (Chapter Three).

2.2.2 Preparation of DBM

DBM was manufactured according to a protocol modified from that used by Urist (Urist, 1965). Porcine bones were obtained from a local abattoir (Cheale Meats, Brentwood, UK) and ovine bones were obtained from a local veterinary institution (Royal Veterinary College, Hatfield, UK). Tibiae (cortical DBM) and lumbar vertebrae (cancellous DBM) of three skeletally mature female ewes and sows were harvested immediately post euthanasia; all soft tissues and periosteum were removed and the bones were cut into longitudinal strips using a band saw (Exact, Hamburg, Germany). Proximal and distal ends of each tibia were excised and the shafts were cut into three longitudinal strips measuring 3-4 mm in thickness, 17 mm (+/- 2 mm) wide, and 200 mm long. The body of each lumbar vertebra was cut into two strips (Figure 2.2).

Figure 2.2: Superior aspect of an ovine lumbar vertebra.

Each strip was demineralised in 0.6*N* HCL at room temperature. The solution was changed every 12 hours and demineralisation was confirmed with radiographs [300 seconds, 30 kilovolts (kV), Faxitron Corporation, Illinois, United States of America (USA)] before washing with phosphate-buffered saline (PBS) until the pH was 7.4 +/- 0.1 (Figures 2.3 and 2.4).

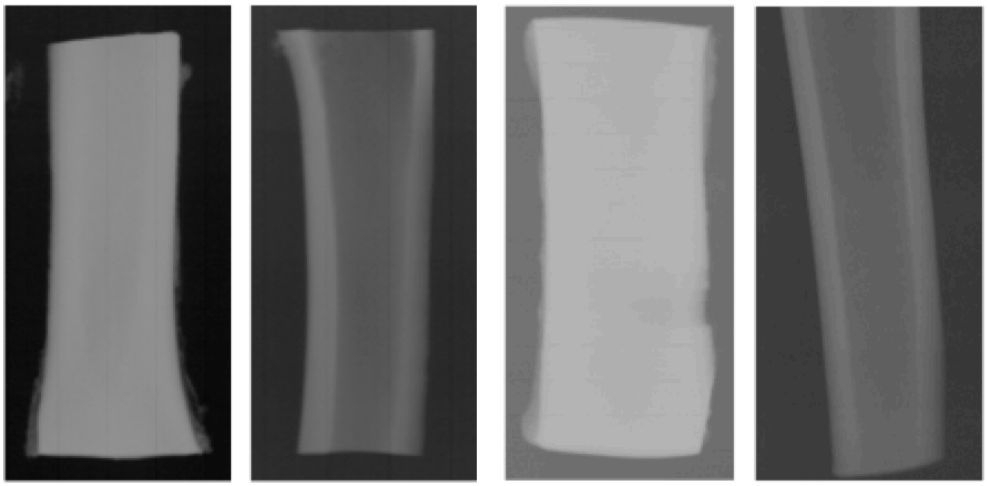

Porcine cortical bone pre-demineralisation	Porcine cortical bone post-demineralisation	Ovine cortical bone pre-demineralisation	Ovine cortical bone post-demineralisation

Figure 2.3: Radiographs of porcine and ovine cortical (tibia) bone pre- and post-demineralisation.

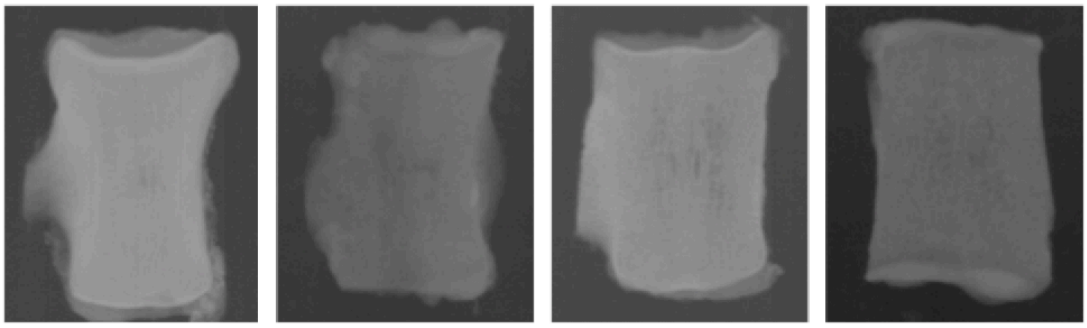

Porcine cancellous bone pre-demineralisation	Porcine cancellous bone post-demineralisation	Ovine cancellous bone pre-demineralisation	Ovine cancellous bone post-demineralisation

Figure 2.4: Radiographs of porcine and ovine cancellous (lumbar vertebra) bone pre- and post-demineralisation.

2.2.3 Ultimate Tensile Strength Testing

Three samples were tested in each group. Each strip was cut into a ‘dog bone’ shape as the wider ends of the sample ensured that stress concentrations were concentrated in the midsection, leading to rupture at the ultimate tensile strength (UTS). In contrast, if failure occurred at the fixed end of the specimen then it could be attributed to improper loading or a pre-existing defect in the material (Driscoll, 1998).

Specimens [3-4 mm in thickness, 17 mm (+/- 2 mm) wide, and 30 mm long] were mounted on a custom made testing machine (Zwick/Roell Group, Ulm, Germany) and secured using a piece of grit paper to prevent slippage (Figure 2.5). Samples were tested until failure at a displacement rate of 10 mm per minute without preconditioning. A stress-strain curve was produced and the UTS was recorded for each strip.

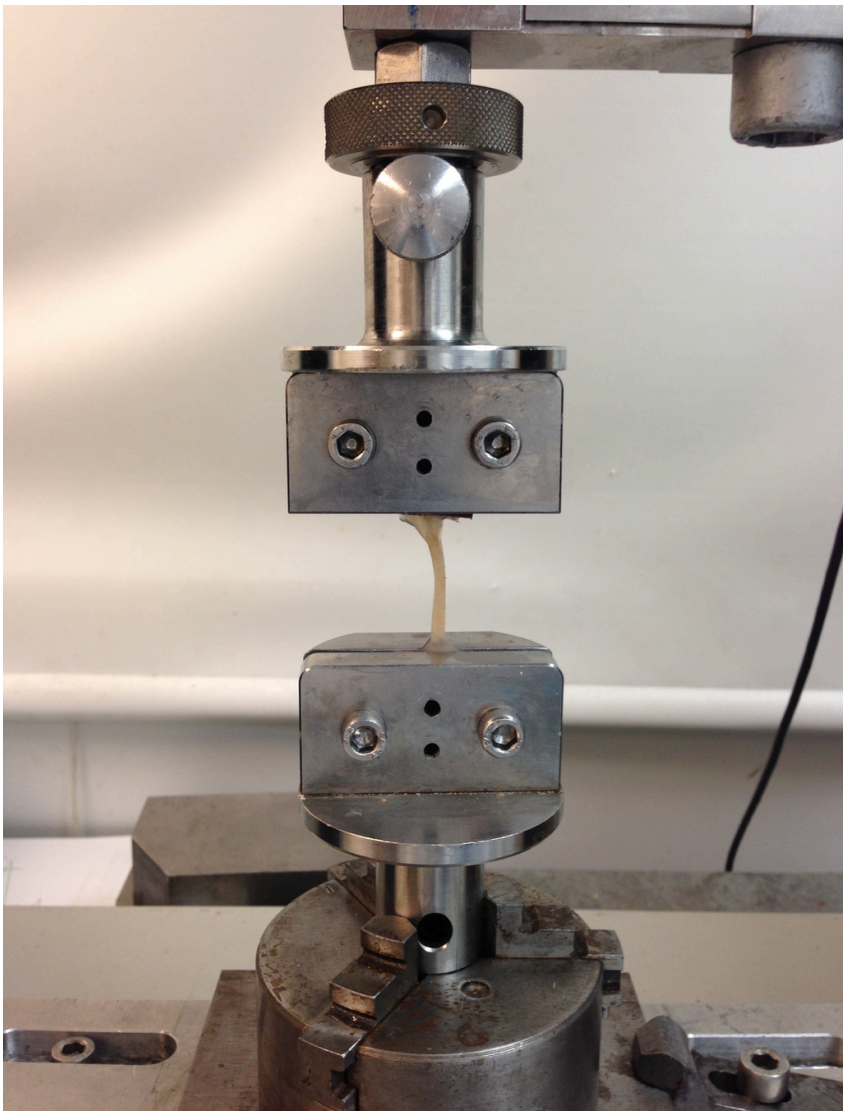

Figure 2.5: Ovine cortical DBM in a custom made tensile testing machine.

2.2.4 Statistical Analysis

Data was analysed using the Mann-Whitney test in IBM SPSS version 22 (Statistical Package for Social Sciences, SPSS Inc., Chicago, Illinois, USA) and statistical significance was considered at $p < 0.05$.

2.3 Results

All samples failed in their mid-substance. Ovine cortical DBM exhibited the greatest UTS with a median force of 142.0 N [95% confidence interval (CI) 125.9 to 161.3]. Porcine cancellous DBM was the weakest scaffold, with a median UTS of 2.5 N (95% CI -6.9 to 17.5). Porcine cortical and ovine cancellous DBM demonstrated a median UTS of 64.4 N (95% CI 23.7 to 124.6) and 16.1 N (95% CI 15.7 to 16.7) respectively (Table 2.1 and Figure 2.6). Each test produced a stress-strain curve characterised by an initial toeing segment, a linear region, and a narrow phase of plastic deformation (Figure 2.7). Stiffness was greatest in cortical DBM.

	Ultimate tensile strength – 1st repetition (N)	Ultimate tensile strength – 2nd repetition (N)	Ultimate tensile strength – 3rd repetition (N)	Median (N)
Porcine cortical DBM	64.4	60.6	97.5	64.4
Porcine cancellous DBM	11	2.5	2.5	2.5
Ovine cortical DBM	136.9	142.9	151.1	142.9
Ovine cancellous DBM	16	16.4	16.1	16.1

Table 2.1: Ultimate tensile strength of porcine and ovine cortical/cancellous DBM.

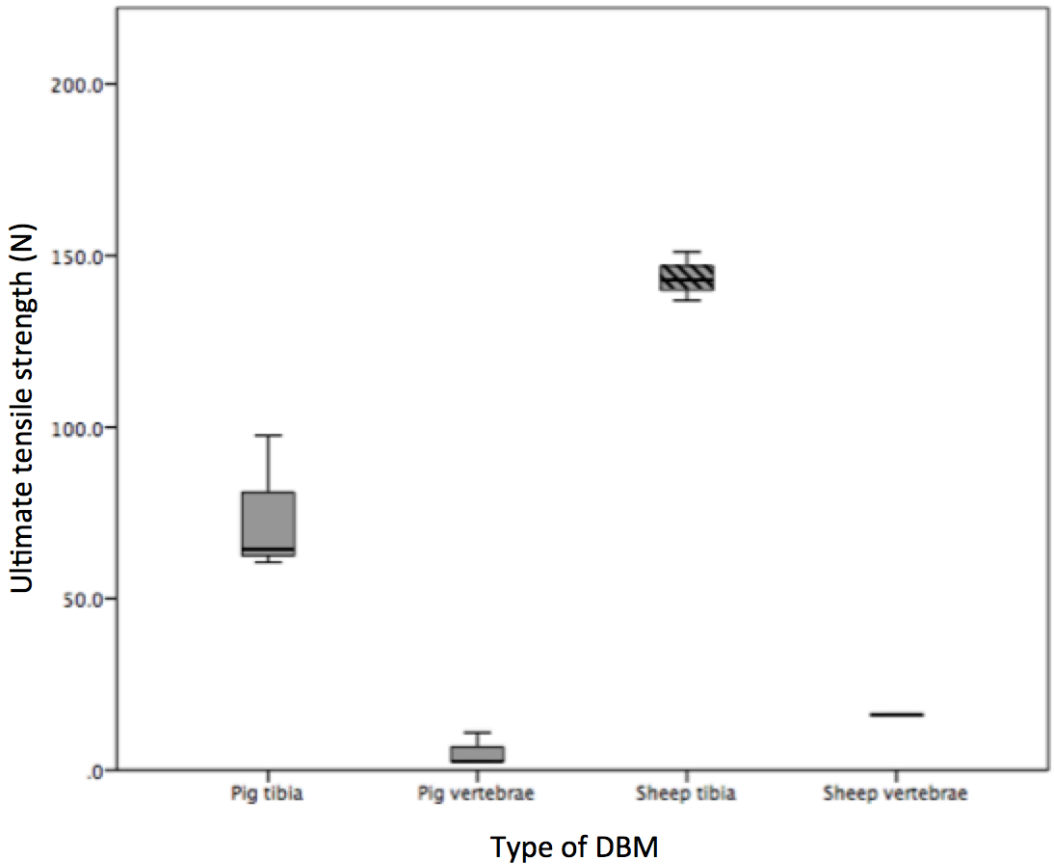

Figure 2.6: Box and whisker plot showing the maximum tensile strength of different DBM groups.

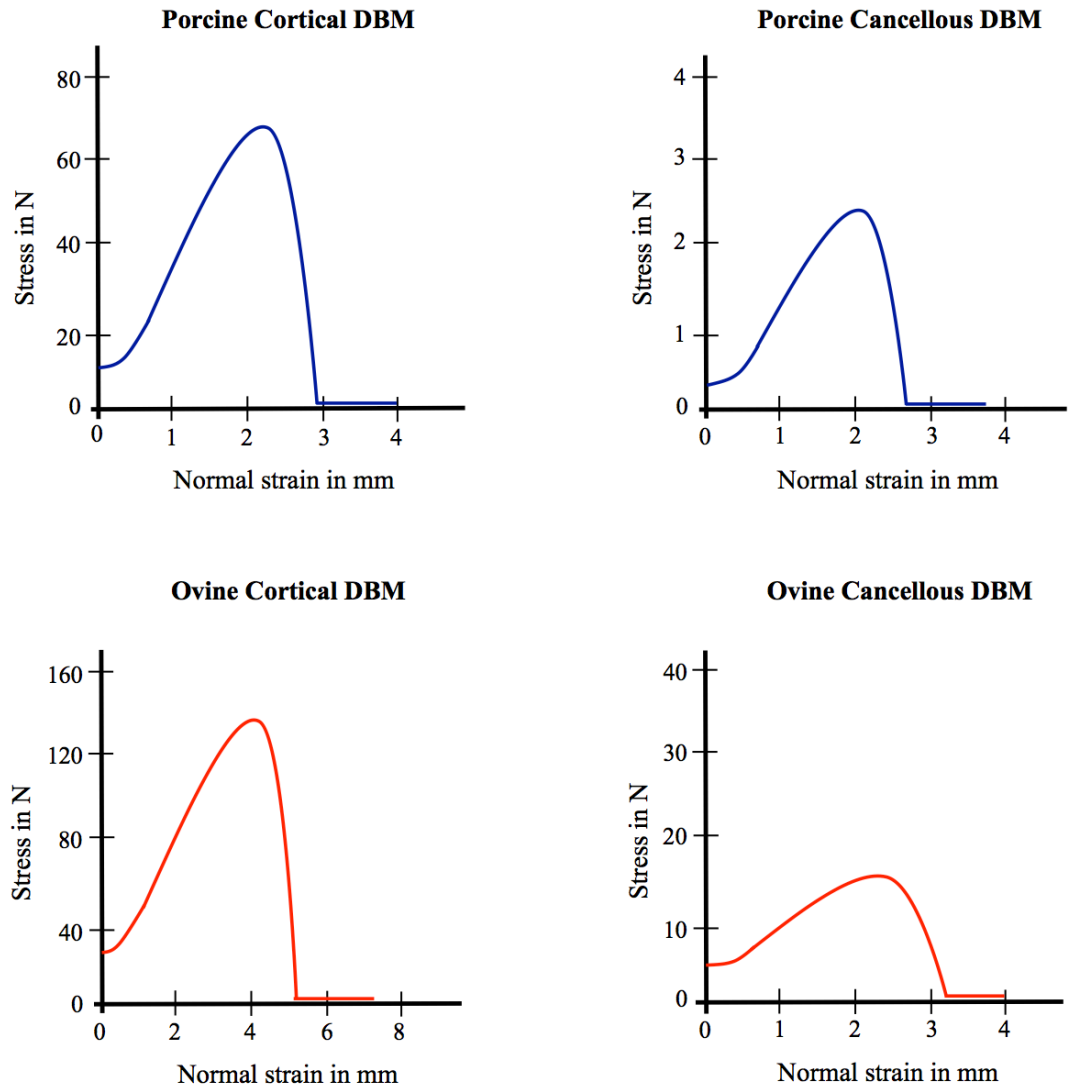

Figure 2.7: Stress-strain curve of representative samples of DBM in each group.

In both ovine and porcine groups, cancellous DBM had the lowest UTS. This reached statistical significance between porcine specimens ($p = 0.046$), and between porcine cancellous and ovine cortical DBM. Ovine cancellous DBM was significantly stronger than its porcine derivative ($p = 0.046$). No difference was demonstrated between cortical and cancellous samples in the ovine group ($p = 0.05$) (Table 2.2).

	Porcine cortical DBM	Porcine cancellous DBM	Ovine cortical DBM	Ovine cancellous DBM
Porcine cortical DBM	-	0.046	0.05	0.05
Porcine cancellous DBM	0.046	-	0.046	0.046
Ovine cortical DBM	0.05	0.046	-	0.05
Ovine cancellous DBM	0.05	0.046	0.05	-

Table 2.2: Statistical significance (p-values) between porcine/ovine cortical and cancellous DBM.

2.4 Discussion

Bone is composed of hydroxyapatite mineral crystals arranged within an organic collagen matrix (Chen and McKittrick, 2011). Tensile testing data from this chapter demonstrates that both cortical and cancellous DBM behave like tendon, in that their stress-strain curves are made up of an initial toeing segment followed by a linear region. Similar findings were noted by Bowman et al (Bowman et al., 1996) who suggested that the early non-linear behaviour of DBM was due to the straightening of crimped collagen fibers, and the subsequent linear behaviour was due to stretching of the straightened collagen fibers. Under tension, DBM therefore behaves like the native collagen present in soft tissues such as tendon, highlighting its suitability as a potential graft material.

Bone is a complex, hierarchical structure made up of type I collagen and carbonated hydroxyapatite. It exists in two forms: cortical (or compact) bone and cancellous (or trabecular) bone. The major difference between the two is in their relative density, defined as the apparent density of bone divided by that of its solid material (bone with a relative density less than 0.7 is classified as cancellous) (Chen and McKittrick, 2011, Gibson, 1985). Cancellous bone can be considered as a cellular solid made up of a network of struts and plates. Its density depends upon the external stresses it experiences (Chen and McKittrick, 2011). In a low stress environment, a strut-like structure develops, whereas a plate-like structure forms when stresses are high. To understand the behaviour of cancellous bone after demineralisation it should be considered as a composite of protein and mineral. Removing either of these constituents reduces the elastic modulus and compressive strength, but preserves the

porous trabecular structure. Reducing the mineral content in particular (as occurs in demineralisation) alters the mechanical response of cancellous bone such that it exhibits plastic deformation (Chen and McKittrick, 2011). The results from this study suggest that the tensile properties of cancellous bone are weaker than that of cortical bone. Whilst this only reached statistical significance in the porcine group, the absolute values were not ignored and still considered when the graft material for the *in vivo* study (Chapter Three) was chosen. The decision was based on both the force transmitted through the human supraspinatus during maximum contraction and the UTS of supraspinatus, which have been estimated to be 196 N and 601 N respectively (Itoi et al., 1995, France et al., 1989).

Interspecies differences are an important factor when choosing an appropriate xenograft. Aerssens et al (Aerssens et al., 1998) examined the difference in bone composition, density, and quality between different species including sheep and pigs. Compared to other animals, the cortical bone of sheep and pigs were found to have less collagen and more non-collagenous protein. In sheep, the cortical bone had a greater proportion of high-density bone particles than pigs. Similar findings were noted in trabecular bone (lumbar vertebrae) composition. Bone mineral content, bone mineral density, and fracture stresses were higher in sheep samples. These findings support the results of this experiment where the ovine scaffold displayed superior mechanical properties than its porcine derivative.

Limitations of this study include the inability to establish the age of the animals used to provide the specimens because they were obtained from an abattoir, and the absence of gamma irradiation in the manufacturing protocol of demineralised bone.

This is a crucial stage when processing DBM in the clinical setting, but gamma irradiation has been shown not to have a significant effect on the mechanical properties of demineralised bone and so it was not used in the present study (Summitt and Reisinger, 2003). Additionally, the inclusion of quantitative data on stiffness and Young's modulus would have provided a more comprehensive assessment of the biomechanical properties of the specimens.

Key findings from this chapter include: (1) Cancellous DBM possessing weaker tensile properties than cortical DBM; (2) Ovine DBM having greater tensile properties than porcine DBM; (3) Ovine cortical DBM having the highest UTS. Since the force transmitted through supraspinatus 196 N during maximum contraction, ovine cortical DBM is the only graft material strong enough to be used *in vivo* to examine tendon-bone healing (Itoi et al., 1995).

2.5 Conclusion

The results from this chapter illustrate that DBM has similar tensile properties to other collagen-based structures such as tendons. The ovine cortical scaffold was the only specimen that could potentially resist the forces transmitted through the native supraspinatus, and will therefore be used in Chapter Three to augment healing in an ovine model of tendon retraction.

Chapter Three: Augmentation of Tendon-Bone Healing using Allogenic and Xenogenic Demineralised Cortical Bone Matrix Enhanced with Minimally Manipulated Mesenchymal Stem Cells in a Non-Degenerative Ovine Model

3.1 Introduction

Chronic tears of the rotator cuff are associated with muscle atrophy, fatty infiltration, muscle fiber shortening, and retraction of the musculotendinous unit (Meyer et al., 2012a, Meyer et al., 2006). A degenerative process has been implicated in these architectural changes, but recently evidence has emerged that in a retracted tendon the pennation angle (the angle between a fasicle's orientation and the tendon axis) increases and allows fatty and fibrous tissue to infiltrate the newly created space between the reoriented muscle fibers (Meyer et al., 2004b). After several weeks, these changes become permanent and represent the main cause of persistent disability following a technically successful tendon repair (Matsumoto et al., 2002, Goutallier et al., 1995). Accordingly, the failure rate following surgery exceeds 50% (Harryman et al., 1991, Zumstein et al., 2008).

Musculotendinous retraction is regarded as one of the most important consequences of a chronic rotator cuff tear as it precludes direct apposition of the tendon stump onto its bony footprint (Dines et al., 2007, Meyer et al., 2012a). This is compounded by diminished elasticity that occurs due to the shortening of muscle fibers, development of scar tissue, and the formation of fibrous tissue within the muscle (Meyer et al., 2004b, Jozsa et al., 1990, Hersche and Gerber, 1998). Retraction is a dynamic process characterised by independent shortening of both muscle and tendon. Tendon shortening contributes the most to retraction and has been demonstrated to be an important factor affecting the outcome following surgery; with longer preoperative tendon stumps associated with lower failure rates (Meyer et al., 2012a, Meyer et al., 2006).

When the tendon cannot be reattached to the bone (irreparable rotator cuff tear) further reconstructive procedures may be required (Merolla et al., 2014). These can involve debridement +/- partial repair (arthroscopic or open), tendon transfer, and non-anatomic/reverse anatomy arthroplasty. Outcomes are varied, with failure occurring in up to 94% of non-arthroplasty cases (Gupta et al., 2013, Castricini et al., 2014, Sclamberg et al., 2004, Galatz et al., 2004, Iannotti et al., 2006). To address this, scaffolds have emerged as a possible solution (Cheung et al., 2010). These aim to decrease gap formation at the repair site as this reduces healing and load to failure (Burkhart et al., 2007, Shea et al., 2012).

Enhancing the function of scaffolds can be achieved using a number of different cell-based strategies (Cheung et al., 2010). MSCs are contained in the bone marrow at a concentration of approximately 10 – 100 per $1x10^6$ bone marrow cells (Kasten et al., 2008). Their use in the clinical setting is restricted due to the high costs associated with time-consuming tissue culture techniques. This can be overcome by isolating the connective tissue progenitor cell-containing mononuclear fraction by centrifugation with a Ficoll gradient (Kasten et al., 2008, Hernigou et al., 2006, Hernigou et al., 2005). Using this technique, bone marrow obtained from the iliac crest has been shown to contain 2579 ± 1121 progenitor cells/cm^3 (Hernigou et al., 2006). Cells obtained in this manner are deemed ‘minimally manipulated MSCs’ and entail lower costs, faster processing, and less chance of an immunogenic reaction (Black et al., 2007, Raposio et al., 2014). In the only study examining this cell population in the treatment of rotator cuff tears, it was associated with a significant improvement in healing compared to non-augmented controls. Tears with retraction were excluded

from this study, thus the role of minimally mmMSCs in their treatment is yet to be established (Hernigou et al., 2014).

Chapter Two demonstrated that cortical DBM possessed sufficient mechanical properties to be considered as a tendon graft. It was therefore used as the basis for this study in order to evaluate the effect of allogenic and xenogenic DBM enhanced with mmMSCs on regeneration of the tendon-bone interface in an ovine model of tendon retraction. Since xenografts are cheaper and more readily available than their allogenic derivatives, their potential for augmenting tendon-bone healing was assessed (Oryan et al., 2014). The hypothesis was that augmentation of a healing tendon-bone interface with DBM and mmMSCs would result in improved function, and restoration of the native enthesis, with no difference between xenogenic and allogenic scaffolds.

3.2 Materials and Methods

3.2.1 Study Design

All animal work was conducted in accordance with a Project License protocol accepted under the UK Home Office Animals (Scientific Procedures) Act 1986. Ten skeletally mature non-pregnant female Friesland ewes, two-to-three years old, weighing between 78 and 97 kilograms (kg) were selected for this study. All 10 animals underwent surgical excision of the distal 1 cm of the right hind limb patellar tendon; the defect was repaired using a strip of xenogenic (porcine)/allogenic (ovine) cortical DBM and mmMSCs. One surgeon carried out all procedures and all animals were randomly allocated (using simple randomisation) to one of the two treatment groups. In keeping with the regulations set out by the UK Home Office Animals (Scientific Procedures) Act 1986, a control group was not used in this study since previous work has shown that a tendon defect does not heal spontaneously, rendering the animals lame (Yokoya et al., 2008, Yokoya et al., 2012). Animals were freely mobilised in individual pens and specimens were retrieved at 12 weeks following euthanasia using intravenous Sodium Pentobarbital. Force plate analysis, radiographs, peripheral quantitative computer tomography (pQCT) scans, and histological analysis were performed.

3.2.2 DBM Manufacture

DBM derived from cortical bone was manufactured according to Urist's protocol, with modifications (Urist, 1965). Six tibiae from three skeletally mature female ewes

(allograft) and sows (xenograft) were harvested immediately post euthanasia; all soft tissues and periosteum were stripped from the bone surface. Proximal and distal ends of each tibia were excised and the shafts were cut into three longitudinal sections corresponding to the three surfaces of the prismatic shape of the tibia using a diamond edged band saw (Exact, Hamburg, Germany). The resulting bone strips were then demineralised in 0.6 *N* HCL at room temperature. Demineralisation was confirmed by taking radiographs (300 seconds, 30 kV, Faxitron Corporation, Illinois, USA). This was followed by prolonged washing in PBS until the pH was 7.4 +/- 0.1. Strips measuring 3-4 mm in thickness, 20 mm (+/- 2 mm) wide, and 15 cm long were cut and stored at -20˚C for two hours and moved to a lyophiliser (Edwards Girovac Ltd, Crawley, West Sussex, UK) for three days. Specimens were sealed in individual plastic bags, sterilised by gamma irradiation at a dose of 25 kilograys (Isotron Limited, Reading, UK), and stored at -20˚C. Samples were rehydrated at the time of surgery in normal saline for 45 minutes prior to use.

3.2.3 Bone Marrow Aspiration and mmMSC Isolation

Following the induction of anaesthesia, 20 ml of marrow was aspirated from the contralateral iliac crest in small fractions to reduce the degree of contamination by peripheral blood. Several aspirations were made through the same skin incision with each being spaced approximately 1 cm apart to avoid dilution from aspiration in the previous channel. All aspirates were stored in vials containing heparin and then concentrated by centrifugation with Ficoll for 30 minutes (Hernigou et al., 2006). The mononuclear layer containing mmMSCs was returned to the operative room after 45 minutes.

3.2.4 Surgical Procedure

A tendon retraction model was developed from a pre-existing ovine model used to investigate tendon-bone healing (Sundar et al., 2009a). All animals were sourced from The Royal Veterinary College (Hatfield, Hertfordshire, UK). Anaesthesia was induced with intravenous Midazolam [2.5 milligrams (mg)] and Ketamine Hydrochloride (2 mg/kg), and then maintained using 2% Isoflurane mixed with pure oxygen via an endotracheal tube.

A longitudinal skin incision was made over the right stifle joint from the patella to the tibial tuberosity (Figure 3.1A). The patellar tendon was identified and a transverse strip of the distal 1 cm was excised from its bony insertion (Figure 3.1B). Using a sagittal saw the superficial 3 mm of the tendon footprint was osteotomised, and two 3.2 mm drill holes were made 1 cm apart on the prepared flat bone surface into which two 5.5 mm metallic suture anchors (Corkscrew, Arthrex, Naples, Florida, USA) for repair of the DBM strip were inserted using a standard surgical technique (Figure 3.1C). The mononuclear layer was combined with the fibrinogen component of a fibrin sealant (Tisseel, Baxter Health Care, Berkshire, United Kingdom) and then mixed with the thrombin component and applied onto the osteotomy site (Kalia et al., 2006, Kalia et al., 2009).

The defect was repaired with allograft in five sheep and xenograft in the remaining five sheep. An interlocking Krakow suture technique was used to secure the DBM strip to the remaining proximal patellar tendon using #2 FiberWire suture (Figure 3.1D). The distal end of the DBM strip overlying the tibial tuberosity was secured to

the surrounding tissue, with the remaining sutures from the suture anchors, to ensure consistent and complete contact with the bone. The dimensions of the DBM strip were adjusted to match the length and width of the host patellar tendon prior to repair: this averaged 20 mm wide and 100 mm long. The surgical wound was closed in layers using absorbable 3'0 Vicryl (Ethicon, Johnson & Johnson Medical Ltd., Berkshire, UK). No restrictions in weight bearing were imposed postoperatively and the sheep were allowed to move freely. Digital lateral radiographs of both hind limbs were taken at 12 weeks.

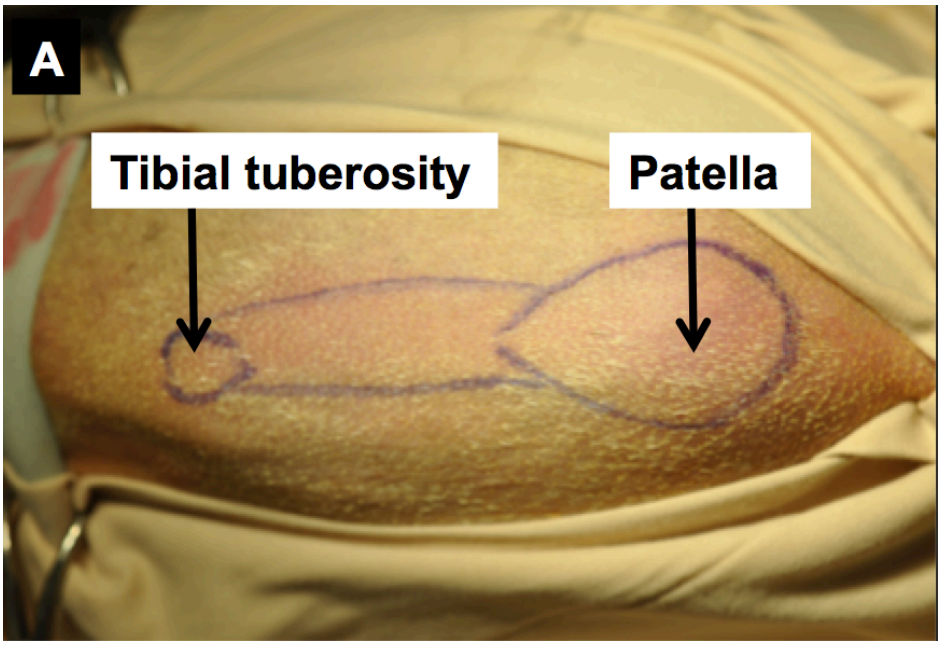

Figure 3.1A: Mid-line skin incision.

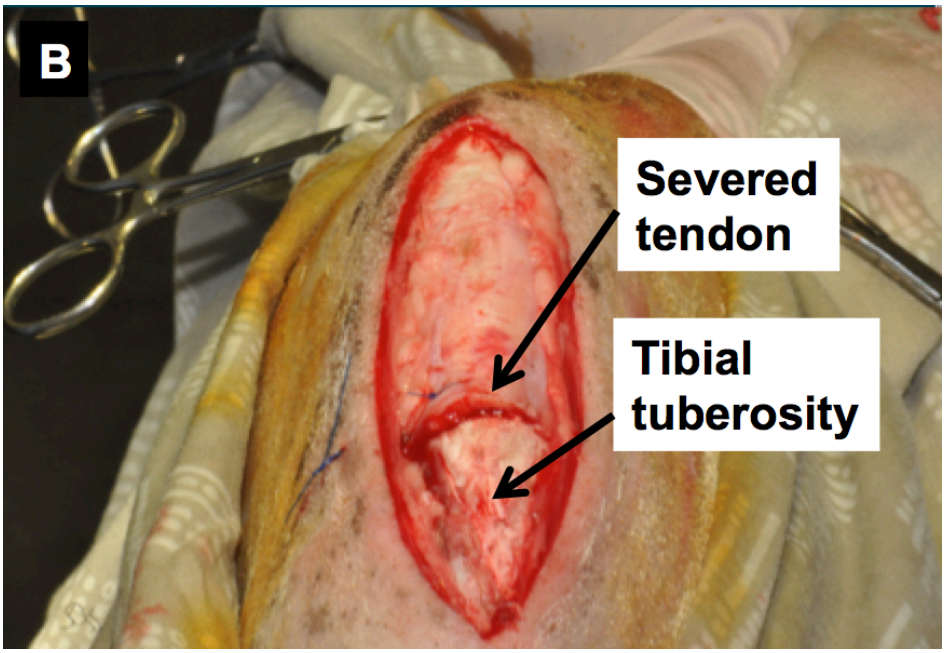

Figure 3.1B: Distal patellar-tendon defect.

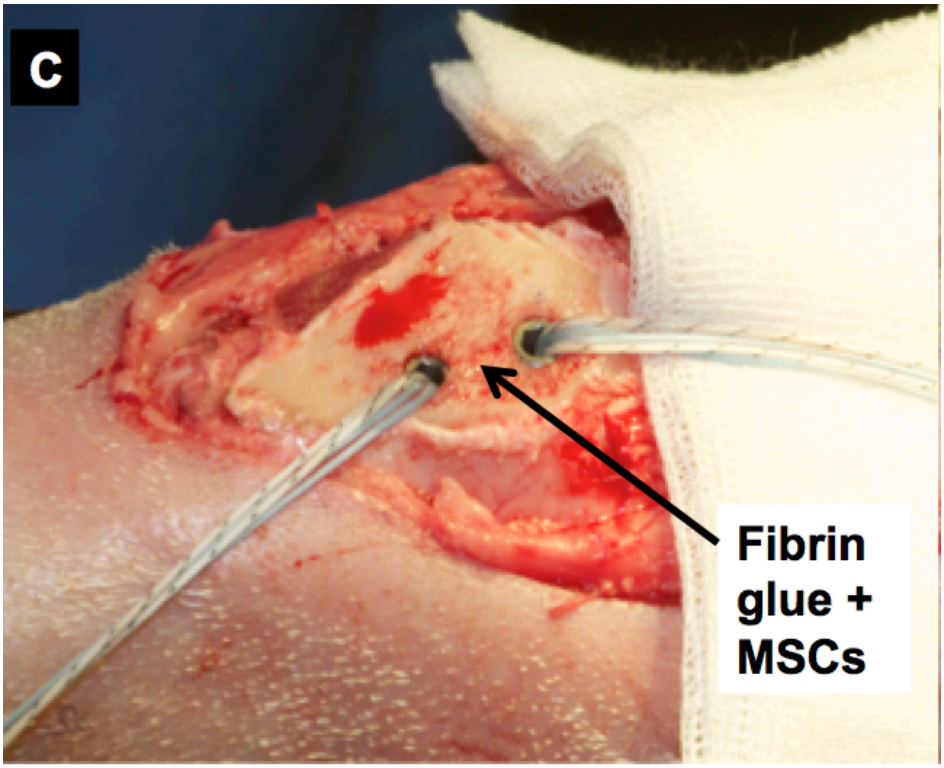

Figure 3.1C: Osteotomised tibial tuberosity with two suture anchors in situ.

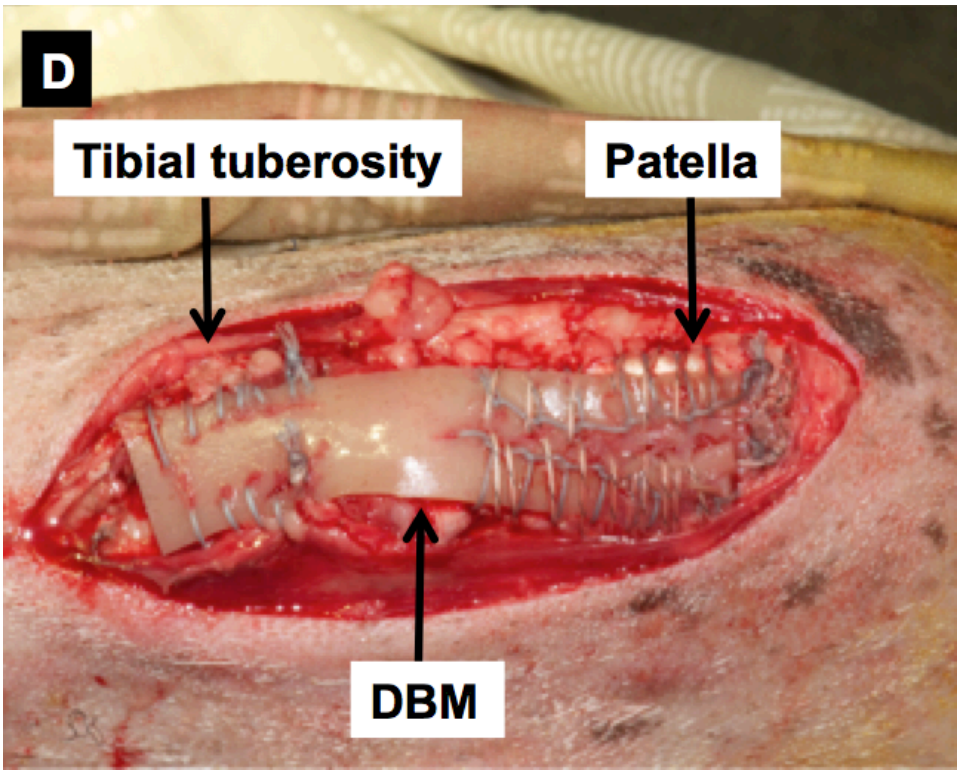

Figure 3.1D: Patellar tendon defect repaired with allogenic DBM.

3.2.5 Force Plate Analysis

Animals underwent force plate analysis pre-operatively and at six, nine, and 12 weeks postoperatively as this has been demonstrated to be an appropriate marker of functional recovery (Sundar et al., 2009a). Twelve readings of each hind limb were taken by walking the animals over a force plate (Kistler Biomechanics Limited, Alton, UK) in a gait analysis laboratory. The mean peak vertical component of the ground reaction force (GRFz) of each hind limb was obtained and normalised for weight (F_{max}/weight). Functional weight bearing (FWB) was expressed as the mean GRFz of the right hind limb as a percentage of the left (control) limb. Improvements in FWB were compared statistically between groups at each time point.

3.2.6 pQCT

pQCT scanning was performed to examine for ossification within the patellar tendon, the DBM, and surrounding tissues. Using an XCT 2000 Bone Scanner (Stratec Medizintechnik Gmbh, Germany) with Software version 6.20, 5 mm CT slices were taken through the tibial tuberosity, patellar tendon/DBM, and patella.

3.2.7 Histology

The patella-patellar tendon/DBM graft-tibial tuberosity complex was harvested at 12 weeks. Visual assessment of the tissue during the dissection, and pQCT were undertaken to determine if ossification had occurred within/around graft. Samples were fixed in 10% formal saline and underwent ascending graded alcohol dehydration, defatting in chloroform, and embedding in LR White Hard Grade Resin (London Resin Company Limited, Reading, UK). Sections were cut, ground, and polished to 70–100 μm before staining with Toluidine Blue and Paragon.
Three distinct zones were defined and evaluated by two observers blinded to the origin of the graft (Figure 3.2). These comprised: zone 1, DBM-patellar tendon interface; zone 2, DBM in the region of the tendon defect; zone 3, DBM neo-enthesis, (the area of the new tendon enthesis over the tibial tuberosity). Sections were assessed semi-qualitatively for new bone formation, inflammatory cells, cellularity, vascularisation, and collagen fiber crimp.

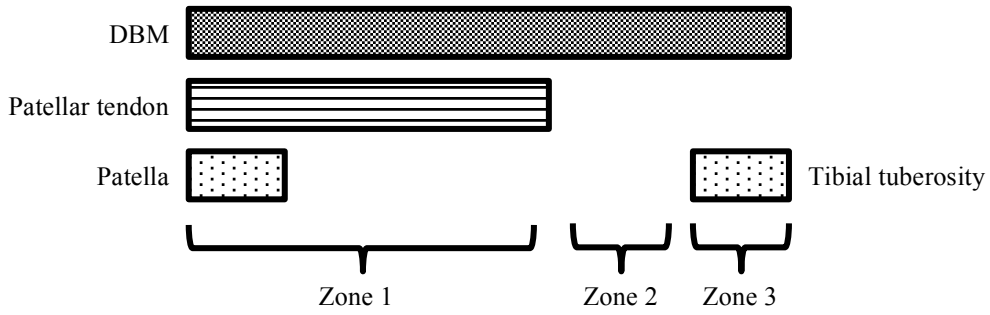

Figure 3.2: Three morphological zones examined histologically. Zone 1: DBM-patellar tendon interface; Zone 2: DBM in the region of the tendon defect; Zone 3: DBM neo-enthesis, examining the area of the new tendon enthesis over the tibial tuberosity.

Semi-quantitative analysis was undertaken for interactions between DBM and the patellar tendon (zone 1), remodeling of the DBM in the tendon defect (zone 2), and the formation of a neo-enthesis (zone 3). In Zone 1, four separate equally spaced regions were analysed in order to comprehensively examine the entire length of the DBM-patellar tendon interface. The maximum score for this area was therefore 20, in contrast to Zones 2 and 3 that could yield a maximum score of 5. Tables 3.1 and 3.2 describe the scoring criteria used for these assessments.

Score	Criteria
1	DBM still present with no evidence of tendon integration
2	DBM: very little evidence of remodelling and integration Collagen: poorly aligned, poorly organised, not parallel
3	DBM: partial remodeling Collagen: partially aligned in a parallel manner, partially organised
4	DBM: almost completely remodeled Collagen: mostly aligned in parallel
5	Completely remodeled DBM Normal tendon: – Parallel aligned collagen fibers – Elongated fibroblast nuclei

Table 3.1: Criteria for semi-quantitative analysis of DBM remodelling (Zones 1 and 2).

Score	Criteria
1	No fibrocartilage No mineralised fibrocartilage
2	Fibrocartilage present No mineralised fibrocartilage
3	Fibrocartilage present Mineralised fibrocartilage present Disorganised arrangement
4	Fibrocartilage present Mineralised fibrocartilage present Organised graduation between distinct regions but no tidemark
5	Fibrocartilage present Mineralised fibrocartilage present Organised graduation between distinct regions with tidemark

Table 3.2: Criteria for semi-quantitative analysis of the tendon-bone interface (Zone 3).

3.2.8 Statistical Analysis

Nonparametric statistical methods were used for all analyses because of the non-normality of the data in the groups being compared. Numerical data were inputted into SPSS software package, version 23 (SPSS Inc, an IBM Company, Chicago, Illinois). Mann Whitney U tests were used to compare data between groups, whilst Wilcoxon Signed Rank tests were used to assess differences within each group over time. Results were considered significant at the $p < 0.05$ level.

3.3 Results

All animals survived the duration of the study and none had post-operative infection or failure of the fixation, as noted on radiographs (Figure 3.3). At 12 weeks, the gait pattern had returned to normal in both groups.

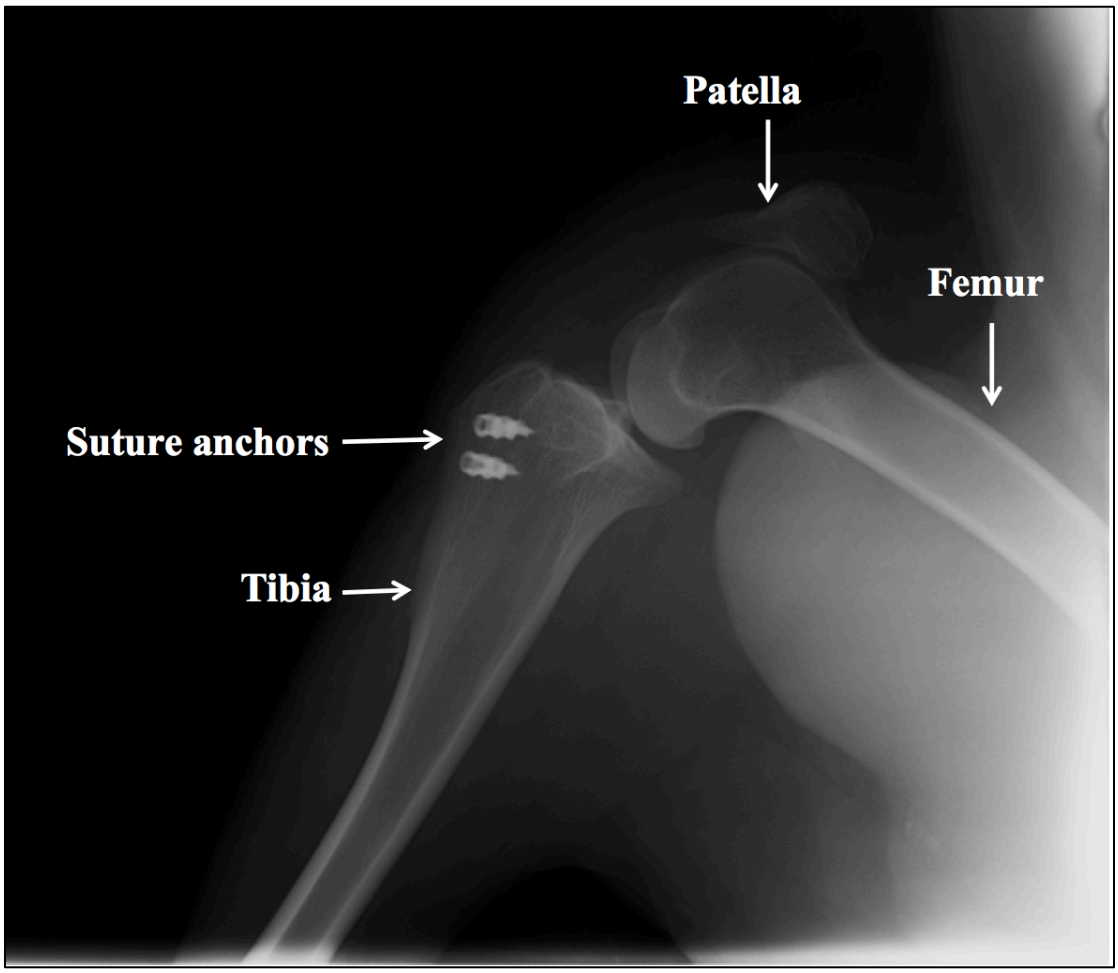

Figure 3.3: Lateral radiograph of the right stifle joint 12 weeks following surgery.

3.3.1 Force Plate Analysis

In the allograft group, FWB reached a median of 55.1% (95% CI 36.6 to 74.9) at six weeks, 68.1% (95% CI 48.4 to 90.7) at nine weeks, and 81.0% (95% CI 78.1 to 86.2) at 12 weeks. A significant improvement was noted between six and nine weeks ($p = 0.043$) but not between nine and 12 weeks ($p = 0.273$). In the xenograft group, FWB reached a median of 39.1% (95% CI 28.8 to 47.1) at six weeks, 43.7% (95% CI 33.3 to 54.4) at nine weeks, and 47.0% (95% CI 35.1 to 67.4) at 12 weeks. A significant improvement was noted between six and nine weeks ($p = 0.043$) but not between nine and 12 weeks ($p = 0.273$). At six, nine, and 12 weeks, FWB was significantly greater in the allograft group compared to the xenograft group ($p = 0.047$, 0.028, and 0.021, respectively) (Figure 3.4).

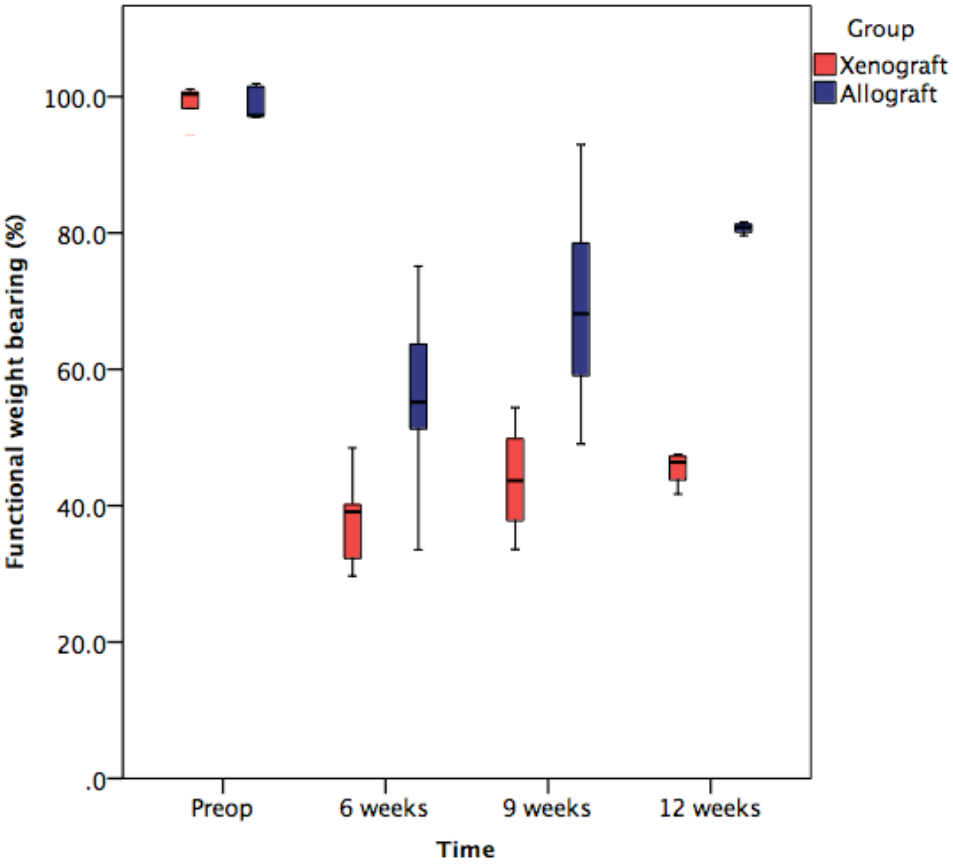

Figure 3.4: Box and whisker plot showing percentage functional weight bearing of allogenic and xenogenic DBM groups at six, nine, and 12 weeks.

3.3.2 pQCT Scans

Ossification within the DBM or the patellar tendon was not found in any of the specimens.

3.3.3 Gross and Histological Findings

Normal post-operative scar tissue was present and there was no evidence of inflammatory reaction, infection, or excessive granulation tissue. The DBM had remodeled and was well integrated into both the patellar tendon and tibial tuberosity. The suture anchors remained well fixed with no evidence of pull out or migration. All suture materials were intact with no evidence of rupture or failure.

3.3.3.1 Qualitative Histology

At 12 weeks, both allogenic and xenogenic DBM had remodeled and integrated into the surrounding tissue with evidence of neovascularisation. In the allograft group, the DBM-patellar tendon interface (zone 1) and tendon defect (zone 2) appeared normal and both were characterised by well-organised, crimped collagen fibers with elongated fibroblast nuclei (Figure 3.5). At the enthesis (zone 3), this was accompanied by mineralised fibrocartilage made up of chondrocytes surrounded by a mineralised matrix (Figure 3.5). This direct type of enthesis, with a distinct transition between bone, mineralised fibrocartilage, demineralised fibrocartilage, and tendon was seen in both groups. However the xenogenic DBM possessed fewer regions of mineralised fibrocartilage at the tendon-bone interface (zone 3) and displayed a more disorganised DBM-patellar tendon interface (zone 1) with fewer crimped collagen fibers (Figure 3.6). No evidence of heterotopic ossification or inflammatory cells were observed in either group.

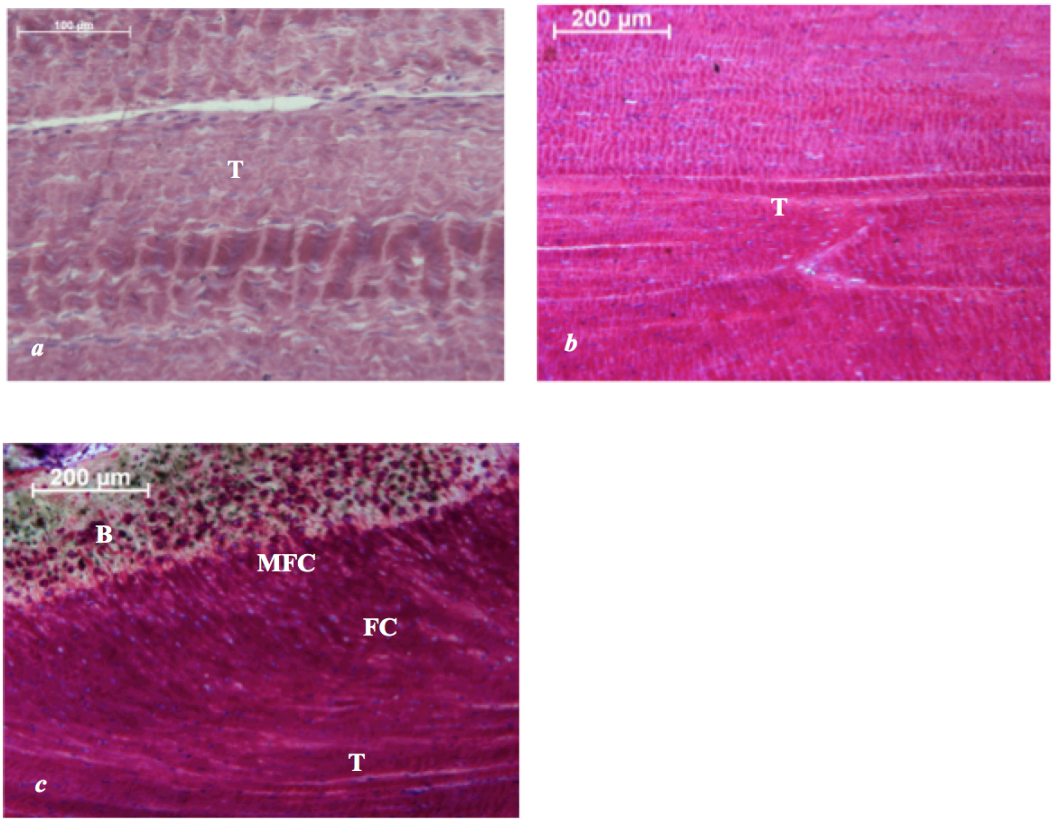

Figure 3.5: Photomicrograph showing appearance of allogenic DBM at 12 weeks. Specimens stained with Toluidine Blue and Paragon. (a) Zone 1: Patellar tendon-DBM interface characterised by well-organised, crimped collagen fibers with elongated fibroblast nuclei. (b) Zone 2: Tendon defect with complete remodeling of DBM and large areas of well-organised, crimped collagen fibers with elongated fibroblast nuclei. (c) Zone 3: DBM neo enthesis comprising tendon (T), fibrocartilage (FC), mineralised fibrocartilage (MFC) and bone (B).

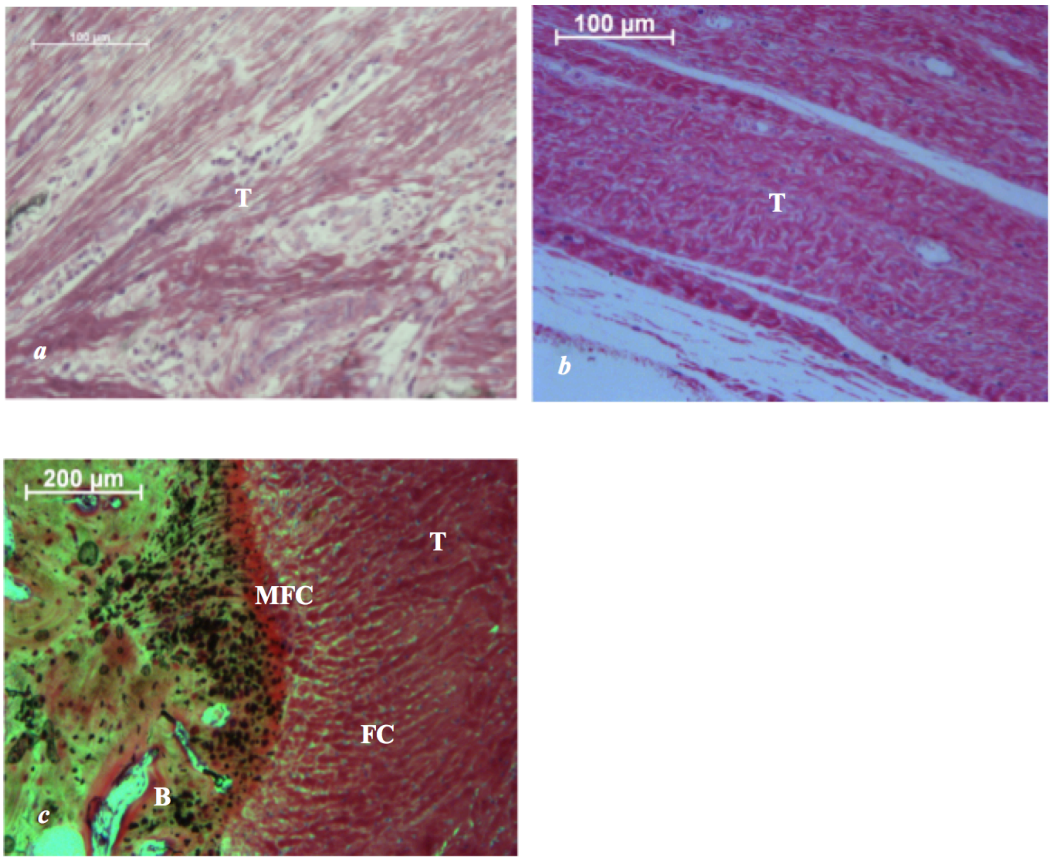

Figure 3.6: Photomicrograph showing appearance of xenogenic DBM at 12 weeks. Specimens stained with Toluidine Blue and Paragon. (a) Zone 1: Patellar tendon-DBM interface characterised by disorganised, crimped collagen fibers with elongated fibroblast nuclei. (b) Zone 2: Tendon defect with complete remodeling of DBM and large areas of disorganised, crimped collagen fibers with elongated fibroblast nuclei. (c) Zone 3: DBM neo enthesis comprising disorganised tendon (T), fibrocartilage (FC), mineralised fibrocartilage (MFC) and bone (B).

3.3.3.2 Quantitative Histology

At 12 weeks, remodeling of the DBM was assessed using the criteria outlined in Table 1. In the region of the DBM-patellar tendon interface (zone 1), this scored a median of 14 (95% CI 12.5 to 15.3) in the allograft group and 12.5 (95% CI 10.5 to 14.2) in the xenograft group. This difference did not reach statistical significance ($p = 0.147$). At the tendon defect (zone 2), this scored a median of 4 (95% CI 3.7 to 4.5) in the allograft group and 3 (95% CI 2.7 to 3.8) in the xenograft group. In this region, the remodeled allograft resembled native tendon tissue significantly more than the xenograft ($p = 0.015$).

Analysis of the neo-enthesis (zone 3) was conducted using the criteria detailed in Table 2 with evaluation of its maturation and presence of four distinct zones (tendon, demineralised fibrocartilage, mineralised fibrocartilage and bone). This scored a median of 4 (95% CI 3.8 to 4.4) in the allograft group and 4 (95% CI 2.9 to 4.1) in the xenograft group. A significantly more mature neo-enthesis was formed in the allograft group ($p = 0.039$).

3.4 Discussion

This experiment suggests that allogenic and xenogenic DBM, used with mmMSCs, can regenerate an enthesis with favorable histological and mechanical properties in an ovine model of tendon retraction. All animals survived the duration of the study and there were no cases of post-operative infection or failure of the fixation. An improvement in functional weight bearing at all time points was noted in both groups, but was significantly greater in those animals that were treated with the allograft. At 12 weeks, the DBM had remodeled across the entire length of the patellar tendon and the defect. This area was made up of well-organised crimped collagen fibers arranged parallel to the direction of load. The construct was well cellularised and vascularised throughout. Compared to the xenograft, the allograft was significantly more mature in the tendon defect and had remodeled into tendon-like tissue with crimped collagen fibers orientated in the direction of the tendon. The tendon-bone interface had been restored in both groups and was defined by the four distinct regions that make up a direct enthesis. This was significantly more mature and organised in the allograft group.

Endochondral ossification has been proposed as a potential mechanism responsible for the development of the native enthesis (Thomopoulos et al., 2010). This involves the release of growth factors (inflammatory phase) and the secretion of a cartilaginous matrix that undergoes mineralisation and remodeling to form bone (Thomopoulos et al., 2010). BMP-2 and BMP-7 mediate this process and additionally cause bony ingrowth into the enthesis, thereby strengthening it (Ma et al., 2007, Schwarting et al., 2015). DBM induces new bone formation by a similar process and may therefore

represent a suitable scaffold to regenerate a functional tendon-bone interface (Urist, 1965). Lovric et al (Lovric et al., 2012) examined the effect of a DBM paste on healing of a bone tunnel during ACL reconstruction in a rodent model. At six weeks, peak load to failure was significantly higher in the DBM group when compared to non-augmented controls. Increased woven bone formation at the healing interface and greater expression of BMP-2 and BMP-7 were thought to be responsible for this. Histology did not show any evidence of fibrocartilage formation and the collagen present at the enthesis was disorganised and immature. Sundar et al (Sundar et al., 2009a) examined functional recovery of the ovine patella tendon-bone interface following tendon reattachment with a DBM scaffold. Repair failure was noted in 33% of non-augmented controls. None of the repairs failed in the DBM group and the resultant enthesis comprised new bone and fibrocartilage. Earlier mobilisation and superior function was noted at all time points.

Kilicoglu et al (Kilicoglu et al., 2012) assessed the effect of DBM on fixation of the extensor digitorum longus tendon within a proximal tibial bone tunnel in a rabbit model. At three weeks a greater proportion of Sharpey's fibers, fibrocartilage, and new bone was found in the DBM group when compared to non-augmented controls. To further evaluate the influence of DBM on tendon-bone healing within a bony tunnel, Hsu and Wang (Hsu and Wang, 2014) used a rabbit model of ACL reconstruction. Similar to previous reports, DBM was associated with new bone formation and greater mineralised fibrocartilage.

The tri-differentiation capacity of MSCs makes them a potentially suitable strategy for the enhancement of tendon-bone healing (Hernigou et al., 2014). Their use in the

clinical setting has been restricted because *in vitro* expansion is costly and time-consuming. To negate the need for expensive laboratory techniques in this study, mmMSCs were isolated from autologous bone marrow aspirates and made available within 45 minutes. This is an appealing 'translational' concept but few studies have treated rotator cuff tears using this method, and none have examined their effect on chronic tears with retraction (Hernigou et al., 2014, Juncosa-Melvin et al., 2006). The majority of studies use tissue culture-expanded MSCs to treat tendon defects but the results are variable. Awad et al (Awad et al., 1999) examined the results of a full thickness patellar tendon defect repaired in rabbits using culture-expanded MSCs within a collagen gel. Compared to controls, the treatment group exhibited superior biomechanical properties but no differences in histological appearance. Juncosa-Melvin et al (Juncosa-Melvin et al., 2006) evaluated the results of a collagen sponge implanted with culture-expanded MSCs that was used to repair a full thickness patellar tendon defect in rabbits. At 12 weeks, there was no difference in cellularity between the MSC group and non-augmented controls. No fibrocartilage was found in either group and the biomechanical properties of the MSC group were superior.

The results from this experiment contrast the aforementioned studies in that both the histological and biomechanical outcomes were improved. This may be due to the increased amounts of BMPs present in DBM (Lovric et al., 2012) causing the locally applied mmMSC population to differentiate down osteoblastic, chondrocytic, and tenocytic lineages (Dorman et al., 2012, Liu et al., 2010, Gulati et al., 2013, Sun et al., 2015). The resultant interface resembled a direct enthesis containing organised fibrocartilage, and was able to resist the strong forces applied to it throughout the postoperative period without failure. Early postoperative weight bearing leading to

mechanotransduction may have contributed to this since applying load to a developing enthesis causes bone at the insertion site to mature, increases fibrocartilage formation, and improves collagen organisation (Thomopoulos et al., 2010). Together, these factors contribute to the formation of a direct enthesis capable of resisting physiological forces.

In this study, an ovine patellar tendon retraction model was used to assess tendon-bone healing with DBM augmentation to simulate the clinical condition of the repair of a retracted tendon. Despite this model not precisely representing chronic rotator cuff tears in the clinical setting due to the lack of degeneration associated with creating an acute tear, it does permit more objective measurements of functional recovery in a healing enthesis as the extensor mechanism in a sheep has no supporting subsidiary structures and is entirely dependent upon the attachment of the patellar tendon to the tibial tuberosity. Detachment of supraspinatus in a sheep, and other animal models, would have had a substantially lesser effect on gait function as other components of the rotator cuff could compensate for its loss (Halder et al., 2002). In this study the use of mmMSCs in the setting of tendon retraction is novel, but it is difficult to be certain of the precise number of cells implanted into each repair site and whether variation between each animal affected their proliferation and/or viability. Other limitations of this study are associated with the lack of a control group. However, not treating the tendon defect would have rendered the animals lame, and therefore the study unethical, since previous work has shown that spontaneous healing does not occur (Yokoya et al., 2008, Yokoya et al., 2012).

3.5 Conclusion

In conclusion, this is the first study to examine the effect of DBM used with mmMSCs on healing of a tendon-bone defect simulating tendon retraction. All animals were allowed unrestricted activity following surgery, which led to no failures. At 12 weeks, the tendon defect had successfully remodeled into tendon-like tissue and was accompanied by a direct enthesis. Functional weight bearing improved at all time points. Superior biomechanical and histological results were noted with the allogenic scaffold, highlighting DBM as a potential solution for the treatment of rotator cuff tears complicated by retraction.

In order to overcome the limitations associated with this work, the next chapter details the development of a small animal model of rotator cuff tendon degeneration akin to what is seen in the clinical setting. This clinically applicable model will subsequently be used to examine the effect of DBM on tendon-bone healing.

Chapter Four: Development of a Degenerative Rat Model of Rotator Cuff Tendon-Bone Healing

4.1 Introduction

Rotator cuff degeneration is common and can result in the development of tears which lead to degenerative changes in the muscle, bone, and tendon (Nho et al., 2008). Structural changes include retraction of the tendon away from the bone surface, muscle atrophy, reduced/increased cellularity, reduced/increased vascularity, fatty infiltration, calcification, and degeneration of the muscle (Loew et al., 2015, Nho et al., 2008). Degeneration can be initiated by a number of factors that are either intrinsic or extrinsic to the cuff itself. The degenerative-microtrauma model is the most important intrinsic factor and encompasses age-related degeneration compounded by repetitive microtrauma, eventually resulting in the development of a tear (Nho et al., 2008).

Extrinsic causes comprise both anatomical and environmental influences. The latter includes increasing age, shoulder overuse, smoking, and any medical condition that impairs the healing response such as diabetes mellitus (Nho et al., 2008). In contrast, abnormal acromial morphology has been highlighted as the principal anatomical variant inciting the degenerative process (Nho et al., 2008). This is characterised by a progressive change in the shape of the acromion (Type 1-flat, Type 2-curved, and Type 3-hooked) and ‘spurs’ forming at its antero-inferior margin. These changes narrow the subacromial space and abut the supraspinatus tendon as it passes below the coracoacromial arch, causing inflammation. This is most prominent during abduction and elevation of the arm and is referred to as the ‘painful arc’ or ‘impingement syndrome’ (Carr et al., 2015a). Delayed treatment may further propagate these

intrinsic and extrinsic processes and compromise repair strategies (Romeo et al., 1999).

Poor healing and recurrent tears frequently occur following repair of a degenerative rotator cuff and are associated with a poor functional outcome (Carr et al., 2015a). In order to accurately determine the effect of biological augmentation on healing, it is imperative to examine such strategies in a degenerative environment akin to what is observed in the clinical setting. Several animal models of tendon degeneration have been developed, but it is the rat's shoulder that seems to have gained the most popularity (Gerber et al., 2004, Buchmann et al., 2011). Advantages of using the rat as a surrogate for rotator cuff function include the presence of an arch-like structure that encloses supraspinatus (similar to the coracoacromial arch) and the high loads passing through the tendon. Alternatively, some primate models possess greater similarities in their anatomy to humans but due to their expense and restricted use, they are an impractical alternative (Soslowsky et al., 1996). Using a rat model, supraspinatus detachment has been shown to lead to degenerative changes comparable to those seen in the clinical setting: tendon degeneration, inflammation, and muscle atrophy combined with a persisting defect. These were most apparent after an interval of three weeks, with longer time points associated with complete closure of the defect (Buchmann et al., 2011).

In a large animal model of tendon retraction, Chapter Three of this thesis demonstrated that allogenic cortical DBM regenerated an enthesis with favorable histological and mechanical properties. This study was limited by the use of a non-degenerative model and so the aim of this chapter was to develop a rat model of

rotator cuff degeneration and assess the development of osteopenia at the bony insertion of supraspinatus following tendon detachment. Osteopenia of the humeral head occurs following a rotator cuff tear in humans and compromises fixation techniques where tendon is reattached to bone (Cadet et al., 2008). DBM induces bone formation by endochondral ossification and may be able to improve tendon-bone healing and reduce the rate of re-tears (Urist, 1965). The hypothesis was that detachment of supraspinatus from the humerus would result in tendon degeneration and osteopenia of the greater tuberosity in a rat model.

4.2 Materials and Methods

4.2.1 Study Design

All animal work was conducted in accordance with a Project License protocol accepted under the UK Home Office Animals (Scientific Procedures) Act 1986. Eighteen randomly allocated (using simple randomisation) female Wistar rats, which had not previously been subject to any experimentation, underwent unilateral detachment of the supraspinatus tendon. One surgeon carried out all procedures. Using a power calculation and previously published data, an n of 6 has been shown to provide a power of 0.8, which provides significance at p =0.05 (Sundar et al., 2009a). Animals were freely mobilised with cage mates and specimens were retrieved at three (n = 6), six (n = 6), and nine weeks (n = 6) postoperatively for histological analysis and pQCT. Euthanasia was carried out using carbon dioxide insufflation.

4.2.2 Surgical Technique

A chronic, degenerative full thickness rotator cuff tear model was developed from one that has previously been used to investigate tendon degeneration (Gulotta et al., 2009). Anaesthesia was induced and maintained using 2% Isoflurane mixed with pure oxygen via a facemask. The right shoulder was used for tendon detachment in all cases and the contralateral left shoulder served as a control. A 1.5 cm skin incision was made directly over the anterolateral border of the acromion. The deltoid was detached from the anterior, lateral, and posterior margins of the acromion and split caudally for 0.5 cm. The acromio-clavicular joint was divided and a traction suture

was placed around the clavicle to facilitate visualisation of supraspinatus (Figure 4.1A). The supraspinatus tendon was marked at its musculotendinous junction with a 5'0 prolene suture to assess retraction during tissue harvest. Under tension of the suture, the tendon was detached using sharp dissection from the greater tuberosity of the humeral head and allowed to retract medially (Figure 4.1B and 4.1C). The deltoid muscle and fascia were closed with 5'0 Vicryl suture (Ethicon, Johnson & Johnson Medical Ltd., Berkshire, UK). Skin closure was achieved using 5'0 Monocryl suture (Ethicon, Johnson & Johnson Medical Ltd., Berkshire, UK) and the animals were permitted unrestricted cage activity (Figure 4.1D). Postoperative pain was assessed daily and analgesia (intra-muscular buprenorphine 0.6 mg) was given every 12 hours for three days.

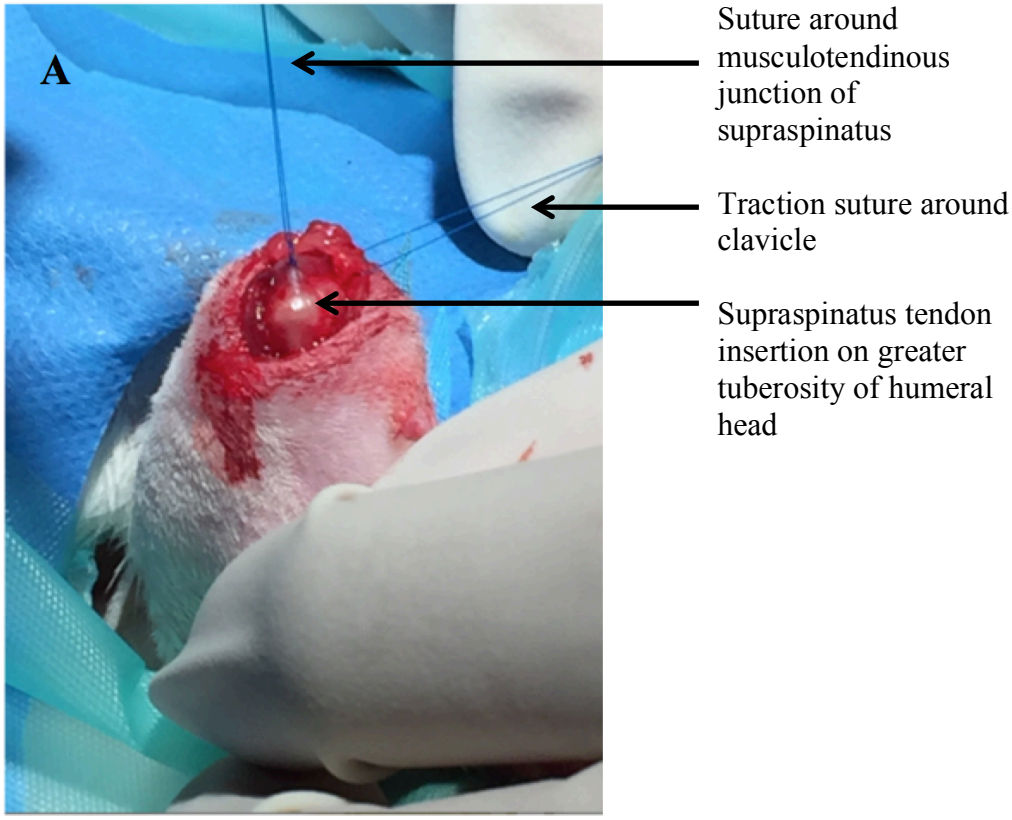

Figure 4.1A: Supraspinatus tendon insertion on the greater tuberosity.

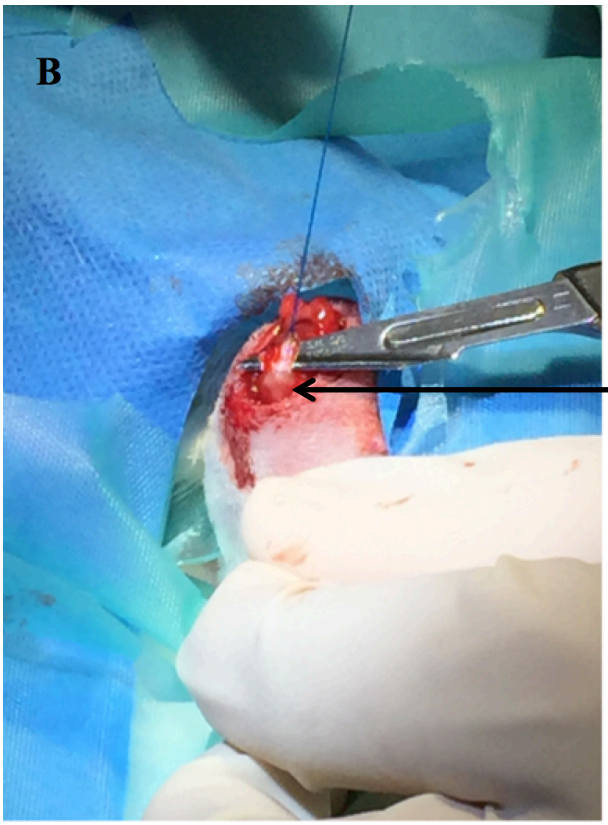

Figure 4.1B: Supraspinatus tendon detachment from greater tuberosity.

Figure 4.1C: Supraspinatus tendon stump following detachment.

Figure 4.1D: Surgical wound following closure.

4.2.3 Macroscopic Assessment

Animals were euthanised at three (n = 6), six (n = 6), and nine weeks (n = 6). Supraspinatus tendon-bone defects were classified as: persistent, partial, and completely closed.

4.2.4 pQCT

After sacrifice pQCT scanning was performed to measure bone mineral density at the humeral head. Using an XCT 2000 Bone Scanner (Stratec Medizintechnik Gmbh,

Germany) with Software version 6.20, 1 mm CT slices were taken through the humeral head and supraspinatus musculotendinous unit.

4.2.5 Histological Assessment

At euthanasia, the right shoulder was dissected and a specimen comprising the humerus with its attached supraspinatus musculotendinous unit was removed. The contralateral left shoulder served as a control (n = 6). Each sample was fixed in 10% formal saline and underwent decalcification in Ethylenediaminetetraacetic acid (EDTA), which was checked by radiography. The specimens were then processed in ascending graded alcohol dehydration followed by defatting in chloroform, and embedding in paraffin wax. Multiple sections were cut in the coronal plane through the humerus, enthesis, supraspinatus musculotendinous unit, and any scar tissue that filled the gap between tendon and bone. Using a Reichert-Jung Model 1130 microtome (Reichert-Jung, Vienna, Austria), these were used to make slides 4 micrometers (μm) thick before H&E staining. The process of sectioning samples was undertaken by Mr Frederick Henshaw (Undergraduate medical student, as part of an MSc Thesis, UCL, London, UK) under supervision.

Two blinded observers evaluated all sections using an Olympus BH-2 light microscope (Olympus, Glasgow, UK). Using a semi-quantitative scoring system (0 = none, 1 = mild, and 2 = severe), four high-powered fields were examined in each muscle to determine the extent of fatty infiltration, cellularity, and inflammation (Buchmann et al., 2011).

Tendon degeneration was assessed according to a modified Movin scale (Movin et al., 1997) and included the following variables: (1) fiber structure, (2) fiber arrangement, (3) rounding of the nuclei, (4) regional variations in cellularity, (5) increased vascularity, and (6) hyalinisation. A four-point scoring system was used: 0 = normal appearance, 1 = slightly abnormal appearance, 2 = a moderately abnormal appearance, and 3 = a markedly abnormal appearance (Longo et al., 2008). Based on this, the total score for any given slide could range from 0 (normal tendon) to 18 (the greatest level of degeneration).

4.2.6 Statistical Analysis

Nonparametric statistical methods were used for all analyses because of the non-normality of the data in the groups being compared. Numerical data were inputted into SPSS software package, version 23 (SPSS Inc, an IBM Company, Chicago, Illinois). Mann Whitney U tests were used to compare data between groups. Results were considered significant at the $p < 0.05$ level.

4.3 Results

All animals survived the duration of the study and none had post-operative infection. Limping was noted for the first three to five postoperative days but a normal gait pattern returned afterwards.

4.3.1 Macroscopic Findings

Scar tissue was noted in all animals. Based on the position of the suture marker, the supraspinatus tendon had retracted approximately 5 mm in all cases. The muscle belly of supraspinatus was atrophic and pale in appearance (Figure 4.2). Some degree of tendon-bone defect closure occurred in all animals at all time points. At three weeks, partial defect closure was evident in all cases. At six weeks, two animals had partial closure of the defect and four animals had complete closure. All animals in the nine-week group had complete closure of the tendon-bone defect (Figure 4.2). The contralateral control group demonstrated no gaps in the supraspinatus tendon-bone interface.

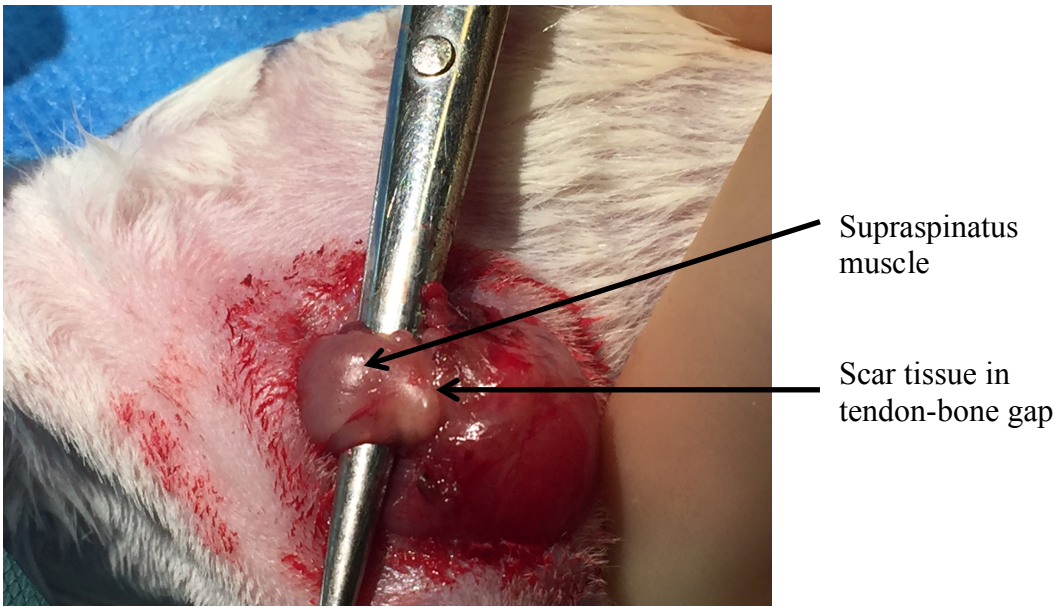

Figure 4.2: Scar tissue in supraspinatus tendon-bone gap at nine weeks following tendon detachment.

4.3.2 pQCT Scans

In controls (contralateral shoulder in which the supraspinatus had not been detached), the median total bone mineral density at the supraspinatus tendon-bone insertion was 793.25 mg/ccm (95% CI 754.24 to 844.70). This significantly decreased three, six, and nine weeks following tendon detachment to a median of 684.70 (95% CI 639.21 to 739.82) ($p = 0.006$), 642.85 (CI 610.74 to 711.33) ($p = 0.004$), and 665.20 mm/ccm (CI 594.01 to 763.62) ($p = 0.025$) respectively (Figure 4.3). No significant change in bone mineral density occurred between three, six, and nine weeks (Table 4.1).

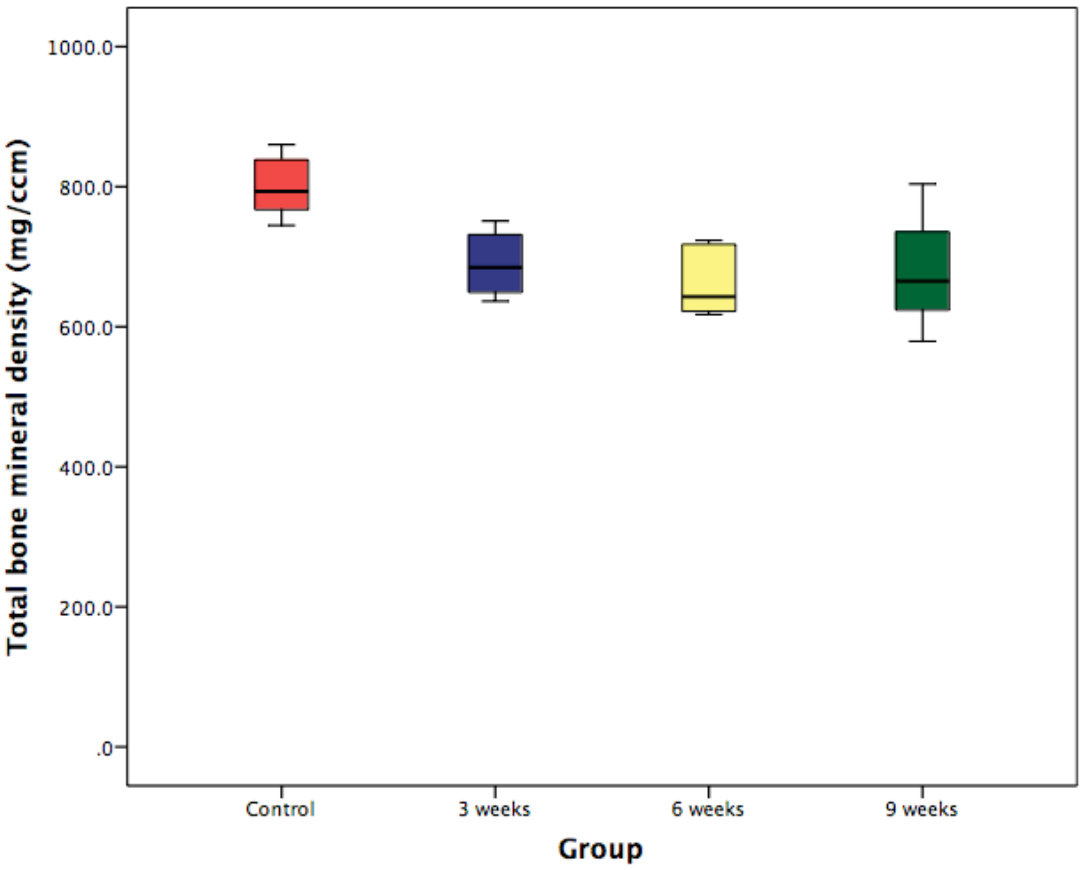

Figure 4.3: Box and whisker plot showing total bone mineral density at the supraspinatus tendon-bone insertion three, six, and nine weeks following tendon detachment.

	Control (non-operated shoulder) group (n = 6)	3 week group (n = 6)	6 week group (n = 6)	9 week group (n = 6)
Control (non-operated shoulder) group (n = 6)	-	0.006	0.004	0.025
3 week group (n = 6)	0.006	-	0.200	0.749
6 week group (n = 6)	0.004	0.200	-	0.631
9 week group (n = 6)	0.025	0.749	0.631	-

Table 4.1: Statistical significance (p-values) between total bone mineral density at the supraspinatus tendon-bone insertion three, six, and nine weeks following tendon detachment.

4.3.3 Histological Findings

4.3.3.1 Muscle Evaluation

A loss of muscle mass was observed at all time points, and was accompanied by degenerative changes (characterised by increased amounts of fibrotic tissue) that were most prominent three weeks after detachment and less evident by nine weeks. No inflammatory changes were present in any of the specimens. All groups demonstrated a degree of fatty infiltration, which peaked at three weeks (Figure 4.4). Compared to controls (where there was no fatty infiltration present) fatty infiltration significantly increased to a median score of 0.5 (95% CI 0.40 to 0.94) (p = 0.002) at three weeks

but reduced to a median score of 0 at six- (95% CI -0.19 to 0.69) (p = 0.140) and nine weeks (95% CI -0.10 to 0.44) (p = 0.138) (Table 4.2) (Figure 4.5).

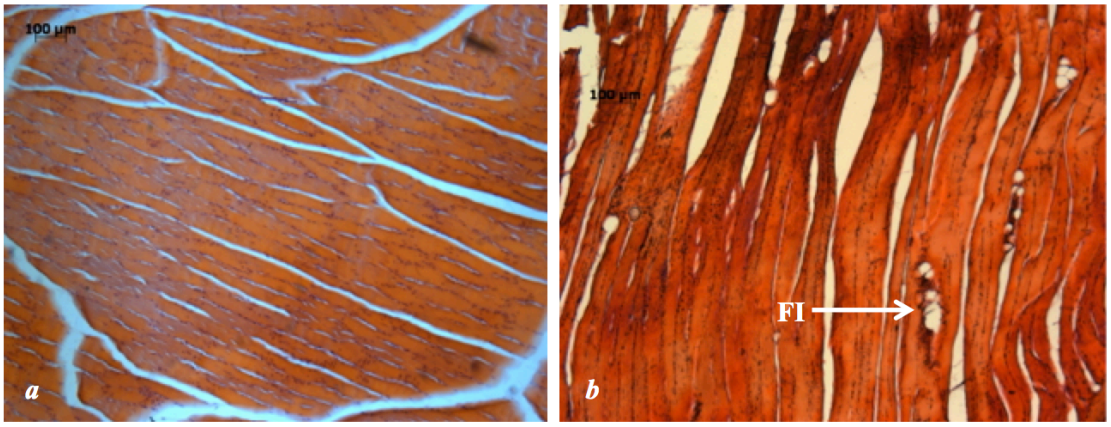

Figure 4.4: Photomicrograph showing fatty infiltration within the supraspinatus muscle belly. (a) Control: no fatty infiltration. (b) Three-week specimen: fatty infiltration (FI).

	Control (non-operated shoulder) group (n = 6)	3 week group (n = 6)	6 week group (n = 6)	9 week group (n = 6)
Control (non-operated shoulder) group (n = 6)	-	0.002	0.140	0.138
3 week group (n = 6)	0.002	-	0.061	0.014
6 week group (n = 6)	0.140	0.061	-	0.847
9 week group (n = 6)	0.138	0.014	0.847	-

Table 4.2: Statistical significance (p-values) between the level of fatty infiltration three, six, and nine weeks after tendon detachment.

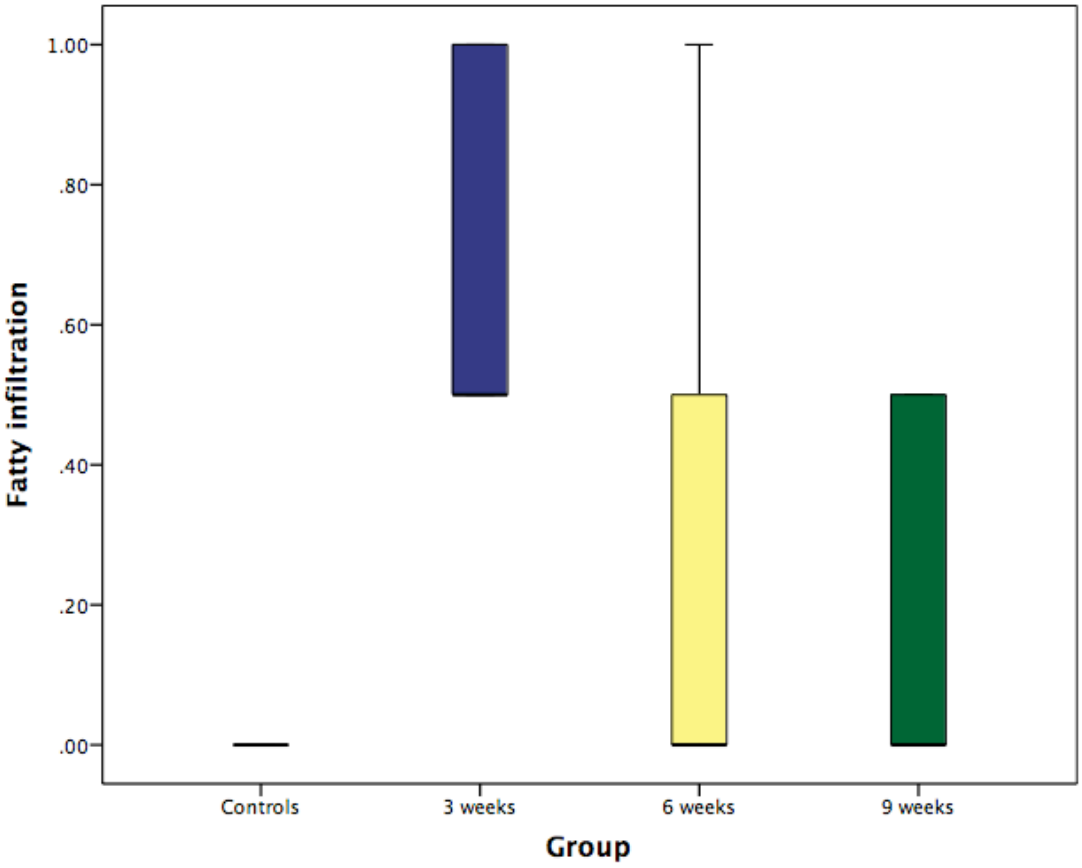

Figure 4.5: Box and whisker plot demonstrating fatty infiltration within the supraspinatus muscle three, six, and nine weeks after tendon detachment.

Cellularity significantly increased at all time-points compared to controls: all control specimens exhibited a normal appearance and therefore scored 0. Compared to controls, cellularity reached a median of 2 (95% CI 2 to 2) at three weeks ($p = 0.001$), 1 (95% CI 0.91 to 1.69) ($p = 0.002$) at six weeks, and 1.5 (95% CI 1.02 to 1.81) ($p = 0.002$) at nine weeks (Table 4.3) (Figure 4.6). Furthermore, cellularity was significantly greater in the three-week group than in the six- and nine-week groups.

	Control (non-operated shoulder) group (n = 6)	3 week group (n = 6)	6 week group (n = 6)	9 week group (n = 6)
Control (non-operated shoulder) group (n = 6)	-	0.001	0.002	0.002
3 week group (n = 6)	0.001	-	0.006	0.007
6 week group (n = 6)	0.002	0.006	-	0.382
9 week group (n = 6)	0.002	0.007	0.382	-

Table 4.3: Statistical significance (p-values) between the level of cellularity three, six, and nine weeks following tendon detachment.

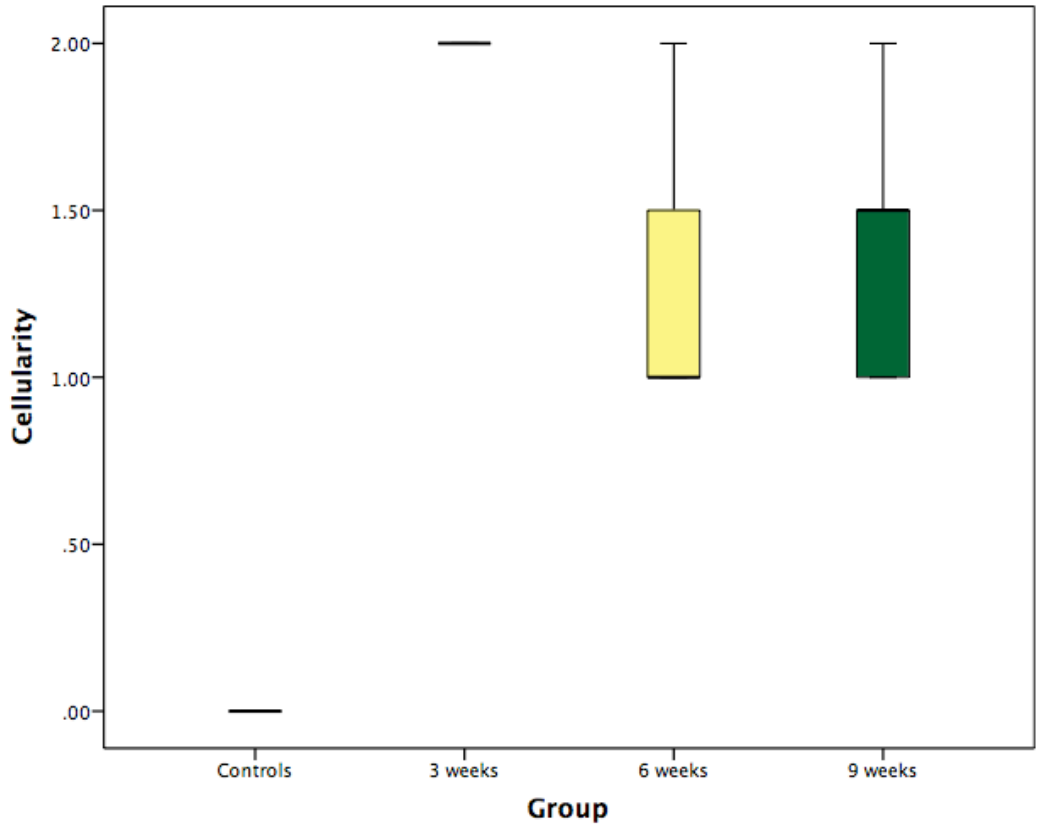

Figure 4.6: Box and whisker plot demonstrating the change in cellularity within the supraspinatus muscle three, six, and nine weeks following tendon detachment.

4.3.3.2 Tendon Evaluation

4.3.3.2.1 Modified Movin Score

The modified Movin score was significantly higher (indicating degeneration) in the three experimental groups compared to the controls ($p = 0.003$: three, six, and nine weeks after supraspinatus tendon detachment) (Table 4.4) (Figure 4.7). Tendon degeneration was most noticeable three weeks after detachment. The median modified Movin score was 0 (95% CI -0.27 to 0.60) in the controls, 8.75 (95% CI 7.08 to 11.26) at three weeks, 7.75 (95% CI 6.45 to 9.38) at six weeks, and 8 (95% CI 7.53 to 9.87) at nine weeks. There were no significant inter-group differences.

	Control (non-operated shoulder) group (n = 6)	3 week group (n = 6)	6 week group (n = 6)	9 week group (n = 6)
Control (non-operated shoulder) group (n = 6)	-	0.003	0.003	0.003
3 week group (n = 6)	0.003	-	0.256	0.326
6 week group (n = 6)	0.003	0.256	-	0.513
9 week group (n = 6)	0.003	0.326	0.513	-

Table 4.4: Statistical significance (p-values) between modified Movin scores three, six, and nine weeks following tendon detachment.

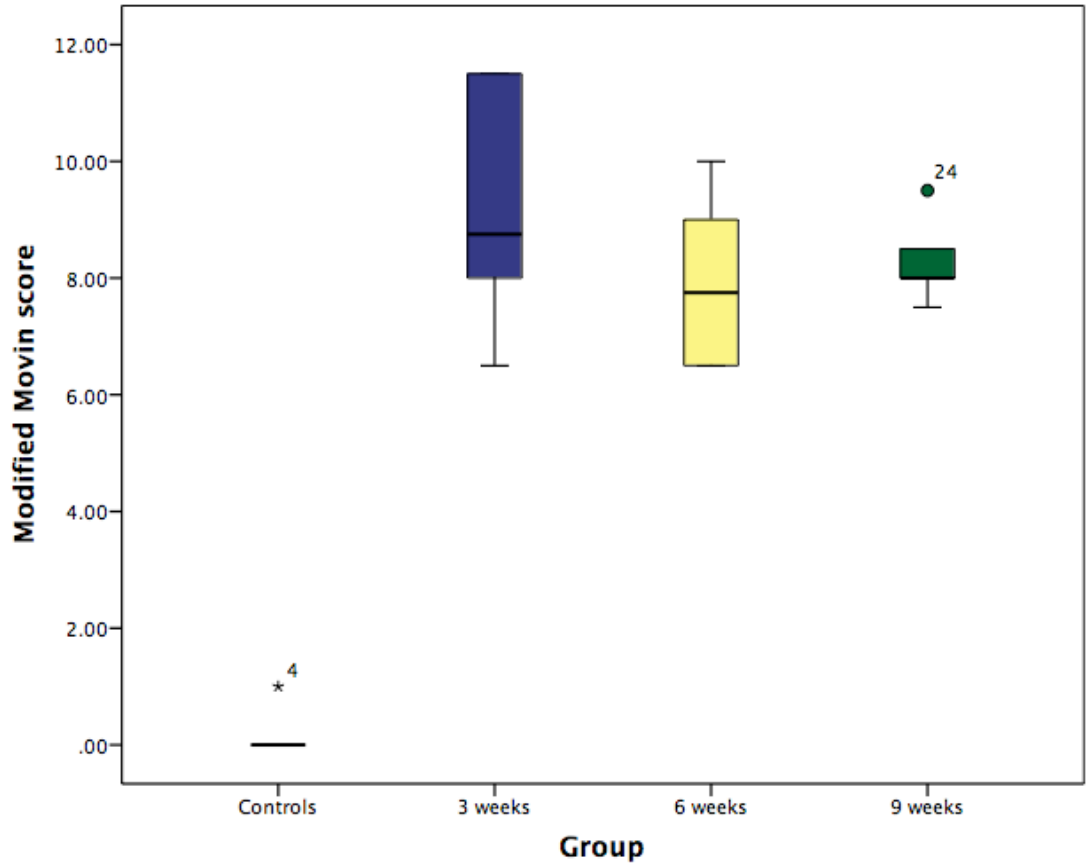

Figure 4.7: Box and whisker plot illustrating the modified Movin scores three, six, and nine weeks following tendon detachment.

4.3.3.2.2 Fiber Structure

In control specimens, collagen fibers were close together and arranged in parallel. Loss of this uniform structure (increased waviness and distance between fibers) to differing degrees characterised abnormal specimens (Figure 4.8). The median scores were 0 (95% CI 0 to 0) for the control tendons, 2 (95% CI 1.56 to 2.10) for the three-week group, 1.75 (95% CI 1.40 to 2.26) for the six-week group, and 2.5 (95% CI 2.40 to 2.94) for the nine-week group. Fiber structure was significantly more abnormal in

the nine-week group compared to the three- ($p = 0.003$) and six-week groups ($p = 0.007$) (Table 4.5) (Figure 4.9).

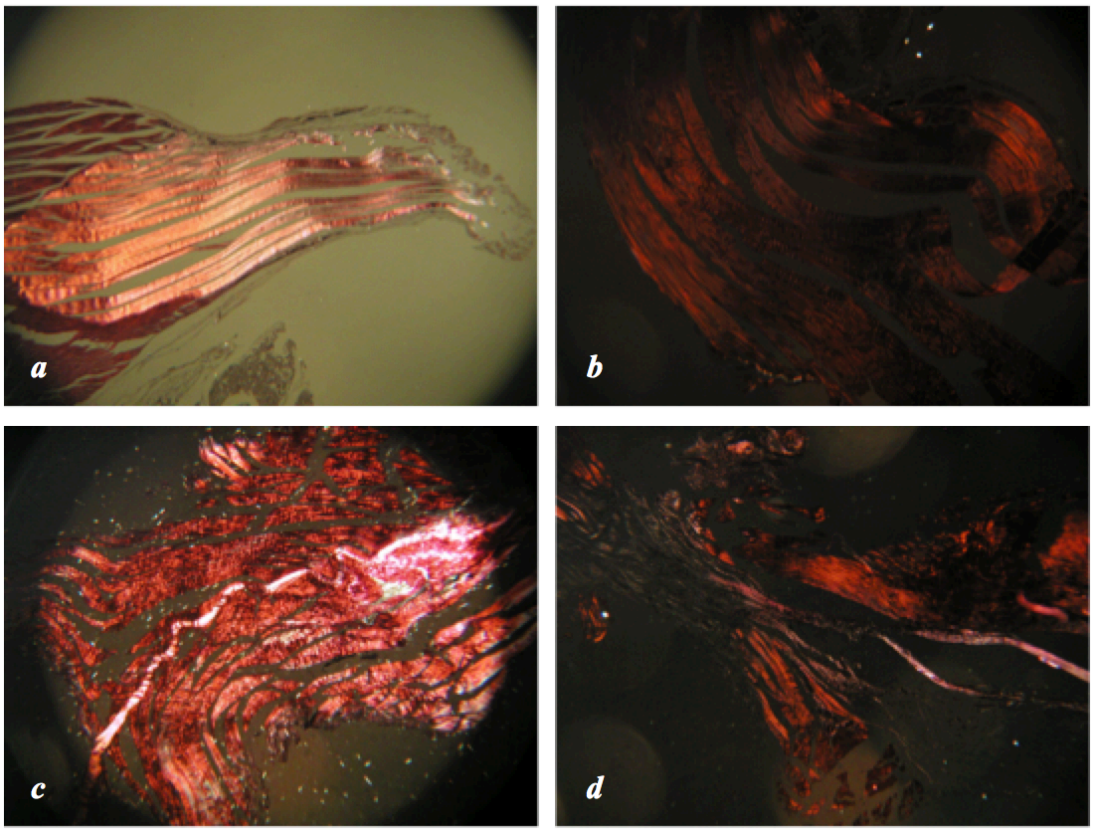

Figure 4.8: Photomicrograph (under polarised light) showing collagen fiber structure. (a) Controls. (b) Three-week group. (c) Six-week group. (d) Nine-week group.

	Control (non-operated shoulder) group (n = 6)	3 week group (n = 6)	6 week group (n = 6)	9 week group (n = 6)
Control (non-operated shoulder) group (n = 6)	-	0	0	0
3 week group (n = 6)	0.002	-	0.859	0.003
6 week group (n = 6)	0.002	0.859	-	0.007
9 week group (n = 6)	0.002	0.003	0.007	-

Table 4.5: Statistical significance (p-values) between fiber structure three, six, and nine weeks following tendon detachment.

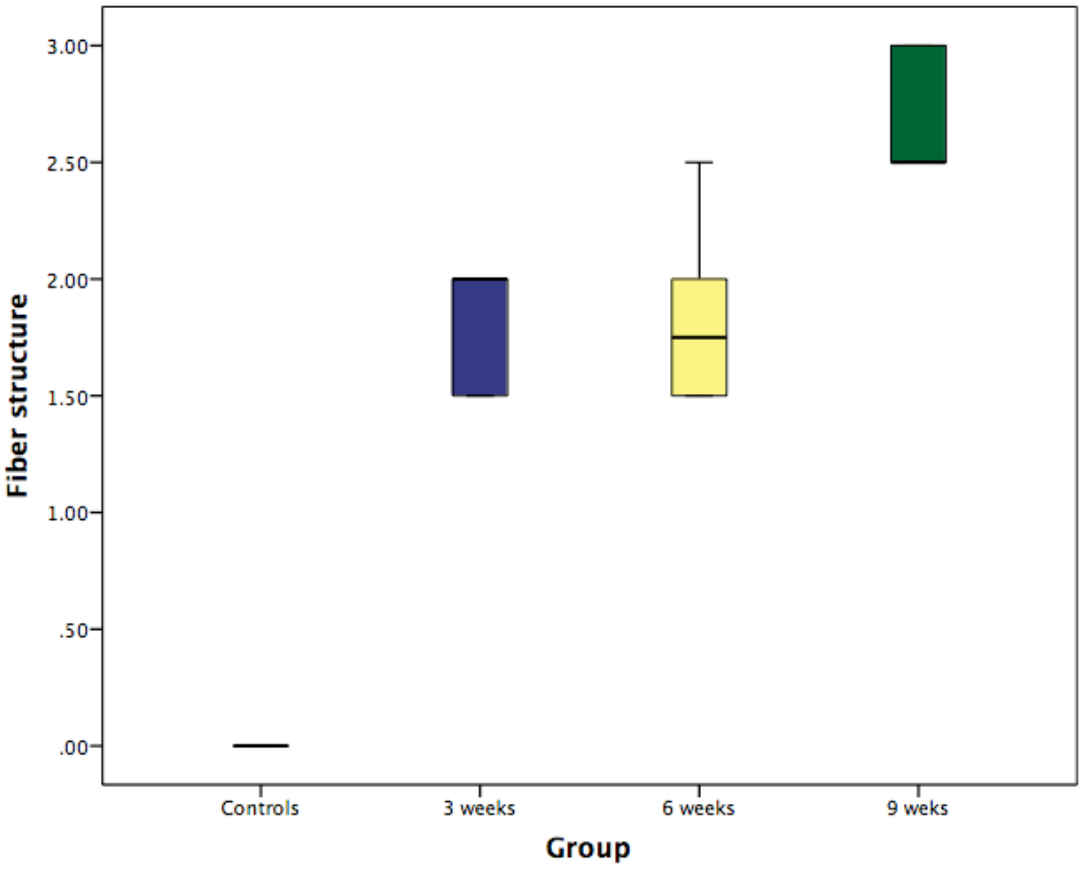

Figure 4.9: Box and whisker plot illustrating the difference in fiber structure three, six, and nine weeks following tendon detachment.

4.3.3.2.3 Fiber Arrangement

In control specimens, the fibers were arranged in parallel. Loss of this arrangement to differing degrees characterised abnormal specimens (Figure 4.8). The median scores were 0 (95% CI 0 to 0) for the control tendons, 2 (95% CI 1.52 to 2.31) for the three-week group, 1.5 (95% CI 1.20 to 1.63) for the six-week group, and 1.5 (95% CI 1.02 to 1.81) for the nine-week group. Fiber arrangement was significantly more abnormal in the three-week group compared to the controls ($p = 0.002$), the six-week group ($p = 0.001$), and the nine-week group ($p = 0.002$) (Table 4.6) (Figure 5.0).

	Control (non-operated shoulder) group (n = 6)	3 week group (n = 6)	6 week group (n = 6)	9 week group (n = 6)
Control (non-operated shoulder) group (n = 6)	-	0.002	0.001	0.002
3 week group (n = 6)	0.002	-	0.019	0.051
6 week group (n = 6)	0.001	0.019	-	0.923
9 week group (n = 6)	0.002	0.051	0.923	-

Table 4.6: Statistical significance (p-values) between fiber arrangement three, six, and nine weeks following tendon detachment.

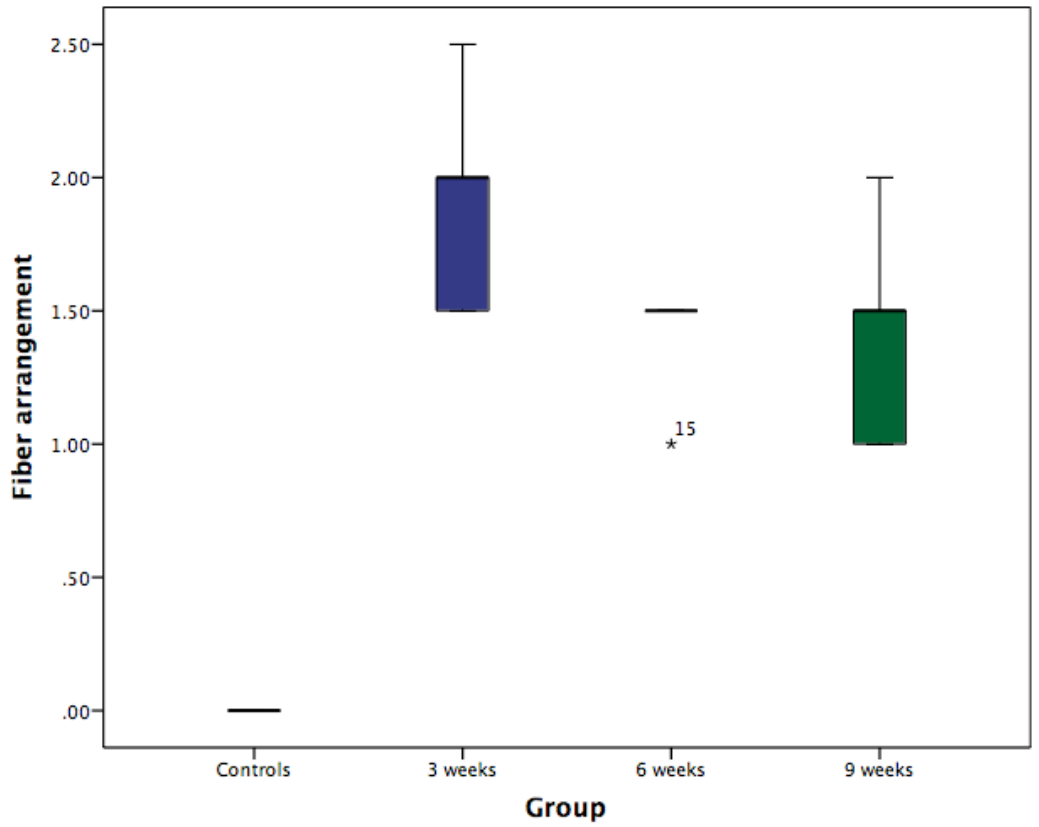

Figure 5.0: Box and whisker plot illustrating the difference in fiber arrangement three, six, and nine weeks following tendon detachment.

4.3.3.2.4 Tenocyte Nuclei

Tenocyte nuclei were flattened and spindle-shaped in control specimens, but following tendon detachment became more rounded (Figure 5.1). The median scores were 0 (95% CI – 0.13 to 0.30) for the control tendons, 2.50 (95% CI 2.06 to 2.60) for the three-week group, 1.75 (95% CI 1.40 to 2.26) for the six-week group, and 2 (95% CI 1.56 to 2.10) for the nine-week group. Tenocyte nuclei were significantly more abnormal than controls following tendon detachment ($p = 0.002$ at three-, $p = 0.003$ at

six-, and p = 0.002 at nine weeks), with the three-week group demonstrating more abnormal rounded nuclei than the six- and nine-week groups (Table 4.7) (Figure 5.2).

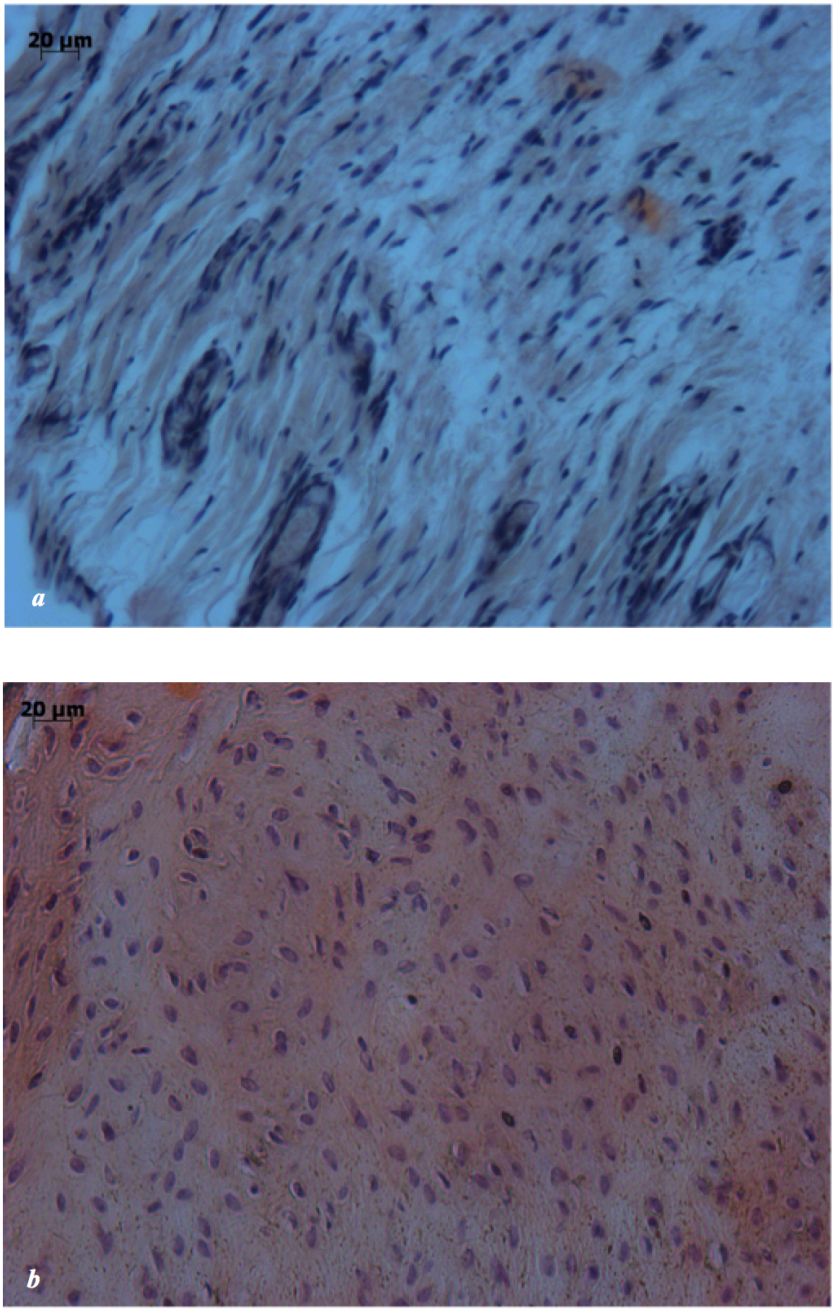

Figure 5.1: Photomicrograph illustrating flattened and spindle-shaped nuclei in controls (a), and rounded nuclei three weeks after tendon detachment (b).

	Control (non-operated shoulder) group (n = 6)	3 week group (n = 6)	6 week group (n = 6)	9 week group (n = 6)
Control (non-operated shoulder) group (n = 6)	-	0.002	0.003	0.002
3 week group (n = 6)	0.002	-	0.041	0.014
6 week group (n = 6)	0.003	0.041	-	0.859
9 week group (n = 6)	0.002	0.014	0.859	-

Table 4.7: Statistical significance (p-values) between tenocyte nuclei morphology three, six, and nine weeks following tendon detachment.

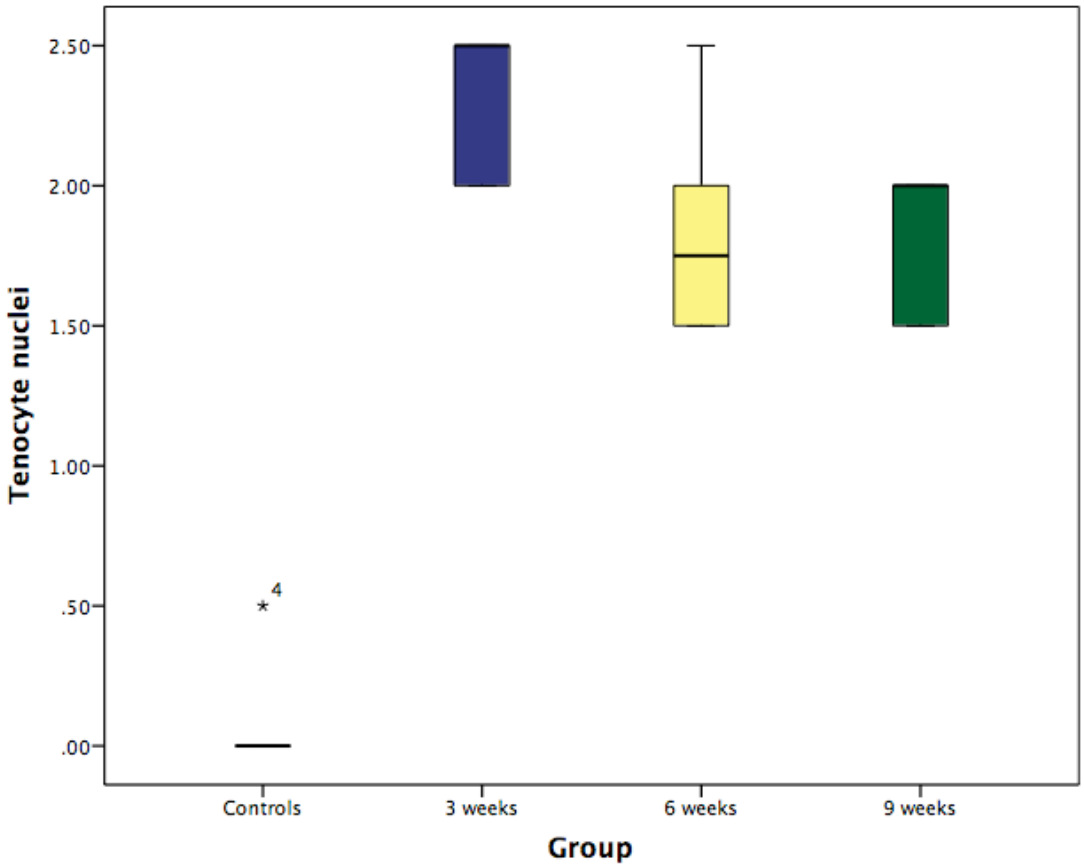

Figure 5.2: Box and whisker plot illustrating the difference between tenocyte nuclei morphology three, six, and nine weeks following tendon detachment.

4.3.3.2.5 Cellularity

Specimens were evaluated for an increase in cellularity. The median scores were 0 (95% CI -0.13 to 0.30) for the control tendons, 1.25 (95% CI 0.84 to 2.16) for the three-week group, 1.75 (95% CI 1.40 to 2.26) for the six-week group, and 1.75 (95% CI 1.46 to 2.03) for the nine-week group. There was a significant increase in cellularity following tendon detachment ($p = 0.003$ at three, $p = 0.003$ at six, and $p = 0.002$ at nine-weeks), however there were no significant differences between experimental groups (Table 4.8) (Figure 5.3).

	Control (non-operated shoulder) group (n = 6)	3 week group (n = 6)	6 week group (n = 6)	9 week group (n = 6)
Control (non-operated shoulder) group (n = 6)	-	0.003	0.003	0.002
3 week group (n = 6)	0.003	-	0.246	0.315
6 week group (n = 6)	0.003	0.246	-	0.789
9 week group (n = 6)	0.002	0.315	0.789	-

Table 4.8: Statistical significance (p-values) between cellularity three, six, and nine weeks following tendon detachment.

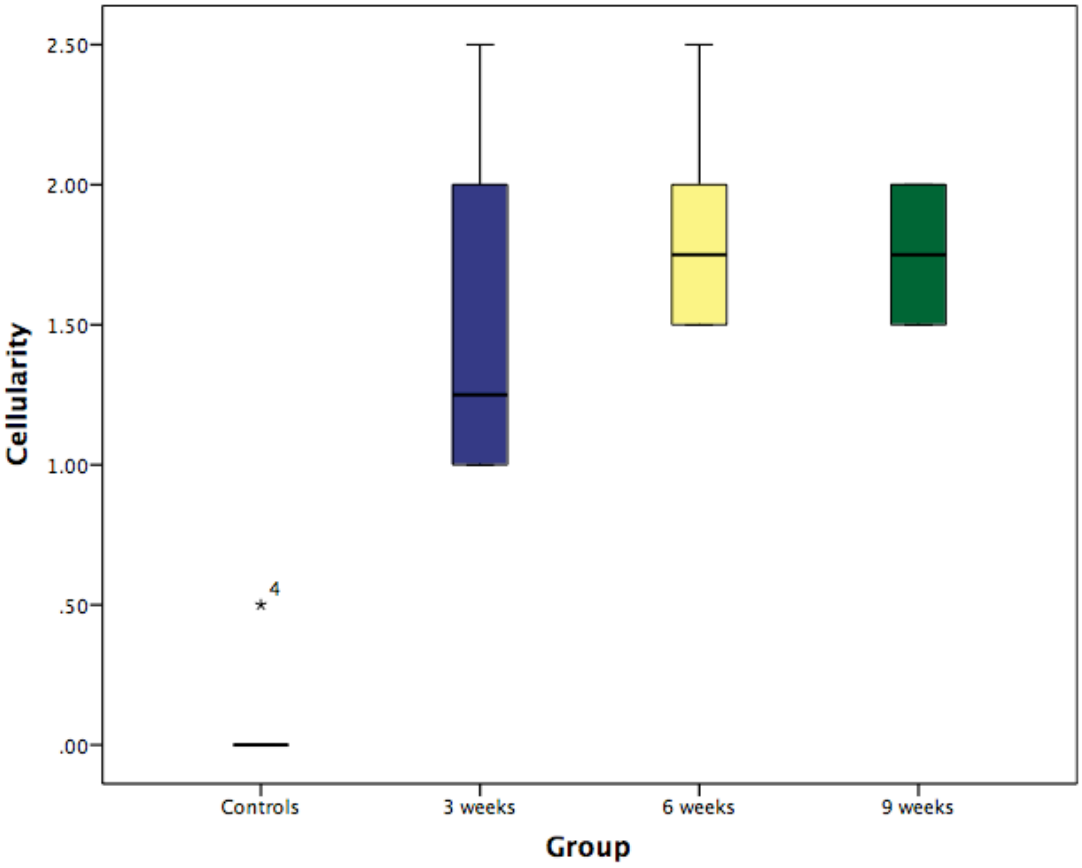

Figure 5.3: Box and whisker plot illustrating the difference in cellularity three, six, and nine weeks following tendon detachment.

4.3.3.2.6 Vascularity

Vascular bundles run with collagen fibers and increase in number with degeneration (Longo et al., 2008). The median scores were 0 (95% CI 0 to 0) for the control tendons, 1.5 (95% CI 0.68 to 2.49) for the three-week group, 1 (95% CI 0.53 to 1.47) for the six-week group, and 0.5 (95% CI 0.67 to 1.10) for the nine-week group. The number of vascular bundles significantly increased at three- ($p = 0.002$), six- ($p = 0.002$), and nine-weeks ($p = 0.006$) following supraspinatus detachment (Table 4.9)

(Figure 5.4). A significant reduction in vascularity was noted between three- and nine-weeks ($p = 0.030$).

	Control (non-operated shoulder) group (n = 6)	3 week group (n = 6)	6 week group (n = 6)	9 week group (n = 6)
Control (non-operated shoulder) group (n = 6)	-	0.002	0	0.006
3 week group (n = 6)	0.002	-	0.249	0.030
6 week group (n = 6)	0.002	0.249	-	0.120
9 week group (n = 6)	0.006	0.030	0.120	-

Table 4.9: Statistical significance (p-values) in vascularity three, six, and nine weeks following tendon detachment.

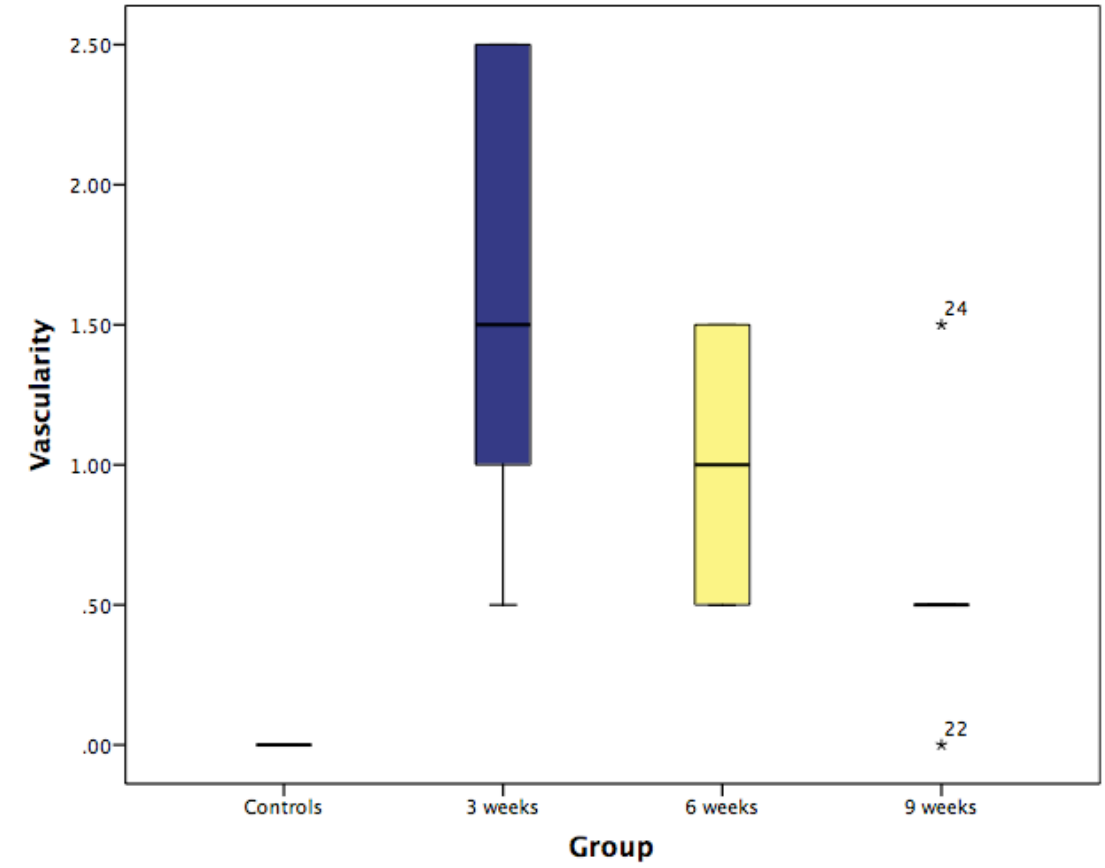

Figure 5.4: Box and whisker plot illustrating the difference in vascularity three, six, and nine weeks following tendon detachment.

4.3.3.2.7 Hyalinisation

Hyalinisation was not observed in any of the specimens.

4.4 Discussion

This study presents a rat model for the investigation of chronic rotator cuff tears. Following detachment of supraspinatus there was a significant rise in the modified Movin score characterised by a loss of muscle mass, fatty infiltration, an increase in musculotendinous cellularity, loss of normal collagen fiber structure/arrangement, rounded tenocyte nuclei, and an increase in the number of vascular bundles. The hypothesis was that tendon detachment would induce supraspinatus musculotendinous degeneration and a reduction in bone mineral density at the enthesis. The results support this, and demonstrate that these changes occur acutely after three weeks duration. However, after this time period, defect closure occurs and results in complete closure at nine weeks. Contrary to previous reports, fatty infiltration was present in muscle specimens at three-weeks but was no longer evident during the latter stages of the study (Buchmann et al., 2011, Barton et al., 2005). These transient changes suggest that with time, there is gradual reconstitution of the tendon-bone interface with fibrous tissue that permits the transfer of load and subsequent remodeling of this neo-enthesis into a tendon-like structure (Barton et al., 2005, Gimbel et al., 2004).

Chronic rotator cuff tears are characterised by retraction, muscle atrophy, reduced/increased cellularity, reduced/increased vascularity, fatty infiltration, calcification, and degeneration of the muscle (Loew et al., 2015, Nho et al., 2008). Several animal models have been developed to reproduce the aforementioned pathological changes but it is the structure and function of the rat's shoulder that most reliably resembles the human rotator cuff. Specifically, the rat possesses a bony arch

comprising the acromion, coracoid, and clavicle through which the supraspinatus tendon passes during movement (Soslowsky et al., 1996). Furthermore, following rotator cuff detachment in a rat the musculotendinous unit undergoes retraction, increased stiffness, and an increase in passive tension (Gimbel et al., 2004, Hersche and Gerber, 1998).

Buchmann et al (Buchmann et al., 2011) performed complete detachment of the supraspinatus tendon in Sprague-Dawley rats and analysed the results after three, six, and nine weeks. The three-week group demonstrated the highest rate of persistent defects and muscle atrophy, whereas the nine-week group exhibited the greatest degree of tendon degeneration and defect closure. Although fatty infiltration was found in some animals, this was not significantly greater than in control specimens. Using a similar model, Barton et al (Barton et al., 2005) examined muscle mass, morphology, and fiber properties. Tendon detachment resulted in a reduction in muscle mass, an increase in the proportion of fast twitch muscle fibers, and an increase in fibrous tissue. At 16-weeks post detachment, muscle mass and fiber properties returned to normal parameters. This acute degenerative response to tendon detachment followed by rapid histological recovery has also been demonstrated in other studies examining the rat model of a chronic rotator cuff tear (Gimbel et al., 2004, Dourte et al., 2010).

Fatty infiltration into the rotator cuff is irreversible and represents an important predisposing factor to repair failure and poor functional outcomes (Deniz et al., 2014). Current rodent models have been unable to establish a significant amount of fat accumulation following tendon detachment, making it difficult to specifically

examine hypotheses related to it (Buchmann et al., 2011, Barton et al., 2005). In this study, there was a significant amount of fatty accumulation into the muscle belly of supraspinatus compared to controls, peaking at three-weeks following tendon detachment and subsiding thereafter. This novel finding may be associated with fundamental inter-species differences between the Wistar rats used in this study and the Sprague-Dawley rats used in others (Buchmann et al., 2011, Barton et al., 2005). Lipoprotein lipase catalyses the hydrolysis of triglycerides and is highly expressed in skeletal tissues. It is regulated differently between Wistar and Sprague-Dawley rats and may account for the lack of fat accumulation in otherwise degenerative muscle tissue in some studies (Galan et al., 1993).

Rotator cuff tears can cause osteopenia at the enthesis due to a loss of physical stimuli (Oh et al., 2014b, Meyer et al., 2004a). During surgery, suture anchors are inserted into the greater tuberosity and therefore any reduction in bone mineral density may cause loosening or pullout before adequate tendon-bone healing can occur (Tingart et al., 2003). Accordingly, this has been recognised to be an independent risk factor predictive of healing, with a higher bone mineral density resulting in better outcomes (Cadet et al., 2008, Chung et al., 2011). The majority of studies ascribe this alteration in bone mineral density to attritional changes secondary to tendon damage, but it is plausible that they may precede the tear and be causative in nature (Chen et al., 2015). In order to examine biological strategies that specifically address bone quality it is imperative that there are suitable animal models available. While the anatomical similarities between the rat and human rotator cuff have been extensively described, there have been no studies to-date evaluating the onset of osteopenia in the rat. This prevents examination of hypotheses directly related to bone mineral density and

strategies targeted towards it. In this study, supraspinatus detachment caused a reduction in bone mineral density at three-, six-, and nine-weeks with no significant change between successive time-points. This may have occurred as a result of a reduction in the forces borne by the greater tuberosity following tendon injury, thus causing an imbalance in bone turnover, favoring bone resorption over bone formation: a principle governed by Wolff's law (Cadet et al., 2008).

Limitations of this study include the small number of specimens tested in each group and that only selected areas in the humeral head were analysed for bone mineral density analysis. Additional time points (two and 12 weeks) would have been beneficial to evaluate the progression and further resolution of degenerative musculotendinous changes, and alterations in bone mineral density. Subtle variations in the degree of rotation of the affected shoulder at the time of pQCT may contribute to minor differences in calculated bone mineral density scores. Given that all animals were limping during the immediate postoperative period, the enthesis of the contra-lateral shoulder may have been influenced by the increased tensile loading, and thus may not have represented the most suitable control.

4.5 Conclusion

In conclusion, this study has determined that three weeks following detachment, the supraspinatus musculotendinous unit in a rat undergoes degeneration, and the greater tuberosity exhibits a reduction in bone mineral density. These changes are similar to those that occur in the clinical setting following a chronic rotator cuff tear, with the difference that scar tissue bridges the defect in a rat whereas in a human the tendon-bone gap is largely maintained.

The results of this chapter indicate that for investigating biological strategies targeted towards improving chronic rotator cuff tendon-bone healing, the detached supraspinatus after three weeks represents a suitable surrogate. The next chapter utilises this model and applies DBM to the healing enthesis three weeks after supraspinatus detachment.

Chapter Five: The Effectiveness of Demineralised Cortical Bone Matrix in a Degenerative Rotator Cuff Repair Model

5.1 Introduction

Tendon-bone healing is an important factor affecting the outcome of rotator cuff repair (Gulotta et al., 2009). Anatomical reattachment of the rotator cuff to its bony insertion is crucial, but musculotendinous degeneration compromises tissue quality and challenges even the most well-performed repair (Nho et al., 2008). In order to facilitate the transmission of forces between tendon and bone, the native enthesis comprises four histological zones arranged in a graded structure (tendon, demineralised fibrocartilage, mineralised fibrocartilage, and bone) (Thomopoulos et al., 2010). Following injury, this is replaced by a weak fibrovascular bridge with inferior biomechanical properties, which renders it prone to rupture (Liu and Baker, 1994, Carpenter et al., 1998, Harryman et al., 1991).

DBM is made up of a collagen scaffold containing several growth factors conducive to endochondral ossification, and has been demonstrated to regenerate an enthesis with favorable histological and mechanical properties (Urist, 1965, Pietrzak et al., 2012, Sundar et al., 2009a). Chapter Three has further illustrated the capacity of DBM to enhance tendon-bone healing in the presence of severe acute retraction. However, this study was undertaken in a non-degenerative large animal model and so its results have limited clinical application since the majority of rotator cuff tears are degenerative (Yamaguchi et al., 2006). To overcome this problem, a chronic rotator cuff tear model was developed in Chapter Four. This study established that degenerative changes were most prominent three weeks after supraspinatus tendon detachment. Osteopenia was evident at this time point and has been identified as a critical factor affecting the quality of tendon-bone fixation as it reduces the pullout

strength of suture anchors that are used as the basis of most repairs (Cadet et al., 2008). In this context, DBM may be able to improve the quality of fixation by inducing new bone formation through a cartilaginous precursor (Urist, 1965).

The aim of this chapter was to assess the effect of DBM on regeneration of a degenerative rotator cuff tear using the model presented in Chapter Four. DBM has previously not been compared to a commercially available augmentation strategy, and so in this study GraftJacket (Wright Medical Technology, Inc., Arlington, TN) was used as an alternative scaffold. GraftJacket is obtained from donated human cadaveric dermal tissue processed to remove its cellular components whilst retaining its ECM. Its acellularity has the advantage of not causing a host inflammatory reaction and it has been safely used in rats to enhance healing of a large acute rotator cuff tear (Ide et al., 2009c). The hypothesis was that compared to a commercially available scaffold (GraftJacket), DBM will result in a higher bone mineral density and regenerate a morphologically superior enthesis characterised by greater fibrocartilage formation and improved collagen fiber organisation, in a rat model of chronic rotator cuff degeneration.

5.2 Materials and Methods

5.2.1 Study Design

All animal work was conducted in accordance with a Project License protocol accepted under the UK Home Office Animals (Scientific Procedures) Act 1986. Eighteen female Wistar rats underwent unilateral detachment of the supraspinatus tendon. Three weeks later, tendon repair was carried out in three groups of randomised animals: Group 1 received augmentation of the repair with cortical allogenic DBM (n = 6); Group 2 received augmentation with non-meshed, ultra-thick GraftJacket (average 1.4 mm thickness) (n = 6); and Group 3 underwent tendon-bone repair without augmentation (n = 6). Using a power calculation and previously published data, an n of 6 has been shown to provide a power of 0.8, which provides significance at p =0.05 (Sundar et al., 2009a). One surgeon carried out all the procedures. Animals were allowed free mobilisation. Specimens were retrieved six weeks after tendon reattachment for histological analysis and pQCT to evaluate bone mineral density at the tendon insertion, reversal of degenerative changes within the tendon, and histological remodeling of the implanted scaffold.

5.2.2 DBM Manufacture

DBM derived from cortical bone was manufactured according to Urist's protocol, with modifications (Urist, 1965). Tibiae of skeletally mature female Wistar rats were harvested immediately post euthanasia; all soft tissues and periosteum were stripped

from the bone surface. Bones measuring approximately 30 mm length by 3 mm width were demineralised in 0.6 *N* HCL at room temperature. Demineralisation was confirmed by taking radiographs (300 seconds, 30 kV, Faxitron Corporation, Illinois, USA). This was followed by washing in PBS until the pH was 7.4 +/- 0.1. Samples were stored at -20˚C for two hours and moved to a lyophiliser (Edwards Girovac Ltd, Crawley, West Sussex, UK) for three days. Specimens were sealed in individual plastic bags, sterilised by gamma irradiation at a dose of 25 kilograys (Isotron Limited, Reading, UK), and stored at -20˚C. Samples were rehydrated at the time of surgery in normal saline for 30 minutes prior to use.

5.2.3 GraftJacket

For this study, non-meshed, ultra-thick GraftJacket (average 1.4 mm thickness) was used (Figure 5.1). Samples were rehydrated at the time of surgery in normal saline for 30 minutes prior to use.

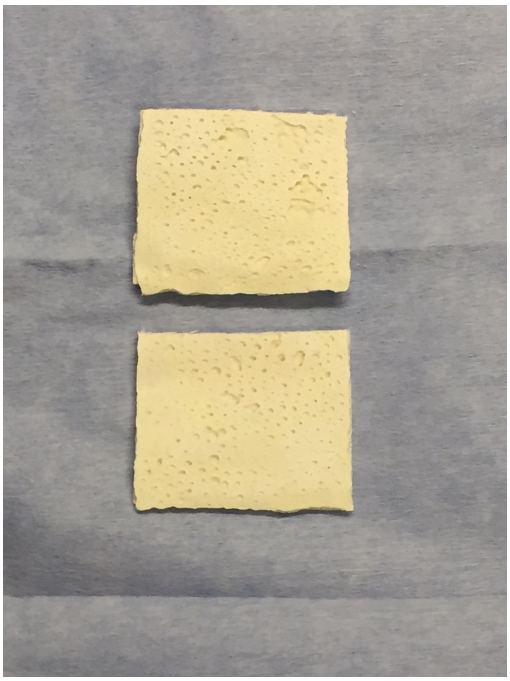

Figure 5.1: Two strips of GraftJacket measuring 1 cm by 1 cm.

5.2.4 Surgical Technique

Two surgeries were performed on each animal: full-thickness supraspinatus tendon detachment and complete tendon reattachment (Figure 5.2). Anaesthesia was induced and maintained using 2% Isoflurane mixed with pure oxygen via a facemask. The right shoulder was operated on in all cases. Tendon detachment was performed as outlined in Chapter Four (section 4.2.2). The second surgery to reattach the tendon was undertaken three weeks after the first procedure. Prior to making the skin incision, the scaffold (DBM or GraftJacket) was rehydrated for 30 minutes in sterile normal saline at the operating table.

A 2 cm skin incision was made in line with the supraspinatus muscle belly, ending anterior to the lateral end of the clavicle. This approach was perpendicular to the incision used for tendon detachment in order to utilise a virgin anatomical plane devoid of scar tissue. The muscle belly of supraspinatus was identified and followed distally to reveal the tendon stump with the suture marker in the musculotendinous junction. Scar tissue was excised and the tendon was grasped using a double-armed 5'0 prolene (Ethicon, Johnson & Johnson Medical Ltd., Berkshire, UK) modified Mason-Allen suture technique (Thomopoulos et al., 2002). Despite traction on the tendon stump, it could not be directly brought back to the humeral head in any of the cases.

The tendon-bone insertion was decorticated using a #11 blade until bleeding was seen. Using a custom-made dental drill, a 1 mm drill hole was made from the neck of the humerus to the bony insertion of the detached supraspinatus. The scaffold (DBM or GraftJacket) was cut into a strip measuring 10 mm long and 3 mm wide. Each limb of the suture was passed through the graft to secure its position. One suture arm was passed through the superior aspect of the drill hole (on the tendon footprint) and the remaining suture arm was passed through the inferior aspect of the drill hole (on the neck of the humerus). The supraspinatus tendon-scaffold complex was attached to the insertion site, with the graft in contact with both the tendon stump proximally and decorticated bone surface distally (Figure 5.2). In the control group the sutures were inserted directly into the drill holes, leaving a 5 mm gap in the tendon-bone interface in all cases.

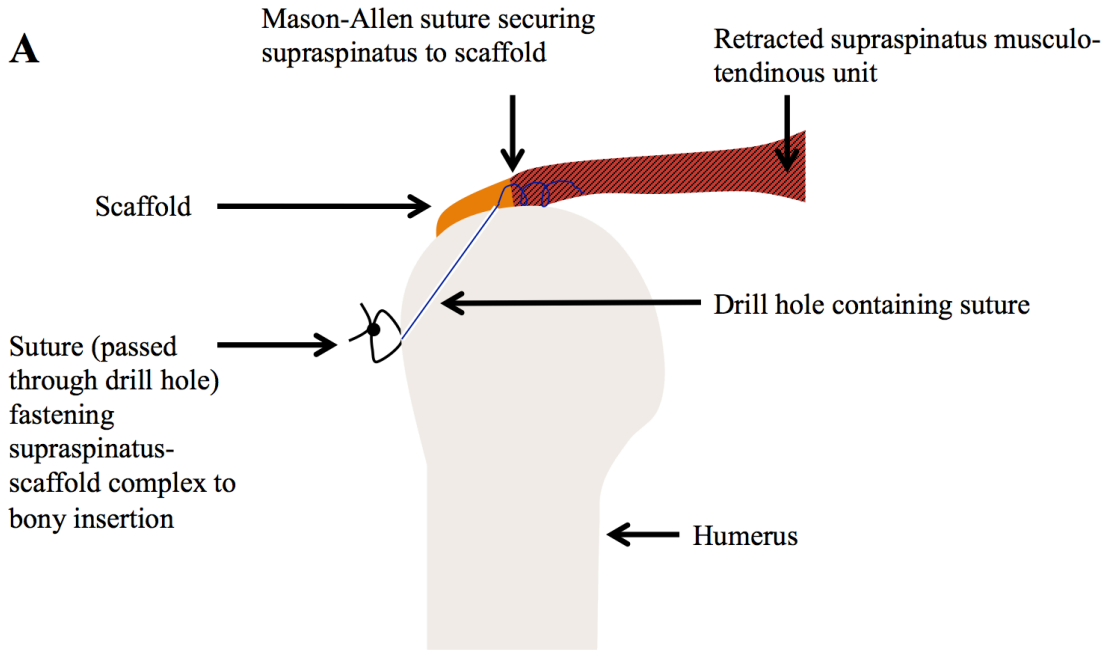

Figure 5.2A: Supraspinatus tendon-bone fixation.

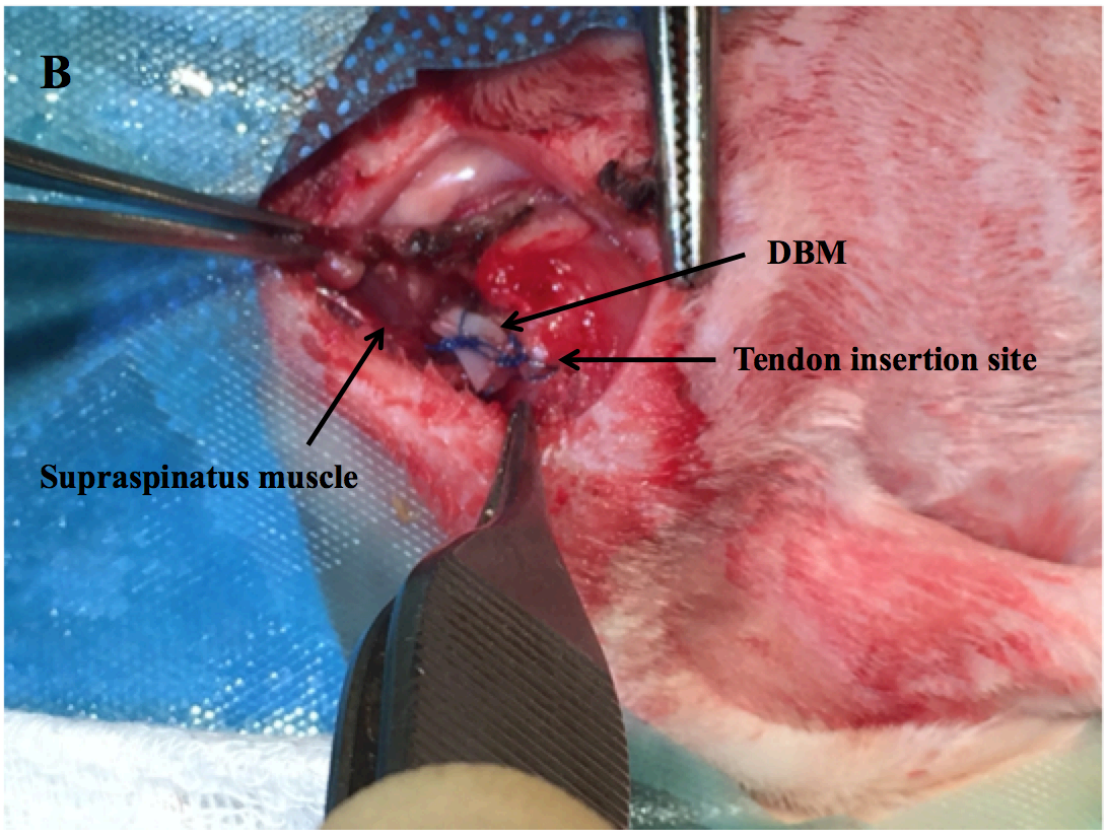

Figure 5.2B: Supraspinatus tendon-bone fixation with cortical DBM.

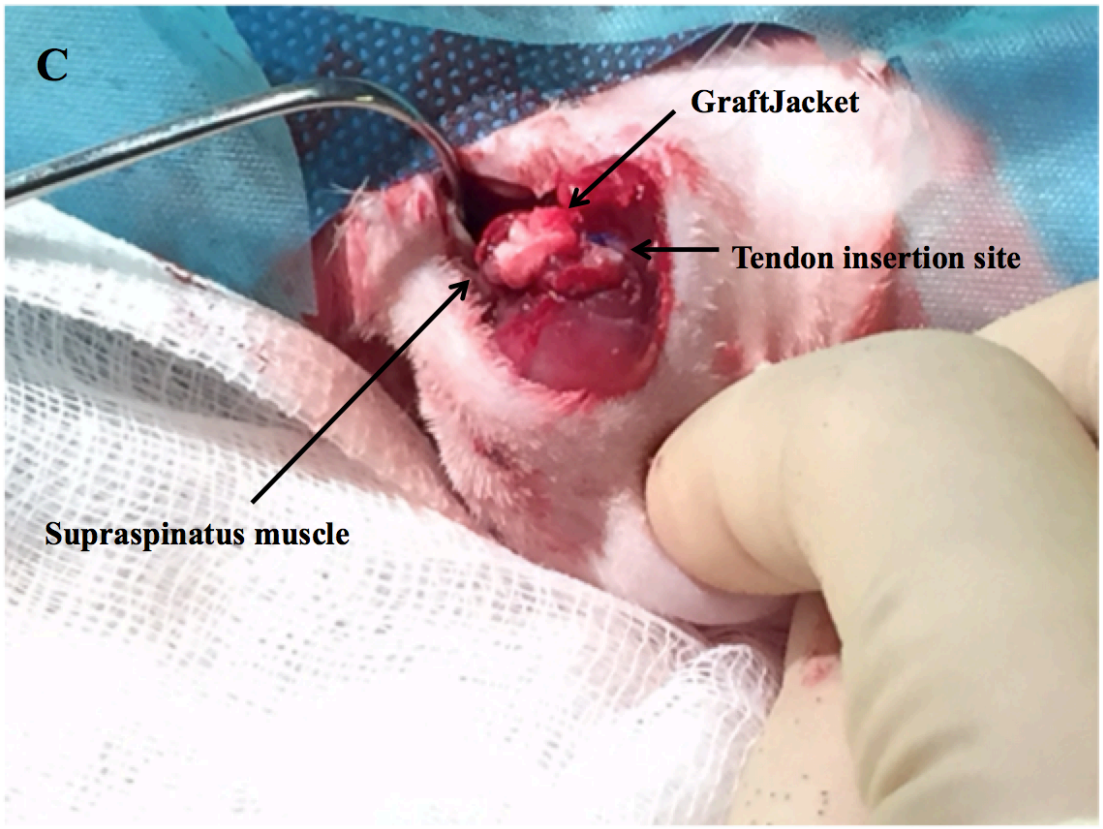

Figure 5.2C: Supraspinatus tendon-bone fixation with GraftJacket.

A layered wound closure was undertaken in a similar manner to the first surgery, and the animals were permitted unrestricted cage activity. Postoperative analgesia (intra-muscular Buprenorphine 0.6 mg) was given every 12 hours for three days.

5.2.5 Histological Assessment

Histological assessment was undertaken six weeks following tendon reattachment using the same method described in Section 4.2.5. In addition to this though, maturation of the enthesis was assessed according to the scoring system developed by Ide et al (Ide et al., 2009c): score 1 – the insertion had continuity without fibrous

tissue or bone ingrowth, score 2 – the insertion had continuity with fibrous tissue ingrowth but no fibrocartilage cells, score 3 – the insertion had continuity with fibrous tissue ingrowth and fibrocartilage cells but no tidemark, and score 4 – the insertion had continuity with fibrous tissue ingrowth, fibrocartilage cells, and a tidemark.

5.2.6 pQCT

Changes in bone mineral density at the humeral head were assessed using pQCT scanning. One millimeter slices were obtained through the humeral head and supraspinatus musculotendinous unit using an XCT 2000 Bone Scanner (Stratec Medizintechnik Gmbh, Germany) with Software version 6.20. Controls were obtained from the contralateral (non-operated) shoulder in six animals subjected to the same rehabilitation conditions as the study groups.

5.2.7 Statistical Analysis

Nonparametric statistical methods were used for all analyses because of the non-normality of the data in the groups being compared. Numerical data were inputted into SPSS software package, version 23 (SPSS Inc, an IBM Company, Chicago, Illinois). Mann Whitney U tests were used to compare data between groups. Results were considered significant at the $p < 0.05$ level.

5.3 Results

All animals survived the duration of the study and none had post-operative infection. Limping was noted for the first three to five postoperative days but a normal gait pattern returned afterwards.

5.3.1 Macroscopic Findings

At the time of euthanasia there was continuity between the repaired tendon and the bone in all groups (Figure 5.3). No signs of infection were noted in any specimen, none of the repairs had failed, and all the sutures were intact. Remodeling of the graft material occurred to a greater extent in the DBM group, whereby the scaffold could not be discerned from other tissues in the regenerated tendon-bone interface. In contrast, GraftJacket was clearly visible at necropsy. Control group specimens demonstrated complete closure of the enthesis.

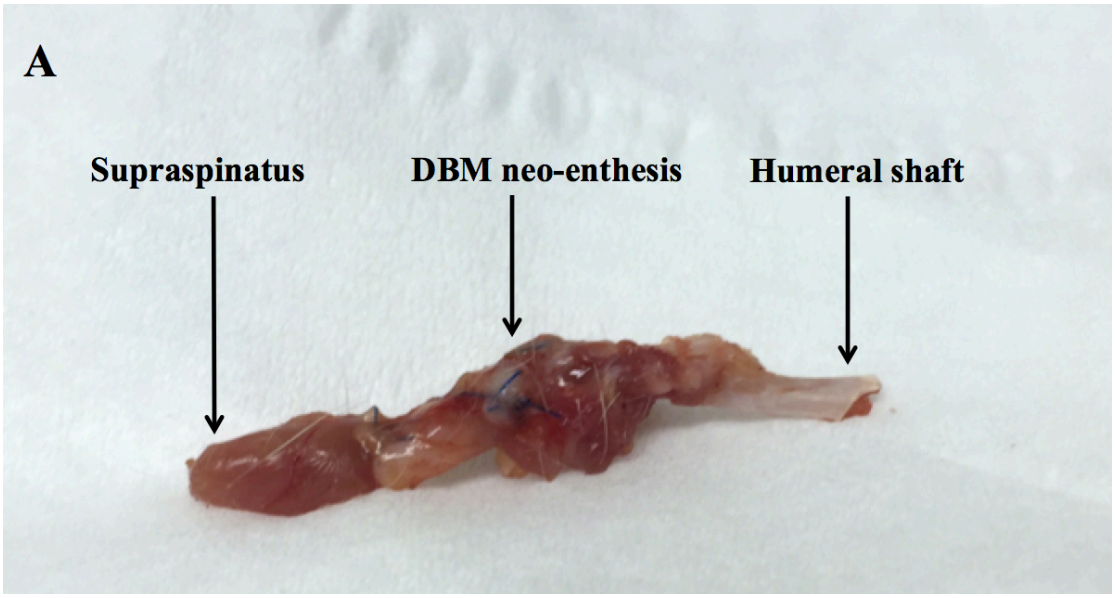

Figure 5.3A: Post-mortem supraspinatus tendon-bone fixation using cortical DBM.

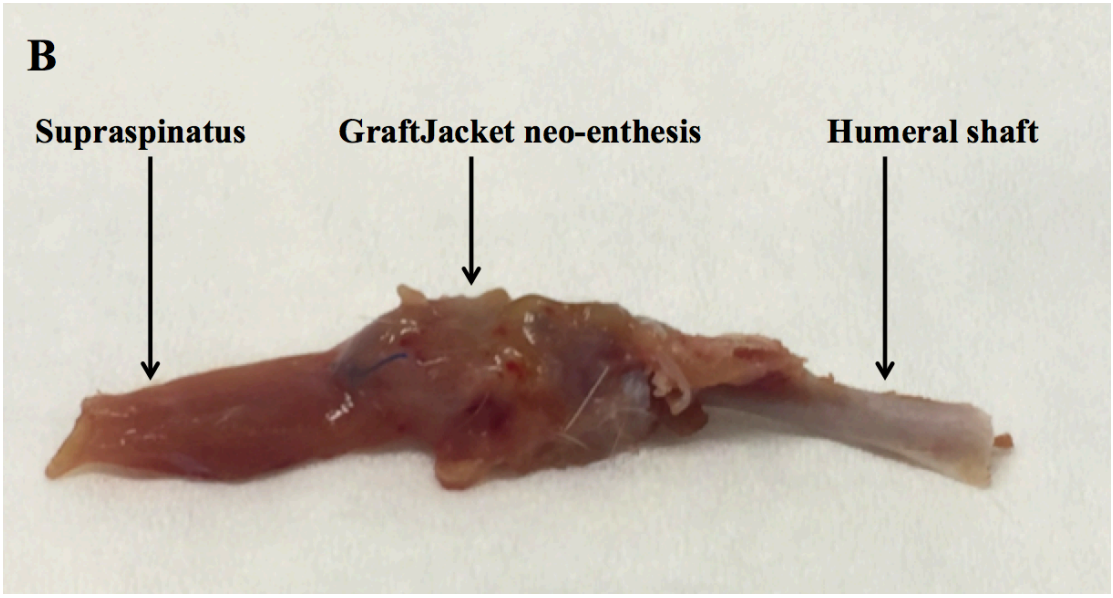

Figure 5.3B: Post-mortem supraspinatus tendon-bone fixation using GraftJacket.

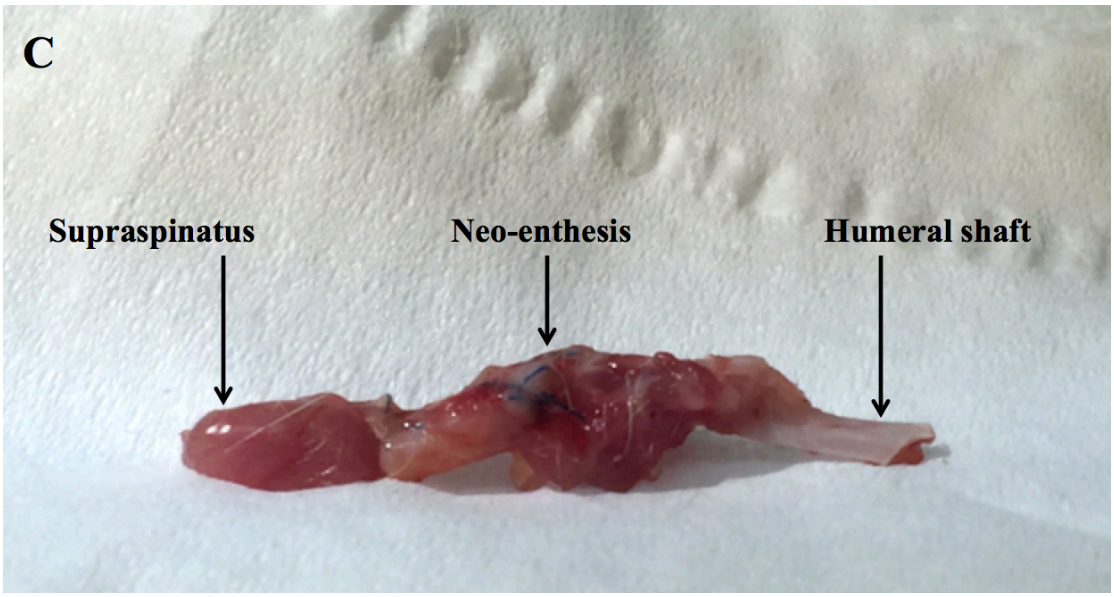

Figure 5.3C: Post-mortem supraspinatus tendon-bone fixation using no augmentation strategy (control group).

5.3.2 Quantitative Histology

5.3.2.1 Enthesis Maturation Score

No significant differences were observed in the enthesis maturation scores between experimental groups. However, the GraftJacket specimens exhibited a more disorganised enthesis than control and DBM groups, which were characterised by a well organised, graded structure (Figure 5.4) (Table 5.1) (Figure 5.5). The median enthesis maturation score was 2.5 (95% CI 1.88 to 3.46) in the controls, 3 (95% CI 2 to 4) in the DBM group, and 2.5 (95% CI 2.02 to 2.81) in the GraftJacket group.

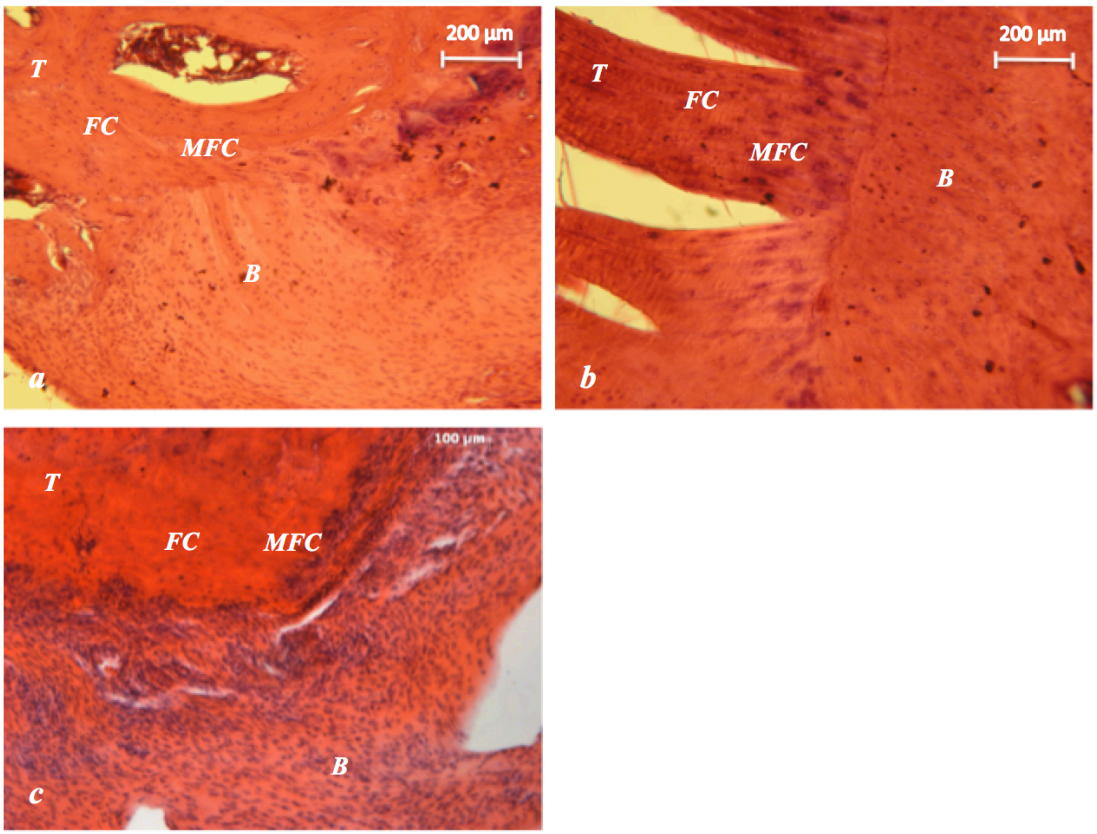

Figure 5.4: Photomicrograph of the enthesis at six weeks. Specimens stained with H&E. (a) Control: Non-augmented tendon-bone repair characterised by a graded enthesis comprising tendon (T), fibrocartilage (FC), mineralised fibrocartilage, and bone (B). (b) DBM: DBM neo enthesis comprising a well organised graded enthesis. (c) GraftJacket: GraftJacket neo enthesis with a disorganised structure.

	Controls	DBM	GraftJacket
Controls	-	0.413	0.672
DBM	0.413	-	0.161
GraftJacket	0.672	0.161	-

Table 5.1: Statistical significance (p-values) between the enthesis maturation scores following tendon reattachment using no augmentation strategy (controls), DBM, and GraftJacket.

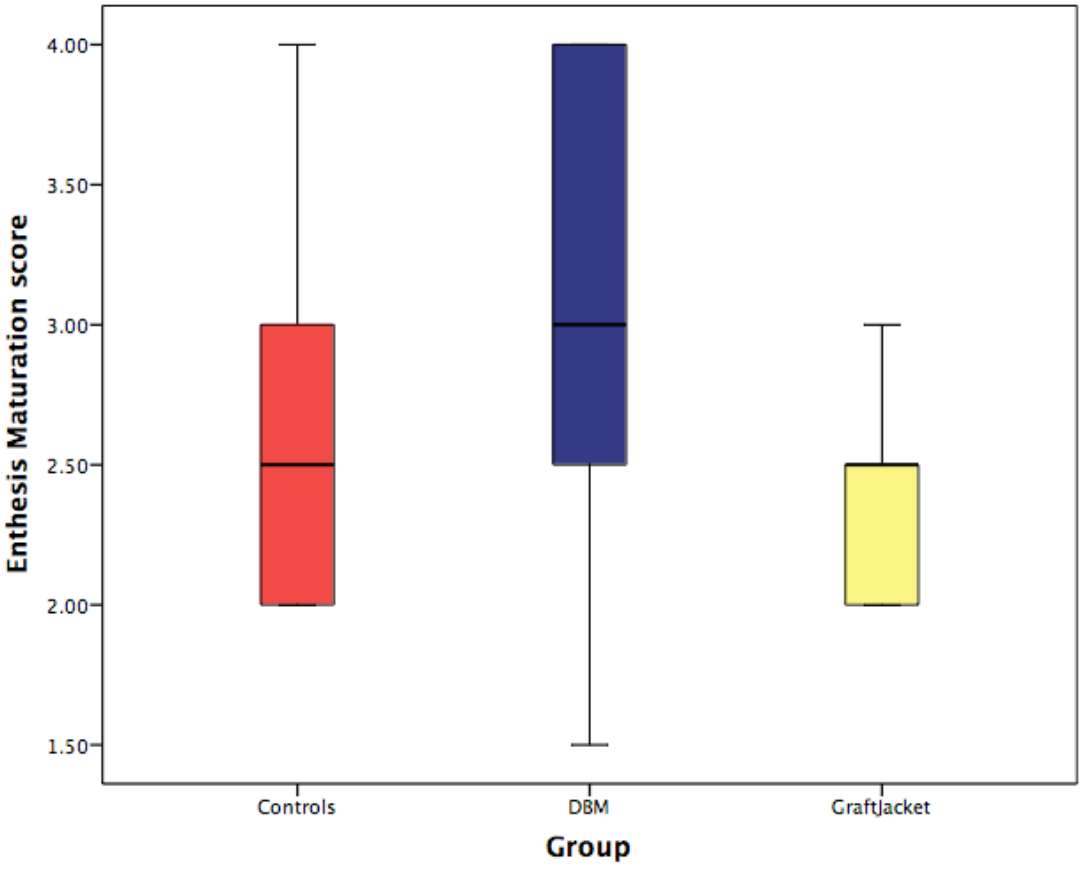

Figure 5.5: Box and whisker plot illustrating the enthesis maturation scores following tendon reattachment using no augmentation strategy (controls), DBM, and GraftJacket.

5.3.2.2 Modified Movin Score

No significant differences in the modified Movin scores (indicating degeneration) were demonstrated between experimental groups (Table 5.2) (Figure 5.6). The median modified Movin score was 7 (95% CI 5.04 to 10.62) in the controls, 6 (95% CI 3.37 to 10.47) in the DBM group, and 9.25 (95% CI 6.94 to 10.89) in the GraftJacket group.

	Controls	DBM	GraftJacket
Controls	-	0.470	0.422
DBM	0.470	-	0.296
GraftJacket	0.422	0.296	-

Table 5.2: Statistical significance (p-values) between the modified Movin scores following tendon reattachment using no augmentation strategy (controls), DBM, and GraftJacket.

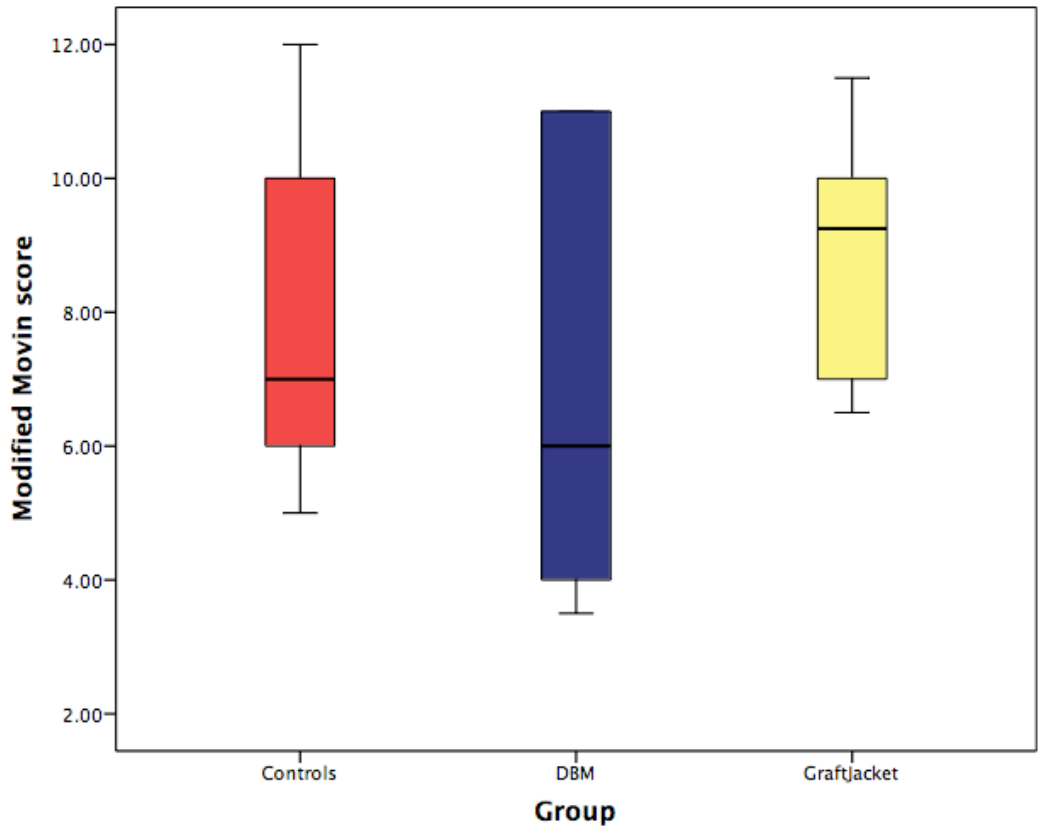

Figure 5.6: Box and whisker plot illustrating the modified Movin scores following tendon reattachment using no augmentation strategy (controls), DBM, and GraftJacket.

5.3.2.3 Fiber Structure

All groups exhibited increased waviness and distance between collagen fibers, compared to the organised structure identified in the control specimens in Chapter Four (Figure 5.7). The median score was 1.75 (95% CI 1.07 to 2.10) in the controls, 1.75 (95% CI 0.66 to 2.83) in the DBM group, and 1.5 (95% CI 0.83 to 2.67) in the GraftJacket group (Table 5.3) (Figure 5.8).

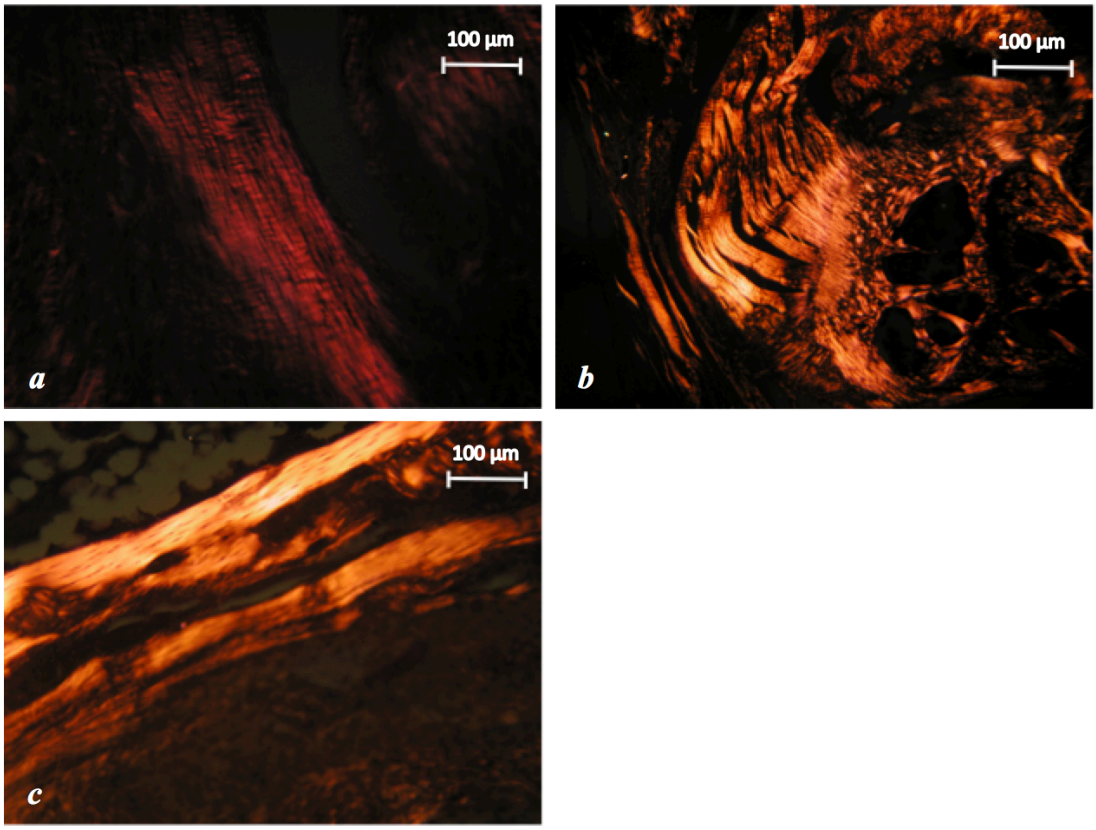

Figure 5.7: Photomicrograph (under polarised light) showing collagen fiber structure. (a) Controls (non-augmented tendon-bone repair). (b) DBM group. (c) GraftJacket group.

	Controls	DBM	GraftJacket
Controls	-	0.742	0.800
DBM	0.742	-	0.933
GraftJacket	0.800	0.933	-

Table 5.3: Statistical significance (p-values) between fiber structure following tendon reattachment using no augmentation strategy (controls), DBM, and GraftJacket.

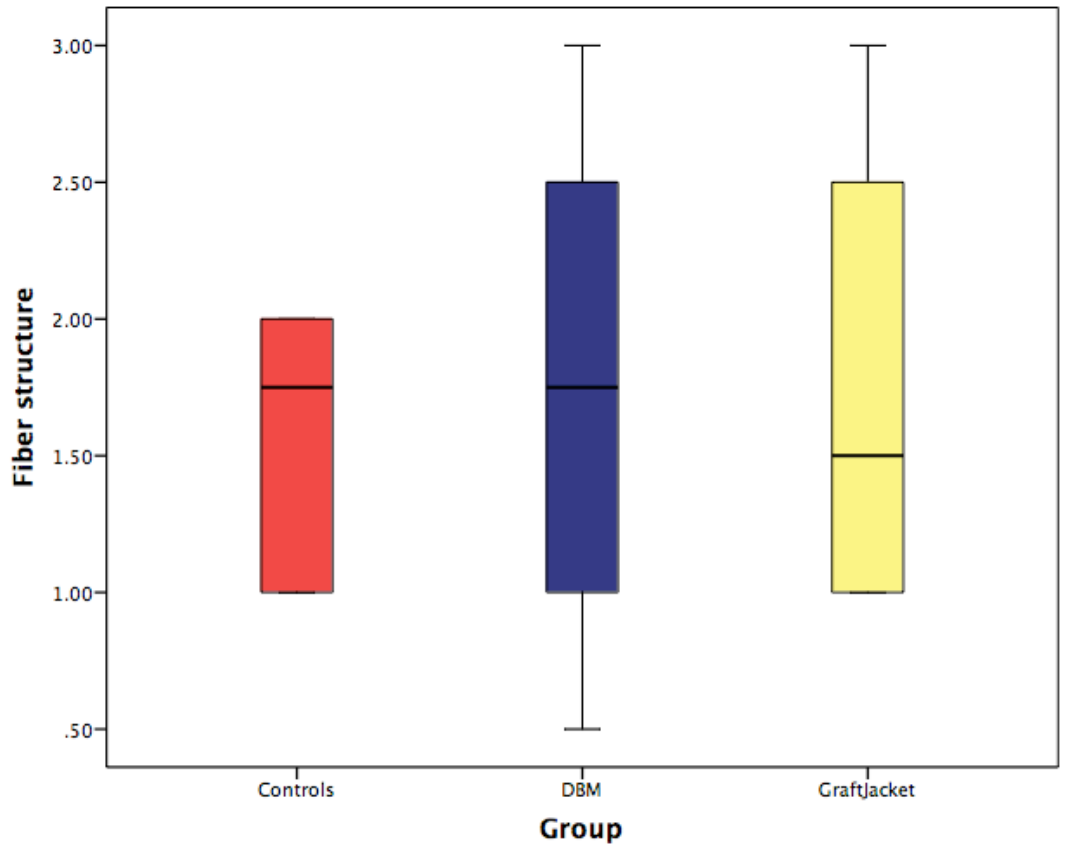

Figure 5.8: Box and whisker plot illustrating the difference in fiber structure following tendon reattachment using no augmentation strategy (controls), DBM, and GraftJacket.

5.3.2.4 Fiber Arrangement

All groups exhibited a loss of the parallel arrangement observed in the control specimens in Chapter Four (Figure 5.7). The median score was 1.5 (95% CI 0.88 to 2.46) in the controls, 1.25 (95% CI 0.84 to 2.16) in the DBM group, and 2.25 (95% CI 1.90 to 2.76) in the GraftJacket group (Table 5.4) (Figure 5.9). Fiber arrangement was significantly more abnormal in the GraftJacket group than in the DBM group ($p = 0.039$).

	Controls	DBM	GraftJacket
Controls	-	0.675	0.071
DBM	0.675	-	0.039
GraftJacket	0.071	0.039	-

Table 5.4: Statistical significance (p-values) between fiber arrangement following tendon reattachment using no augmentation strategy (controls), DBM, and GraftJacket.

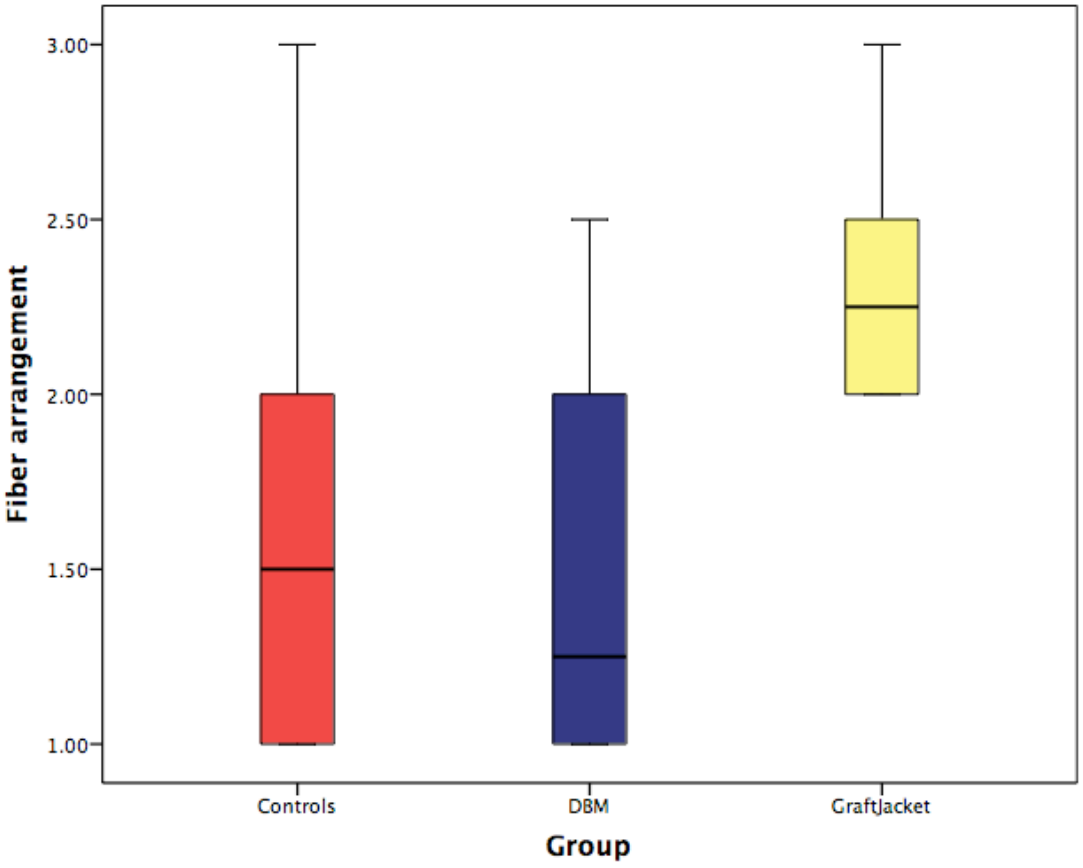

Figure 5.9: Box and whisker plot illustrating the difference in fiber arrangement following tendon reattachment using no augmentation strategy (controls), DBM, and GraftJacket.

5.3.2.5 Tenocyte Nuclei

Rounding of nuclei (indicating persistent degeneration) was identified in all groups following tendon reattachment (Figure 6.0). The median score was 1.75 (95% CI 1.12 to 2.55) in the controls, 1.50 (95% CI 1.03 to 1.97) in the DBM group, and 2 (95% CI 1.56 to 2.10) in the GraftJacket group (Table 5.5) (Figure 6.1). There were no significant inter-group differences.

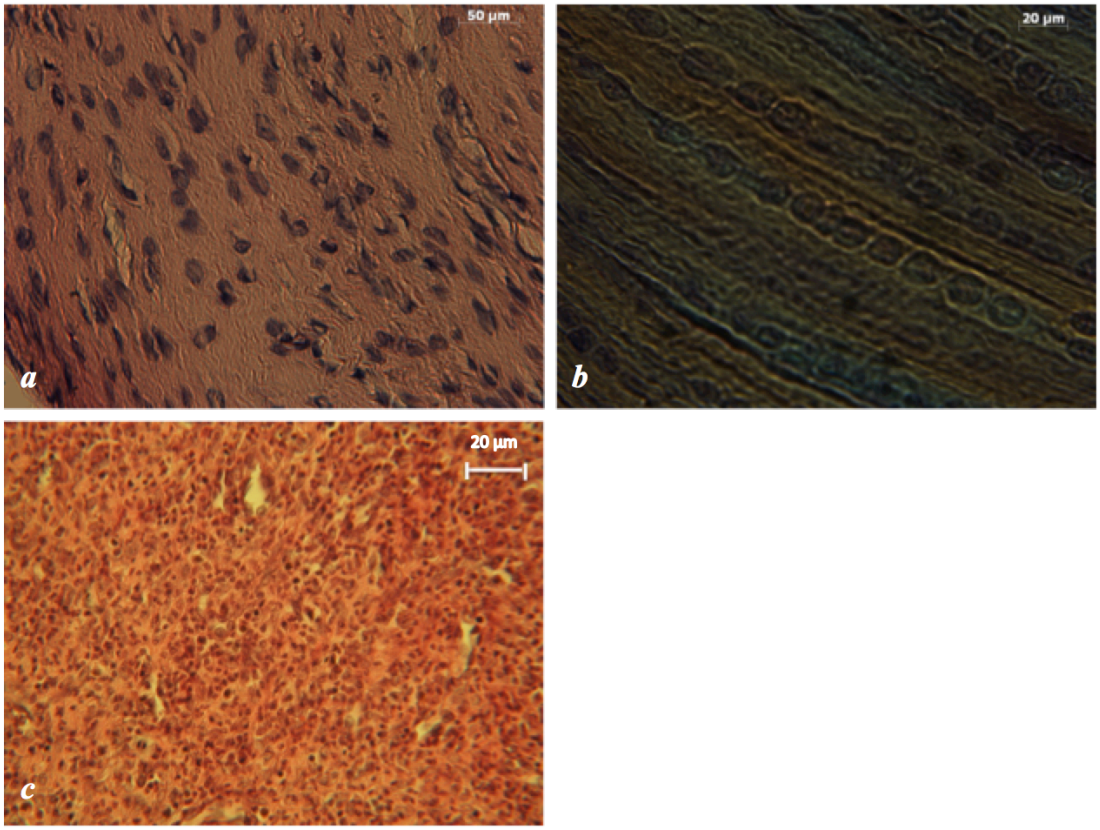

Figure 6: Photomicrograph illustrating rounded nuclei. (a) Controls (non-augmented tendon-bone repair). (b) DBM group. (c) GraftJacket group.

	Controls	DBM	GraftJacket
Controls	-	0.403	0.727
DBM	0.403	-	0.162
GraftJacket	0.727	0.162	-

Table 5.5: Statistical significance (p-values) between tenocyte nuclei morphology following tendon reattachment using no augmentation strategy (controls), DBM, and GraftJacket.

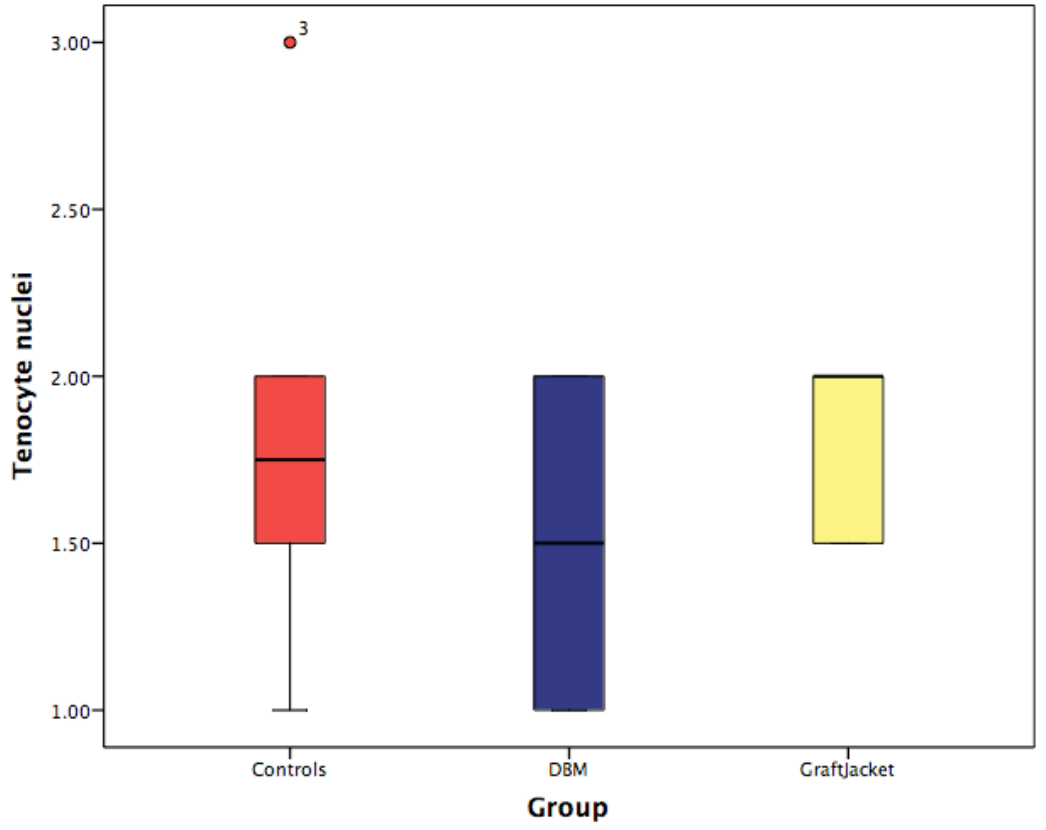

Figure 6.1: Box and whisker plot illustrating the differences in tenocyte nuclei morphology following tendon reattachment using no augmentation strategy (controls), DBM, and GraftJacket.

5.3.2.6 Cellularity

Specimens were evaluated for an increase in cellularity, indicating persistent degeneration. The median score was 1.50 (95% CI 0.97 to 2.20) in the controls, 1.25 (95% CI 0.70 to 1.97) in the DBM group, and 2 (95% CI 1.69 to 2.48) in the GraftJacket group (Table 5.6) (Figure 6.2). Cellularity was significantly less in the DBM group than in the GraftJacket group ($p = 0.037$), but there were no other significant inter-group differences.

	Controls	DBM	GraftJacket
Controls	-	0.508	0.115
DBM	0.508	-	0.037
GraftJacket	0.115	0.037	-

Table 5.6: Statistical significance (p-values) between cellularity following tendon reattachment using no augmentation strategy (controls), DBM, and GraftJacket.

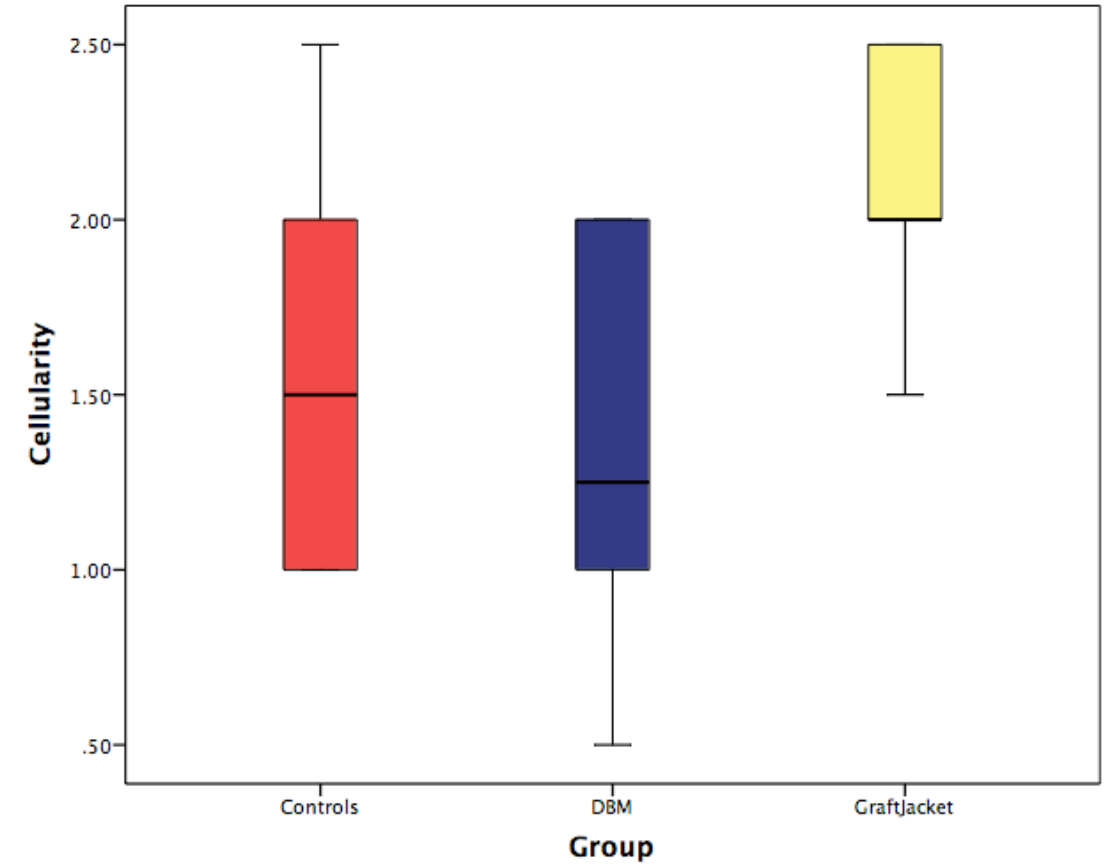

Figure 6.2: Box and whisker plot illustrating the differences in cellularity following tendon reattachment using no augmentation strategy (controls), DBM, and GraftJacket.

5.3.2.7 Vascularity

Specimens were evaluated for an increase in vascularity, indicating persistent degeneration (Longo et al., 2008). The median score was 1.50 (95% CI 0.54 to 2.12) in the controls, 0.25 (95% CI -0.35 to 2.01) in the DBM group, and 1 (95% CI 0.30 to 1.53) in the GraftJacket group (Table 5.7) (Figure 6.3). There were no significant inter-group differences.

	Controls	DBM	GraftJacket
Controls	-	0.459	0.216
DBM	0.459	-	0.623
GraftJacket	0.216	0.623	-

Table 5.7: Statistical significance (p-values) in vascularity following tendon reattachment using no augmentation strategy (controls), DBM, and GraftJacket.

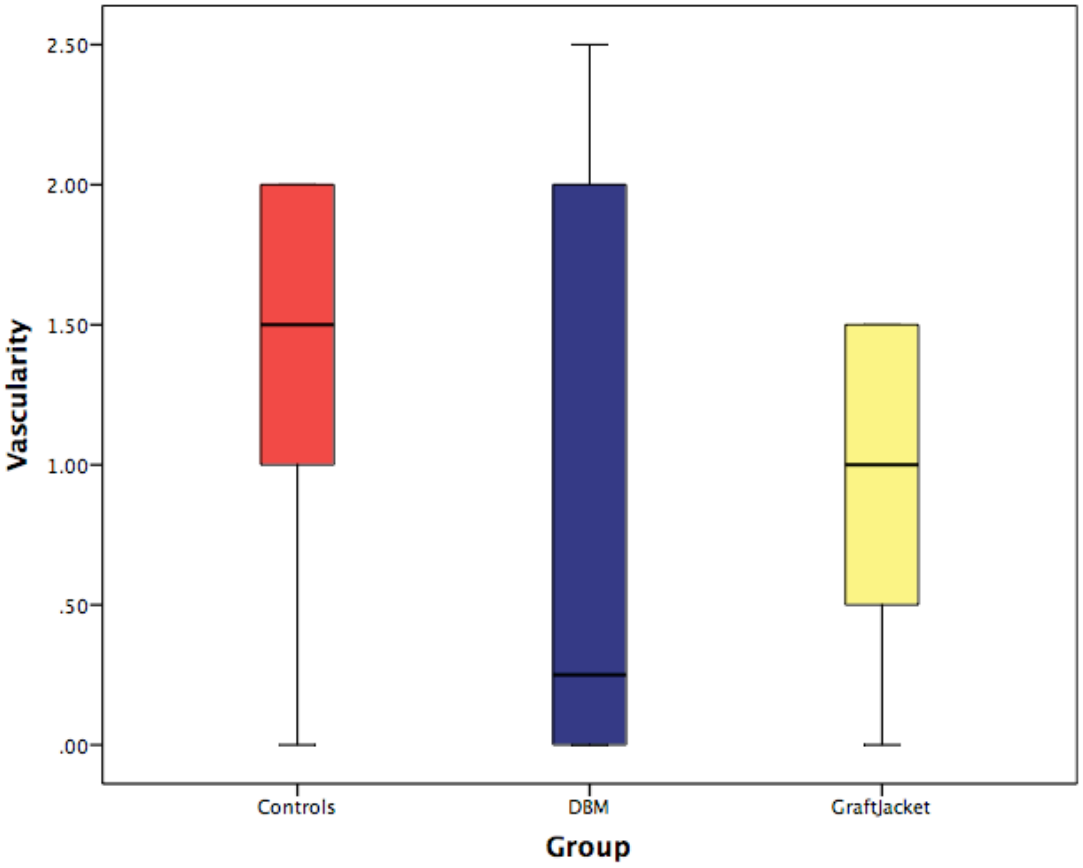

Figure 6.3: Box and whisker plot illustrating the differences in vascularity following tendon reattachment using no augmentation strategy (controls), DBM, and GraftJacket.

5.3.2.8 Hyalinisation

Hyalinisation was not observed in any of the specimens.

5.3.3 pQCT

Control specimens comprised the contralateral shoulder of animals that had undergone unilateral tendon detachment three weeks earlier, as outlined in Chapter Four. In this group (n = 6), the median total bone mineral density at the supraspinatus tendon-bone insertion was 793.25 mg/ccm (95% CI 754.24 to 844.70) (Figure 6.4). This significantly decreased six weeks following tendon repair with DBM and GraftJacket to a median of 721.20 (95% CI 537.52 to 771.68) (p = 0.004) and 620.55 mg/ccm (95% CI 551.01 to 733.80) (p = 0.006) respectively (Table 5.8). Following non-augmented repair of the supraspinatus tendon to bone without the addition of an augmentation strategy, median bone mineral density was 756.30 mg/ccm (95% CI 648.01 to 818.46). This was not significantly different to controls (p = 0.078).

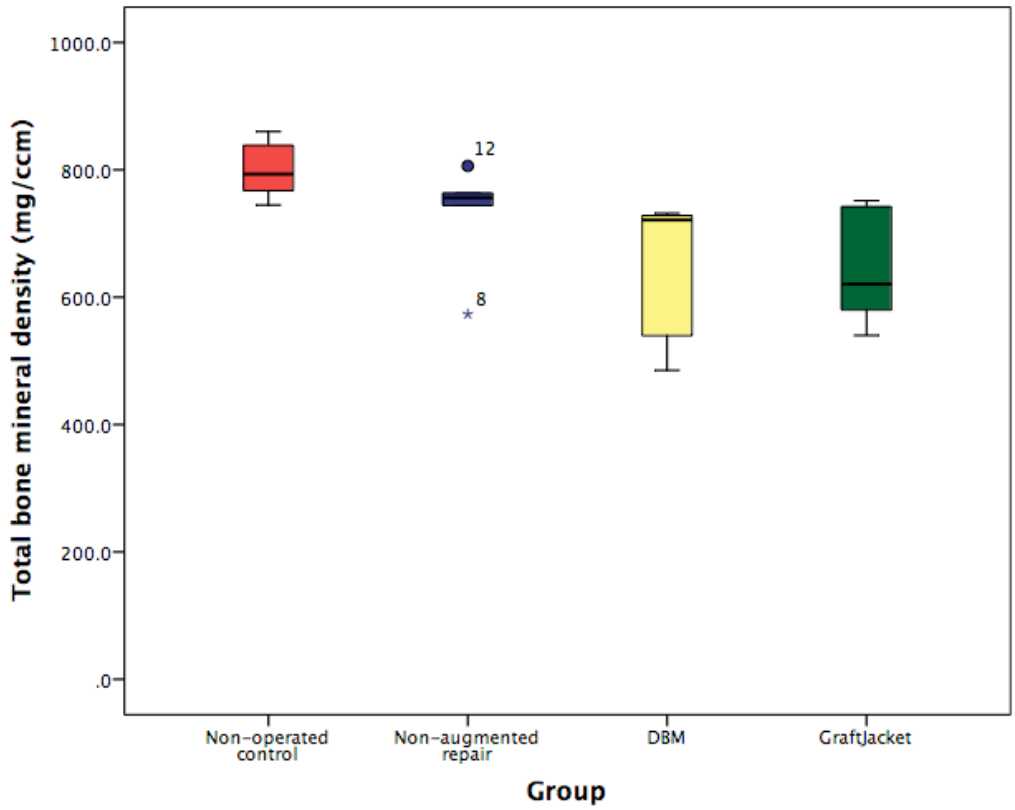

Figure 6.4: Box and whisker plot showing total bone mineral density at the supraspinatus tendon-bone insertion six weeks following non-augmented tendon-bone repair, repair with cortical DBM, and repair with GraftJacket.

	Non-operated control	Non-augmented repair	DBM	GraftJacket
Non-operated control	-	0.078	0.004	0.006
Non-augmented repair	0.078	-	0.025	0.055
DBM	0.004	0.025	-	0.749
GraftJacket	0.006	0.055	0.749	-

Table 5.8: Statistical significance (p-values) between total bone mineral density at the supraspinatus tendon-bone insertion six weeks following non-augmented tendon-bone repair, repair with DBM, and repair with GraftJacket.

5.4 Discussion

In this study, it was hypothesised that compared to a commercially available scaffold (GraftJacket), DBM would regenerate a morphologically superior enthesis characterised by greater fibrocartilage formation and improved collagen fiber organisation. It was further hypothesised that DBM would result in a higher bone mineral density at the insertion site. However, the results do not support this hypothesis. Using a rat model of chronic rotator cuff degeneration, the supraspinatus tendon was reattached to its bony insertion with DBM, GraftJacket, and no augmentation strategy (controls) and analysed after six weeks. All groups demonstrated closure of the tendon-bone gap with a fibrocartilaginous interface, but the degenerative process at this time point could not be reversed (as illustrated by a persistently high Modified Movin score). Although there was no significant difference in enthesis maturation scores at the conclusion of the study, the GraftJacket specimens exhibited a disorganised structure with significantly more abnormal collagen fiber arrangement and cellularity than the DBM repairs (indicating more severe degeneration).

Bone mineral density at the enthesis was the second parameter examined because it has been shown to determine the quality and degree of tendon-bone healing, and the pullout strength of suture anchors in the clinical setting (Lovric et al., 2012, Cadet et al., 2008). Following tendon reattachment with DBM and GraftJacket, this did not recover to the baseline levels established in Chapter Four (bone mineral density at the non-operated tendon insertion site). In contrast, the non-augmented repairs exhibited a significantly higher bone mineral density than DBM and GraftJacket specimens, and

were not significantly different to the control specimens in Chapter Four. This indicates that at this time point bone density had not recovered to normal levels. Several *in vivo* studies have demonstrated the ability of DBM to enhance tendon-bone healing, but none in a degenerative rotator cuff tear model (Sundar et al., 2009a, Kilicoglu et al., 2012, Lovric et al., 2012). In the first study to examine the use of DBM at the healing enthesis, Sundar et al (Sundar et al., 2009a) created an acute tear in an ovine patellar tendon model and repaired it with the scaffold. Compared to controls at 12-weeks, the DBM group showed increased amounts of mineralised fibrocartilage and improved functional weight bearing. To determine the effect of DBM on tendon healing within a bone tunnel, Kilicoglu et al (Kilicoglu et al., 2012) developed a rabbit model and retrieved specimens three, six, and nine weeks after surgery. At three weeks, a higher number of Sharpey's fibers, marginally increased fibrocartilage formation, and new bone formation was observed in the DBM group, but this difference was not significant at later time-points. In a further study examining the healing potential of a DBM paste in a tendon-bone tunnel, Lovric et al (Lovric et al., 2012) created a rat model of ACL reconstruction. No reconstitution of the fibrocartilage layer was observed in either the DBM or control groups. The main finding was a significantly greater amount of new bone formation in DBM-augmented animals associated with a significantly higher peak load to failure of the tendon-bone interface at six weeks.

The current study could not reproduce the results of DBM-induced tendon-bone healing observed in other animal models, including those described in Chapter Three of this thesis. Considering that the overall contact area between tendon and bone is a major determinant of healing, the limited tendon-bone surface area in a rat model

does not present an environment that is as conducive to healing as large animal models and those that utilise a tendon-bone tunnel (Greis et al., 2001). Furthermore, the high shear forces from contraction of supraspinatus are distributed over a relatively small surface area and therefore may not have allowed adequate tendon healing to take place (Gulotta et al., 2009). The next important finding of this study was that the non-augmented control group demonstrated an equivalent histological outcome to those tendons repaired with DBM and GraftJacket, and also resulted in a bone mineral density at the tendon insertion comparable to the non-operated controls described in Chapter Four. This may be due to the two bulky scaffolds inhibiting motion of the shoulder joint and thus remodeling of the grafts into a native tendon-bone interface, within the allocated time frame of six weeks.

There are several limitations to this study. Previous work has shown that most control tendons in a rat model heal by eight weeks, making it challenging to detect differences between control and experimental groups because it is difficult to improve upon a solid mass of healed tissue (Gulotta et al., 2009). Earlier time points in the healing phase (two and four weeks) may have highlighted differences that later became non-significant between groups. Similarly, later time points (nine and 12 weeks) may have allowed greater time for the scaffolds to remodel and exert their restorative effect on the tendon-bone interface. Finally, biomechanical evaluation of the repair construct would have strengthened the results of this study, but due to the limited number of specimens this could not be performed.

5.5 Conclusion

This study has highlighted the difficulty of developing a suitable model of a chronic rotator cuff tear, and a scaffold to improve healing of the rotator cuff tendon-bone interface. Although the application of DBM to a chronic rotator cuff tear does result in a fibrocartilaginous enthesis, this was not significantly more mature than non-augmented controls or a commercially available alternative scaffold (GraftJacket). However, without further time points for histological analysis it is not possible to discern between subtle differences in the healing interface, early and late in the remodelling process of tendon healing. It is possible that the addition of cell-based strategies to the healing enthesis may enhance the results observed in this study, and so the next chapter investigates the use of MSCs in chronic rotator cuff healing.

Chapter Six: Application of Demineralised Cortical Bone Matrix and Mesenchymal Stem Cells to a Degenerative Rotator Cuff Repair Model

6.1 Introduction

Approximately 75,000 rotator cuff repairs are performed each year in the United States (Vitale et al., 2007). Up to 94% of tendons fail to heal back to bone and result in a worse functional outcome than those tendons that do go onto heal (Carr et al., 2015a, Galatz et al., 2004). The native enthesis is a graded structure that allows stresses to be evenly distributed between tendon and bone (Thomopoulos et al., 2010). Following surgery, scar tissue is deposited at the healing interface and has been identified as a potential cause of the high failure rate because it possesses weak mechanical properties and does not contain mineralised fibrocartilage (St Pierre et al., 1995, Cooper and Misol, 1970) (Cooper and Misol, 1970, Gerber et al., 1999, Koike et al., 2006, St Pierre et al., 1995). In order to improve rotator cuff healing, biological strategies must enhance tissue regeneration and provide an optimal mechanical environment to resist tearing during the crucial postoperative rehabilitation period (Miller et al., 2011).

MSCs are multipotent cells that are capable of differentiating into several cell types, including chondrocytes, adipocytes, and osteoblasts (Chamberlain et al., 2007). *In vivo* examination of MSCs on enthesis regeneration have reported the absence of a fibrocartilaginous interface, citing the lack of signaling as a reason for the transplanted cells not differentiating and improving healing (Gulotta et al., 2009). To enhance their effect studies have engineered stem cells *in vitro* to express specific proteins (Gulotta et al., 2010, Gulotta et al., 2011a). In doing so, fibrocartilage production and strength of the repair have been increased (Gulotta et al., 2010).

DBM consists of a network of collagen fibers that provide a sustained release of growth factors such as BMPs (Pietrzak et al., 2012). Wurgler-Hari et al (Wurgler-Hauri et al., 2007) demonstrated that a slow release of growth factors is required for tendon-bone healing, and there is evidence to indicate that BMPs are important proponents of a naturally graded, mechanically favorable enthesis (Longo et al., 2011, Aspenberg and Forslund, 1999, Pauly et al., 2012). Differentiation of MSCs can be directed by the introduction of BMPs; a property that may be utilised to increase production of mineralised fibrocartilage at the healing enthesis (Dorman et al., 2012, Liu et al., 2010, Gulati et al., 2013, Sun et al., 2015). In an acute tear model of tendon-bone healing, DBM has been shown to regenerate a strong enthesis with mineralised fibrocartilage (Sundar et al., 2009a). Chapters Three and Five of this thesis have further highlighted the potential of DBM to be used as a graft material for tendon repair to bone, in a model of severe retraction (Chapter Three) and degeneration (Chapter Five). Since the ultimate strength of the tendon-bone interface is dependent upon bony ingrowth into healing tissue containing fibrocartilage, the addition of MSCs into the DBM-based repair construct may produce an enthesis resembling the native insertion site with a natural gradation between tendon, demineralised fibrocartilage, mineralised fibrocartilage, and bone.

The purpose of this study was to determine if DBM enhanced with MSCs could improve healing when applied to a degenerative model of rotator cuff repair. As in Chapter Five, DBM was compared to GraftJacket (Wright Medical Technology, Inc., Arlington, TN), as this is a commonly used scaffold in clinical practice (Bond et al., 2008). The hypothesis was that compared to MSCs alone, DBM enhanced with MSCs will regenerate a morphologically superior enthesis with a higher bone mineral

density in a rat model of a chronic rotator cuff tear. To determine whether MSCs could enhance the structure of the healing enthesis compared to repairs without stem cells, the results of this study were compared to those from Chapter Five. It was hypothesised that the addition of MSCs would yield a morphologically superior interface and increased bone mineral density at the tendon insertion.

6.2 Materials and Methods

6.2.1 Study Design

All animal work was conducted in accordance with a Project License protocol accepted under the UK Home Office Animals (Scientific Procedures) Act 1986. Eighteen female Wistar rats underwent unilateral detachment of the supraspinatus tendon, and an additional one animal from the same genus was used to obtain bone marrow-derived MSCs. Previously published data was used to calculate the number of animals (n = 6) required to generate a power of 0.8 with significance at the 0.05 level (Sundar et al., 2009a). Three weeks later, tendon repair was carried out in animals randomised into three groups: Group 1 received augmentation of the repair with cortical allogenic DBM (n = 6); Group 2 received augmentation with non-meshed, ultra-thick GraftJacket; and Group 3 underwent tendon-bone repair without a scaffold (n = 6). All animals received 1×10^6 MSCs in a fibrin sealant Tisseel® kit (Baxter, Vienna, Austria) and one animal from each study group received MSCs labeled with Quantum Dot nanoparticles (Thermo Fisher Scientific, Massachusetts, United States) (QDs) for cell tracking. Fibrin glue without MSCs has previously been shown not to enhance healing of the enthesis and therefore it was not used as an experimental group in this study in order to minimise the number of animals used, as per UK Home Office regulations (Gulotta et al., 2009, Shoemaker et al., 1989, Yamazaki et al., 2005).

All procedures were carried out by one surgeon. Animals were freely mobilised and specimens were retrieved at six weeks (following euthanasia with carbon dioxide

insufflation) postoperatively for histological analysis and pQCT to evaluate bone mineral density at the tendon insertion, reversal of degenerative changes within the tendon, and histological remodeling of the implanted graft material.

6.2.2 DBM Manufacture

Cortical DBM derived from the tibiae of skeletally mature female Wistar rats were manufactured using the same technique described in Chapter Five (section 5.2.2). Samples were rehydrated at the time of surgery in normal saline for 30 minutes prior to use.

6.2.3 GraftJacket

As in Chapter Five, non-meshed, ultra-thick GraftJacket with an average thickness of 1.4 mm was used in all cases. Samples were rehydrated at the time of surgery in normal saline for 30 minutes prior to use.

6.2.4 Bone Marrow-Derived Mesenchymal Stem Cell Harvest and Culture

One six-month-old female Wistar rat was euthanised by carbon dioxide inhalation and bilateral femurs were harvested under sterile conditions. MSCs were harvested by lavaging the intramedullary canals with Dulbecco's modified Eagle's medium (DMEM) (Invitrogen, Paisley, UK) containing 10% fetal calf serum (FCS) (HyClone, Logan, Utah, USA). Cells were washed with sterile PBS three times and centrifuged

at 2000 revolutions per minute (rpm) for five minutes. The supernatant was discarded and the cell pellet was resuspended in 20 ml DMEM containing 1% penicillin/streptomycin solution and 10% FCS, and plated onto T-175 culture flasks. Cells were cultured at 37°C in a 5% carbon dioxide incubator. After two days, the contents of the flask were removed and washed with media, leaving behind MSCs that adhered to the bottom of the flask. Afterwards, media was changed twice a week for 14 days. Once confluent, the MSCs were detached with trypsin and serially subcultured. Third-passage cells were used for implantation. Previous studies have shown that this protocol is a reliable method of obtaining MSCs, and that their pluripotency is maintained up to the third passage (Gulotta et al., 2009, Gulotta et al., 2010, Akhan et al., 2015, Pittenger et al., 1999, Toh et al., 2005). No immunogenic reaction was anticipated with stem cell implantation because the rats from where they were harvested were the same strain as those receiving them.

6.2.5 Surgical Technique

Tendon detachment and subsequent reattachment were undertaken using the same operative protocol described in Chapter Five (section 5.2.4), with the exception that MSCs were incorporated into the repair. The fibrin sealant Tisseel® (Baxter, Vienna, Austria) contained two parts: a vapor-heated Tisseel® powder dissolved in aprotinin solution and a vapor-heated thrombin powder, dissolved in calcium chloride solution. One milliliter of the Tisseel® solution contained 100–130 mg of total protein, of which 75–115 mg was fibrinogen. One milliliter of thrombin solution contained 45–55 mg of total protein, of which 500 International Units (IU) [2] was thrombin (Kalia et

al., 2006). Preoperatively, MSCs were implanted into the thrombin component *in vitro* at a concentration of 1×10^6 cells/100 µl and mixed with the Tisseel® solution. The fibrin glue was injected into a custom-made square-shaped stainless steel mold measuring 1 cm by 1cm containing DMEM, which provided nutrition to the cells up to the point at which they were implanted (Figure 6.1).

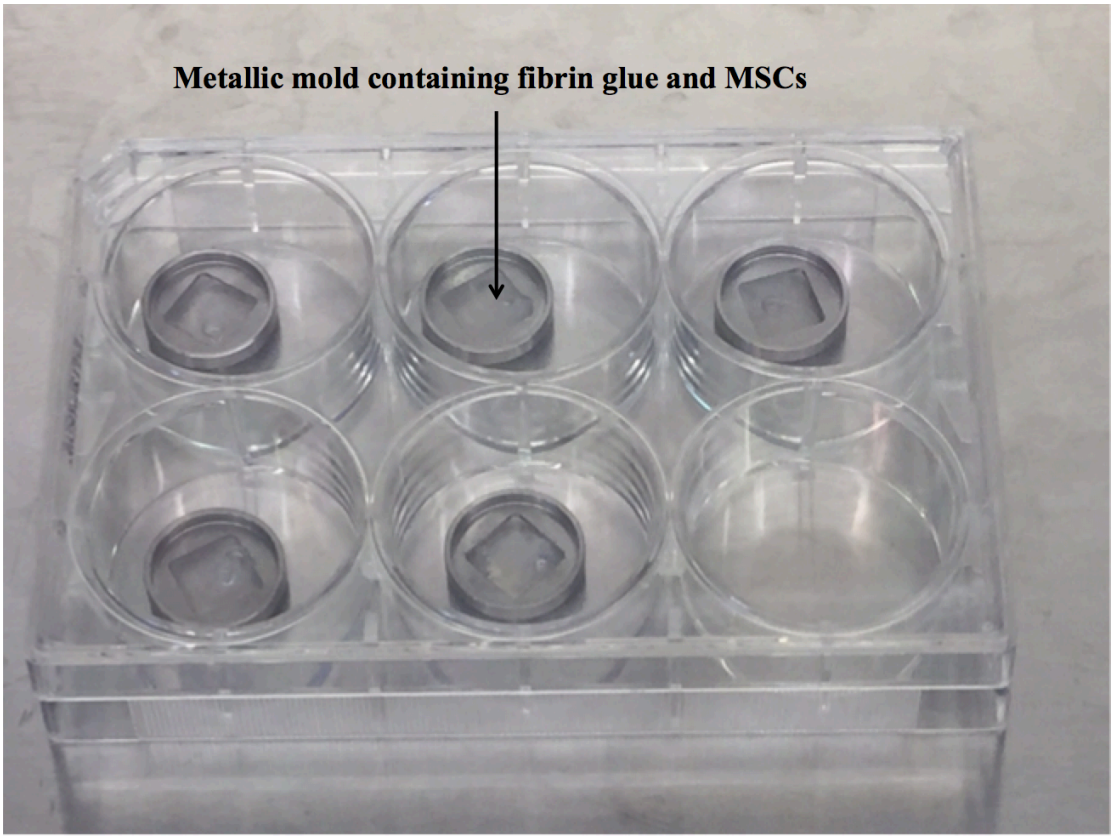

Figure 6.1: Metallic molds containing fibrin glue and MSCs *in vitro*.

Prior to securing the graft material (cortical DBM or GraftJacket) during tendon reattachment surgery, the sheet of fibrin glue containing MSCs was placed on the decorticated humeral head whilst lying in contact with the proximal tendon stump

(Figure 6.2). All grafts used to augment healing measured approximately 1.5 cm in length and 3-5 mm in width.

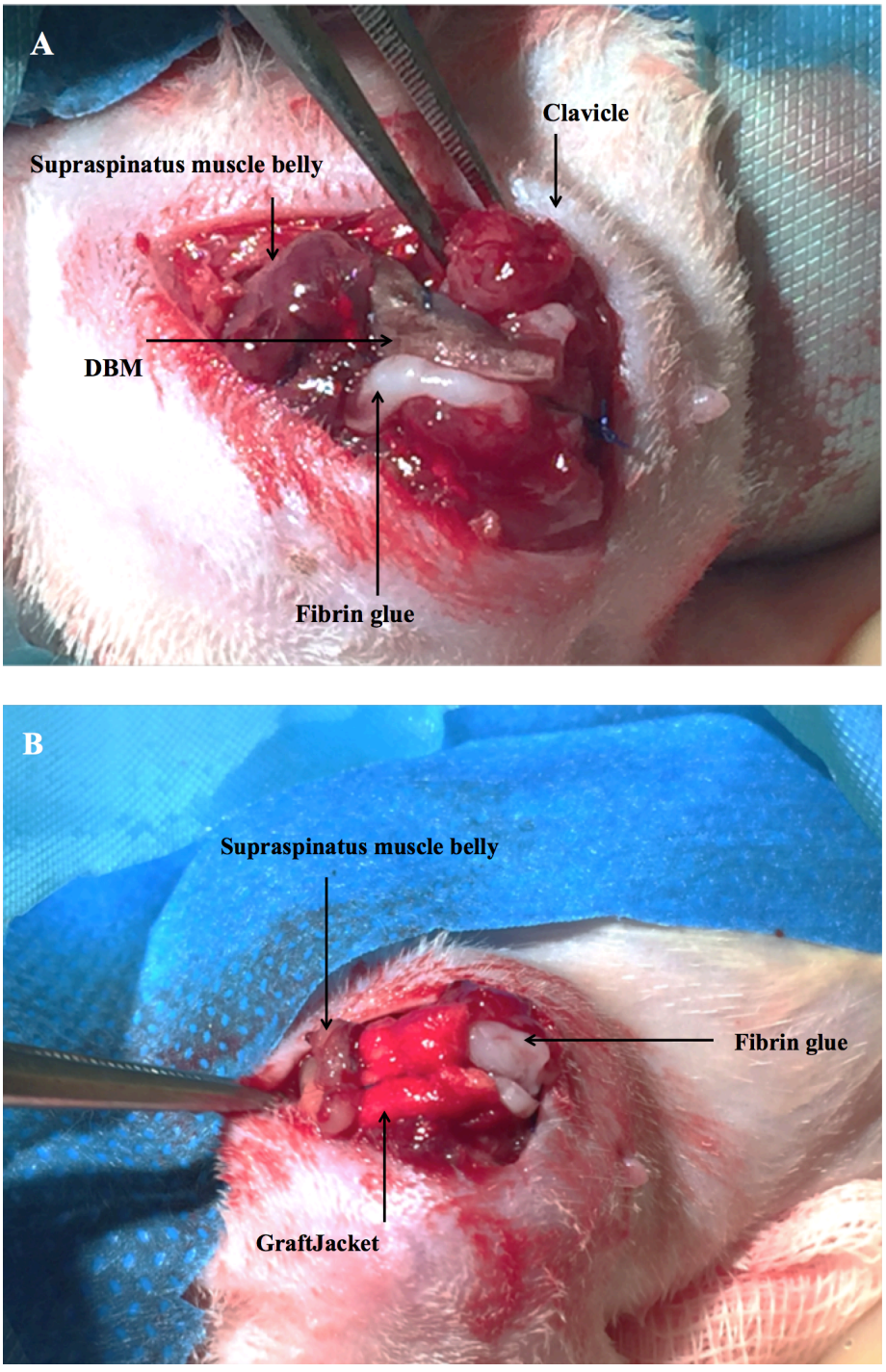

Figure 6.2: Supraspinatus tendon-bone interface with cortical DBM + MSCs (A) and GraftJacket + MSCs (B).

In the group where MSCs were used in isolation, the fibrin glue bridged the gap between the retracted supraspinatus musculotendinous unit and its bony insertion. The repair construct resembled a laminated structure: superficial layer – cortical DBM/GraftJacket, central layer – fibrin glue with MSCs, and deep layer – humeral head with tendon footprint (Figure 6.3).

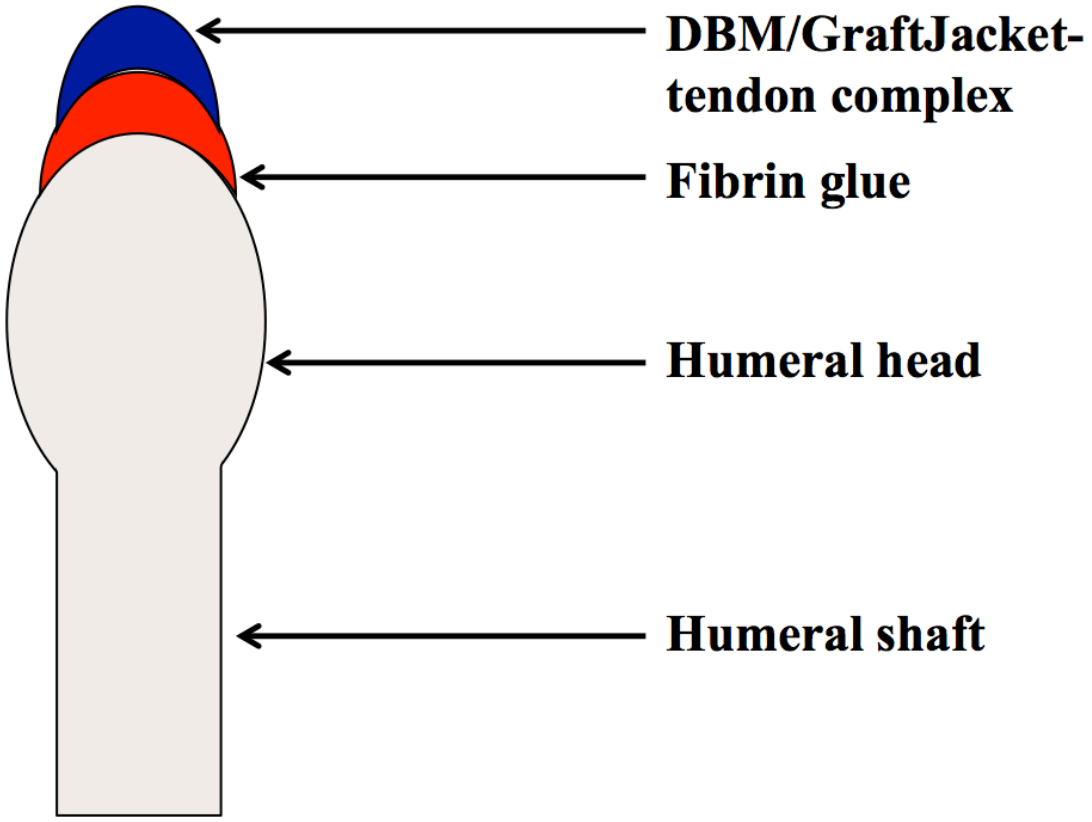

Figure 6.3: Lateral view of the tendon-bone repair construct comprising superficial layer – cortical DBM/GraftJacket, central layer – fibrin glue with MSCs, and deep layer – humeral head with tendon footprint.

6.2.6 Mesenchymal Stem Cell Tracking

QDs are semiconductor nanoparticles that are phagocytosed or take up by pinocytosis into cells and distributed within cytoplasmic vesicles, causing intense fluorescence (Muller-Borer et al., 2007). Using them in this study was crucial to establishing whether the implanted MSCs remained at the healing enthesis to exert their effect locally. Properties that make QDs suitable for cell tracking include their compatibility with MSCs without effecting proliferation and differentiation, and their resistance to chemical and metabolic degradation (Muller-Borer et al., 2007, Collins et al., 2012, Alivisatos, 2004, Chan et al., 2002, Dubertret et al., 2002, Jaiswal et al., 2003).

In this study, three animals (one from each experimental group) received MSCs labeled with a Q-Tracker 655 Cell Labeling kit (Thermo Fisher Scientific, Massachusetts, United States). QDs were applied to cells at a concentration of 300,000 particle units/1 × 10^6 MSCs. This was achieved using the following protocol issued from the manufacturer: 1 μL of Qtracker® Reagent A and Component B were mixed in a 1.5 mL micro-centrifuge tube and incubated for five minutes at room temperature, 0.2 mL of fresh complete growth medium was added to the tube and vortexed for 30 seconds, 0.2 mL of the labeling solution was added to a well-plate containing MSCs, the sample was incubated at 37 ° C for 45-60 minutes, and the cells were washed twice with fresh complete growth medium. On the morning of surgery transduced MSCs were suspended in the fibrin sealant, stored in DMEM, and implanted at the repair site as described above.

6.2.7 Histological Assessment

Histological assessment was undertaken six weeks following tendon reattachment using the same method described in Section 5.2.5.

Presence of red fluorescence using fluorescein isothiocyanate (FITC) microscopy was used to confirm the position and distribution of the MSCs containing QDs.

6.2.8 pQCT

Changes in bone mineral density at the humeral head were assessed using the same method outlined in Section 5.2.6.

6.2.9 Statistical Analysis

Nonparametric statistical methods were used for all analyses because of the non-normality of the data in the groups being compared. Numerical data were inputted into SPSS software package, version 23 (SPSS Inc, an IBM Company, Chicago, Illinois). Mann Whitney U tests were used to compare data between groups. Results were considered significant at the $p < 0.05$ level. In order to determine whether there was any benefit in using MSCs, the data from this chapter was compared to that of Chapter Five.

6.3 Results

All animals survived the duration of the study and none had post-operative infection. Limping was noted for the first three to five postoperative days but a normal gait pattern returned afterwards.

6.3.1 Mesenchymal Stem Cell Tracking

QDs were demonstrated in all specimens where they were implanted, suggesting that the MSCs remained at the tendon-bone interface (Figure 6.4).

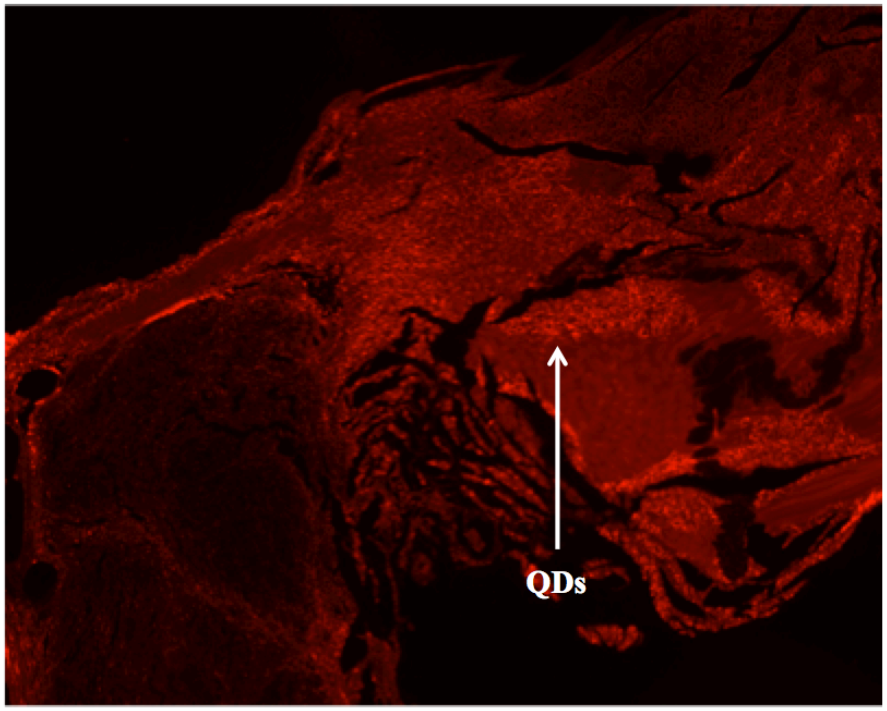

Figure 6.4: QDs at the tendon-bone interface denoted by red florescent cells; when viewed under a FITC filter.

6.3.2 Macroscopic Findings

At the time of euthanasia there was continuity between the repaired tendon and the bone in all groups. There were no infections and none of the repairs had failed as illustrated by the intact sutures. Remodeling of the graft material occurred to a greater extent in DBM group, whereby the scaffold could not be discerned from other tissue-types in the regenerated tendon-bone interface. In contrast, the GraftJacket group was clearly visible at necropsy. MSC-only specimens demonstrated complete closure of the enthesis. These were similar findings to Chapter Five, where MSCs were not used.

6.3.3 Quantitative Histology

6.3.3.1 Enthesis Maturation Score

No significant differences were observed in the enthesis maturation scores between experimental groups (Figure 6.5) (Table 5.9) (Figure 6.6). DBM had remodeled to a greater extent than GraftJacket, although not completely in all specimens. The median enthesis maturation score was 3 (95% CI 2.47 to 3.70) in the MSC group, 3 (95% CI 3 to 3) in the DBM + MSC group, and 2.5 (95% CI 1.88 to 3.46) in the GraftJacket + MSC group.

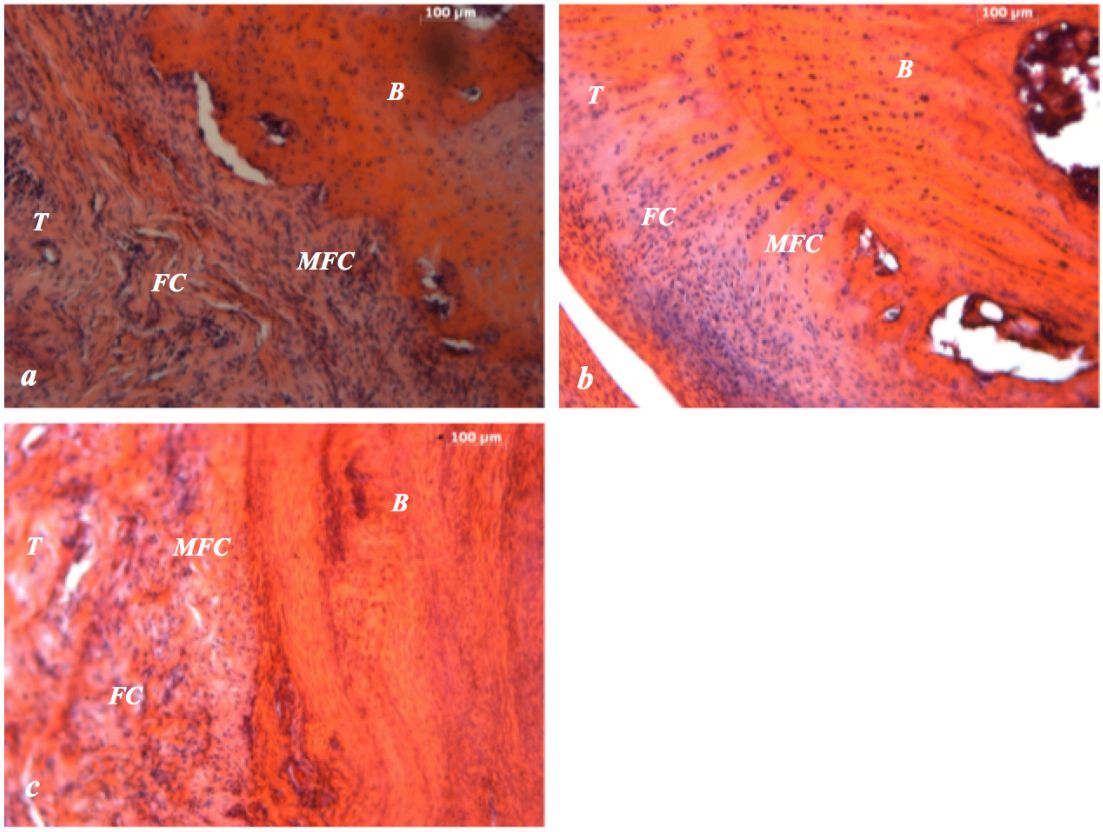

Figure 6.5: Photomicrograph of the enthesis at six weeks. Specimens stained with H&E. (a) Control: Tendon-bone repair with MSCs, characterised by a graded enthesis comprising tendon (T), fibrocartilage (FC), mineralised fibrocartilage, and bone (B). (b) DBM + MSCs: DBM neo enthesis comprising a well-organised, graded enthesis. (c) GraftJacket + MSCs: GraftJacket neo enthesis with a disorganised structure.

	MSCs alone	DBM + MSCs	GraftJacket + MSCs
MSCs alone	-	1	0.216
DBM+MSCs	1	-	0.107
GraftJacket+MSCs	0.216	0.107	-

Table 5.9: Statistical significance (p-values) between the enthesis maturation scores following tendon reattachment using MSCs alone, DBM + MSCs, and GraftJacket + MSCs.

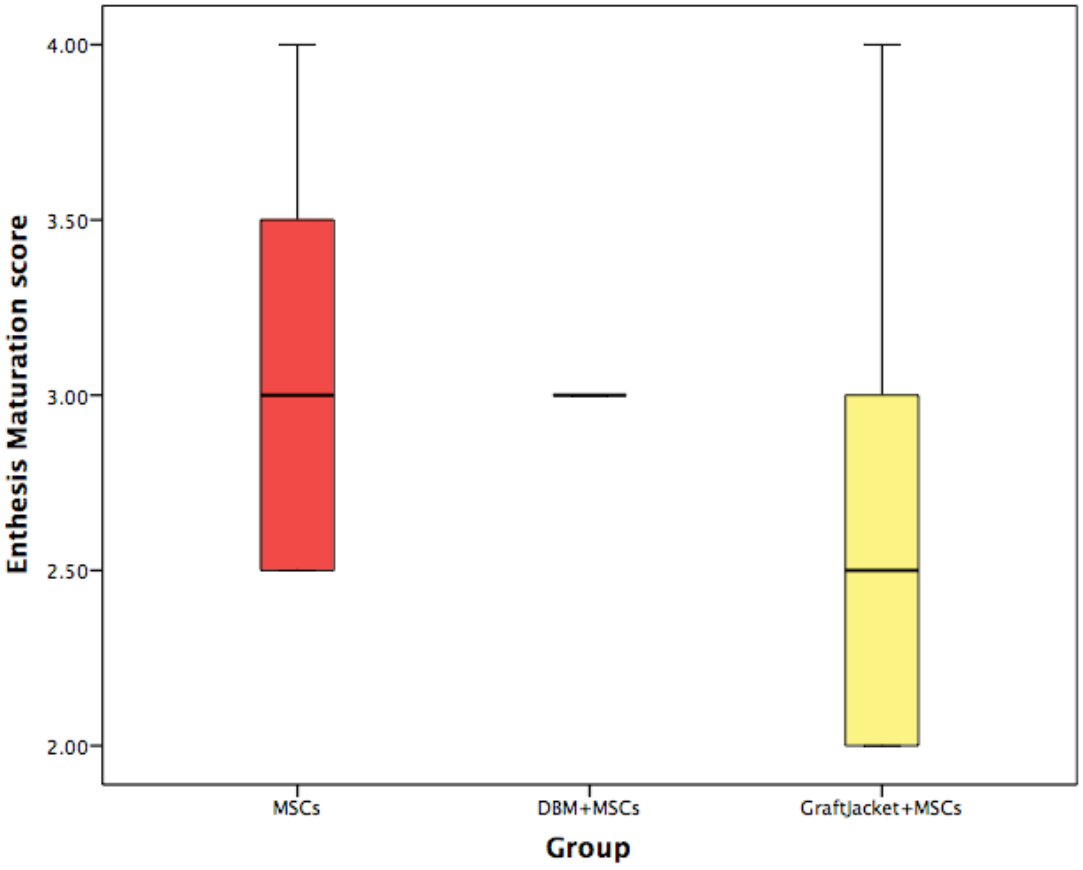

Figure 6.6: Box and whisker plot illustrating the enthesis maturation scores following tendon reattachment using MSCs alone, DBM + MSCs, and GraftJacket + MSCs.

6.3.3.2 Modified Movin Score

No significant differences in the modified Movin scores (indicating degeneration) were demonstrated between experimental groups (Table 6.0) (Figure 6.7). The median modified Movin score was 4.25 (95% CI 2.19 to 5.48) in the MSC group, 6.75 (95% CI 3.46 to 9.04) in the DBM + MSC group, and 5.75 (95% CI 4.55 to 7.62) in the GraftJacket + MSC group.

	MSCs alone	DBM+MSCs	GraftJacket+MSCs
MSCs alone	-	0.126	0.053
DBM+MSCs	0.126	-	0.746
GraftJacket+MSCs	0.053	0.746	-

Table 6.0: Statistical significance (p-values) between the modified Movin scores following tendon reattachment using MSCs alone, DBM + MSCs, and GraftJacket + MSCs.

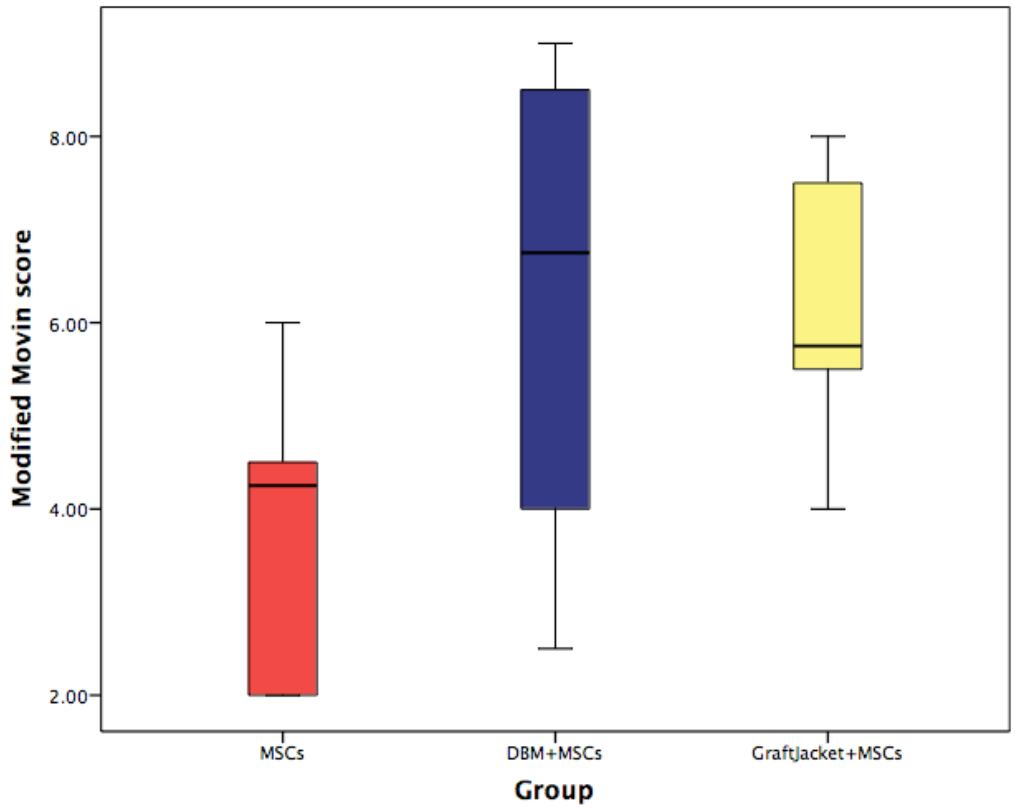

Figure 6.7: Box and whisker plot illustrating the modified Movin scores following tendon reattachment using MSCs alone, DBM + MSCs, and GraftJacket + MSCs.

6.3.3.3 Fiber Structure

All groups exhibited increased waviness and distance between collagen fibers, compared to the organised structure identified in the control specimens in Chapter Four (intact tendon-bone interface) (Figure 6.8). The median score was 1 (95% CI 0.12 to 1.55) in the MSC group, 1.75 (95% CI 1.03 to 2.30) in the DBM + MSC group, and 1.25 (95% CI 0.34 to 1.66) in the GraftJacket + MSC group (Table 6.1) (Figure 6.9).

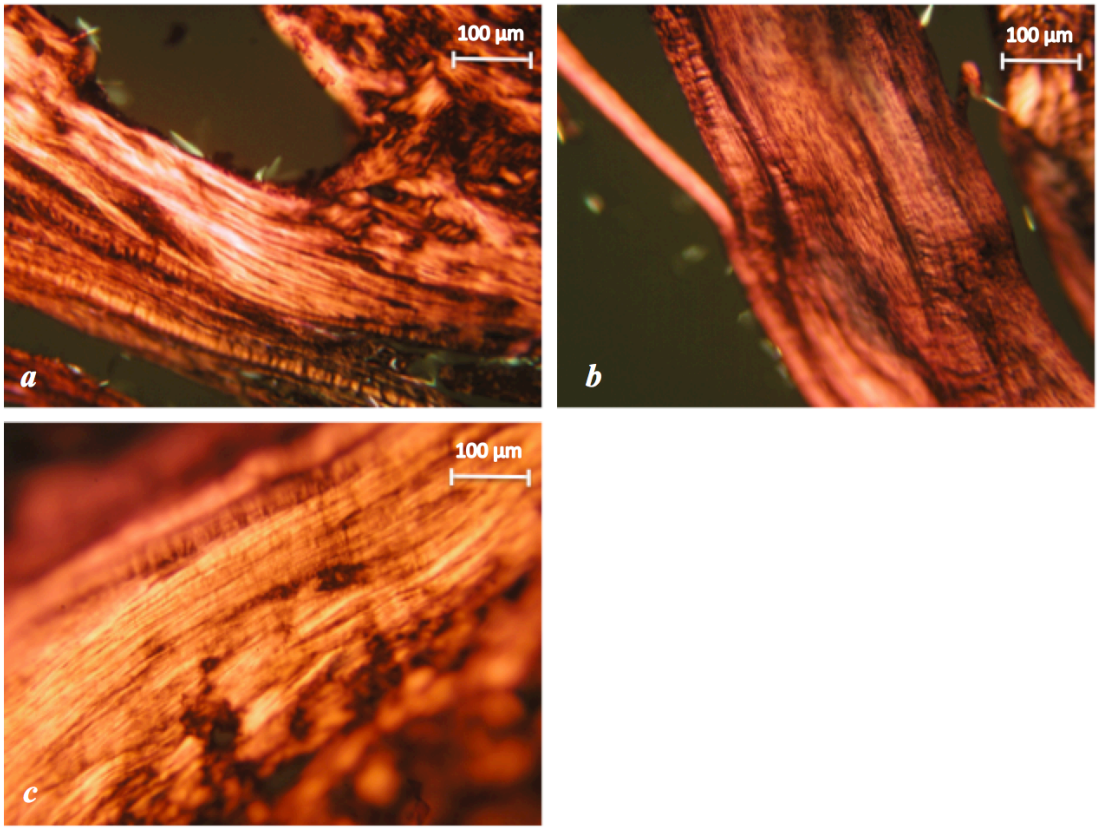

Figure 6.8: Photomicrograph (under polarised light) showing collagen fiber structure: (a) tendon-bone repair using MSCs alone, (b) DBM + MSCs, and (c) GraftJacket + MSCs.

	MSCs alone	DBM+MSCs	GraftJacket+MSCs
MSCs alone	-	0.070	0.613
DBM+MSCs	0.070	-	0.118
GraftJacket+MSCs	0.613	0.118	-

Table 6.1: Statistical significance (p-values) between fiber structure following tendon reattachment using MSCs alone, DBM + MSCs, and GraftJacket + MSCs.

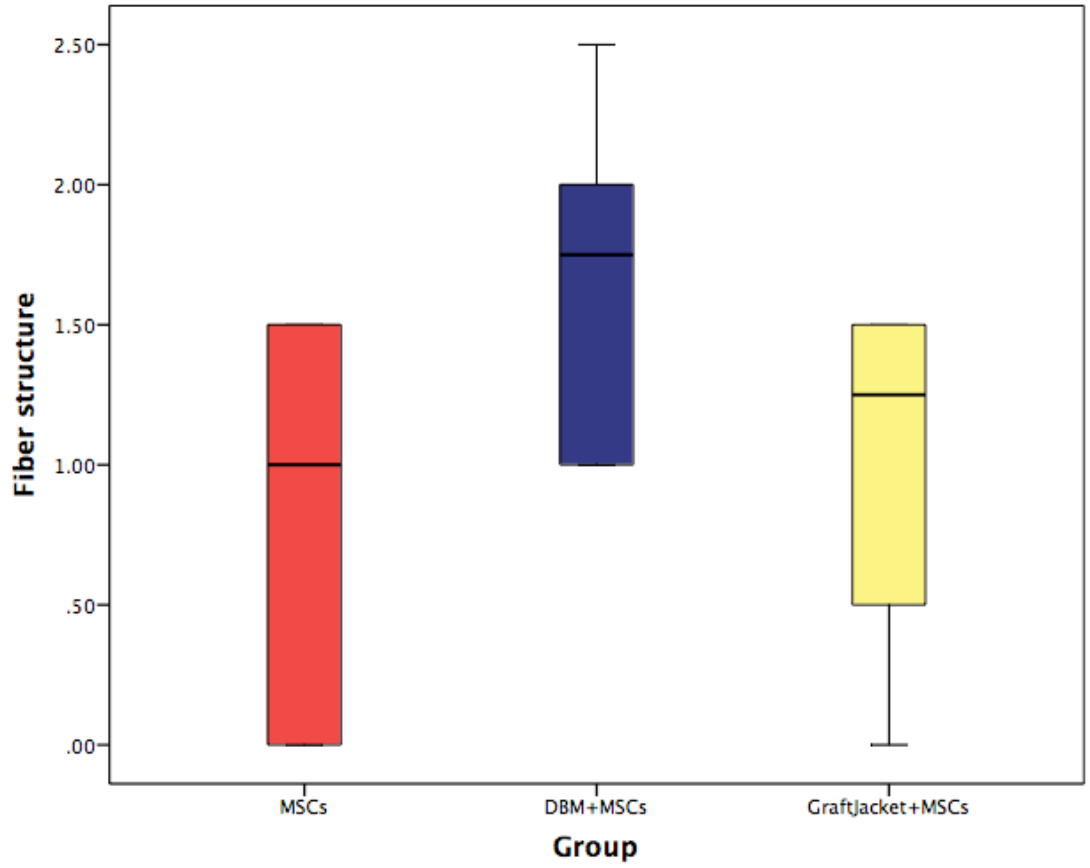

Figure 6.9: Box and whisker plot illustrating the difference in fiber structure following tendon reattachment using MSCs alone, DBM + MSCs, and GraftJacket + MSCs.

6.3.3.4 Fiber Arrangement

All groups exhibited a loss of the parallel arrangement observed in the control specimens in Chapter Four (intact tendon-bone interface) (Figure 6.8). The median score was 1 (95% CI 0.52 to 1.31) in the MSC group, 1 (95% CI 0.81 to 1.69) in the DBM + MSC group, and 2 (95% CI 1.70 to 2.13) in the GraftJacket + MSC group (Table 6.2) (Figure 6.10). Fiber arrangement was significantly more abnormal in the

GraftJacket group than in the DBM group ($p = 0.014$) and the MSC group ($p = 0.003$).

	MSCs alone	DBM+MSCs	GraftJacket+MSCs
MSCs alone	-	0.179	0.003
DBM+MSCs	0.179	-	0.014
GraftJacket+MSCs	0.003	0.014	-

Table 6.2: Statistical significance (p-values) between fiber arrangement following tendon reattachment using MSCs alone, DBM + MSCs, and GraftJacket + MSCs.

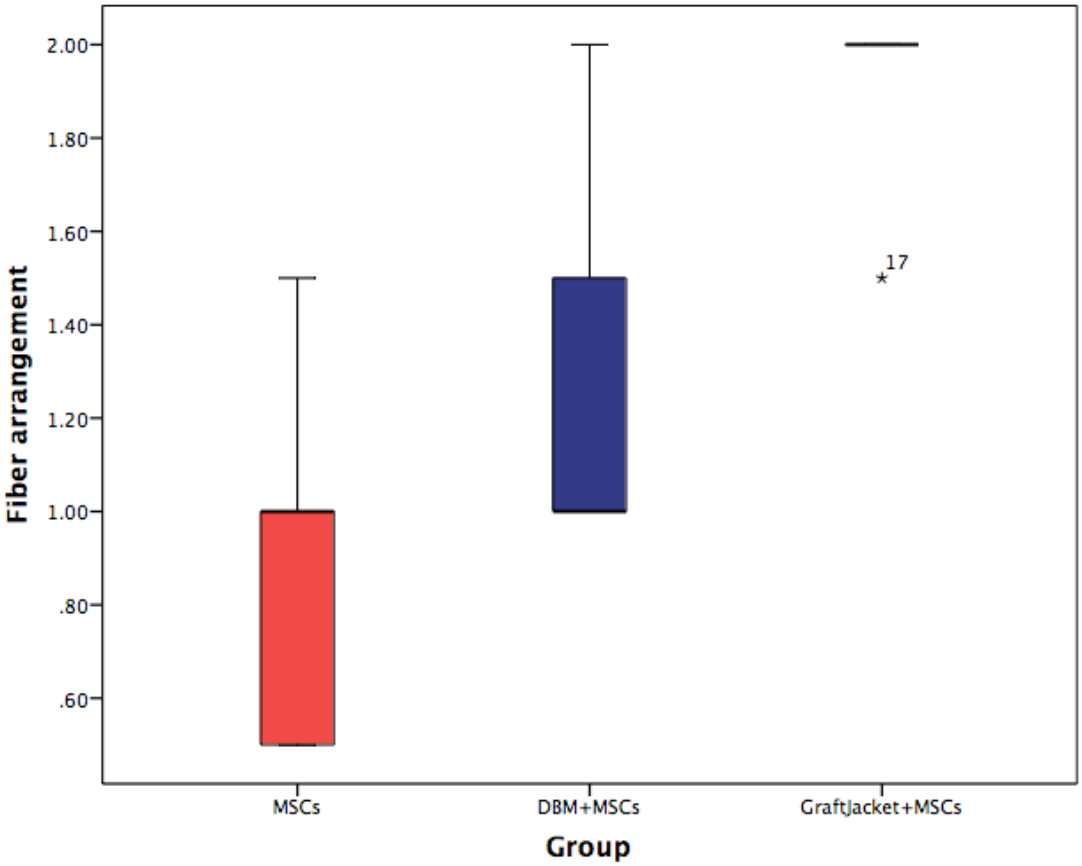

Figure 6.10: Box and whisker plot illustrating the difference in fiber arrangement following tendon reattachment using MSCs alone, DBM + MSCs, and GraftJacket + MSCs.

6.3.3.5 Tenocyte Nuclei

Rounding of nuclei (indicating persistent degeneration) was identified in all groups following tendon reattachment (Figure 6.11). The median score was 1 (95% CI 0.74 to 1.60) in the MSC group, 1.50 (95% CI 0.48 to 2.19) in the DBM + MSC group, and 1 (95% CI 0.79 to 1.88) in the GraftJacket + MSC group (Table 6.3) (Figure 6.12).

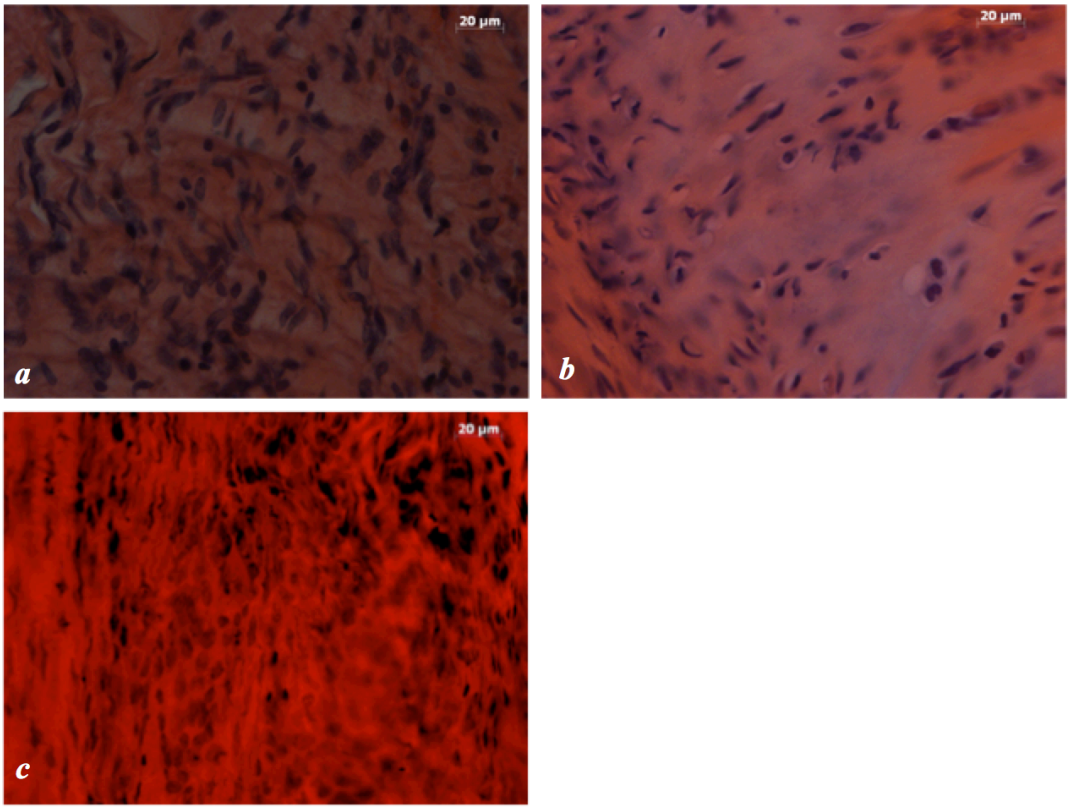

Figure 6.11: Photomicrograph illustrating rounded nuclei. (a) Controls (tendon-bone repair with MSCs alone). (b) DBM + MSC group. (c) GraftJacket + MSC group.

	MSCs alone	DBM+MSCs	GraftJacket+MSCs
MSCs alone	-	0.523	0.523
DBM+MSCs	0.523	-	0.859
GraftJacket+MSCs	0.523	0.859	-

Table 6.3: Statistical significance (p-values) between tenocyte nuclei morphology following tendon reattachment using MSCs alone, DBM + MSCs, and GraftJacket + MSCs.

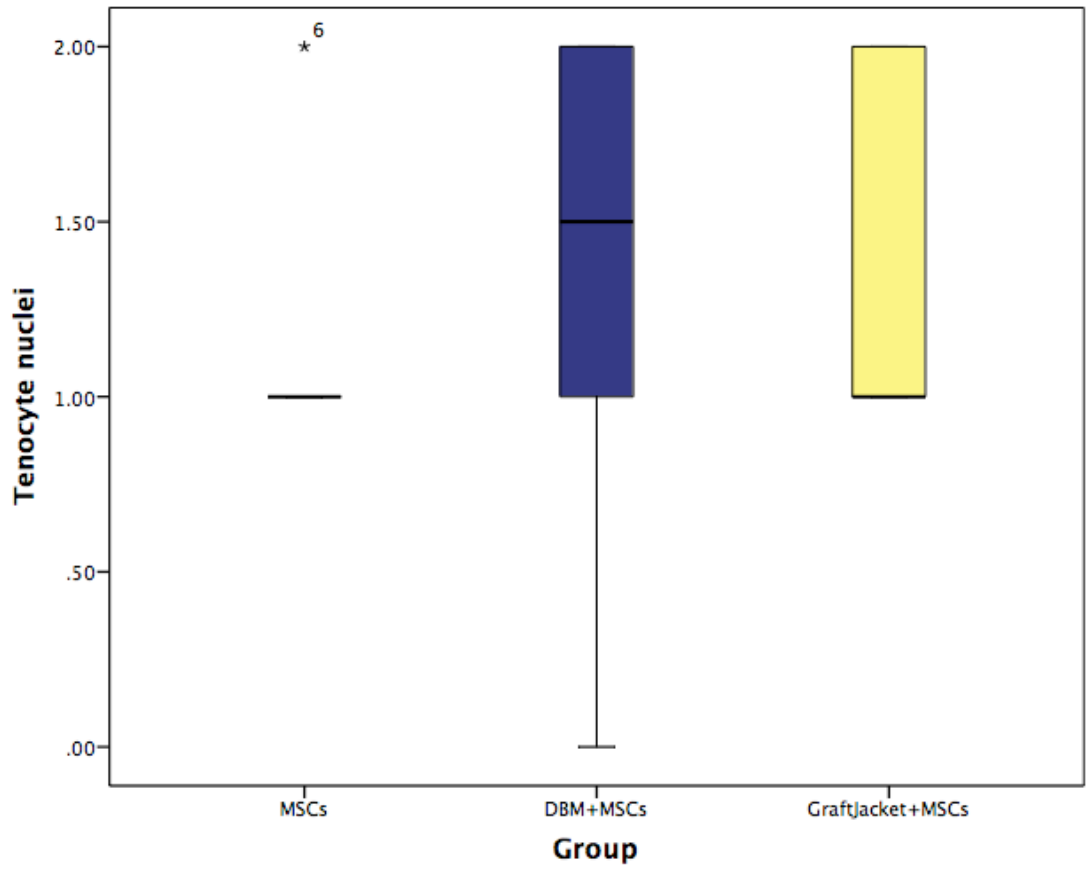

Figure 6.12: Box and whisker plot illustrating the difference in tenocyte nuclei morphology following tendon reattachment using MSCs alone, DBM + MSCs, and GraftJacket + MSCs.

6.3.3.6 Cellularity

Specimens were evaluated for an increase in cellularity, indicating persistent degeneration. The median score was 1 (95% CI 0.56 to 1.10) in the MSC group, 1.50 (95% CI 0.72 to 2.11) in the DBM + MSC group, and 1.25 (95% CI 0.90 to 1.93) in the GraftJacket + MSC group (Table 6.4) (Figure 6.13). Cellularity was significantly

less (indicating less noticeable degeneration) in the MSC group than in the GraftJacket group (p = 0.031).

	MSCs alone	DBM+MSCs	GraftJacket+MSCs
MSCs alone	-	0.118	0.031
DBM+MSCs	0.118	-	1
GraftJacket+MSCs	0.031	1	-

Table 6.4: Statistical significance (p-values) between cellularity following tendon reattachment using MSCs alone, DBM + MSCs, and GraftJacket + MSCs.

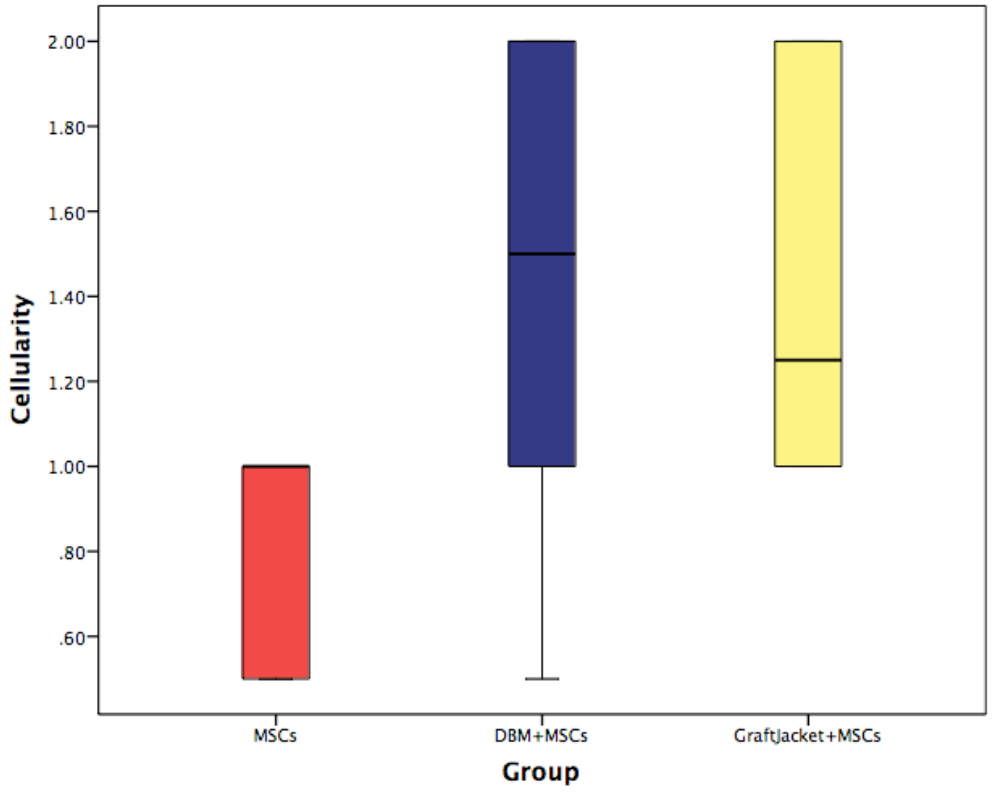

Figure 6.13: Box and whisker plot illustrating the difference in cellularity following tendon reattachment using MSCs alone, DBM + MSCs, and GraftJacket + MSCs.

6.3.3.7 Vascularity

Specimens were evaluated for an increase in vascularity, indicating persistent degeneration (Longo et al., 2008). The median score was 0 (95% CI -0.13 to 0.30) in the MSC group, 0.25 (95% CI -0.26 to 1.42) in the DBM + MSC group, and 0.5 (95% CI 0.02 to 0.81) in the GraftJacket + MSC group (Table 6.5) (Figure 6.14).

	MSCs alone	DBM+MSCs	GraftJacket+MSCs
MSCs alone	-	0.181	0.083
DBM+MSCs	0.181	-	1
GraftJacket+MSCs	0.083	1	-

Table 6.5: Statistical significance (p-values) in vascularity following tendon reattachment using MSCs alone, DBM + MSCs, and GraftJacket + MSCs.

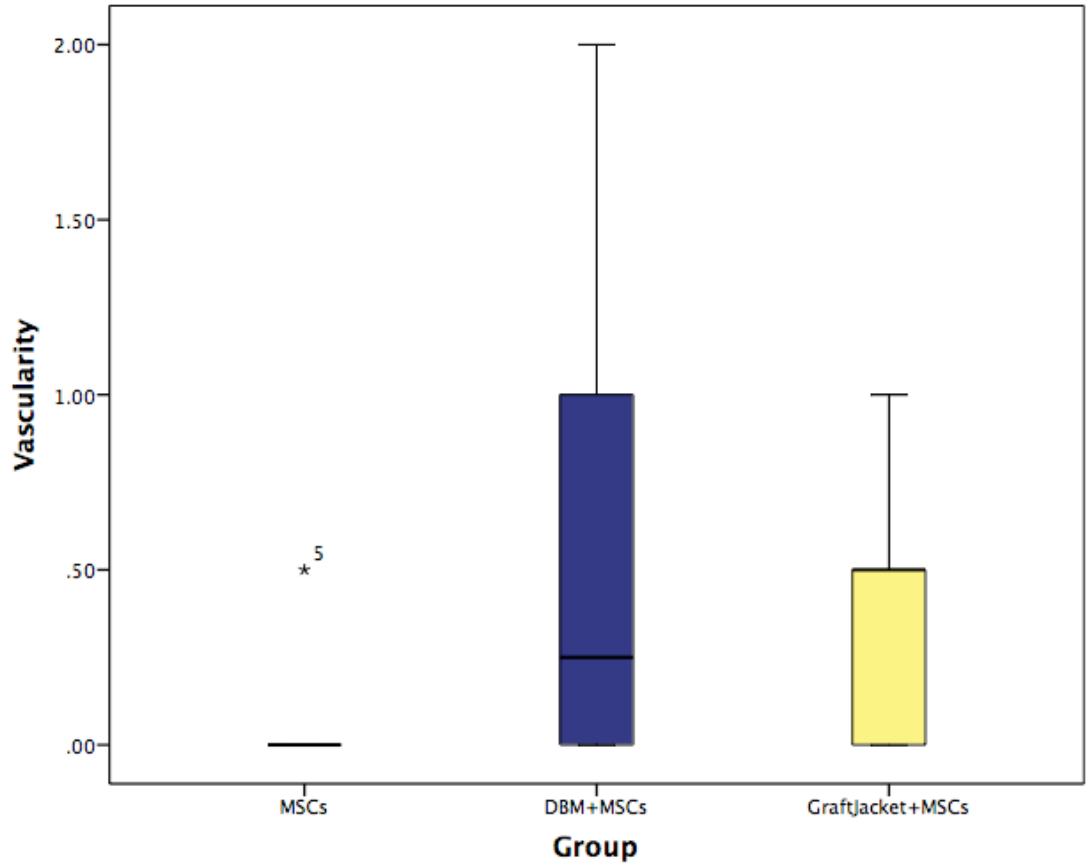

Figure 6.14: Box and whisker plot illustrating the difference in vascularity following tendon reattachment using MSCs alone, DBM + MSCs, and GraftJacket + MSCs.

6.3.3.8 Hyalinisation

Hyalinisation was not observed in any of the specimens.

6.3.4 Comparison of Quantitative Histology: MSCs vs No MSCs

Results discussed from herein are a direct comparison between the histological outcomes in Chapters Five and Six, i.e. MSCs (Chapter Six) versus no MSCs (Chapter Five). In this section, the Mann Whitney U test was used to compare the results between the two groups.

6.3.4.1 Enthesis Maturation Score

Repairs with MSCs alone and DBM + MSCs resulted in a significantly more mature enthesis than repairs augmented with GraftJacket alone ($p = 0.044$ and 0.007 respectively). There were no significant differences between other experimental groups (Table 6.6) (Figure 6.15).

	Controls (Non-augmented tendon-bone repair)	DBM	GraftJacket
MSCs alone	0.216	1	0.044
DBM+MSCs	0.107	1	0.007
GraftJacket+MSCs	1	0.413	0.672

Table 6.6: Statistical significance (p-values) between the enthesis maturation scores following tendon reattachment between MSC and non-MSC groups.

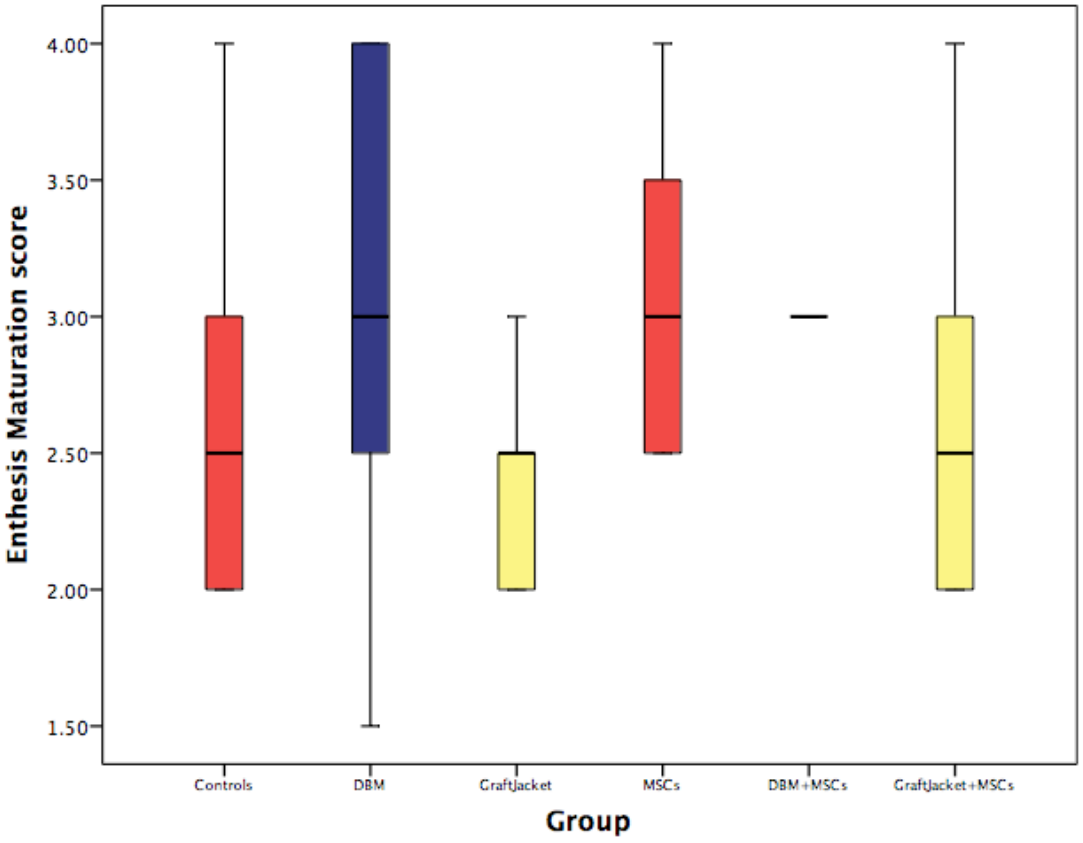

Figure 6.15: Box and whisker plot illustrating the enthesis maturation scores following tendon reattachment between MSC and non-MSC groups.

6.3.4.2 Modified Movin Score

Repairs with MSCs alone resulted in a significantly less degenerative tendon than repairs augmented with GraftJacket and non-augmented controls ($p = 0.004$ and 0.008 respectively). Furthermore, the addition of MSCs to GraftJacket produced a tendon that was significantly less degenerative ($p = 0.025$). There were no significant differences between other experimental groups (Table 6.7) (Figure 6.16).

	Controls (Non-augmented tendon-bone repair)	DBM	GraftJacket
MSCs alone	0.008	0.126	0.004
DBM+MSCs	0.423	0.810	0.065
GraftJacket+MSCs	0.260	0.936	0.025

Table 6.7: Statistical significance (p-values) between the modified Movin scores following tendon reattachment between MSC and non-MSC groups.

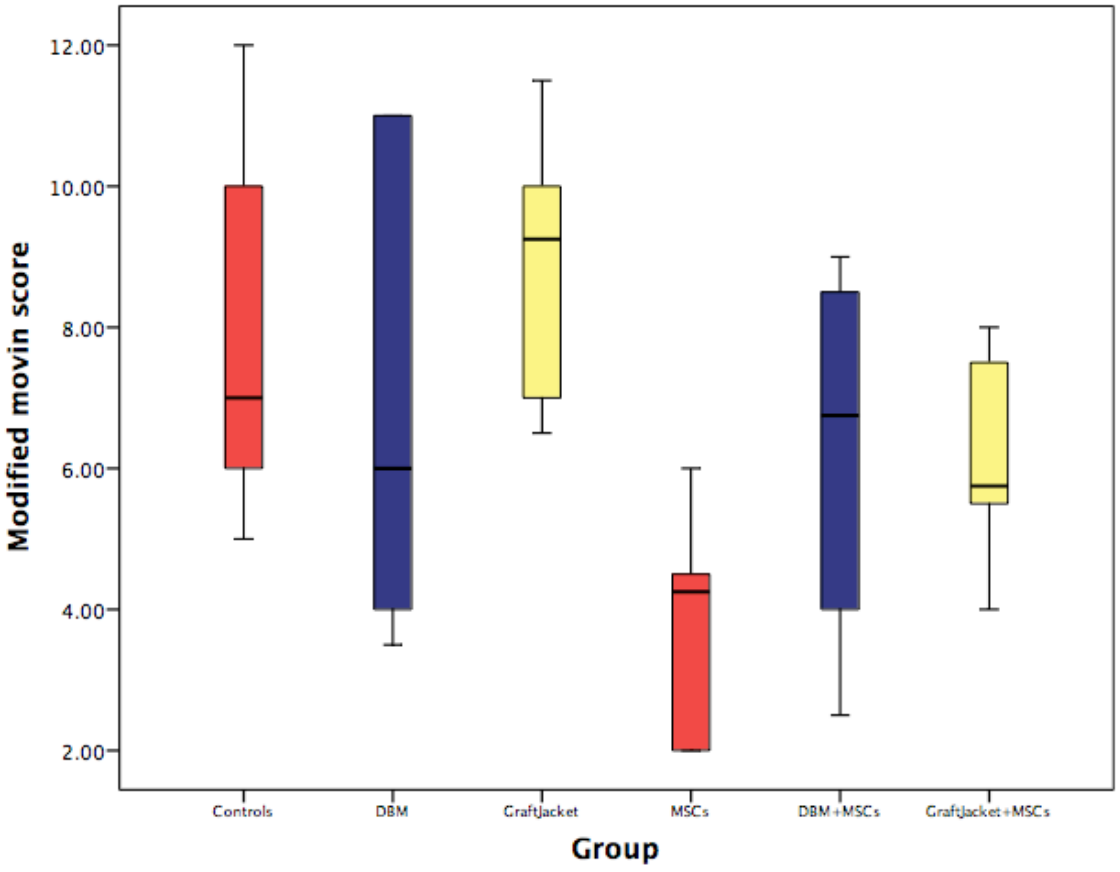

Figure 6.16: Box and whisker plot illustrating the modified Movin scores following tendon reattachment between MSC and non-MSC groups.

6.3.4.3 Fiber Structure

The addition of MSCs did not result in any significant improvement in fiber structure compared to repairs performed without stem cells (Table 6.8) (Figure 6.17).

	Controls (Non-augmented tendon-bone repair)	DBM	GraftJacket
MSCs alone	0.068	0.190	0.134
DBM+MSCs	0.799	0.869	0.933
GraftJacket+MSCs	0.116	0.289	0.218

Table 6.8: Statistical significance (p-values) between the modified Movin scores following tendon reattachment between MSC and non-MSC groups.

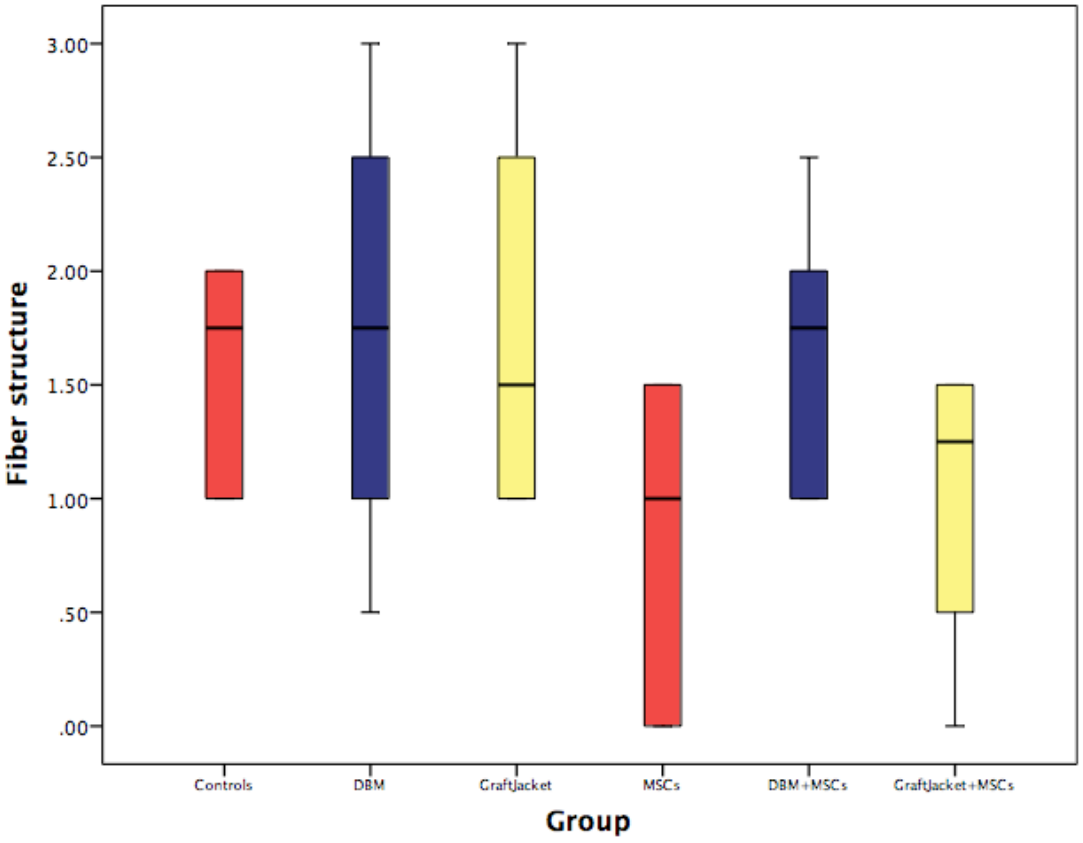

Figure 6.17: Box and whisker plot illustrating the modified Movin scores following tendon reattachment between MSC and non-MSC groups.

6.3.4.4 Fiber Arrangement

Fiber arrangement was significantly less abnormal (characterised by a more parallel arrangement) in all three MSC groups compared to GraftJacket alone, and the addition of MSCs resulted in significantly less abnormal fiber structure compared to non-augmented controls ($p = 0.044$). There were no significant differences between other experimental groups (Table 6.9) (Figure 6.18).

	Controls (Non-augmented tendon-bone repair)	DBM	GraftJacket
MSCs alone	0.044	0.086	0.003
DBM+MSCs	0.262	0.473	0.006
GraftJacket+MSCs	0.195	0.167	0.045

Table 6.9: Statistical significance (p-values) between fiber arrangement following tendon reattachment between MSC and non-MSC groups.

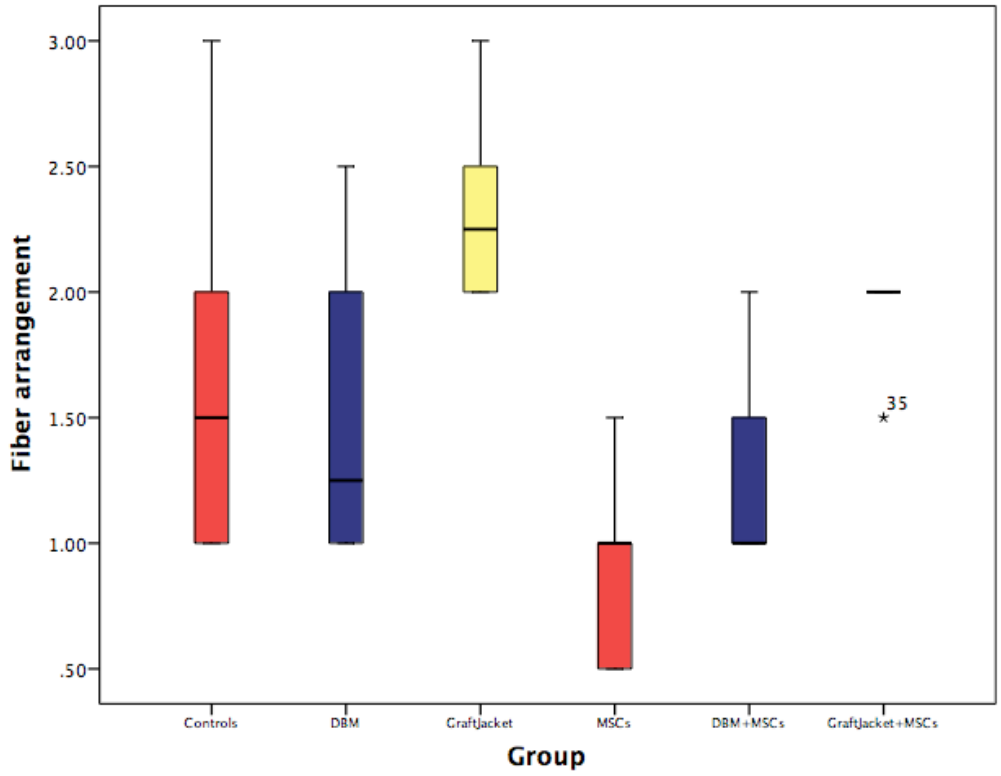

Figure 6.18: Box and whisker plot illustrating the difference in fiber arrangement following tendon reattachment between MSC and non-MSC groups.

6.3.4.5 Tenocyte Nuclei

Significantly less rounded tenocyte nuclei (indicating less degeneration) were identified in cases of tendon-bone repair with MSCs alone compared to repairs with no augmentation strategy and with GraftJacket ($p = 0.047$ and 0.015 respectively). There were no significant differences between other experimental groups (Table 6.10) (Figure 6.19).

	Controls (Non-augmented tendon-bone repair)	DBM	GraftJacket
MSCs alone	0.047	0.149	0.015
DBM+MSCs	0.402	0.865	0.282
GraftJacket+MSCs	0.175	0.484	0.080

Table 6.10: Statistical significance (p-values) between tenocyte nuclei morphology following tendon reattachment between MSC and non-MSC groups.

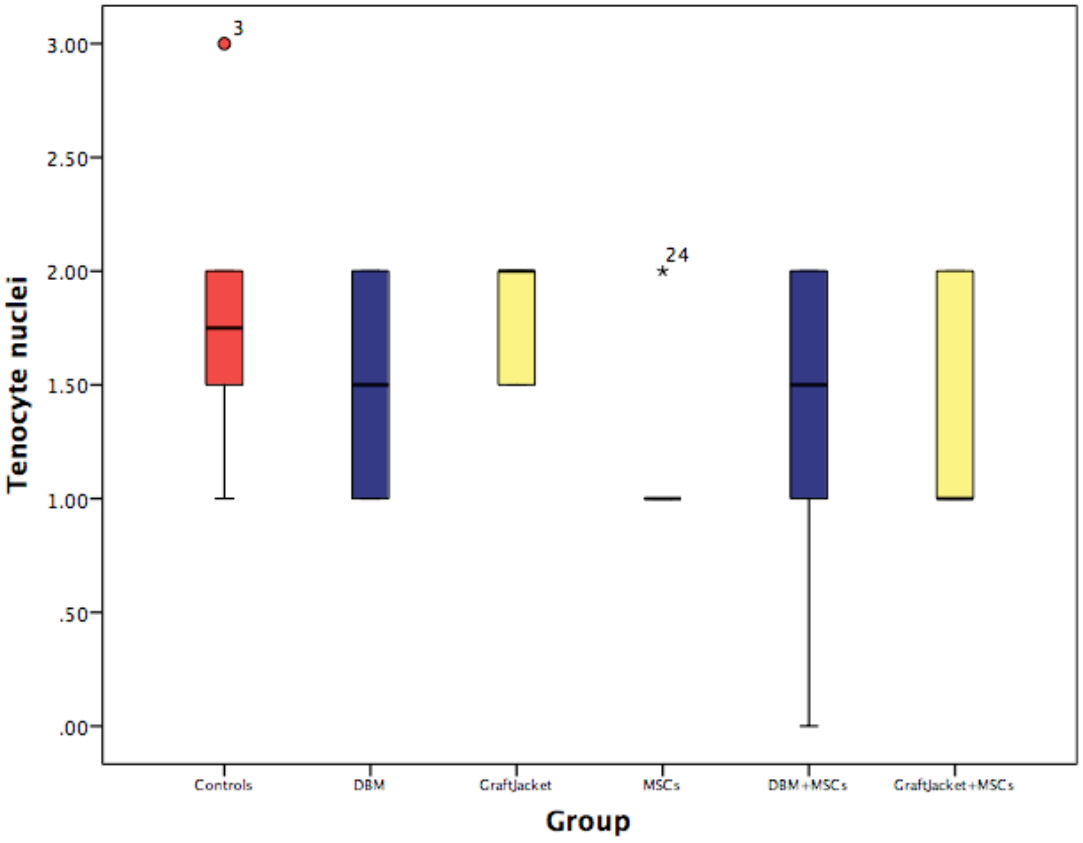

Figure 6.19: Box and whisker plot illustrating the difference in tenocyte nuclei morphology following tendon reattachment between MSC and non-MSC groups.

6.3.4.6 Cellularity

Significantly less cellularity (indicating less degeneration) was identified in cases of tendon-bone repair with MSCs alone compared to repairs without stem cells and a scaffold, and with GraftJacket ($p = 0.016$ and 0.003 respectively). Furthermore, the addition of MSCs to GraftJacket resulted in significantly less cellularity ($p = 0.036$). There were no significant differences between other experimental groups (Table 6.11) (Figure 6.20).

	Controls (Non-augmented tendon-bone repair)	DBM	GraftJacket
MSCs alone	0.016	0.120	0.003
DBM+MSCs	0.677	0.799	0.072
GraftJacket+MSCs	0.613	0.799	0.036

Table 6.11: Statistical significance (p-values) between cellularity following tendon reattachment between MSC and non-MSC groups.

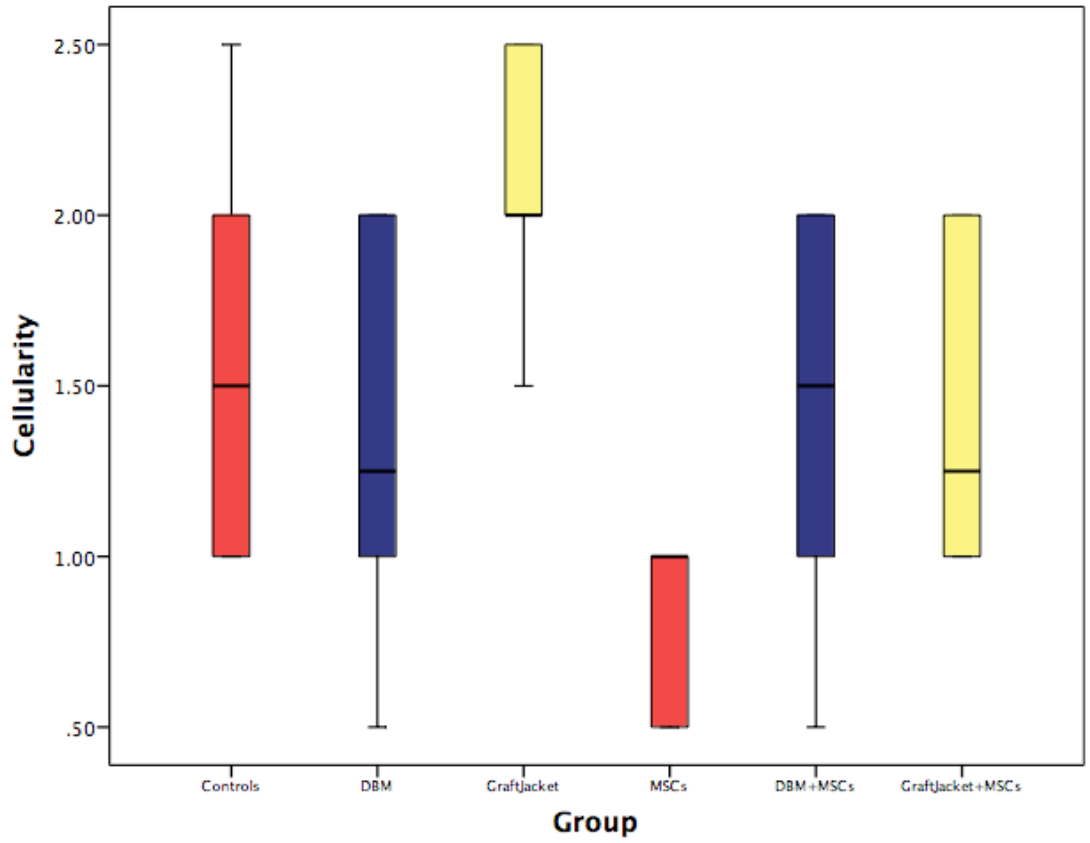

Figure 6.20: Box and whisker plot illustrating the difference in cellularity following tendon reattachment between MSC and non-MSC groups.

6.3.4.7 Vascularity

Significantly fewer vascular bundles (indicating less degeneration) were identified in cases of tendon-bone repair with MSCs alone compared to repairs without stem cells and a scaffold, and with GraftJacket ($p = 0.013$ and 0.016 respectively). Furthermore, repairs with GraftJacket + MSCs were significantly less vascular than cases of tendon-bone repair without a scaffold ($p = 0.041$). There were no significant differences between other experimental groups (Table 6.12) (Figure 6.21).

	Controls (Non-augmented tendon-bone repair)	DBM	GraftJacket
MSCs alone	0.013	0.181	0.016
DBM+MSCs	0.138	0.797	0.323
GraftJacket+MSCs	0.041	0.933	0.115

Table 6.12: Statistical significance (p-values) in vascularity following tendon reattachment between MSC and non-MSC groups.

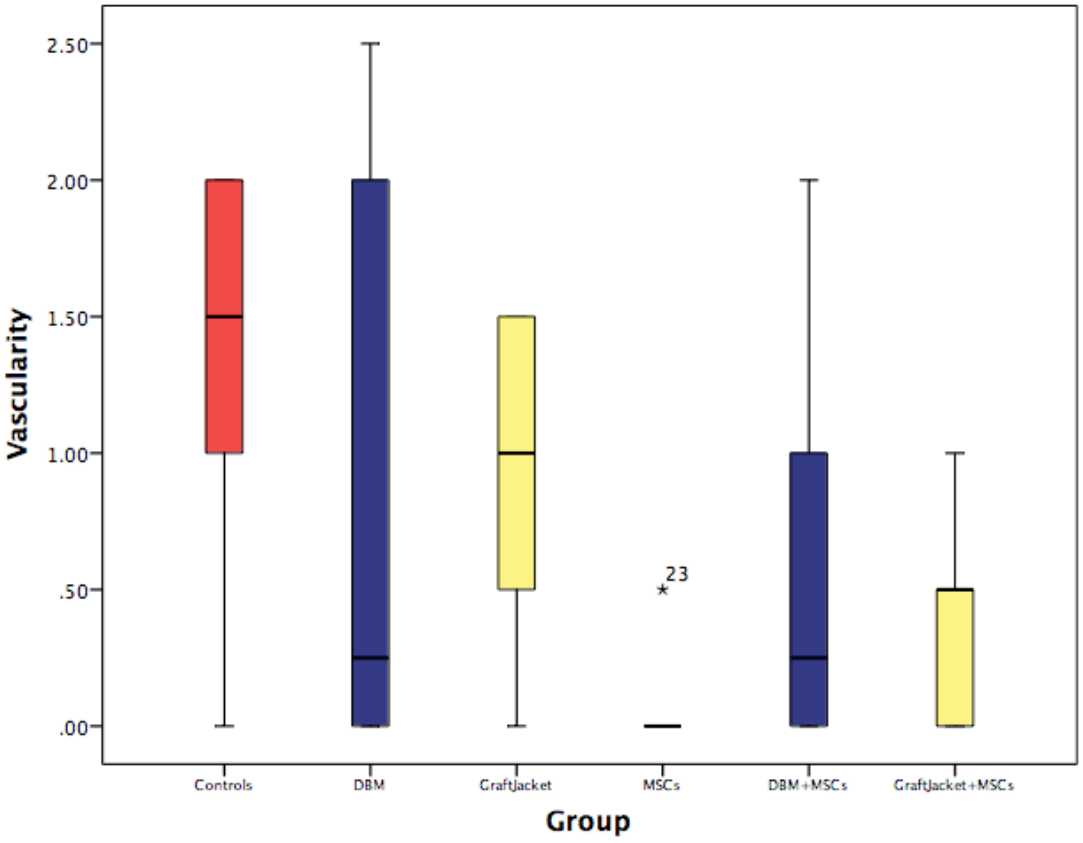

Figure 6.21: Box and whisker plot illustrating the difference in vascularity following tendon reattachment between MSC and non-MSC groups.

6.3.4.8 Hyalinisation

Hyalinisation was not observed in any of the specimens.

6.3.5 pQCT

Control specimens comprised the contralateral shoulder of animals that had undergone unilateral tendon detachment three weeks earlier (as discussed in Chapter Four). In this group (n = 6), the median total bone mineral density at the supraspinatus tendon-bone insertion was 793.25 mg/ccm (95% CI 754.24 to 844.70) (Figure 6.22). This significantly decreased six weeks following repair with GraftJacket + MSCs and repair with MSCs alone to a median 717.25 mg/ccm (95% CI 582.54 to 782.39) (p = 0.010) and 719.65 (95% CI 666.80 to 765.27) (p = 0.010) respectively (Table 6.13). In repairs with DBM + MSCs, median bone mineral density was 701.20 mg/ccm (95% CI 621.27 to 794.73). This was not significantly different to controls (p = 0.055). No significant increase in bone mineral density was conferred by the addition of MSCs to the healing interface (Figure 6.23) (Table 6.14).

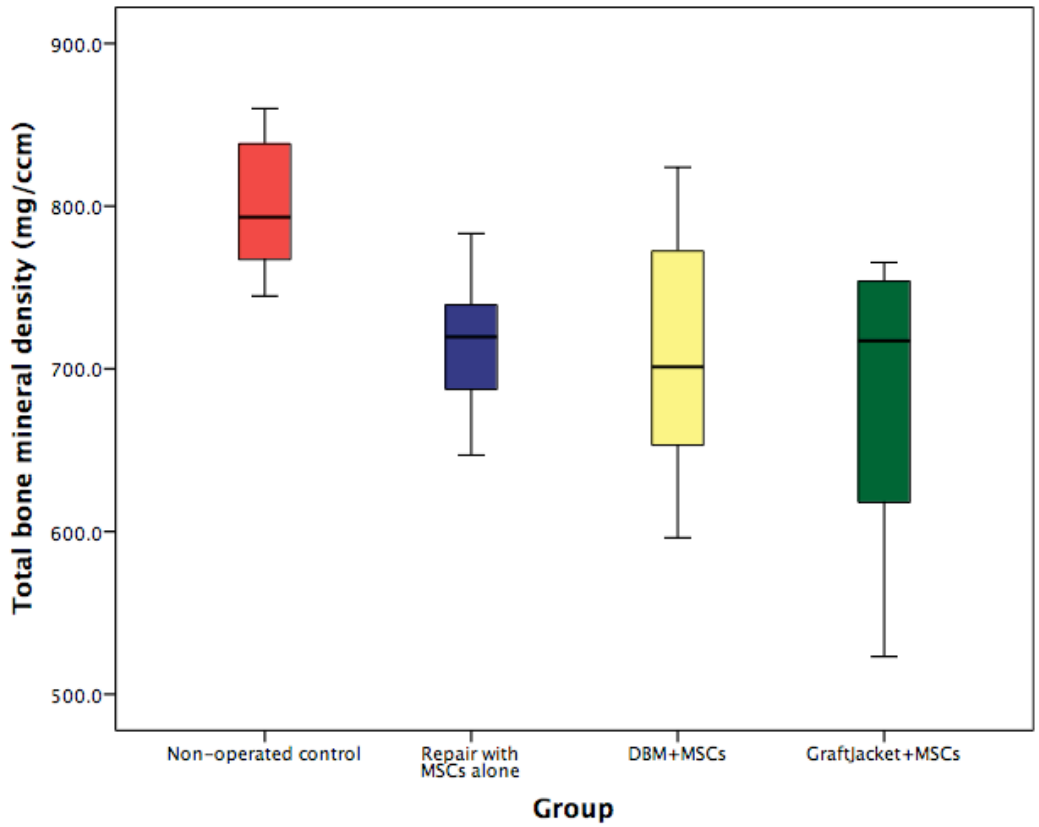

Figure 6.22: Box and whisker plot showing total bone mineral density at the supraspinatus tendon-bone insertion six weeks following repair with MSCs alone, cortical DBM and MSCs, and GraftJacket and MSCs.

	Non-operated control	Repair with MSCs alone	DBM with MSCs	GraftJacket with MSCs
Non-operated control	-	0.010	0.055	0.010
Repair with MSCs alone	0.010	-	0.749	0.873
DBM with MSCs	0.055	0.749	-	0.749
GraftJacket with MSCs	0.010	0.873	0.749	-

Table 6.13: Statistical significance (p-values) between total bone mineral density at the supraspinatus tendon-bone insertion six weeks following repair with MSCs alone, cortical DBM and MSCs, and GraftJacket and MSCs.

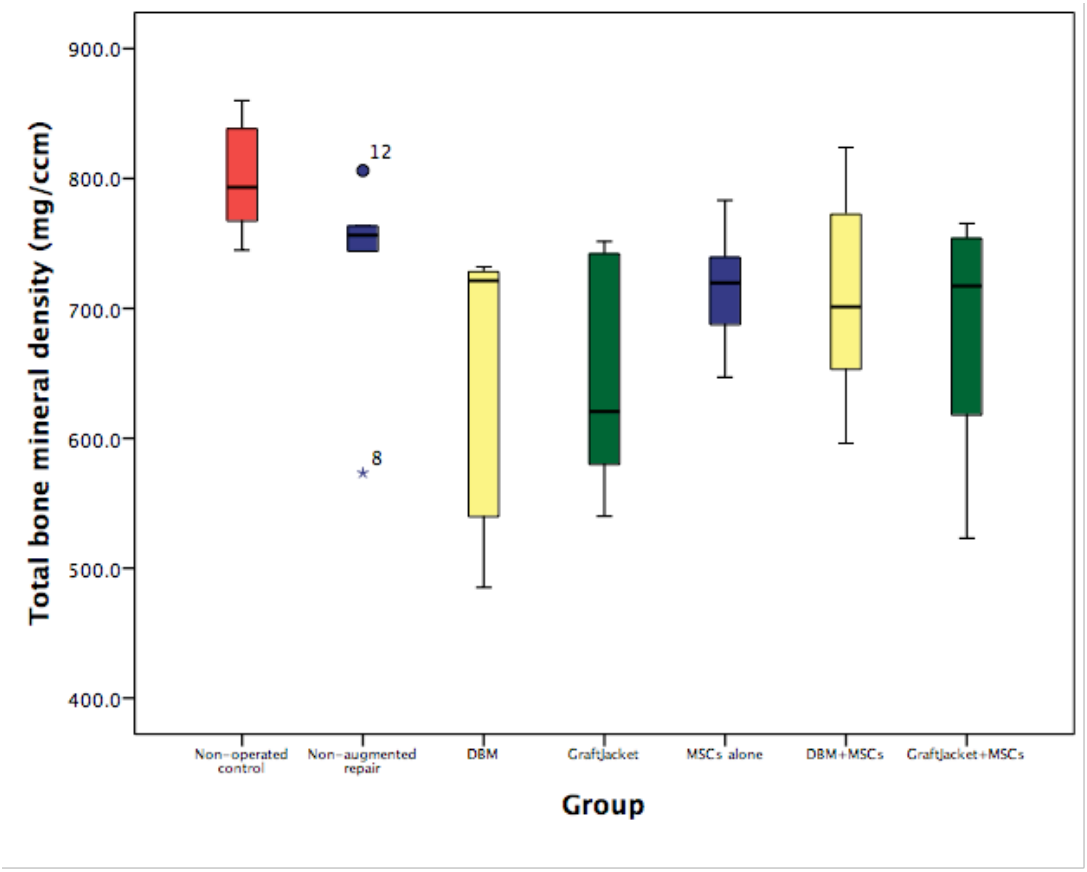

Figure 6.23: Box and whisker plot showing total bone mineral density at the supraspinatus tendon-bone insertion six weeks following repair with and without MSCs.

	Controls (Non-augmented tendon-bone repair)	DBM	GraftJacket
MSCs alone	0.200	0.337	0.200
DBM+MSCs	0.631	0.522	0.200
GraftJacket+MSCs	0.200	0.423	0.337

Table 6.14: Statistical significance (p-values) between total bone mineral density at the supraspinatus tendon-bone insertion six weeks following repair with and without MSCs.

6.4 Discussion

In this chapter, it was hypothesised that compared to MSCs alone, DBM + MSCs would regenerate a morphologically superior enthesis characterised by greater fibrocartilage formation and improved collagen fiber organisation in a rat model of a chronic rotator cuff tear. It was further hypothesised that DBM would result in a higher bone mineral density at the insertion site. These hypotheses though, are only partially supported by the results.

Using a rat model of chronic rotator cuff degeneration, tendons were reattached to their bony insertion with DBM + MSCs, GraftJacket + MSCs, and MSCs alone (controls), and analysed after six weeks. MSCs were confined to the healing enthesis as illustrated by the presence of QDs on confocal microscopy. All groups demonstrated closure of the tendon-bone gap with a fibrocartilaginous enthesis, but the degenerative process could not be reversed (as illustrated by a persistently high Modified Movin score). Although there were no significant differences in the enthesis maturation and Modified Movin scores, repairs augmented with GraftJacket + MSCs exhibited a disorganised enthesis, abnormal collagen fiber arrangement, and greater cellularity (indicating persistent degeneration) compared to other MSC groups. In addition to these histological parameters, bone mineral density at the enthesis was examined. This showed that only repairs augmented with DBM + MSCs reached a bone mineral density not significantly lower than non-operated controls. This suggests that MSCs were able to enhance this aspect of DBM's function because a similar outcome was not observed when DBM was used in isolation (Chapter Five).

To determine whether MSCs could enhance the structure of the healing enthesis compared to repairs without stem cells, the results of this experiment were compared to those from Chapter Five. It was hypothesised that the addition of MSCs would yield a morphologically superior interface. This was partially supported by the results, in that groups treated with MSCs alone and DBM + MSCs resulted in a more mature enthesis (characterised by a significantly higher enthesis maturation score) than those repaired with GraftJacket. The addition of MSCs to GraftJacket produced a tendon that was significantly less degenerative (characterised by a lower Modified Movin score). Furthermore, repairs with MSCs alone produced a tendon that was significantly less degenerative than non-augmented controls and repairs enhanced with GraftJacket. This highlights a supplementary role of MSCs in enthesis healing when used in conjunction with biological scaffolds.

Several *in vivo* studies have evaluated the use of MSCs in tendon-bone healing (Gulotta et al., 2010, Gulotta et al., 2011a, Hernigou et al., 2014, Gulotta et al., 2009). In a non-degenerative rotator cuff tear model, Gulotta et al (Gulotta et al., 2009) applied MSCs to an acutely detached supraspinatus tendon. At four weeks, the biomechanical strengths of the repairs were equal between MSC and control groups, and there was no difference in the amount of new cartilage formation or collagen fiber organisation. This was attributed to a lack of growth/transcription factors and so further studies evaluated the effect of MT1-MMP on MSCs and MSCs transduced with Ad-Scx (Gulotta et al., 2010, Gulotta et al., 2011a). The results suggested that MSCs used in this context could result in more fibrocartilage, a higher ultimate load to failure, and a higher ultimate stress to failure.

The current study could not reproduce the results of MSC-induced tendon-bone healing observed in other animal models, even in the presence of DBM (Gulotta et al., 2010, Gulotta et al., 2011a). This is most likely due to the limited tendon-bone surface area in a rat model not presenting an environment that is as conducive to healing as large animal models and those that utilise a tendon-bone tunnel (Greis et al., 2001, Gulotta et al., 2009). DBM contains multiple growth factors such as BMPs and TGFs (Sawkins et al., 2013, Veillette and McKee, 2007, Urist, 1965, Urist et al., 1983, Reddi, 1998). It is plausible that these were released slowly with time and were therefore unable to completely exert their effect on the MSCs during the six weeks where enthesis healing was permitted to take place. The next important finding of this study was that it was only in the DBM group where bone mineral density did not significantly differ from controls, suggesting that there was a predominance of bone formation over bone resorption. This is likely to be due to endogenous supplies of BMP-2 and TGF-β within DBM acting on MSCs to form new bone in the developing enthesis (Sundar et al., 2009b, Urist, 1965).

Limitations of this study are principally due to the short time-period (six weeks) that the healing enthesis was allowed to develop over. It is feasible that with a longer study protocol, the new bony ingrowth in the DBM group that led to a preservation of bone mineral density compared to other experimental groups where bone mineral density had decreased, could have developed into fibrocartilage and mineralised fibrocartilage. Only one concentration of MSCs was used, as this was extrapolated from the existing literature. With greater cell numbers it is possible that a greater difference between MSC and non-MSC groups would have been identified. A larger number of animals within the groups may have resulted in more significant values and

a clearer indication of the benefits or drawbacks of the treatments. The lack of biomechanical testing prevents any discussion about functional recovery of the enthesis, which is a particularly important consideration in the clinical setting as this may affect the success of postoperative rehabilitation.

6.5 Conclusion

This study demonstrated that when DBM and MSCs were applied to the healing enthesis in a chronic rotator cuff tear model, a fibrocartilaginous-based structure was produced, albeit not significantly more mature than other experimental groups. In comparison to the results of Chapter Five where stem cells were not used, MSCs were found to enhance the effects of GraftJacket and tendon-bone repair without a scaffold. Aside from these important histological findings, pQCT analysis showed that it was only in the DBM + MSC specimens where bone mineral density was not significantly different to non-operated controls.

Chapter Seven: General Discussion and Conclusions

7.1 Key Findings and Contributions to Current Knowledge

This thesis aimed to investigate the effect of DBM on regeneration of the tendon-bone interface, and whether its function could be augmented by MSCs. Particular emphasis was given to tendon retraction as this often complicates rotator cuff tears in the clinical setting and is associated with a poor outcome (Galatz et al., 2004). The following hypothesis was examined:

DBM will improve tendon-bone healing in an enthesis defect model, and its effect may be further enhanced by the incorporation of MSCs.

7.2 Mechanical Integrity of Rotator Cuff Repairs

DBM is a collagen-based scaffold containing several growth factors and has been postulated to induce tendon-bone regeneration through a cartilaginous precursor (Sundar et al., 2009a). Previous studies have examined DBM in models of acute tendon rupture, but this is a scenario infrequently encountered in the clinical setting where the ruptured rotator cuff tendon retracts and precludes a tension-free repair due to the onset of degenerative changes (Sundar et al., 2009a, Meyer et al., 2012a). These tendinopathic changes sometimes precede a tear and have additionally been recognised in asymptomatic shoulders (Mall et al., 2010).

Scaffolds used in the context of a retracted tendon tear act as an interpositional graft and may be the subject of high tensile forces as the musculo-tendinous unit contracts. In order to determine the suitability of DBM for this purpose, its mechanical

properties were characterised. Porcine and ovine cortical/cancellous scaffolds were subjected to tensile forces to evaluate whether cancellous bone could withstand without failure, given their higher porosity. Load-deformation analysis for DBM indicated that it had an initial non-linear toe region, followed by a linear region, and subsequent failure without yielding. The visco-elastic behaviour of demineralised bone is similar to tendon tissue and due to the initial straightening of coiled collagen fibers followed by stretching. Accordingly, it is plausible that DBM possesses similar ductility, toughness, and resistance to fatigue as tendon. Further comparative analysis of cortical and cancellous specimens revealed that cancellous scaffolds had such a low UTS that it would be unable to resist the forces transmitted through the rotator cuff tendon-bone interface without failure. Although this could be enhance by increasing the thickness of the graft, it would adversely affect joint movement due to the limited space available for other musculo-tendinous units thereby increasing the risk of 'internal impingement.'

7.3 Repair of a Retracted Tendon

When DBM was applied to a large animal model of acute tendon retraction, superior results were associated with use of the allograft although it could not be determined whether this was due to its mechanical properties or an immunogenic reaction to the xenograft due to presence of the α-Gal epitope. Other studies examining healing of a retracted tendon using an MSC-collagen gel construct have not been able to produce the histological and functional results observed in this study (Awad et al., 1999, Juncosa-Melvin et al., 2006). This illustrates the importance of having a strong

interpositional graft bridging the tendon-bone interface whilst simultaneously having biological factors capable of inducing neo-tendon formation.

7.4 Repair of a Chronic Rotator Cuff Tear

Several animal models of tendon degeneration have been described in the literature but none have evaluated the onset of osteopenia at the enthesis or demonstrated fatty infiltration (a critical feature observed in the clinical setting and one that is associated with poor surgical outcomes) (Goutallier et al., 2003). Accurately reproducing the histological conditions that accompany a chronic rotator cuff tear (abnormal collagen orientation, abnormal tenocyte morphology, increased cellularity, and increased vascularity) is crucial to investigating strategies targeted towards reversing this process (Longo et al., 2008). Three weeks after supraspinatus detachment in a Wistar rat the musculotendinous unit underwent degeneration and fatty infiltration, and the greater tuberosity exhibited a reduction in bone mineral density (Longo et al., 2008). These novel findings may have been associated with fundamental inter-species differences between the Wistar rats used in this study and the Sprague-Dawley rats used in others (Buchmann et al., 2011, Barton et al., 2005, Galan et al., 1993). Lipoprotein lipase catalyses the hydrolysis of triglycerides and is highly expressed in skeletal tissues. It is regulated differently between Wistar and Sprague-Dawley rats and may account for the lack of fat accumulation in otherwise degenerative muscle tissue in some studies (Galan et al., 1993).

This model was subsequently used to evaluate the affect of DBM on tendon regeneration, and compared to a commercial scaffold that is used widely in clinical

practice GraftJacket) and a non-augmented control (direct tendon-bone healing) (Wong et al., 2010, Bond et al., 2008). Perhaps the most important finding of this study was that the non-augmented control group demonstrated a similar histological outcome to those tendons repaired with DBM and dermal collagen, and also resulted in a bone mineral density at the tendon insertion comparable to non-operated controls. This raises considerable doubt as to the suitability of the rat as a surrogate for chronic rotator cuff tendon-bone healing, because in humans spontaneous healing does not to occur. The preservation of bone mineral density is advantageous as it may limit micromotion of suture anchors within the tendon footprint thereby allowing early tendon rehabilitation during the immediate postoperative period without the risk of implant failure. This is appealing since applying load to a developing enthesis causes bone at the insertion site to mature, an increase in fibrocartilage formation, and an improvement in collagen organisation (Thomopoulos et al., 2010).

Stem cells formulate an integral part of many cell-based strategies used to improve tendon-bone healing because of their capacity to differentiate and produce mineralised fibrocartilage. BMPs are able to enhance their role by promoting chondrocytic and osteoblastic differentiation in order to promote a naturally graded enthesis with new bone formation providing mechanical integrity (Dorman et al., 2012, Liu et al., 2010, Gulati et al., 2013, Sun et al., 2015). Contrary to other studies though, when applied to the aforementioned degenerative rotator cuff tear model, it was not found to have a supplementary effect (Gulotta et al., 2010, Gulotta et al., 2011a). However, this may have been due to the isolated time point used for analysis (six weeks) and its inability to discern between subtle differences in collagen structure and cellularity that occurred either earlier or later in the healing process.

7.5 Applications

As a result of the work carried out in this thesis there is now increasing evidence supporting the use of DBM for tendon-bone healing. Not only is this applicable to the rotator cuff, but to other anatomical sites of tendon-bone injury where healing can be comprised by degeneration and retraction such as the Achilles tendon and extensor/flexor tendons of the hand.

7.6 Limitations

This thesis is centered around two *in vivo* models of tendon-bone healing: the ovine patellar tendon and the rat's supraspinatus. Initially, the former was used to assess the regenerative capacity of DBM, as it is not reliant upon subsidiary structures for stability, and therefore can accurately evaluate the effect of biological scaffolds on tendon-bone healing. However, it is not possible to create a degenerative model based on this, because detachment of the patellar tendon (to induce degeneration) would render the animals permanently lame and thus be unethical. For this reason the rat's shoulder presented an appealing alternative. The results though, indicate that the detached supraspinatus tendon in a rat undergoes spontaneous healing within six weeks. Macroscopically it was not possible to discern non-augmented tendon repairs from augmented ones, although with earlier/longer time points, subtle differences may have been detected. This raises doubts as to the suitability of the rat as a model of rotator cuff function and is the main limitation of this thesis.

Considerable histological differences were observed between entheses treated with DBM (organised structure) and GraftJacket (disorganised structure), although these did not reach statistical significance. It is plausible that the histological scoring system used to assess these changes was not sensitive enough as it did not adequately discriminate between organised and disorganised areas of mineralised fibrocartilage. Furthermore, due to restrictions in the number of animals that could be used for each *in vivo* study, biomechanical testing of the repair construct could not be undertaken and therefore limits the interpretation of the histological results.

7.7 General Conclusions

1. The UTS of demineralised cortical bone is greater than that of cancellous bone.
2. The UTS of ovine demineralised bone is greater than that of porcine bone.
3. In an acute model of severe tendon retraction, DBM + mmMSCs are able to remodel across the entire length of the tendon and result in a fibrocartilaginous enthesis.
4. Allogenic DBM is associated with superior histological and mechanical properties than its xenogenic derivative in an acute model of severe tendon retraction.
5. Three weeks following supraspinatus tendon detachment in a Wistar rat the musculotendinous unit undergoes degeneration including fatty infiltration, and the bony insertion develops osteopenia.
6. Application of DBM to a chronic rotator cuff tear results in a fibrocartilaginous enthesis not significantly more mature than non-augmented controls or a commercially available alternative scaffold (GraftJacket).

7. Application of DBM to a chronic rotator cuff tear does not reverse the degenerative changes in the supraspinatus musculo-tendinous unit.
8. Application of DBM to a chronic rotator cuff tear does not increase bone mineral density to pre-injury levels.
9. Application of DBM + MSCs to a chronic rotator cuff tear results in a fibrocartilaginous enthesis not significantly more mature than non-augmented controls or a commercially available alternative scaffold (GraftJacket).
10. Application of DBM + MSCs to a chronic rotator cuff tear does not reverse the degenerative changes in the supraspinatus musculo-tendinous unit.
11. Application of DBM + MSCs to a chronic rotator cuff tear preserves bone mineral density to pre-injury levels.

7.8 Future Work

7.8.1 In Vitro

DBM has been demonstrated to enhance tendon-bone healing but the precise cellular mechanisms governing this process are unknown. Several growth factors have been identified within demineralised bone but so far it is only the elution of BMP-7 that has been characterised (Pietrzak et al., 2012). Other proteins such as BMP-2 and TGF exert a stimulatory effect on the healing enthesis but these have not been studied in the same way (Rodeo et al., 2007). In particular, BMPs have been shown to cause MSC differentiation and so future studies should evaluate MSC seeding on DBM to see if it can be harnessed to enhance stem cell function and therefore improve regeneration of a direct enthesis (Dorman et al., 2012, Toh et al., 2005).

Xenografts were associated with inferior mechanical and histological properties when compared to their allogenic derivatives in a large animal model of tendon retraction (Chapter Three). Hyper-acute rejection may have been responsible for this and should be investigated by staining the scaffold with human serum containing the anti-Gal antibody, and then identifying the α-Gal epitope using a sialic acid-binding lectin (Zheng et al., 2005, McDevitt et al., 2003, Mathapati et al., 2011, Kim et al., 2009).

Evaluation of the material properties of human demineralised cortical/cancellous bone would provide useful information for any potential future translational work. This would include defining its stress/strain, ultimate tensile strength, Young's modulus, ductility, fatigue, toughness, and creep. Comparing these values to those obtained from the human supraspinatus tendon would determine the suitability of DBM as a potential graft material in the clinical setting.

7.8.2 In Vivo

Future *in vivo* studies should focus on developing a model of rotator cuff function characterised by degeneration, a lack of spontaneous healing, an arch-like structure covering the supraspinatus tendon (similar to the coraco-acromial arch in humans), the influence of other shoulder muscles such as the deltoid, and movement in both the sagittal and coronal planes. The ovine model of chronic rotator cuff degeneration (involving detachment and subsequent reattachment of infraspinatus) may be suitable because it possesses many of these features, including fatty infiltration, which has not been previously observed in a rat model other than in Chapter Four of this thesis (Gerber et al., 2004, Buchmann et al., 2011, Melrose et al., 2013). The rat model

specifically is commonly used to investigate biological strategies at the healing enthesis but its ability to self-regenerate viable and functional tendon tissue even in the presence of a tissue-defect does raise some concerns. Wistar rats warrant further study as they develop fatty infiltration following tendon detachment unlike their Sprague-Dawley counterparts.

Following further *in vivo* work there may be sufficient evidence to commence a pilot study with humans as a precursor to a randomised controlled clinical trial.

Appendix: List of Publications.

1. Thangarajah T, Sanghani-Kerai A, Henshaw F, Lambert SM, Pendegrass CJ, Blunn GW. *Research Paper-Application of Demineralised Cortical Bone Matrix and Bone-Marrow Derived Mesenchymal Stem Cells in a Chronic Rotator Cuff Tear Model.* The American Journal of Sports Medicine 2017. PMID: 28949253.

2. Thangarajah T, Henshaw F, Sanghani-Kerai A, Lambert SM, Pendegrass CJ, Blunn GW. *Research Paper-Supraspinatus Detachment Causes Musculotendinous Degeneration and a Reduction in Bone Mineral Density at the Enthesis in a Rat Model of Chronic Rotator Cuff Degeneration.* Shoulder and Elbow 2017 Jul;9(3):178-187. PMID: 28588658.

3. Thangarajah T, Henshaw F, Sanghani-Kerai A, Lambert SM, Blunn GW, Pendegrass CJ. *Research Paper-The Effectiveness of Demineralised Cortical Bone Matrix in a Chronic Rotator Cuff Tear Model.* The Journal of Shoulder and Elbow Surgery 2017 Apr;26(4):619-626. PMID: 28162888.

4. Thangarajah T, Pendegrass C, Shahbazi S, Lambert SM, Alexander S, Blunn GW. *Research Paper-Tendon Reattachment to Bone in an Ovine Model of Tendon Retraction Using Allogenic and Xenogenic Demineralized Bone Matrix Incorporated with Mesenchymal Stem Cells.* PLoS One 2016 Sep 8;11(9):e0161473. PMID: 27606597.

5. Thangarajah T, Pendegrass C, Shahbazi S, Lambert SM, Alexander S, Blunn GW. *Review Article-Augmentation of Rotator Cuff Repair with Soft Tissue Scaffolds.* Orthopaedic Journal of Sports Medicine 2015 June;3(6):2325967115587495. PMID: 26665095.

Bibliography

AERSSENS, J., BOONEN, S., LOWET, G. & DEQUEKER, J. 1998. Interspecies differences in bone composition, density, and quality: potential implications for in vivo bone research. *Endocrinology,* 139**,** 663-70.

AKHAN, E., TUNCEL, D. & AKCALI, K. C. 2015. Nanoparticle labeling of bone marrow-derived rat mesenchymal stem cells: their use in differentiation and tracking. *Biomed Res Int,* 2015**,** 298430.

ALIVISATOS, P. 2004. The use of nanocrystals in biological detection. *Nat Biotechnol,* 22**,** 47-52.

AMIEL, D., FRANK, C., HARWOOD, F., FRONEK, J. & AKESON, W. 1984. Tendons and ligaments: a morphological and biochemical comparison. *J Orthop Res,* 1**,** 257-65.

ASPENBERG, P. & FORSLUND, C. 1999. Enhanced tendon healing with GDF 5 and 6. *Acta Orthop Scand,* 70**,** 51-4.

AURORA, A., MCCARRON, J. A., VAN DEN BOGERT, A. J., GATICA, J. E., IANNOTTI, J. P. & DERWIN, K. A. 2012. The biomechanical role of scaffolds in augmented rotator cuff tendon repairs. *J Shoulder Elbow Surg,* 21**,** 1064-71.

AWAD, H. A., BUTLER, D. L., BOIVIN, G. P., SMITH, F. N., MALAVIYA, P., HUIBREGTSE, B. & CAPLAN, A. I. 1999. Autologous mesenchymal stem cell-mediated repair of tendon. *Tissue Eng,* 5**,** 267-77.

BADDOO, M., HILL, K., WILKINSON, R., GAUPP, D., HUGHES, C., KOPEN, G. C. & PHINNEY, D. G. 2003. Characterization of mesenchymal stem cells

isolated from murine bone marrow by negative selection. *J Cell Biochem,* 89**,** 1235-49.

BADYLAK, S. F., RECORD, R., LINDBERG, K., HODDE, J. & PARK, K. 1998. Small intestinal submucosa: a substrate for in vitro cell growth. *J Biomater Sci Polym Ed,* 9**,** 863-78.

BARBER, F. A. 2016. Triple-Loaded Single-Row Versus Suture-Bridge Double-Row Rotator Cuff Tendon Repair With Platelet-Rich Plasma Fibrin Membrane: A Randomized Controlled Trial. *Arthroscopy*.

BARBER, F. A., BURNS, J. P., DEUTSCH, A., LABBE, M. R. & LITCHFIELD, R. B. 2012. A prospective, randomized evaluation of acellular human dermal matrix augmentation for arthroscopic rotator cuff repair. *Arthroscopy,* 28**,** 8-15.

BARTHOLOMEW, A., STURGEON, C., SIATSKAS, M., FERRER, K., MCINTOSH, K., PATIL, S., HARDY, W., DEVINE, S., UCKER, D., DEANS, R., MOSELEY, A. & HOFFMAN, R. 2002. Mesenchymal stem cells suppress lymphocyte proliferation in vitro and prolong skin graft survival in vivo. *Exp Hematol,* 30**,** 42-8.

BARTON, E. R., GIMBEL, J. A., WILLIAMS, G. R. & SOSLOWSKY, L. J. 2005. Rat supraspinatus muscle atrophy after tendon detachment. *J Orthop Res,* 23**,** 259-65.

BASSETT, R. W. & COFIELD, R. H. 1983. Acute tears of the rotator cuff. The timing of surgical repair. *Clin Orthop Relat Res***,** 18-24.

BEDI, A., DINES, J., WARREN, R. F. & DINES, D. M. 2010. Massive tears of the rotator cuff. *J Bone Joint Surg Am,* 92**,** 1894-908.

BEDI, A., MAAK, T., WALSH, C., RODEO, S. A., GRANDE, D., DINES, D. M. & DINES, J. S. 2012. Cytokines in rotator cuff degeneration and repair. *J Shoulder Elbow Surg,* 21**,** 218-27.

BEITZEL, K., MCCARTHY, M. B., COTE, M. P., RUSSELL, R. P., APOSTOLAKOS, J., RAMOS, D. M., KUMBAR, S. G., IMHOFF, A. B., ARCIERO, R. A. & MAZZOCCA, A. D. 2014. Properties of biologic scaffolds and their response to mesenchymal stem cells. *Arthroscopy,* 30**,** 289-98.

BELEMA-BEDADA, F., UCHIDA, S., MARTIRE, A., KOSTIN, S. & BRAUN, T. 2008. Efficient homing of multipotent adult mesenchymal stem cells depends on FROUNT-mediated clustering of CCR2. *Cell Stem Cell,* 2**,** 566-75.

BENJAMIN, M., EVANS, E. J. & COPP, L. 1986. The histology of tendon attachments to bone in man. *J Anat,* 149**,** 89-100.

BISHOP, J., KLEPPS, S., LO, I. K., BIRD, J., GLADSTONE, J. N. & FLATOW, E. L. 2006. Cuff integrity after arthroscopic versus open rotator cuff repair: a prospective study. *J Shoulder Elbow Surg,* 15**,** 290-9.

BLACK, L. L., GAYNOR, J., GAHRING, D., ADAMS, C., ARON, D., HARMAN, S., GINGERICH, D. A. & HARMAN, R. 2007. Effect of adipose-derived mesenchymal stem and regenerative cells on lameness in dogs with chronic osteoarthritis of the coxofemoral joints: a randomized, double-blinded, multicenter, controlled trial. *Vet Ther,* 8**,** 272-84.

BLOCK, J. E. & RUSSELL, J. L. 1998. Spine fusion with demineralized bone. *J Neurosurg,* 88**,** 354-6.

BOILEAU, P., BRASSART, N., WATKINSON, D. J., CARLES, M., HATZIDAKIS, A. M. & KRISHNAN, S. G. 2005. Arthroscopic repair of full-thickness tears

of the supraspinatus: does the tendon really heal? *J Bone Joint Surg Am,* 87**,** 1229-40.

BOND, J. L., DOPIRAK, R. M., HIGGINS, J., BURNS, J. & SNYDER, S. J. 2008. Arthroscopic replacement of massive, irreparable rotator cuff tears using a GraftJacket allograft: technique and preliminary results. *Arthroscopy,* 24**,** 403-409.e1.

BOWMAN, S. M., ZEIND, J., GIBSON, L. J., HAYES, W. C. & MCMAHON, T. A. 1996. The tensile behavior of demineralized bovine cortical bone. *J Biomech,* 29**,** 1497-501.

BRAUNE, C., VON EISENHART-ROTHE, R., WELSCH, F., TEUFEL, M. & JAEGER, A. 2003. Mid-term results and quantitative comparison of postoperative shoulder function in traumatic and non-traumatic rotator cuff tears. *Arch Orthop Trauma Surg,* 123**,** 419-24.

BRAUNSTEIN, V., OCKERT, B., WINDOLF, M., SPRECHER, C. M., MUTSCHLER, W., IMHOFF, A., POSTL, L. K., BIBERTHALER, P. & KIRCHHOFF, C. 2015. Increasing pullout strength of suture anchors in osteoporotic bone using augmentation--a cadaver study. *Clin Biomech (Bristol, Avon),* 30**,** 243-7.

BRENNEKE, S. L. & MORGAN, C. J. 1992. Evaluation of ultrasonography as a diagnostic technique in the assessment of rotator cuff tendon tears. *Am J Sports Med,* 20**,** 287-9.

BRYANT, L., SHNIER, R., BRYANT, C. & MURRELL, G. A. 2002. A comparison of clinical estimation, ultrasonography, magnetic resonance imaging, and arthroscopy in determining the size of rotator cuff tears. *J Shoulder Elbow Surg,* 11**,** 219-24.

BUCHMANN, S., WALZ, L., SANDMANN, G. H., HOPPE, H., BEITZEL, K., WEXEL, G., BATTMANN, A., VOGT, S., HINTERWIMMER, S. & IMHOFF, A. B. 2011. Rotator cuff changes in a full thickness tear rat model: verification of the optimal time interval until reconstruction for comparison to the healing process of chronic lesions in humans. *Arch Orthop Trauma Surg,* 131**,** 429-35.

BURKHART, S. S., BARTH, J. R., RICHARDS, D. P., ZLATKIN, M. B. & LARSEN, M. 2007. Arthroscopic repair of massive rotator cuff tears with stage 3 and 4 fatty degeneration. *Arthroscopy,* 23**,** 347-54.

BURKHART, S. S., ESCH, J. C. & JOLSON, R. S. 1993. The rotator crescent and rotator cable: an anatomic description of the shoulder's "suspension bridge". *Arthroscopy,* 9**,** 611-6.

BUTLER, D. L., GROOD, E. S., NOYES, F. R. & ZERNICKE, R. F. 1978. Biomechanics of ligaments and tendons. *Exerc Sport Sci Rev,* 6**,** 125-81.

BUTLER, D. L., JUNCOSA-MELVIN, N., BOIVIN, G. P., GALLOWAY, M. T., SHEARN, J. T., GOOCH, C. & AWAD, H. 2008. Functional tissue engineering for tendon repair: A multidisciplinary strategy using mesenchymal stem cells, bioscaffolds, and mechanical stimulation. *J Orthop Res,* 26**,** 1-9.

CADET, E. R., HSU, J. W., LEVINE, W. N., BIGLIANI, L. U. & AHMAD, C. S. 2008. The relationship between greater tuberosity osteopenia and the chronicity of rotator cuff tears. *J Shoulder Elbow Surg,* 17**,** 73-7.

CAMPBELL, B. H., AGARWAL, C. & WANG, J. H. 2004. TGF-beta1, TGF-beta3, and PGE(2) regulate contraction of human patellar tendon fibroblasts. *Biomech Model Mechanobiol,* 2**,** 239-45.

CAPLAN, A. I. 2007. Adult mesenchymal stem cells for tissue engineering versus regenerative medicine. *J Cell Physiol,* 213**,** 341-7.

CAPLAN, A. I. & DENNIS, J. E. 2006. Mesenchymal stem cells as trophic mediators. *J Cell Biochem,* 98**,** 1076-84.

CARPENTER, J. E., THOMOPOULOS, S., FLANAGAN, C. L., DEBANO, C. M. & SOSLOWSKY, L. J. 1998. Rotator cuff defect healing: a biomechanical and histologic analysis in an animal model. *J Shoulder Elbow Surg,* 7**,** 599-605.

CARR, A. J., COOPER, C. D., CAMPBELL, M. K., REES, J. L., MOSER, J., BEARD, D. J., FITZPATRICK, R., GRAY, A., DAWSON, J., MURPHY, J., BRUHN, H., COOPER, D. & RAMSAY, C. R. 2015a. Clinical effectiveness and cost-effectiveness of open and arthroscopic rotator cuff repair [the UK Rotator Cuff Surgery (UKUFF) randomised trial]. *Health Technol Assess,* 19**,** 1-218.

CARR, A. J., MURPHY, R., DAKIN, S. G., ROMBACH, I., WHEWAY, K., WATKINS, B. & FRANKLIN, S. L. 2015b. Platelet-Rich Plasma Injection With Arthroscopic Acromioplasty for Chronic Rotator Cuff Tendinopathy: A Randomized Controlled Trial. *Am J Sports Med,* 43**,** 2891-7.

CASTRICINI, R., LONGO, U. G., DE BENEDETTO, M., LOPPINI, M., ZINI, R., MAFFULLI, N. & DENARO, V. 2014. Arthroscopic-Assisted Latissimus Dorsi Transfer for the Management of Irreparable Rotator Cuff Tears: Short-Term Results. *J Bone Joint Surg Am,* 96**,** e119.

CASTRO-MALASPINA, H., GAY, R. E., RESNICK, G., KAPOOR, N., MEYERS, P., CHIARIERI, D., MCKENZIE, S., BROXMEYER, H. E. & MOORE, M. A. 1980. Characterization of human bone marrow fibroblast colony-forming cells (CFU-F) and their progeny. *Blood,* 56**,** 289-301.

CHAKKALAKAL, D. A., STRATES, B. S., MASHOOF, A. A., GARVIN, K. L., NOVAK, J. R., FRITZ, E. D., MOLLNER, T. J. & MCGUIRE, M. H. 1999. Repair of segmental bone defects in the rat: an experimental model of human fracture healing. *Bone,* 25**,** 321-32.

CHAMBERLAIN, G., FOX, J., ASHTON, B. & MIDDLETON, J. 2007. Concise review: mesenchymal stem cells: their phenotype, differentiation capacity, immunological features, and potential for homing. *Stem Cells,* 25**,** 2739-49.

CHAN, W. C., MAXWELL, D. J., GAO, X., BAILEY, R. E., HAN, M. & NIE, S. 2002. Luminescent quantum dots for multiplexed biological detection and imaging. *Curr Opin Biotechnol,* 13**,** 40-6.

CHANG, E. Y. & CHUNG, C. B. 2014. Current concepts on imaging diagnosis of rotator cuff disease. *Semin Musculoskelet Radiol,* 18**,** 412-24.

CHAROUSSET, C., BELLAICHE, L., KALRA, K. & PETROVER, D. 2010. Arthroscopic repair of full-thickness rotator cuff tears: is there tendon healing in patients aged 65 years or older? *Arthroscopy,* 26**,** 302-9.

CHEN, P. Y. & MCKITTRICK, J. 2011. Compressive mechanical properties of demineralized and deproteinized cancellous bone. *J Mech Behav Biomed Mater,* 4**,** 961-73.

CHEN, X., GIAMBINI, H., BEN-ABRAHAM, E., AN, K. N., NASSR, A. & ZHAO, C. 2015. Effect of Bone Mineral Density on Rotator Cuff Tear: An Osteoporotic Rabbit Model. *PLoS One,* 10**,** e0139384.

CHENG, Z., OU, L., ZHOU, X., LI, F., JIA, X., ZHANG, Y., LIU, X., LI, Y., WARD, C. A., MELO, L. G. & KONG, D. 2008. Targeted migration of mesenchymal stem cells modified with CXCR4 gene to infarcted myocardium improves cardiac performance. *Mol Ther,* 16**,** 571-9.

CHEUNG, E. V., SILVERIO, L. & SPERLING, J. W. 2010. Strategies in biologic augmentation of rotator cuff repair: a review. *Clin Orthop Relat Res,* 468**,** 1476-84.

CHO, N. S. & RHEE, Y. G. 2009. The factors affecting the clinical outcome and integrity of arthroscopically repaired rotator cuff tears of the shoulder. *Clin Orthop Surg,* 1**,** 96-104.

CHUNG, S. W., KIM, J. Y., KIM, M. H., KIM, S. H. & OH, J. H. 2013. Arthroscopic repair of massive rotator cuff tears: outcome and analysis of factors associated with healing failure or poor postoperative function. *Am J Sports Med,* 41**,** 1674-83.

CHUNG, S. W., OH, J. H., GONG, H. S., KIM, J. Y. & KIM, S. H. 2011. Factors affecting rotator cuff healing after arthroscopic repair: osteoporosis as one of the independent risk factors. *Am J Sports Med,* 39**,** 2099-107.

CIAMPI, P., SCOTTI, C., NONIS, A., VITALI, M., DI SERIO, C., PERETTI, G. M. & FRASCHINI, G. 2014. The benefit of synthetic versus biological patch augmentation in the repair of posterosuperior massive rotator cuff tears: a 3-year follow-up study. *Am J Sports Med,* 42**,** 1169-75.

CLARK, J. M. & HARRYMAN, D. T., 2ND 1992. Tendons, ligaments, and capsule of the rotator cuff. Gross and microscopic anatomy. *J Bone Joint Surg Am,* 74**,** 713-25.

COLLINS, M. C., GUNST, P. R., CASCIO, W. E., KYPSON, A. P. & MULLER-BORER, B. J. 2012. Labeling and imaging mesenchymal stem cells with quantum dots. *Methods Mol Biol,* 906**,** 199-210.

COLVIN, A. C., EGOROVA, N., HARRISON, A. K., MOSKOWITZ, A. & FLATOW, E. L. 2012. National trends in rotator cuff repair. *J Bone Joint Surg Am,* 94**,** 227-33.

CONGET, P. A. & MINGUELL, J. J. 1999. Phenotypical and functional properties of human bone marrow mesenchymal progenitor cells. *J Cell Physiol,* 181**,** 67-73.

COOPER, R. R. & MISOL, S. 1970. Tendon and ligament insertion. A light and electron microscopic study. *J Bone Joint Surg Am,* 52**,** 1-20.

COSTOUROS, J. G., PORRAMATIKUL, M., LIE, D. T. & WARNER, J. J. 2007. Reversal of suprascapular neuropathy following arthroscopic repair of massive supraspinatus and infraspinatus rotator cuff tears. *Arthroscopy,* 23**,** 1152-61.

CRASS, J. R., CRAIG, E. V., THOMPSON, R. C. & FEINBERG, S. B. 1984. Ultrasonography of the rotator cuff: surgical correlation. *J Clin Ultrasound,* 12**,** 487-91.

CRISOSTOMO, P. R., WANG, Y., MARKEL, T. A., WANG, M., LAHM, T. & MELDRUM, D. R. 2008. Human mesenchymal stem cells stimulated by TNF-alpha, LPS, or hypoxia produce growth factors by an NF kappa B- but not JNK-dependent mechanism. *Am J Physiol Cell Physiol,* 294**,** C675-82.

CURTIS, A. S., BURBANK, K. M., TIERNEY, J. J., SCHELLER, A. D. & CURRAN, A. R. 2006. The insertional footprint of the rotator cuff: an anatomic study. *Arthroscopy,* 22**,** 609.e1.

DALLARI, D., STAGNI, C., RANI, N., SABBIONI, G., PELOTTI, P., TORRICELLI, P., TSCHON, M. & GIAVARESI, G. 2016. Ultrasound-Guided Injection of Platelet-Rich Plasma and Hyaluronic Acid, Separately and

in Combination, for Hip Osteoarthritis: A Randomized Controlled Study. *Am J Sports Med*.

DENIZ, G., KOSE, O., TUGAY, A., GULER, F. & TURAN, A. 2014. Fatty degeneration and atrophy of the rotator cuff muscles after arthroscopic repair: does it improve, halt or deteriorate? *Arch Orthop Trauma Surg,* 134**,** 985-90.

DEORIO, J. K. & COFIELD, R. H. 1984. Results of a second attempt at surgical repair of a failed initial rotator-cuff repair. *J Bone Joint Surg Am,* 66**,** 563-7.

DERWIN, K. A., BADYLAK, S. F., STEINMANN, S. P. & IANNOTTI, J. P. 2010. Extracellular matrix scaffold devices for rotator cuff repair. *J Shoulder Elbow Surg,* 19**,** 467-76.

DI NICOLA, M., CARLO-STELLA, C., MAGNI, M., MILANESI, M., LONGONI, P. D., MATTEUCCI, P., GRISANTI, S. & GIANNI, A. M. 2002. Human bone marrow stromal cells suppress T-lymphocyte proliferation induced by cellular or nonspecific mitogenic stimuli. *Blood,* 99**,** 3838-43.

DINES, D. M., MOYNIHAN, D. P., DINES, J. S. & MCCANN, P. 2007. Irreparable rotator cuff tears: what to do and when to do it; the surgeon's dilemma. *Instr Course Lect,* 56**,** 13-22.

DOMINICI, M., LE BLANC, K., MUELLER, I., SLAPER-CORTENBACH, I., MARINI, F., KRAUSE, D., DEANS, R., KEATING, A., PROCKOP, D. & HORWITZ, E. 2006. Minimal criteria for defining multipotent mesenchymal stromal cells. The International Society for Cellular Therapy position statement. *Cytotherapy,* 8**,** 315-7.

DORMAN, L. J., TUCCI, M. & BENGHUZZI, H. 2012. In vitro effects of bmp-2, bmp-7, and bmp-13 on proliferation and differentation of mouse mesenchymal stem cells. *Biomed Sci Instrum,* 48**,** 81-7.

DORMER, N. H., BERKLAND, C. J. & DETAMORE, M. S. 2010. Emerging techniques in stratified designs and continuous gradients for tissue engineering of interfaces. *Ann Biomed Eng,* 38**,** 2121-41.

DOURTE, L. M., PERRY, S. M., GETZ, C. L. & SOSLOWSKY, L. J. 2010. Tendon properties remain altered in a chronic rat rotator cuff model. *Clin Orthop Relat Res,* 468**,** 1485-92.

DRISCOLL, S. B. 1998. *The Basics of Testing Plastics: Mechanical Properties, Flame Exposure, and General Guidelines* Astm Intl.

DUBERTRET, B., SKOURIDES, P., NORRIS, D. J., NOIREAUX, V., BRIVANLOU, A. H. & LIBCHABER, A. 2002. In vivo imaging of quantum dots encapsulated in phospholipid micelles. *Science,* 298**,** 1759-62.

DUNN, W. R., KUHN, J. E., SANDERS, R., AN, Q., BAUMGARTEN, K. M., BISHOP, J. Y., BROPHY, R. H., CAREY, J. L., HOLLOWAY, G. B., JONES, G. L., MA, C. B., MARX, R. G., MCCARTY, E. C., PODDAR, S. K., SMITH, M. V., SPENCER, E. E., VIDAL, A. F., WOLF, B. R. & WRIGHT, R. W. 2014. Symptoms of pain do not correlate with rotator cuff tear severity: a cross-sectional study of 393 patients with a symptomatic atraumatic full-thickness rotator cuff tear. *J Bone Joint Surg Am,* 96**,** 793-800.

DYKYJ, D. & JULES, K. T. 1991. The clinical anatomy of tendons. *J Am Podiatr Med Assoc,* 81**,** 358-65.

ELLERA GOMES, J. L., DA SILVA, R. C., SILLA, L. M., ABREU, M. R. & PELLANDA, R. 2012. Conventional rotator cuff repair complemented by the aid of mononuclear autologous stem cells. *Knee Surg Sports Traumatol Arthrosc,* 20**,** 373-7.

ESCAMILLA, R. F., YAMASHIRO, K., PAULOS, L. & ANDREWS, J. R. 2009. Shoulder muscle activity and function in common shoulder rehabilitation exercises. *Sports Med,* 39**,** 663-85.

EVANKO, S. P. & VOGEL, K. G. 1990. Ultrastructure and proteoglycan composition in the developing fibrocartilaginous region of bovine tendon. *Matrix,* 10**,** 420-36.

EVERTS, P. A., KNAPE, J. T., WEIBRICH, G., SCHONBERGER, J. P., HOFFMANN, J., OVERDEVEST, E. P., BOX, H. A. & VAN ZUNDERT, A. 2006. Platelet-rich plasma and platelet gel: a review. *J Extra Corpor Technol,* 38**,** 174-87.

FINI, M., BONDIOLI, E., CASTAGNA, A., TORRICELLI, P., GIAVARESI, G., ROTINI, R., MARINELLI, A., GUERRA, E., ORLANDI, C., CARBONI, A., AITI, A., BENEDETTINI, E., GIARDINO, R. & MELANDRI, D. 2012. Decellularized human dermis to treat massive rotator cuff tears: in vitro evaluations. *Connect Tissue Res,* 53**,** 298-306.

FRANCE, E. P., PAULOS, L. E., HARNER, C. D. & STRAIGHT, C. B. 1989. Biomechanical evaluation of rotator cuff fixation methods. *Am J Sports Med,* 17**,** 176-81.

FRANCESCHI, F., PAPALIA, R., FRANCESCHETTI, E., PALUMBO, A., DEL BUONO, A., PACIOTTI, M., MAFFULLI, N. & DENARO, V. 2016. Double-Row Repair Lowers the Retear Risk After Accelerated Rehabilitation. *Am J Sports Med*.

FUKUDA, H. 2000. Partial-thickness rotator cuff tears: a modern view on Codman's classic. *J Shoulder Elbow Surg,* 9**,** 163-8.

FUKUTA, S., OYAMA, M., KAVALKOVICH, K., FU, F. H. & NIYIBIZI, C. 1998. Identification of types II, IX and X collagens at the insertion site of the bovine achilles tendon. *Matrix Biol,* 17**,** 65-73.

GALAN, X., LLOBERA, M. & RAMIREZ, I. 1993. Lipoprotein lipase in developing rat tissues: differences between Wistar and Sprague-Dawley rats. *Biol Neonate,* 64**,** 295-303.

GALATZ, L., ROTHERMICH, S., VANDERPLOEG, K., PETERSEN, B., SANDELL, L. & THOMOPOULOS, S. 2007. Development of the supraspinatus tendon-to-bone insertion: localized expression of extracellular matrix and growth factor genes. *J Orthop Res,* 25**,** 1621-8.

GALATZ, L. M., BALL, C. M., TEEFEY, S. A., MIDDLETON, W. D. & YAMAGUCHI, K. 2004. The outcome and repair integrity of completely arthroscopically repaired large and massive rotator cuff tears. *J Bone Joint Surg Am,* 86-a**,** 219-24.

GALMICHE, M. C., KOTELIANSKY, V. E., BRIERE, J., HERVE, P. & CHARBORD, P. 1993. Stromal cells from human long-term marrow cultures are mesenchymal cells that differentiate following a vascular smooth muscle differentiation pathway. *Blood,* 82**,** 66-76.

GAO, J., RASANEN, T., PERSLIDEN, J. & MESSNER, K. 1996. The morphology of ligament insertions after failure at low strain velocity: an evaluation of ligament entheses in the rabbit knee. *J Anat,* 189 (Pt 1)**,** 127-33.

GERBER, C. & KRUSHELL, R. J. 1991. Isolated rupture of the tendon of the subscapularis muscle. Clinical features in 16 cases. *J Bone Joint Surg Br,* 73**,** 389-94.

GERBER, C., MEYER, D. C., SCHNEEBERGER, A. G., HOPPELER, H. & VON RECHENBERG, B. 2004. Effect of tendon release and delayed repair on the structure of the muscles of the rotator cuff: an experimental study in sheep. *J Bone Joint Surg Am,* 86-a**,** 1973-82.

GERBER, C., SCHNEEBERGER, A. G., PERREN, S. M. & NYFFELER, R. W. 1999. Experimental rotator cuff repair. A preliminary study. *J Bone Joint Surg Am,* 81**,** 1281-90.

GIBSON, L. J. 1985. The mechanical behaviour of cancellous bone. *J Biomech,* 18**,** 317-28.

GILBERT, T. W., FREUND, J. M. & BADYLAK, S. F. 2009. Quantification of DNA in biologic scaffold materials. *J Surg Res,* 152**,** 135-9.

GIMBEL, J. A., VAN KLEUNEN, J. P., MEHTA, S., PERRY, S. M., WILLIAMS, G. R. & SOSLOWSKY, L. J. 2004. Supraspinatus tendon organizational and mechanical properties in a chronic rotator cuff tear animal model. *J Biomech,* 37**,** 739-49.

GINDRAUX, F., SELMANI, Z., OBERT, L., DAVANI, S., TIBERGHIEN, P., HERVE, P. & DESCHASEAUX, F. 2007. Human and rodent bone marrow mesenchymal stem cells that express primitive stem cell markers can be directly enriched by using the CD49a molecule. *Cell Tissue Res,* 327**,** 471-83.

GIPHART, J. E., BRUNKHORST, J. P., HORN, N. H., SHELBURNE, K. B., TORRY, M. R. & MILLETT, P. J. 2013. Effect of plane of arm elevation on glenohumeral kinematics: a normative biplane fluoroscopy study. *J Bone Joint Surg Am,* 95**,** 238-45.

GOMIERO, C., BERTOLUTTI, G., MARTINELLO, T., VAN BRUAENE, N., BROECKX, S. Y., PATRUNO, M. & SPAAS, J. H. 2016. Tenogenic

induction of equine mesenchymal stem cells by means of growth factors and low-level laser technology. *Vet Res Commun*.

GOUTALLIER, D., POSTEL, J. M., BERNAGEAU, J., LAVAU, L. & VOISIN, M. C. 1995. Fatty infiltration of disrupted rotator cuff muscles. *Rev Rhum Engl Ed,* 62**,** 415-22.

GOUTALLIER, D., POSTEL, J. M., GLEYZE, P., LEGUILLOUX, P. & VAN DRIESSCHE, S. 2003. Influence of cuff muscle fatty degeneration on anatomic and functional outcomes after simple suture of full-thickness tears. *J Shoulder Elbow Surg,* 12**,** 550-4.

GREEN, A. 2003. Chronic massive rotator cuff tears: evaluation and management. *J Am Acad Orthop Surg,* 11**,** 321-31.

GREENSPOON, J. A., PETRI, M., WARTH, R. J. & MILLETT, P. J. 2015. Massive rotator cuff tears: pathomechanics, current treatment options, and clinical outcomes. *J Shoulder Elbow Surg,* 24**,** 1493-505.

GREIS, P. E., BURKS, R. T., BACHUS, K. & LUKER, M. G. 2001. The influence of tendon length and fit on the strength of a tendon-bone tunnel complex. A biomechanical and histologic study in the dog. *Am J Sports Med,* 29**,** 493-7.

GULATI, B. R., KUMAR, R., MOHANTY, N., KUMAR, P., SOMASUNDARAM, R. K. & YADAV, P. S. 2013. Bone morphogenetic protein-12 induces tenogenic differentiation of mesenchymal stem cells derived from equine amniotic fluid. *Cells Tissues Organs,* 198**,** 377-89.

GULOTTA, L. V., KOVACEVIC, D., EHTESHAMI, J. R., DAGHER, E., PACKER, J. D. & RODEO, S. A. 2009. Application of bone marrow-derived mesenchymal stem cells in a rotator cuff repair model. *Am J Sports Med,* 37**,** 2126-33.

GULOTTA, L. V., KOVACEVIC, D., MONTGOMERY, S., EHTESHAMI, J. R., PACKER, J. D. & RODEO, S. A. 2010. Stem cells genetically modified with the developmental gene MT1-MMP improve regeneration of the supraspinatus tendon-to-bone insertion site. *Am J Sports Med,* 38**,** 1429-37.

GULOTTA, L. V., KOVACEVIC, D., PACKER, J. D., DENG, X. H. & RODEO, S. A. 2011a. Bone marrow-derived mesenchymal stem cells transduced with scleraxis improve rotator cuff healing in a rat model. *Am J Sports Med,* 39**,** 1282-9.

GULOTTA, L. V., KOVACEVIC, D., PACKER, J. D., EHTESHAMI, J. R. & RODEO, S. A. 2011b. Adenoviral-mediated gene transfer of human bone morphogenetic protein-13 does not improve rotator cuff healing in a rat model. *Am J Sports Med,* 39**,** 180-7.

GULOTTA, L. V. & RODEO, S. A. 2009. Growth factors for rotator cuff repair. *Clin Sports Med,* 28**,** 13-23.

GUPTA, A. K., HUG, K., BOGGESS, B., GAVIGAN, M. & TOTH, A. P. 2013. Massive or 2-tendon rotator cuff tears in active patients with minimal glenohumeral arthritis: clinical and radiographic outcomes of reconstruction using dermal tissue matrix xenograft. *Am J Sports Med,* 41**,** 872-9.

HAKIMI, O., MOUTHUY, P. A. & CARR, A. 2013. Synthetic and degradable patches: an emerging solution for rotator cuff repair. *Int J Exp Pathol,* 94**,** 287-92.

HALDER, A. M., O'DRISCOLL, S. W., HEERS, G., MURA, N., ZOBITZ, M. E., AN, K. N. & KREUSCH-BRINKER, R. 2002. Biomechanical comparison of effects of supraspinatus tendon detachments, tendon defects, and muscle retractions. *J Bone Joint Surg Am,* 84-a**,** 780-5.

HAN, Z., JING, Y., ZHANG, S., LIU, Y., SHI, Y. & WEI, L. 2012. The role of immunosuppression of mesenchymal stem cells in tissue repair and tumor growth. *Cell Biosci,* 2**,** 8.

HARRYMAN, D. T., 2ND, MACK, L. A., WANG, K. Y., JACKINS, S. E., RICHARDSON, M. L. & MATSEN, F. A., 3RD 1991. Repairs of the rotator cuff. Correlation of functional results with integrity of the cuff. *J Bone Joint Surg Am,* 73**,** 982-9.

HAWKINS, R. J. & KENNEDY, J. C. 1980. Impingement syndrome in athletes. *Am J Sports Med,* 8**,** 151-8.

HAYNESWORTH, S. E., BABER, M. A. & CAPLAN, A. I. 1992. Cell surface antigens on human marrow-derived mesenchymal cells are detected by monoclonal antibodies. *Bone,* 13**,** 69-80.

HERNIGOU, P., FLOUZAT LACHANIETTE, C. H., DELAMBRE, J., ZILBER, S., DUFFIET, P., CHEVALLIER, N. & ROUARD, H. 2014. Biologic augmentation of rotator cuff repair with mesenchymal stem cells during arthroscopy improves healing and prevents further tears: a case-controlled study. *Int Orthop,* 38**,** 1811-8.

HERNIGOU, P., MATHIEU, G., POIGNARD, A., MANICOM, O., BEAUJEAN, F. & ROUARD, H. 2006. Percutaneous autologous bone-marrow grafting for nonunions. Surgical technique. *J Bone Joint Surg Am,* 88 Suppl 1 Pt 2**,** 322-7.

HERNIGOU, P., MEROUSE, G., DUFFIET, P., CHEVALIER, N. & ROUARD, H. 2015. Reduced levels of mesenchymal stem cells at the tendon-bone interface tuberosity in patients with symptomatic rotator cuff tear. *Int Orthop*.

HERNIGOU, P., POIGNARD, A., BEAUJEAN, F. & ROUARD, H. 2005. Percutaneous autologous bone-marrow grafting for nonunions. Influence of

the number and concentration of progenitor cells. *J Bone Joint Surg Am,* 87**,** 1430-7.

HERSCHE, O. & GERBER, C. 1998. Passive tension in the supraspinatus musculotendinous unit after long-standing rupture of its tendon: a preliminary report. *J Shoulder Elbow Surg,* 7**,** 393-6.

HESS, G. P., CAPPIELLO, W. L., POOLE, R. M. & HUNTER, S. C. 1989. Prevention and treatment of overuse tendon injuries. *Sports Med,* 8**,** 371-84.

HIDALGO-BASTIDA, L. A. & CARTMELL, S. H. 2010. Mesenchymal stem cells, osteoblasts and extracellular matrix proteins: enhancing cell adhesion and differentiation for bone tissue engineering. *Tissue Eng Part B Rev,* 16**,** 405-12.

HOPPE, S., ALINI, M., BENNEKER, L. M., MILZ, S., BOILEAU, P. & ZUMSTEIN, M. A. 2013. Tenocytes of chronic rotator cuff tendon tears can be stimulated by platelet-released growth factors. *J Shoulder Elbow Surg,* 22**,** 340-9.

HSU, S. L. & WANG, C. J. 2014. The use of demineralized bone matrix for anterior cruciate ligament reconstruction: a radiographic, histologic, and immunohistochemical study in rabbits. *J Surg Res,* 187**,** 219-24.

HUGHES, P. C., TAYLOR, N. F. & GREEN, R. A. 2008. Most clinical tests cannot accurately diagnose rotator cuff pathology: a systematic review. *Aust J Physiother,* 54**,** 159-70.

HUGHES, R. E. & AN, K. N. 1996. Force analysis of rotator cuff muscles. *Clin Orthop Relat Res***,** 75-83.

IANNOTTI, J. P. 1994. Full-Thickness Rotator Cuff Tears: Factors Affecting Surgical Outcome. *J Am Acad Orthop Surg,* 2**,** 87-95.

IANNOTTI, J. P., CICCONE, J., BUSS, D. D., VISOTSKY, J. L., MASCHA, E., COTMAN, K. & RAWOOL, N. M. 2005. Accuracy of office-based ultrasonography of the shoulder for the diagnosis of rotator cuff tears. *J Bone Joint Surg Am,* 87**,** 1305-11.

IANNOTTI, J. P., CODSI, M. J., KWON, Y. W., DERWIN, K., CICCONE, J. & BREMS, J. J. 2006. Porcine small intestine submucosa augmentation of surgical repair of chronic two-tendon rotator cuff tears. A randomized, controlled trial. *J Bone Joint Surg Am,* 88**,** 1238-44.

IANNOTTI, J. P., DEUTSCH, A., GREEN, A., RUDICEL, S., CHRISTENSEN, J., MARRAFFINO, S. & RODEO, S. 2013. Time to failure after rotator cuff repair: a prospective imaging study. *J Bone Joint Surg Am,* 95**,** 965-71.

IANNOTTI, J. P., ZLATKIN, M. B., ESTERHAI, J. L., KRESSEL, H. Y., DALINKA, M. K. & SPINDLER, K. P. 1991. Magnetic resonance imaging of the shoulder. Sensitivity, specificity, and predictive value. *J Bone Joint Surg Am,* 73**,** 17-29.

IDE, J., KIKUKAWA, K., HIROSE, J., IYAMA, K., SAKAMOTO, H., FUJIMOTO, T. & MIZUTA, H. 2009a. The effect of a local application of fibroblast growth factor-2 on tendon-to-bone remodeling in rats with acute injury and repair of the supraspinatus tendon. *J Shoulder Elbow Surg,* 18**,** 391-8.

IDE, J., KIKUKAWA, K., HIROSE, J., IYAMA, K., SAKAMOTO, H. & MIZUTA, H. 2009b. The effects of fibroblast growth factor-2 on rotator cuff reconstruction with acellular dermal matrix grafts. *Arthroscopy,* 25**,** 608-16.

IDE, J., KIKUKAWA, K., HIROSE, J., IYAMA, K., SAKAMOTO, H. & MIZUTA, H. 2009c. Reconstruction of large rotator-cuff tears with acellular dermal matrix grafts in rats. *J Shoulder Elbow Surg,* 18**,** 288-95.

ISAAC, C., GHARAIBEH, B., WITT, M., WRIGHT, V. J. & HUARD, J. 2012. Biologic approaches to enhance rotator cuff healing after injury. *J Shoulder Elbow Surg,* 21**,** 181-90.

ITOI, E., BERGLUND, L. J., GRABOWSKI, J. J., SCHULTZ, F. M., GROWNEY, E. S., MORREY, B. F. & AN, K. N. 1995. Tensile properties of the supraspinatus tendon. *J Orthop Res,* 13**,** 578-84.

JAISWAL, J. K., MATTOUSSI, H., MAURO, J. M. & SIMON, S. M. 2003. Long-term multiple color imaging of live cells using quantum dot bioconjugates. *Nat Biotechnol,* 21**,** 47-51.

JAMES, R., KESTURU, G., BALIAN, G. & CHHABRA, A. B. 2008. Tendon: biology, biomechanics, repair, growth factors, and evolving treatment options. *J Hand Surg Am,* 33**,** 102-12.

JAVAZON, E. H., BEGGS, K. J. & FLAKE, A. W. 2004. Mesenchymal stem cells: paradoxes of passaging. *Exp Hematol,* 32**,** 414-25.

JING, Y., HAN, Z., ZHANG, S., LIU, Y. & WEI, L. 2011. Epithelial-Mesenchymal Transition in tumor microenvironment. *Cell Biosci,* 1**,** 29.

JONES, E. A., KINSEY, S. E., ENGLISH, A., JONES, R. A., STRASZYNSKI, L., MEREDITH, D. M., MARKHAM, A. F., JACK, A., EMERY, P. & MCGONAGLE, D. 2002. Isolation and characterization of bone marrow multipotential mesenchymal progenitor cells. *Arthritis Rheum,* 46**,** 3349-60.

JOZSA, L., KANNUS, P., THORING, J., REFFY, A., JARVINEN, M. & KVIST, M. 1990. The effect of tenotomy and immobilisation on intramuscular connective tissue. A morphometric and microscopic study in rat calf muscles. *J Bone Joint Surg Br,* 72**,** 293-7.

JU, Y. J., MUNETA, T., YOSHIMURA, H., KOGA, H. & SEKIYA, I. 2008. Synovial mesenchymal stem cells accelerate early remodeling of tendon-bone healing. *Cell Tissue Res,* 332**,** 469-78.

JUNCOSA-MELVIN, N., BOIVIN, G. P., GOOCH, C., GALLOWAY, M. T., WEST, J. R., DUNN, M. G. & BUTLER, D. L. 2006. The effect of autologous mesenchymal stem cells on the biomechanics and histology of gel-collagen sponge constructs used for rabbit patellar tendon repair. *Tissue Eng,* 12**,** 369-79.

JUNCOSA-MELVIN, N., MATLIN, K. S., HOLDCRAFT, R. W., NIRMALANANDHAN, V. S. & BUTLER, D. L. 2007. Mechanical stimulation increases collagen type I and collagen type III gene expression of stem cell-collagen sponge constructs for patellar tendon repair. *Tissue Eng,* 13**,** 1219-26.

KALIA, P., BLUNN, G. W., MILLER, J., BHALLA, A., WISEMAN, M. & COATHUP, M. J. 2006. Do autologous mesenchymal stem cells augment bone growth and contact to massive bone tumor implants? *Tissue Eng,* 12**,** 1617-26.

KALIA, P., COATHUP, M. J., OUSSEDIK, S., KONAN, S., DODD, M., HADDAD, F. S. & BLUNN, G. W. 2009. Augmentation of bone growth onto the acetabular cup surface using bone marrow stromal cells in total hip replacement surgery. *Tissue Eng Part A,* 15**,** 3689-96.

KARTHIKEYAN, S., GRIFFIN, D. R., PARSONS, N., LAWRENCE, T. M., MODI, C. S., DREW, S. J. & SMITH, C. D. 2015. Microvascular blood flow in normal and pathologic rotator cuffs. *J Shoulder Elbow Surg,* 24**,** 1954-60.

KASTELIC, J. & BAER, E. 1980. Deformation in tendon collagen. *Symp Soc Exp Biol,* 34**,** 397-435.

KASTELIC, J., GALESKI, A. & BAER, E. 1978. The multicomposite structure of tendon. *Connect Tissue Res,* 6**,** 11-23.

KASTEN, P., BEYEN, I., EGERMANN, M., SUDA, A. J., MOGHADDAM, A. A., ZIMMERMANN, G. & LUGINBUHL, R. 2008. Instant stem cell therapy: characterization and concentration of human mesenchymal stem cells in vitro. *Eur Cell Mater,* 16**,** 47-55.

KASTRINAKI, M. C., ANDREAKOU, I., CHARBORD, P. & PAPADAKI, H. A. 2008. Isolation of human bone marrow mesenchymal stem cells using different membrane markers: comparison of colony/cloning efficiency, differentiation potential, and molecular profile. *Tissue Eng Part C Methods,* 14**,** 333-9.

KEENER, J. D., GALATZ, L. M., TEEFEY, S. A., MIDDLETON, W. D., STEGER-MAY, K., STOBBS-CUCCHI, G., PATTON, R. & YAMAGUCHI, K. 2015. A prospective evaluation of survivorship of asymptomatic degenerative rotator cuff tears. *J Bone Joint Surg Am,* 97**,** 89-98.

KILICOGLU, O. I., DIKMEN, G., KOYUNCU, O., BILGIC, B. & ALTURFAN, A. K. 2012. Effects of demineralized bone matrix on tendon-bone healing: an in vivo, experimental study on rabbits. *Acta Orthop Traumatol Turc,* 46**,** 443-8.

KILINCOGLU, V., YETER, A., SERVET, E., KANGAL, M. & YILDIRIM, M. 2015. Short term results comparison of intraarticular platelet-rich plasma (prp) and hyaluronic acid (ha) applications in early stage of knee osteoarthritis. *Int J Clin Exp Med,* 8**,** 18807-12.

KILLIAN, J. T., WILKINSON, L., WHITE, S. & BRASSARD, M. 1998. Treatment of unicameral bone cyst with demineralized bone matrix. *J Pediatr Orthop,* 18**,** 621-4.

KIM, D. H., ELATTRACHE, N. S., TIBONE, J. E., JUN, B. J., DELAMORA, S. N., KVITNE, R. S. & LEE, T. Q. 2006. Biomechanical comparison of a single-row versus double-row suture anchor technique for rotator cuff repair. *Am J Sports Med,* 34**,** 407-14.

KIM, H. M., DAHIYA, N., TEEFEY, S. A., MIDDLETON, W. D., STOBBS, G., STEGER-MAY, K., YAMAGUCHI, K. & KEENER, J. D. 2010. Location and initiation of degenerative rotator cuff tears: an analysis of three hundred and sixty shoulders. *J Bone Joint Surg Am,* 92**,** 1088-96.

KIM, Y. G., OH, J. Y., GIL, G. C., KIM, M. K., KO, J. H., LEE, S., LEE, H. J., WEE, W. R. & KIM, B. G. 2009. Identification of alpha-Gal and non-Gal epitopes in pig corneal endothelial cells and keratocytes by using mass spectrometry. *Curr Eye Res,* 34**,** 877-95.

KIRKENDALL, D. T. & GARRETT, W. E. 1997. Function and biomechanics of tendons. *Scand J Med Sci Sports,* 7**,** 62-6.

KLEIN, M. B., YALAMANCHI, N., PHAM, H., LONGAKER, M. T. & CHANG, J. 2002. Flexor tendon healing in vitro: effects of TGF-beta on tendon cell collagen production. *J Hand Surg Am,* 27**,** 615-20.

KLEPPS, S., BISHOP, J., LIN, J., CAHLON, O., STRAUSS, A., HAYES, P. & FLATOW, E. L. 2004. Prospective evaluation of the effect of rotator cuff integrity on the outcome of open rotator cuff repairs. *Am J Sports Med,* 32**,** 1716-22.

KOBAYASHI, M., ITOI, E., MINAGAWA, H., MIYAKOSHI, N., TAKAHASHI, S., TUOHETI, Y., OKADA, K. & SHIMADA, Y. 2006. Expression of growth factors in the early phase of supraspinatus tendon healing in rabbits. *J Shoulder Elbow Surg,* 15**,** 371-7.

KOIKE, Y., TRUDEL, G., CURRAN, D. & UHTHOFF, H. K. 2006. Delay of supraspinatus repair by up to 12 weeks does not impair enthesis formation: a quantitative histologic study in rabbits. *J Orthop Res,* 24**,** 202-10.

KOPEN, G. C., PROCKOP, D. J. & PHINNEY, D. G. 1999. Marrow stromal cells migrate throughout forebrain and cerebellum, and they differentiate into astrocytes after injection into neonatal mouse brains. *Proc Natl Acad Sci U S A,* 96**,** 10711-6.

KOVACEVIC, D., FOX, A. J., BEDI, A., YING, L., DENG, X. H., WARREN, R. F. & RODEO, S. A. 2011. Calcium-phosphate matrix with or without TGF-beta3 improves tendon-bone healing after rotator cuff repair. *Am J Sports Med,* 39**,** 811-9.

KOVACEVIC, D., GULOTTA, L. V., YING, L., EHTESHAMI, J. R., DENG, X. H. & RODEO, S. A. 2015. rhPDGF-BB promotes early healing in a rat rotator cuff repair model. *Clin Orthop Relat Res,* 473**,** 1644-54.

KOVACEVIC, D. & RODEO, S. A. 2008. Biological augmentation of rotator cuff tendon repair. *Clin Orthop Relat Res,* 466**,** 622-33.

KRAMPERA, M., GLENNIE, S., DYSON, J., SCOTT, D., LAYLOR, R., SIMPSON, E. & DAZZI, F. 2003. Bone marrow mesenchymal stem cells inhibit the response of naive and memory antigen-specific T cells to their cognate peptide. *Blood,* 101**,** 3722-9.

KUHN, J. E., DUNN, W. R., MA, B., WRIGHT, R. W., JONES, G., SPENCER, E. E., WOLF, B., SAFRAN, M., SPINDLER, K. P., MCCARTY, E., KELLY, B. & HOLLOWAY, B. 2007. Interobserver agreement in the classification of rotator cuff tears. *Am J Sports Med,* 35**,** 437-41.

KUKKONEN, J., JOUKAINEN, A., LEHTINEN, J., MATTILA, K. T., TUOMINEN, E. K., KAUKO, T. & AARIMAA, V. 2015. Treatment of Nontraumatic Rotator Cuff Tears: A Randomized Controlled Trial with Two Years of Clinical and Imaging Follow-up. *J Bone Joint Surg Am,* 97**,** 1729-37.

KUMAGAI, J., SARKAR, K., UHTHOFF, H. K., OKAWARA, Y. & OOSHIMA, A. 1994. Immunohistochemical distribution of type I, II and III collagens in the rabbit supraspinatus tendon insertion. *J Anat,* 185 (Pt 2)**,** 279-84.

KVIST, M., JOZSA, L., JARVINEN, M. & KVIST, H. 1985. Fine structural alterations in chronic Achilles paratenonitis in athletes. *Pathol Res Pract,* 180**,** 416-23.

KVIST, M., JOZSA, L., KANNUS, P., ISOLA, J., VIENO, T., JARVINEN, M. & LEHTO, M. 1991. Morphology and histochemistry of the myotendineal junction of the rat calf muscles. Histochemical, immunohistochemical and electron-microscopic study. *Acta Anat (Basel),* 141**,** 199-205.

LAMBERS HEERSPINK, F. O., VAN RAAY, J. J., KOOREVAAR, R. C., VAN EERDEN, P. J., WESTERBEEK, R. E., VAN 'T RIET, E., VAN DEN AKKER-SCHEEK, I. & DIERCKS, R. L. 2015. Comparing surgical repair with conservative treatment for degenerative rotator cuff tears: a randomized controlled trial. *J Shoulder Elbow Surg,* 24**,** 1274-81.

LE BLANC, K., TAMMIK, C., ROSENDAHL, K., ZETTERBERG, E. & RINGDEN, O. 2003a. HLA expression and immunologic properties of

differentiated and undifferentiated mesenchymal stem cells. *Exp Hematol,* 31**,** 890-6.

LE BLANC, K., TAMMIK, L., SUNDBERG, B., HAYNESWORTH, S. E. & RINGDEN, O. 2003b. Mesenchymal stem cells inhibit and stimulate mixed lymphocyte cultures and mitogenic responses independently of the major histocompatibility complex. *Scand J Immunol,* 57**,** 11-20.

LEE, O. K., COATHUP, M. J., GOODSHIP, A. E. & BLUNN, G. W. 2005. Use of mesenchymal stem cells to facilitate bone regeneration in normal and chemotherapy-treated rats. *Tissue Eng,* 11**,** 1727-35.

LINDSAY, W. K. & BIRCH, J. R. 1964. THE FIBROBLAST IN FLEXOR TENDON HEALING. *Plast Reconstr Surg,* 34**,** 223-32.

LITTLEWOOD, C., ASHTON, J., MAWSON, S., MAY, S. & WALTERS, S. 2012. A mixed methods study to evaluate the clinical and cost-effectiveness of a self-managed exercise programme versus usual physiotherapy for chronic rotator cuff disorders: protocol for the SELF study. *BMC Musculoskelet Disord,* 13**,** 62.

LIU, G., LI, Y., SUN, J., ZHOU, H., ZHANG, W., CUI, L. & CAO, Y. 2010. In vitro and in vivo evaluation of osteogenesis of human umbilical cord blood-derived mesenchymal stem cells on partially demineralized bone matrix. *Tissue Eng Part A,* 16**,** 971-82.

LIU, S. H. & BAKER, C. L. 1994. Arthroscopically assisted rotator cuff repair: correlation of functional results with integrity of the cuff. *Arthroscopy,* 10**,** 54-60.

LIU, Y., HAN, Z. P., ZHANG, S. S., JING, Y. Y., BU, X. X., WANG, C. Y., SUN, K., JIANG, G. C., ZHAO, X., LI, R., GAO, L., ZHAO, Q. D., WU, M. C. &

WEI, L. X. 2011. Effects of inflammatory factors on mesenchymal stem cells and their role in the promotion of tumor angiogenesis in colon cancer. *J Biol Chem,* 286**,** 25007-15.

LOEW, M., MAGOSCH, P., LICHTENBERG, S., HABERMEYER, P. & PORSCHKE, F. 2015. How to discriminate between acute traumatic and chronic degenerative rotator cuff lesions: an analysis of specific criteria on radiography and magnetic resonance imaging. *J Shoulder Elbow Surg,* 24**,** 1685-93.

LONGO, U. G., FRANCESCHI, F., RUZZINI, L., RABITTI, C., MORINI, S., MAFFULLI, N. & DENARO, V. 2008. Histopathology of the supraspinatus tendon in rotator cuff tears. *Am J Sports Med,* 36**,** 533-8.

LONGO, U. G., LAMBERTI, A., MAFFULLI, N. & DENARO, V. 2011. Tissue engineered biological augmentation for tendon healing: a systematic review. *Br Med Bull,* 98**,** 31-59.

LOVRIC, V., CHEN, D., YU, Y., OLIVER, R. A., GENIN, F. & WALSH, W. R. 2012. Effects of demineralized bone matrix on tendon-bone healing in an intra-articular rodent model. *Am J Sports Med,* 40**,** 2365-74.

MA, C. B., KAWAMURA, S., DENG, X. H., YING, L., SCHNEIDKRAUT, J., HAYS, P. & RODEO, S. A. 2007. Bone morphogenetic proteins-signaling plays a role in tendon-to-bone healing: a study of rhBMP-2 and noggin. *Am J Sports Med,* 35**,** 597-604.

MACK, L. A., NYBERG, D. A., MATSEN, F. R., 3RD, KILCOYNE, R. F. & HARVEY, D. 1988. Sonography of the postoperative shoulder. *AJR Am J Roentgenol,* 150**,** 1089-93.

MALCARNEY, H. L., BONAR, F. & MURRELL, G. A. 2005. Early inflammatory reaction after rotator cuff repair with a porcine small intestine submucosal implant: a report of 4 cases. *Am J Sports Med,* 33**,** 907-11.

MALL, N. A., KIM, H. M., KEENER, J. D., STEGER-MAY, K., TEEFEY, S. A., MIDDLETON, W. D., STOBBS, G. & YAMAGUCHI, K. 2010. Symptomatic progression of asymptomatic rotator cuff tears: a prospective study of clinical and sonographic variables. *J Bone Joint Surg Am,* 92**,** 2623-33.

MALL, N. A., TANAKA, M. J., CHOI, L. S. & PALETTA, G. A., JR. 2014. Factors affecting rotator cuff healing. *J Bone Joint Surg Am,* 96**,** 778-88.

MALLON, W. J., WILSON, R. J. & BASAMANIA, C. J. 2006. The association of suprascapular neuropathy with massive rotator cuff tears: a preliminary report. *J Shoulder Elbow Surg,* 15**,** 395-8.

MAMAN, E., HARRIS, C., WHITE, L., TOMLINSON, G., SHASHANK, M. & BOYNTON, E. 2009. Outcome of nonoperative treatment of symptomatic rotator cuff tears monitored by magnetic resonance imaging. *J Bone Joint Surg Am,* 91**,** 1898-906.

MANNING, C. N., KIM, H. M., SAKIYAMA-ELBERT, S., GALATZ, L. M., HAVLIOGLU, N. & THOMOPOULOS, S. 2011. Sustained delivery of transforming growth factor beta three enhances tendon-to-bone healing in a rat model. *J Orthop Res,* 29**,** 1099-105.

MATHAPATI, S., VERMA, R. S., CHERIAN, K. M. & GUHATHAKURTA, S. 2011. Inflammatory responses of tissue-engineered xenografts in a clinical scenario. *Interact Cardiovasc Thorac Surg,* 12**,** 360-5.

MATSUMOTO, F., UHTHOFF, H. K., TRUDEL, G. & LOEHR, J. F. 2002. Delayed tendon reattachment does not reverse atrophy and fat accumulation of the supraspinatus--an experimental study in rabbits. *J Orthop Res,* 20**,** 357-63.

MCDEVITT, C. A., WILDEY, G. M. & CUTRONE, R. M. 2003. Transforming growth factor-beta1 in a sterilized tissue derived from the pig small intestine submucosa. *J Biomed Mater Res A,* 67**,** 637-40.

MCPHERSON, T. B., LIANG, H., RECORD, R. D. & BADYLAK, S. F. 2000. Galalpha(1,3)Gal epitope in porcine small intestinal submucosa. *Tissue Eng,* 6**,** 233-9.

MELROSE, J., SMITH, M. M., SMITH, S. M., RAVI, V., YOUNG, A. A., DART, A. J., SONNABEND, D. H. & LITTLE, C. B. 2013. Altered stress induced by partial transection of the infraspinatus tendon leads to perlecan (HSPG2) accumulation in an ovine model of tendinopathy. *Tissue Cell,* 45**,** 77-82.

MEROLLA, G., CHILLEMI, C., FRANCESCHINI, V., CERCIELLO, S., IPPOLITO, G., PALADINI, P. & PORCELLINI, G. 2014. Tendon transfer for irreparable rotator cuff tears: indications and surgical rationale. *Muscles Ligaments Tendons J,* 4**,** 425-32.

MEYER, D. C., FUCENTESE, S. F., KOLLER, B. & GERBER, C. 2004a. Association of osteopenia of the humeral head with full-thickness rotator cuff tears. *J Shoulder Elbow Surg,* 13**,** 333-7.

MEYER, D. C., HOPPELER, H., VON RECHENBERG, B. & GERBER, C. 2004b. A pathomechanical concept explains muscle loss and fatty muscular changes following surgical tendon release. *J Orthop Res,* 22**,** 1004-7.

MEYER, D. C., LAJTAI, G., VON RECHENBERG, B., PFIRRMANN, C. W. & GERBER, C. 2006. Tendon retracts more than muscle in experimental chronic tears of the rotator cuff. *J Bone Joint Surg Br,* 88**,** 1533-8.

MEYER, D. C., WIESER, K., FARSHAD, M. & GERBER, C. 2012a. Retraction of supraspinatus muscle and tendon as predictors of success of rotator cuff repair. *Am J Sports Med,* 40**,** 2242-7.

MEYER, F., WARDALE, J., BEST, S., CAMERON, R., RUSHTON, N. & BROOKS, R. 2012b. Effects of lactic acid and glycolic acid on human osteoblasts: a way to understand PLGA involvement in PLGA/calcium phosphate composite failure. *J Orthop Res,* 30**,** 864-71.

MICHNA, H. 1983. A peculiar myofibrillar pattern in the murine muscle-tendon junction. *Cell Tissue Res,* 233**,** 227-31.

MIHATA, T., WATANABE, C., FUKUNISHI, K., OHUE, M., TSUJIMURA, T., FUJIWARA, K. & KINOSHITA, M. 2011. Functional and structural outcomes of single-row versus double-row versus combined double-row and suture-bridge repair for rotator cuff tears. *Am J Sports Med,* 39**,** 2091-8.

MILLER, B. S., DOWNIE, B. K., KOHEN, R. B., KIJEK, T., LESNIAK, B., JACOBSON, J. A., HUGHES, R. E. & CARPENTER, J. E. 2011. When do rotator cuff repairs fail? Serial ultrasound examination after arthroscopic repair of large and massive rotator cuff tears. *Am J Sports Med,* 39**,** 2064-70.

MIMATA, Y., NISHIDA, J., SATO, K., SUZUKI, Y. & DOITA, M. 2015. Glenohumeral arthrodesis for malignant tumor of the shoulder girdle. *J Shoulder Elbow Surg,* 24**,** 174-8.

MINK, J. H., HARRIS, E. & RAPPAPORT, M. 1985. Rotator cuff tears: evaluation using double-contrast shoulder arthrography. *Radiology,* 157**,** 621-3.

MOOSMAYER, S., LUND, G., SELJOM, U. S., HALDORSEN, B., SVEGE, I. C., HENNIG, T., PRIPP, A. H. & SMITH, H. J. 2014. Tendon repair compared with physiotherapy in the treatment of rotator cuff tears: a randomized controlled study in 103 cases with a five-year follow-up. *J Bone Joint Surg Am,* 96**,** 1504-14.

MOSLER, E., FOLKHARD, W., KNORZER, E., NEMETSCHEK-GANSLER, H., NEMETSCHEK, T. & KOCH, M. H. 1985. Stress-induced molecular rearrangement in tendon collagen. *J Mol Biol,* 182**,** 589-96.

MOVIN, T., GAD, A., REINHOLT, F. P. & ROLF, C. 1997. Tendon pathology in long-standing achillodynia. Biopsy findings in 40 patients. *Acta Orthop Scand,* 68**,** 170-5.

MULLER-BORER, B. J., COLLINS, M. C., GUNST, P. R., CASCIO, W. E. & KYPSON, A. P. 2007. Quantum dot labeling of mesenchymal stem cells. *J Nanobiotechnology,* 5**,** 9.

NA, K., KIM, S. W., SUN, B. K., WOO, D. G., YANG, H. N., CHUNG, H. M. & PARK, K. H. 2007. Osteogenic differentiation of rabbit mesenchymal stem cells in thermo-reversible hydrogel constructs containing hydroxyapatite and bone morphogenic protein-2 (BMP-2). *Biomaterials,* 28**,** 2631-7.

NHO, S. J., SHINDLE, M. K., ADLER, R. S., WARREN, R. F., ALTCHEK, D. W. & MACGILLIVRAY, J. D. 2009. Prospective analysis of arthroscopic rotator cuff repair: subgroup analysis. *J Shoulder Elbow Surg,* 18**,** 697-704.

NHO, S. J., YADAV, H., SHINDLE, M. K. & MACGILLIVRAY, J. D. 2008. Rotator cuff degeneration: etiology and pathogenesis. *Am J Sports Med,* 36**,** 987-93.

NIXON, A. J., DAHLGREN, L. A., HAUPT, J. L., YEAGER, A. E. & WARD, D. L. 2008. Effect of adipose-derived nucleated cell fractions on tendon repair in horses with collagenase-induced tendinitis. *Am J Vet Res,* 69**,** 928-37.

NIXON, A. J., WATTS, A. E. & SCHNABEL, L. V. 2012. Cell- and gene-based approaches to tendon regeneration. *J Shoulder Elbow Surg,* 21**,** 278-94.

O'BRIEN, M. 1992. Functional anatomy and physiology of tendons. *Clin Sports Med,* 11**,** 505-20.

OH, J. H., CHUNG, S. W., KIM, S. H., CHUNG, J. Y. & KIM, J. Y. 2014a. 2013 Neer Award: Effect of the adipose-derived stem cell for the improvement of fatty degeneration and rotator cuff healing in rabbit model. *J Shoulder Elbow Surg,* 23**,** 445-55.

OH, J. H., SONG, B. W., KIM, S. H., CHOI, J. A., LEE, J. W., CHUNG, S. W. & RHIE, T. Y. 2014b. The measurement of bone mineral density of bilateral proximal humeri using DXA in patients with unilateral rotator cuff tear. *Osteoporos Int,* 25**,** 2639-48.

ORYAN, A., ALIDADI, S., MOSHIRI, A. & MAFFULLI, N. 2014. Bone regenerative medicine: classic options, novel strategies, and future directions. *J Orthop Surg Res,* 9**,** 18.

OXLUND, H. 1986. Relationships between the biomechanical properties, composition and molecular structure of connective tissues. *Connect Tissue Res,* 15**,** 65-72.

PATTE, D. 1990. Classification of rotator cuff lesions. *Clin Orthop Relat Res***,** 81-6.

PAULY, S., KLATTE, F., STROBEL, C., SCHMIDMAIER, G., GREINER, S., SCHEIBEL, M. & WILDEMANN, B. 2012. BMP-2 and BMP-7 affect human rotator cuff tendon cells in vitro. *J Shoulder Elbow Surg,* 21**,** 464-73.

PEDOWITZ, R. A., YAMAGUCHI, K., AHMAD, C. S., BURKS, R. T., FLATOW, E. L., GREEN, A., WIES, J. L., ST ANDRE, J., BOYER, K., IANNOTTI, J. P., MILLER, B. S., TASHJIAN, R., WATTERS, W. C., 3RD, WEBER, K., TURKELSON, C. M., RAYMOND, L., SLUKA, P. & MCGOWAN, R. 2012. American Academy of Orthopaedic Surgeons Clinical Practice Guideline on: optimizing the management of rotator cuff problems. *J Bone Joint Surg Am,* 94**,** 163-7.

PHIPATANAKUL, W. P. & PETERSEN, S. A. 2009. Porcine small intestine submucosa xenograft augmentation in repair of massive rotator cuff tears. *Am J Orthop (Belle Mead NJ),* 38**,** 572-5.

PIETRZAK, W. S., DOW, M., GOMEZ, J., SOULVIE, M. & TSIAGALIS, G. 2012. The in vitro elution of BMP-7 from demineralized bone matrix. *Cell Tissue Bank,* 13**,** 653-61.

PILL, S. G., PHILLIPS, J., KISSENBERTH, M. J. & HAWKINS, R. J. 2012. Decision making in massive rotator cuff tears. *Instr Course Lect,* 61**,** 97-111.

PITTENGER, M. F., MACKAY, A. M., BECK, S. C., JAISWAL, R. K., DOUGLAS, R., MOSCA, J. D., MOORMAN, M. A., SIMONETTI, D. W., CRAIG, S. & MARSHAK, D. R. 1999. Multilineage potential of adult human mesenchymal stem cells. *Science,* 284**,** 143-7.

POSTL, L. K., BRAUNSTEIN, V., VON EISENHART-ROTHE, R. & KIRCHHOFF, C. 2013. Footprint reconstruction in a rotator cuff tear associated cyst of the greater tuberosity: augmented anchorage. *Arch Orthop Trauma Surg,* 133**,** 81-5.

PROCTOR, C. S. 2014. Long-term successful arthroscopic repair of large and massive rotator cuff tears with a functional and degradable reinforcement device. *J Shoulder Elbow Surg*.

RALPHS, J. R., BENJAMIN, M., WAGGETT, A. D., RUSSELL, D. C., MESSNER, K. & GAO, J. 1998. Regional differences in cell shape and gap junction expression in rat Achilles tendon: relation to fibrocartilage differentiation. *J Anat,* 193 (Pt 2)**,** 215-22.

RANDELLI, P. S., ARRIGONI, P., CABITZA, P., VOLPI, P. & MAFFULLI, N. 2008. Autologous platelet rich plasma for arthroscopic rotator cuff repair. A pilot study. *Disabil Rehabil,* 30**,** 1584-9.

RAPOSIO, E., CARUANA, G., BONOMINI, S. & LIBONDI, G. 2014. A novel and effective strategy for the isolation of adipose-derived stem cells: minimally manipulated adipose-derived stem cells for more rapid and safe stem cell therapy. *Plast Reconstr Surg,* 133**,** 1406-9.

REDDI, A. H. 1998. Initiation of fracture repair by bone morphogenetic proteins. *Clin Orthop Relat Res***,** S66-72.

RODEO, S. A., ARNOCZKY, S. P., TORZILLI, P. A., HIDAKA, C. & WARREN, R. F. 1993. Tendon-healing in a bone tunnel. A biomechanical and histological study in the dog. *J Bone Joint Surg Am,* 75**,** 1795-803.

RODEO, S. A., POTTER, H. G., KAWAMURA, S., TURNER, A. S., KIM, H. J. & ATKINSON, B. L. 2007. Biologic augmentation of rotator cuff tendon-healing with use of a mixture of osteoinductive growth factors. *J Bone Joint Surg Am,* 89**,** 2485-97.

ROHL, L., LARSEN, E., LINDE, F., ODGAARD, A. & JORGENSEN, J. 1991. Tensile and compressive properties of cancellous bone. *J Biomech,* 24**,** 1143-9.

ROMEO, A. A., HANG, D. W., BACH, B. R., JR. & SHOTT, S. 1999. Repair of full thickness rotator cuff tears. Gender, age, and other factors affecting outcome. *Clin Orthop Relat Res***,** 243-55.

RUTLEDGE, K., CHENG, Q., PRYZHKOVA, M., HARRIS, G. M. & JABBARZADEH, E. 2014. Enhanced differentiation of human embryonic stem cells on extracellular matrix-containing osteomimetic scaffolds for bone tissue engineering. *Tissue Eng Part C Methods,* 20**,** 865-74.

SACHS, D. H. 1994. The pig as a potential xenograft donor. *Vet Immunol Immunopathol,* 43**,** 185-91.

SAGARRIGA VISCONTI, C., KAVALKOVICH, K., WU, J. & NIYIBIZI, C. 1996. Biochemical analysis of collagens at the ligament-bone interface reveals presence of cartilage-specific collagens. *Arch Biochem Biophys,* 328**,** 135-42.

SALTZMAN, B. M., JAIN, A., CAMPBELL, K. A., MASCARENHAS, R., ROMEO, A. A., VERMA, N. N. & COLE, B. J. 2015. Does the Use of Platelet-Rich Plasma at the Time of Surgery Improve Clinical Outcomes in Arthroscopic Rotator Cuff Repair When Compared With Control Cohorts? A Systematic Review of Meta-analyses. *Arthroscopy*.

SAWKINS, M. J., BOWEN, W., DHADDA, P., MARKIDES, H., SIDNEY, L. E., TAYLOR, A. J., ROSE, F. R., BADYLAK, S. F., SHAKESHEFF, K. M. & WHITE, L. J. 2013. Hydrogels derived from demineralized and decellularized bone extracellular matrix. *Acta Biomater,* 9**,** 7865-73.

SCHNABEL, L. V., LYNCH, M. E., VAN DER MEULEN, M. C., YEAGER, A. E., KORNATOWSKI, M. A. & NIXON, A. J. 2009. Mesenchymal stem cells and insulin-like growth factor-I gene-enhanced mesenchymal stem cells improve structural aspects of healing in equine flexor digitorum superficialis tendons. *J Orthop Res,* 27**,** 1392-8.

SCHWARTING, T., LECHLER, P., STRUEWER, J., AMBROCK, M., FRANGEN, T. M., RUCHHOLTZ, S., ZIRING, E. & FRINK, M. 2015. Bone morphogenetic protein 7 (BMP-7) influences tendon-bone integration in vitro. *PLoS One,* 10**,** e0116833.

SCHWARTZ, M. A. & DESIMONE, D. W. 2008. Cell adhesion receptors in mechanotransduction. *Curr Opin Cell Biol,* 20**,** 551-6.

SCLAMBERG, S. G., TIBONE, J. E., ITAMURA, J. M. & KASRAEIAN, S. 2004. Six-month magnetic resonance imaging follow-up of large and massive rotator cuff repairs reinforced with porcine small intestinal submucosa. *J Shoulder Elbow Surg,* 13**,** 538-41.

SEEHERMAN, H. J., ARCHAMBAULT, J. M., RODEO, S. A., TURNER, A. S., ZEKAS, L., D'AUGUSTA, D., LI, X. J., SMITH, E. & WOZNEY, J. M. 2008. rhBMP-12 accelerates healing of rotator cuff repairs in a sheep model. *J Bone Joint Surg Am,* 90**,** 2206-19.

SHARKEY, N. A. & MARDER, R. A. 1995. The rotator cuff opposes superior translation of the humeral head. *Am J Sports Med,* 23**,** 270-5.

SHARMA, P. & MAFFULLI, N. 2005. Tendon injury and tendinopathy: healing and repair. *J Bone Joint Surg Am,* 87**,** 187-202.

SHEA, K. P., OBOPILWE, E., SPERLING, J. W. & IANNOTTI, J. P. 2012. A biomechanical analysis of gap formation and failure mechanics of a xenograft-

reinforced rotator cuff repair in a cadaveric model. *J Shoulder Elbow Surg,* 21**,** 1072-9.

SHEN, H., MA, Y., LUO, Y., LIU, X., ZHANG, Z. & DAI, J. 2015. Directed osteogenic differentiation of mesenchymal stem cell in three-dimensional biodegradable methylcellulose-based scaffolds. *Colloids Surf B Biointerfaces,* 135**,** 332-8.

SHI, L. L., BOYKIN, R. E., LIN, A. & WARNER, J. J. 2014. Association of suprascapular neuropathy with rotator cuff tendon tears and fatty degeneration. *J Shoulder Elbow Surg,* 23**,** 339-46.

SHOEMAKER, S. C., RECHL, H., CAMPBELL, P., KRAM, H. B. & SANCHEZ, M. 1989. Effects of fibrin sealant on incorporation of autograft and xenograft tendons within bone tunnels. A preliminary study. *Am J Sports Med,* 17**,** 318-24.

SMIT, T. H., ODGAARD, A. & SCHNEIDER, E. 1997. Structure and function of vertebral trabecular bone. *Spine (Phila Pa 1976),* 22**,** 2823-33.

SORDI, V., MALOSIO, M. L., MARCHESI, F., MERCALLI, A., MELZI, R., GIORDANO, T., BELMONTE, N., FERRARI, G., LEONE, B. E., BERTUZZI, F., ZERBINI, G., ALLAVENA, P., BONIFACIO, E. & PIEMONTI, L. 2005. Bone marrow mesenchymal stem cells express a restricted set of functionally active chemokine receptors capable of promoting migration to pancreatic islets. *Blood,* 106**,** 419-27.

SOSLOWSKY, L. J., CARPENTER, J. E., DEBANO, C. M., BANERJI, I. & MOALLI, M. R. 1996. Development and use of an animal model for investigations on rotator cuff disease. *J Shoulder Elbow Surg,* 5**,** 383-92.

SPALAZZI, J. P., DAGHER, E., DOTY, S. B., GUO, X. E., RODEO, S. A. & LU, H. H. 2008. In vivo evaluation of a multiphased scaffold designed for orthopaedic interface tissue engineering and soft tissue-to-bone integration. *J Biomed Mater Res A,* 86**,** 1-12.

SPALAZZI, J. P., DOTY, S. B., MOFFAT, K. L., LEVINE, W. N. & LU, H. H. 2006. Development of controlled matrix heterogeneity on a triphasic scaffold for orthopedic interface tissue engineering. *Tissue Eng,* 12**,** 3497-508.

ST PIERRE, P., OLSON, E. J., ELLIOTT, J. J., O'HAIR, K. C., MCKINNEY, L. A. & RYAN, J. 1995. Tendon-healing to cortical bone compared with healing to a cancellous trough. A biomechanical and histological evaluation in goats. *J Bone Joint Surg Am,* 77**,** 1858-66.

SUMMITT, M. C. & REISINGER, K. D. 2003. Characterization of the mechanical properties of demineralized bone. *J Biomed Mater Res A,* 67**,** 742-50.

SUN, J., LI, J., LI, C. & YU, Y. 2015. Role of bone morphogenetic protein-2 in osteogenic differentiation of mesenchymal stem cells. *Mol Med Rep,* 12**,** 4230-7.

SUNDAR, S., PENDEGRASS, C. J. & BLUNN, G. W. 2009a. Tendon bone healing can be enhanced by demineralized bone matrix: a functional and histological study. *J Biomed Mater Res B Appl Biomater,* 88**,** 115-22.

SUNDAR, S., PENDEGRASS, C. J., ODDY, M. J. & BLUNN, G. W. 2009b. Tendon re-attachment to metal prostheses in an in vivo animal model using demineralised bone matrix. *J Bone Joint Surg Br,* 91**,** 1257-62.

TAKAHASHI, S., NAKAJIMA, M., KOBAYASHI, M., WAKABAYASHI, I., MIYAKOSHI, N., MINAGAWA, H. & ITOI, E. 2002. Effect of recombinant

basic fibroblast growth factor (bFGF) on fibroblast-like cells from human rotator cuff tendon. *Tohoku J Exp Med,* 198**,** 207-14.

TASHJIAN, R. Z., HOLLINS, A. M., KIM, H. M., TEEFEY, S. A., MIDDLETON, W. D., STEGER-MAY, K., GALATZ, L. M. & YAMAGUCHI, K. 2010. Factors affecting healing rates after arthroscopic double-row rotator cuff repair. *Am J Sports Med,* 38**,** 2435-42.

TAYLOR, M. S., DANIELS, A. U., ANDRIANO, K. P. & HELLER, J. 1994. Six bioabsorbable polymers: in vitro acute toxicity of accumulated degradation products. *J Appl Biomater,* 5**,** 151-7.

TEEFEY, S. A., RUBIN, D. A., MIDDLETON, W. D., HILDEBOLT, C. F., LEIBOLD, R. A. & YAMAGUCHI, K. 2004. Detection and quantification of rotator cuff tears. Comparison of ultrasonographic, magnetic resonance imaging, and arthroscopic findings in seventy-one consecutive cases. *J Bone Joint Surg Am,* 86-a**,** 708-16.

THOMOPOULOS, S., GENIN, G. M. & GALATZ, L. M. 2010. The development and morphogenesis of the tendon-to-bone insertion - what development can teach us about healing. *J Musculoskelet Neuronal Interact,* 10**,** 35-45.

THOMOPOULOS, S., HATTERSLEY, G., ROSEN, V., MERTENS, M., GALATZ, L., WILLIAMS, G. R. & SOSLOWSKY, L. J. 2002. The localized expression of extracellular matrix components in healing tendon insertion sites: an in situ hybridization study. *J Orthop Res,* 20**,** 454-63.

THOMOPOULOS, S., WILLIAMS, G. R., GIMBEL, J. A., FAVATA, M. & SOSLOWSKY, L. J. 2003. Variation of biomechanical, structural, and compositional properties along the tendon to bone insertion site. *J Orthop Res,* 21**,** 413-9.

TIDBALL, J. G. & DANIEL, T. L. 1986. Myotendinous junctions of tonic muscle cells: structure and loading. *Cell Tissue Res,* 245**,** 315-22.

TINGART, M. J., APRELEVA, M., ZURAKOWSKI, D. & WARNER, J. J. 2003. Pullout strength of suture anchors used in rotator cuff repair. *J Bone Joint Surg Am,* 85-a**,** 2190-8.

TOH, W. S., LIU, H., HENG, B. C., RUFAIHAH, A. J., YE, C. P. & CAO, T. 2005. Combined effects of TGFbeta1 and BMP2 in serum-free chondrogenic differentiation of mesenchymal stem cells induced hyaline-like cartilage formation. *Growth Factors,* 23**,** 313-21.

TOKUNAGA, T., IDE, J., ARIMURA, H., NAKAMURA, T., UEHARA, Y., SAKAMOTO, H. & MIZUTA, H. 2015. Local Application of Gelatin Hydrogel Sheets Impregnated With Platelet-Derived Growth Factor BB Promotes Tendon-to-Bone Healing After Rotator Cuff Repair in Rats. *Arthroscopy,* 31**,** 1482-91.

TROTTER, J. A. & BACA, J. M. 1987. A stereological comparison of the muscle-tendon junctions of fast and slow fibers in the chicken. *Anat Rec,* 218**,** 256-66.

UCCELLI, A., MORETTA, L. & PISTOIA, V. 2008. Mesenchymal stem cells in health and disease. *Nat Rev Immunol,* 8**,** 726-36.

URIST, M. R. 1965. Bone: formation by autoinduction. *Science,* 150**,** 893-9.

URIST, M. R., DELANGE, R. J. & FINERMAN, G. A. 1983. Bone cell differentiation and growth factors. *Science,* 220**,** 680-6.

VEILLETTE, C. J. & MCKEE, M. D. 2007. Growth factors--BMPs, DBMs, and buffy coat products: are there any proven differences amongst them? *Injury,* 38 Suppl 1**,** S38-48.

VIIDIK, A. 1973. Functional properties of collagenous tissues. *Int Rev Connect Tissue Res,* 6**,** 127-215.

VITALE, M. A., VITALE, M. G., ZIVIN, J. G., BRAMAN, J. P., BIGLIANI, L. U. & FLATOW, E. L. 2007. Rotator cuff repair: an analysis of utility scores and cost-effectiveness. *J Shoulder Elbow Surg,* 16**,** 181-7.

VOGEL, K. G., SANDY, J. D., POGANY, G. & ROBBINS, J. R. 1994. Aggrecan in bovine tendon. *Matrix Biol,* 14**,** 171-9.

VON LUTTICHAU, I., NOTOHAMIPRODJO, M., WECHSELBERGER, A., PETERS, C., HENGER, A., SELIGER, C., DJAFARZADEH, R., HUSS, R. & NELSON, P. J. 2005. Human adult CD34- progenitor cells functionally express the chemokine receptors CCR1, CCR4, CCR7, CXCR5, and CCR10 but not CXCR4. *Stem Cells Dev,* 14**,** 329-36.

WAGGETT, A. D., RALPHS, J. R., KWAN, A. P., WOODNUTT, D. & BENJAMIN, M. 1998. Characterization of collagens and proteoglycans at the insertion of the human Achilles tendon. *Matrix Biol,* 16**,** 457-70.

WAGNER, J., KEAN, T., YOUNG, R., DENNIS, J. E. & CAPLAN, A. I. 2009. Optimizing mesenchymal stem cell-based therapeutics. *Curr Opin Biotechnol,* 20**,** 531-6.

WALDORFF, E. I., LINDNER, J., KIJEK, T. G., DOWNIE, B. K., HUGHES, R. E., CARPENTER, J. E. & MILLER, B. S. 2011. Bone density of the greater tuberosity is decreased in rotator cuff disease with and without full-thickness tears. *J Shoulder Elbow Surg,* 20**,** 904-8.

WALTON, J. R., BOWMAN, N. K., KHATIB, Y., LINKLATER, J. & MURRELL, G. A. 2007. Restore orthobiologic implant: not recommended for augmentation of rotator cuff repairs. *J Bone Joint Surg Am,* 89**,** 786-91.

WANG, A., MCCANN, P., COLLIVER, J., KOH, E., ACKLAND, T., JOSS, B., ZHENG, M. & BREIDAHL, B. 2015. Do postoperative platelet-rich plasma injections accelerate early tendon healing and functional recovery after arthroscopic supraspinatus repair? A randomized controlled trial. *Am J Sports Med,* 43**,** 1430-7.

WEI, X., YANG, X., HAN, Z. P., QU, F. F., SHAO, L. & SHI, Y. F. 2013. Mesenchymal stem cells: a new trend for cell therapy. *Acta Pharmacol Sin,* 34**,** 747-54.

WHANG, K., HEALY, K. E., ELENZ, D. R., NAM, E. K., TSAI, D. C., THOMAS, C. H., NUBER, G. W., GLORIEUX, F. H., TRAVERS, R. & SPRAGUE, S. M. 1999. Engineering bone regeneration with bioabsorbable scaffolds with novel microarchitecture. *Tissue Eng,* 5**,** 35-51.

WIENER, S. N. & SEITZ, W. H., JR. 1993. Sonography of the shoulder in patients with tears of the rotator cuff: accuracy and value for selecting surgical options. *AJR Am J Roentgenol,* 160**,** 103-7; discussion 109-10.

WOLFF, A. B., SETHI, P., SUTTON, K. M., COVEY, A. S., MAGIT, D. P. & MEDVECKY, M. 2006. Partial-thickness rotator cuff tears. *J Am Acad Orthop Surg,* 14**,** 715-25.

WOLFGANG, G. L. 1974. Surgical repair of tears of the rotator cuff of the shoulder. Factors influencing the result. *J Bone Joint Surg Am,* 56**,** 14-26.

WONG, I., BURNS, J. & SNYDER, S. 2010. Arthroscopic GraftJacket repair of rotator cuff tears. *J Shoulder Elbow Surg,* 19**,** 104-9.

WOO SL, A. K., FRANK CB, LIVESAY GA, MA CB, ZEMINSKI JA, WAYNE JS, MYERS BS. 2000. Anatomy, biology, and biome- chanics of tendon and ligament. . *Orthopaedic Basic Sci- ence. 2 ed. Rosemont, IL: AAOS***,** 581-616.

WOO, S. L. & BUCKWALTER, J. A. 1988. AAOS/NIH/ORS workshop. Injury and repair of the musculoskeletal soft tissues. Savannah, Georgia, June 18-20, 1987. *J Orthop Res,* 6**,** 907-31.

WURGLER-HAURI, C. C., DOURTE, L. M., BARADET, T. C., WILLIAMS, G. R. & SOSLOWSKY, L. J. 2007. Temporal expression of 8 growth factors in tendon-to-bone healing in a rat supraspinatus model. *J Shoulder Elbow Surg,* 16**,** S198-203.

WYLIE, J. D., SUTER, T., POTTER, M. Q., GRANGER, E. K. & TASHJIAN, R. Z. 2016. Mental Health Has a Stronger Association with Patient-Reported Shoulder Pain and Function Than Tear Size in Patients with Full-Thickness Rotator Cuff Tears. *J Bone Joint Surg Am,* 98**,** 251-6.

WYNN, R. F., HART, C. A., CORRADI-PERINI, C., O'NEILL, L., EVANS, C. A., WRAITH, J. E., FAIRBAIRN, L. J. & BELLANTUONO, I. 2004. A small proportion of mesenchymal stem cells strongly expresses functionally active CXCR4 receptor capable of promoting migration to bone marrow. *Blood,* 104**,** 2643-5.

XU, G., ZHANG, Y., ZHANG, L., REN, G. & SHI, Y. 2007. The role of IL-6 in inhibition of lymphocyte apoptosis by mesenchymal stem cells. *Biochem Biophys Res Commun,* 361**,** 745-50.

YAMAGUCHI, K., DITSIOS, K., MIDDLETON, W. D., HILDEBOLT, C. F., GALATZ, L. M. & TEEFEY, S. A. 2006. The demographic and morphological features of rotator cuff disease. A comparison of asymptomatic and symptomatic shoulders. *J Bone Joint Surg Am,* 88**,** 1699-704.

YAMAGUCHI, K., TETRO, A. M., BLAM, O., EVANOFF, B. A., TEEFEY, S. A. & MIDDLETON, W. D. 2001. Natural history of asymptomatic rotator cuff

tears: a longitudinal analysis of asymptomatic tears detected sonographically. *J Shoulder Elbow Surg,* 10**,** 199-203.

YAMAZAKI, S., YASUDA, K., TOMITA, F., TOHYAMA, H. & MINAMI, A. 2005. The effect of transforming growth factor-beta1 on intraosseous healing of flexor tendon autograft replacement of anterior cruciate ligament in dogs. *Arthroscopy,* 21**,** 1034-41.

YOKOYA, S., MOCHIZUKI, Y., NAGATA, Y., DEIE, M. & OCHI, M. 2008. Tendon-bone insertion repair and regeneration using polyglycolic acid sheet in the rabbit rotator cuff injury model. *Am J Sports Med,* 36**,** 1298-309.

YOKOYA, S., MOCHIZUKI, Y., NATSU, K., OMAE, H., NAGATA, Y. & OCHI, M. 2012. Rotator cuff regeneration using a bioabsorbable material with bone marrow-derived mesenchymal stem cells in a rabbit model. *Am J Sports Med,* 40**,** 1259-68.

ZHAO, S., ZHAO, J., DONG, S., HUANGFU, X., LI, B., YANG, H., ZHAO, J. & CUI, W. 2014. Biological augmentation of rotator cuff repair using bFGF-loaded electrospun poly(lactide-co-glycolide) fibrous membranes. *Int J Nanomedicine,* 9**,** 2373-85.

ZHENG, M. H., CHEN, J., KIRILAK, Y., WILLERS, C., XU, J. & WOOD, D. 2005. Porcine small intestine submucosa (SIS) is not an acellular collagenous matrix and contains porcine DNA: possible implications in human implantation. *J Biomed Mater Res B Appl Biomater,* 73**,** 61-7.

ZUMSTEIN, M. A., JOST, B., HEMPEL, J., HODLER, J. & GERBER, C. 2008. The clinical and structural long-term results of open repair of massive tears of the rotator cuff. *J Bone Joint Surg Am,* 90**,** 2423-31.